Design and Development of Fluorescent Probes based on Poly(*p*-phenylene) for Sensing Applications

A thesis submitted by

Sameer Hussain

Roll No. 11612235

to

Indian Institute of Technology Guwahati

for the award of the degree of

Doctor of Philosophy

Department of Chemistry
Indian Institute of Technology Guwahati
Guwahati - 781039
India

August-2016

Design and Development of Fluorescent Probes based on Poly(*p*-phenylene) for Sensing Applications

A thesis submitted by

Sameer Hussain

Roll No. 11612235

to

Indian Institute of Technology Guwahati

for the award of the degree of

Doctor of Philosophy

Department of Chemistry
Indian Institute of Technology Guwahati
Guwahati - 781039
India

August-2016

Dedicated To My Parents

INDIAN INSTITUTE OF TECHNOLOGY GUWAHATI
Department of Chemistry

STATEMENT

I do hereby declare that the work contained in the thesis entitled "**Design and Development of Fluorescent Probes based on Poly(*p*-phenylene) for Sensing Applications**" is the result of investigations carried out by me in the Department of Chemistry, Indian Institute of Technology Guwahati, Guwahati, Assam India under the supervision of Prof. Parameswar Krishnan Iyer, Professor, Department of Chemistry, Indian Institute of Technology Guwahati, Guwahati, Assam, India. This work has not been submitted elsewhere for the award of any degree.

August, 2016 **Sameer Hussain**

IIT Guwahati

INDIAN INSTITUTE OF TECHNOLOGY GUWAHATI
Department of Chemistry

CERTIFICATE

This is to certify that the work contained in the thesis entitled **"Design and Development of Fluorescent Probes based on Poly(*p*-phenylene) for Sensing Applications"** by **Sameer Hussain**, a Ph.D. student of Department of Chemistry, Indian Institute of Technology Guwahati, for the award of degree of Doctor of Philosophy has been carried out under my supervision and this work has not been submitted elsewhere for any degree.

August, 2016
Guwahati

Prof. Parameswar Krishnan Iyer
Thesis Supervisor
Department of Chemistry
Indian Institute of Technology Guwahati
Guwahati – 781039
Assam, India.

Acknowledgements

At this stage of ending truly memorable and overwhelming journey towards my intellectual destination, it is really hard to list all the people who sincerely helped me and I would like to thank all of them who have made this thesis possible.

First of all, I would like to express my sincere gratitude to my supervisor Prof. Parameswar Krishnan Iyer for his expert guidance, advice, prudent suggestions and help me out in their busy schedule. I earnestly thank him for his astute supervision, freedom to work, encouragement, inspiration and creative ideas, which helped me to enhance my knowledge. I deem it my good fortune to have worked under his able and expert guidance.

I would like to thank my doctoral committee members, Prof. Bhisma Kumar Patel (Chairman), Prof. Abu Taleb Khan (ex-Chairman), Dr. Bhubaneswar Mandal and Dr. Vishal Trivedi for their insightful advices, suggestions and crucial comments which certainly helped me a lot in the betterment of my thesis.

I am grateful to all faculty members in the Department of Chemistry, IIT Guwahati for their help and encouragement and also the non-teaching staff of the Department for their technical support. I am thankful to the Central Instruments Facility (CIF), IIT Guwahati for various characterization facilities.

I gratefully acknowledge all my teachers especially Suhail Sabir sir, Shahid sir, Zain sir at AMU, Aligarh for their best teachings, constant motivations and precious advices which certainly are of great impact on me.

I convey my special thanks to Akhtar Hussain Malik for his emotional support, affection, respect, continuing encouragement, invaluable advices and assistance in my thesis work. I am lucky and honoured to have such a lovely and caring sister like friend Anamika Kalita who helped me a lot in the research work and during ups and down of my life to get out through difficult times. I am grateful to my oldest best friend Mohd Adil Afroz for everything he has done for me starting from academics upto extra-curricular. My best regards with Arvin, Sayan, Niranjan and Maimur for their unconditional love, respect, assistance and moral support. I have found wonderful human beings and friends in all of them for the rest of my life.

It is a pleasure to express my deep sense of gratitude to all my dear labmates working in synthesis lab as well as organic electronics lab, Priyanka di, Radha bhaiyya, Suresh, Bhim, Anamika Kalita, Anamika Dey, Ashish, Dipjyoti, Akhtar, Arvin, Sayan, Gopi, Rahul, Niranjan, Raman, Indrani, Ramesh ji, Subrata, Maimur, Nystha, Nehal, Rithesh for giving me friendly environment in lab and making my days memorable with them. I am

indebted to my former lab seniors Prasanta da, Atul da, Subbarao bhaiyya, Meenakshi mam and Jupitara mam for their valuable guidance and encouragement. I would like to acknowledge my former labmates, Debojit, Paran and all the interns/project fellows (past and present) for their profound respect and love. Thanks also to all other departmental seniors, batch mates and juniors for sharing valuable experiences and unforgettable moments.

I take this opportunity to express gratitude to my dear friends and colleagues, Reshma, Nausheen, Sajjad, Firoz, Sabera, Afsana, Priyam, Saugata, Kobirul, Julfiqar, Nirmali, Tulsi, Himadri, Namami, Ujjwol, Bornali, Priyanka, for their timely suggestions, inspiration and moral support. I would also like to express deep gratitude to my seniors and juniors from AMU, Musawwer bhai, Zia bhai, Ajaz bhai, Palash bhai, Akhtar, Wajid, Sahnawaz, Krapa, Adil, Shaad, Kafeel, Maimur, Akhtar Alam, Rather, Bilal, Munendra, Sana, Rabiul for giving me unforgettable experiences and cherishable moments. I will especially miss the wonderful moments shared with Shaad, Adil and Wajid during my stay at hostel.

Finally, my PhD endeavour could not be completed without the endless love, unending support, tolerance and blessings from my family. I would like to express my sincere gratitude with great honour to my family members who give me lots of love, strength, kind support and prayers which made me to reach this stage. I am fortunate and blessed to have such a caring and supportive mother Mrs. Anis Khatoon and father Mr. Zameer Hussain who struggle and sacrifice a lot to make my career. I am grateful to my elder sister Dr. Asma Khatoon, younger brother Er. Anzar Anwar and brother-in-law Dr. Ashraf Imam for their eternal love, cooperation and emotional support which were immensely needed to complete this work.

Last but not the least, I would like to thank the Almighty Allah for continuously showering his blessings and for providing me a talented supervisor cum mentor, a loving and supporting family, and wonderful friends who have helped me to achieve these remarkable steps.

Sameer Hussain

Synopsis

The content of this thesis report entitled **"Design and Development of Fluorescent Probes based on Poly(*p*−phenylene) for Sensing Applications"** is divided into five chapters. Chapter I described the respective research area where the scope and significance of the subsequent chapters are discussed. Chapter II discussed the synthesis of a neutral conjugated polymer PPT, a derivative of poly(*p*−phenylene) and its application in the colorimetric and fluorometric detection of iodide and mercury in aqueous environment, both in solution state as well as on solid platform. Chapter III described the synthesis of a new water soluble cationic conjugated polymer PMI and its application in the detection and discrimination of widely used anionic surfactants SDS/SDBS in the natural water systems. Chapter III also discussed about the practicability of polymer PMI in illicit−drug analysis. Chapter IV highlighted the application of polymer PMI in the detection of potent explosive and highly water soluble pollutant picric acid both in solution as well as solid phase. Chapter V deals with the detection and discrimination of flavins (RF, FMN and FAD) by polymer PMI under physiological conditions.

Chapter I: Introduction

The use of conjugated polymers (CPs) as highly sensitive material represents a new and promising direction in multi−disciplinary areas of chemical sciences, biological sciences and material sciences. Several research groups have demonstrated that CP based sensing platforms are very efficient in detecting various chemical and biological species utilizing its unique opto−electronic properties, excellent film forming abilities, viability in biosystems etc. Owing to these numerous features of CPs, they are considered as an important class of materials for optoelectronic devices and used worldwide for light emitting diodes (LEDs), organic−field effect transistors (OFETs), photovoltaics, plastic lasers and sensors. CPs exhibit strong absorption and emission due to migration of excitons along the backbone chain. These excitons can be transferred to low energy/electron acceptor sites over a particular distance that subsequently results in signal amplification of the acceptors or amplified quenching of the fluorescence of CPs. The photophysical properties of CPs depend on effective conjugation length, chemical nature, intramolecular arrangements and intermolecular packing that provide suitable mechanisms for sensing applications. Sensors based on CP are considered more sensitive than small molecule due to their ability to amplify the signal from a recognition event. On binding of an analyte to a receptor attached to CP, the conducting properties of the entire

backbone or various absorbing units are collectively affected. Such recognition process eventually results in signal amplification or super quenching (turn−off) of the fluorescence compared to small molecule based sensors where change in fluorescence usually occurred due to single chromophore after binding event. This signal amplification process in CPs was first discovered by Swager in 1995 and termed as "molecular−wire effect". Such remarkable feature of CPs is crucial for chemo− and biosensing applications, since extremely dilute concentrations of the probe is required. When "turn−on" sensing mechanism is implemented, the analyte binding perturbs the electron density along the polymer backbone or alter the conformation of the polymer chain that subsequently results in appearance of emission. Figure 1 demonstrates the effect of dimensionality on sensitivity of CPs *via* quenching and de−quenching mechanisms. Note that quenching mechanisms in CP based sensors are generally more sensitive than de−quenching mechanism. Higher dimension materials exhibit greater sensitivity than 1-Dimensional or isolated polymer chains.

CPs can be acquired with variable backbone chain, *viz.* poly(*p*−phenylene vinylene) (PPV), poly(*p*−phenylenes) (PPP), poly(*p*−phenylene ethynylene) (PPE), polyfluorene (PF), polythiophene (PT), polypyrrole (PPy), polyaniline (PANI) etc. The solubility of CP in water is essential for performing sensing in biological environments. This can be

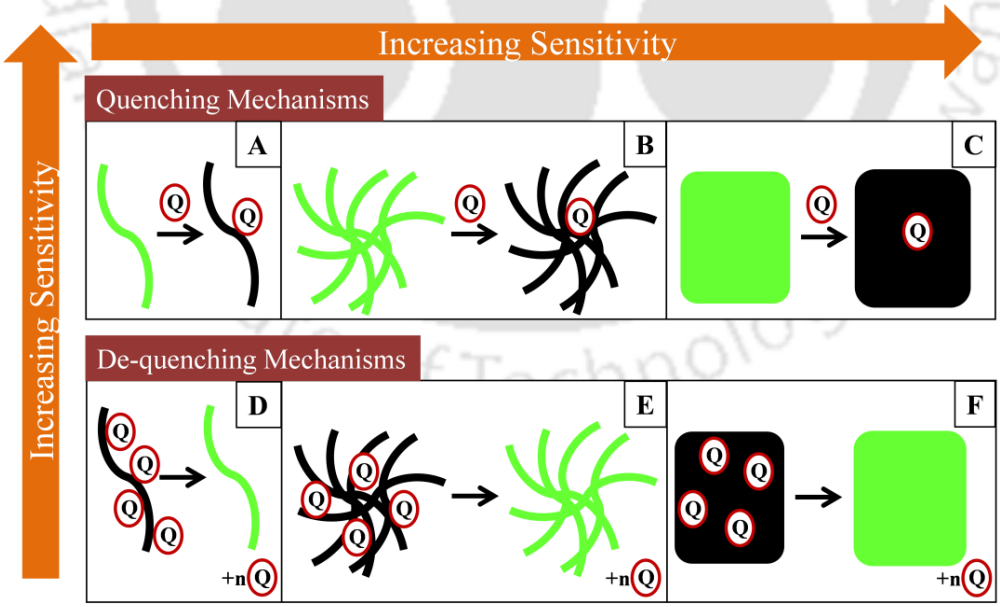

Figure 1. Effect of dimensionality on the sensitivity of conjugated polymers *via* quenching and de−quenching mechanism. Reprinted with permission from ref 10 (Chapter 1). Copyright 2013 American Chemical Society.

accomplished by incorporating suitable ionic pendant groups like sulphate, sulphonate, carboxylate, quaternary ammonium, imidazolium etc. onto the side chains of polymer. In addition to providing the solubility in aqueous media, charged character of CPs further facilitates the electrostatic interactions between the desirable sensing analyte and probe that assists in efficient signal transduction process. Furthermore, these ionic groups sometimes act as specific recognition site for detection of a particular analyte. Thus, the combined water solubility and light harvesting property of CPs offer exceptional opportunities for the development of chemical and biological sensors with enhanced sensitivity that is superior to small molecule based sensors. The main objective of this thesis was to design and synthesize new conjugated polymers and utilize them in the detection of various chemical and biological important species with the aim to overcome the challenges and drawbacks arises in the existing sensing systems.

Chapter II: Thiazole-containing conjugated polymer as a visual and fluorometric sensor for iodide and mercury

This chapter described the synthesis of a new derivative of poly(*p*−phenylene) i.e. poly(1,4−bis−(8−(4−phenylthiazole−2−thiol)−octyloxy)−benzene) (PPT). The polymer PPT was prepared by a simple and economical method of oxidative polymerization reaction. PPT displayed fluorescence "turn−off/turn−on" characteristics and colorimetric responses to I^- and Hg^{2+} in 4:1 THF/water mixture (Figure 2). The UV−vis and fluorescence spectra of the PPT showed significant shift in λ_{max} by addition of iodides and mercury. A colorless PPT solution turns to deep yellow in the presence of iodide salts which subsequently becomes colorless again on addition of Hg^{2+} salts that could be easily detected visually by the naked eye. The K_{sv} value obtained for the detection of iodide is 0.13×10^5 M^{-1} confirming very high sensitivity of this polymer for iodide salts. The detection limit calculated for Hg^{2+} using the PPT polymer was found to be 2.1 nM which is comparable with the maximum permissibility limit of 10 nM set by WHO and US−EPA. The detection of both iodide and mercury was also possible in solid state by using a membrane film prepared by mixing 1% PPT in polystyrene. This membrane changes color in presence of iodide as well as mercury salts. These results confirm that the PPT polymer can be applied as colorimetric as well as fluorometric sensing of iodide and mercury ions in competing environment in solution as well as in solid state using a membrane film rapidly.

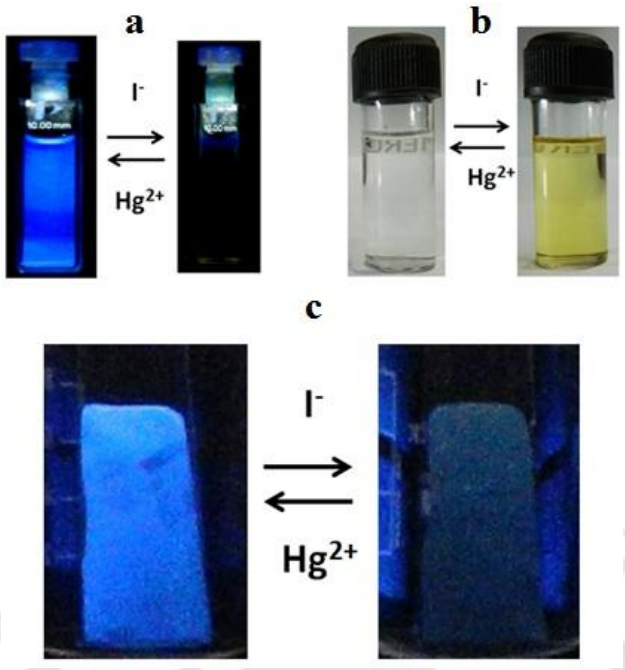

Figure 2. Color of the PPT solution in 4:1 THF/water under (a) UV light and (b) naked-eye. A bright blue Polystyrene + PPT membrane (left image) under UV light in water loses its fluorescence (right image) upon being dipped in a 3.3×10^{-5} M I^- solution in water. This film regains its fluorescence upon being dipped in a fresh 5×10^{-5} M solution of Hg^{2+}.

Chapter III: Highly precise detection, discrimination, and removal of anionic surfactants over the full pH range *via* cationic conjugated polymer: An efficient strategy to facilitate illicit−drug analysis

This chapter discussed the synthesis of a new water−soluble cationic conjugated polyelectrolyte (CPE), poly(1,4−bis(6−(1−methylimidazolium)−hexyloxy)−benzene bromide) (PMI) that displays extraordinary stability over the full pH range of 1−14 as well as in seawater, brine, urine and other solutions. The polymer PMI performs efficient detection, discrimination and removal of moderately dissimilar anionic surfactants *viz.*, sodium dodecyl benzenesulfonate (SDBS) and sodium dodecyl sulfate (SDS) at very low levels (31.7 and 17.3 parts per billion (ppb)), respectively (Figure 3). PMI formed stable hydrogels in the presence of SDS that remained unaffected by strong acids/bases, heating, ultrasonication, or exposure to light, whereas SDBS formed precipitate with PMI as a result of its different inter−polymer cofacial arrangement *via* Columbic attraction. The complex−forming ability of PMI with SDS and SDBS facilitated their elimination from

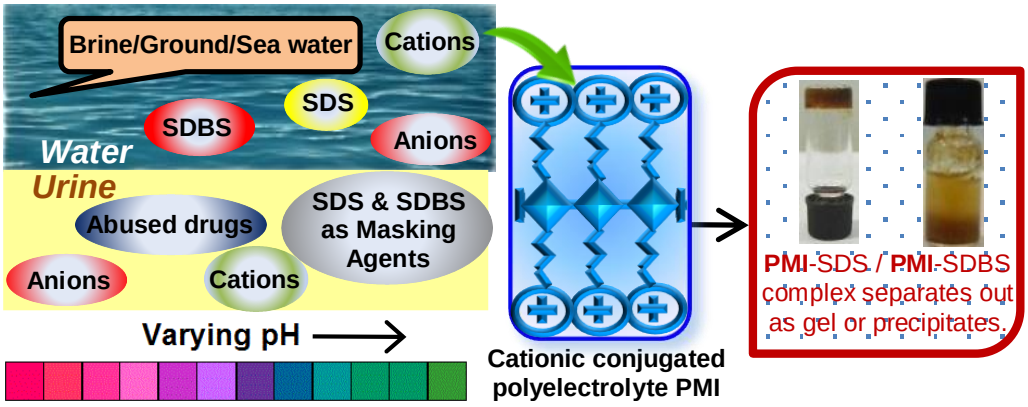

Figure 3. Cationic polymer PMI performs detection of widespread surfactants SDS/SDBS in various conditions.

water or drug−doped urine samples without the use of any organic solvent, chromatographic technique, or solid support. This protocol, the first of its kind for the removal of anionic surfactants at very low concentrations from any type of solution and competitive environments, demonstrates an original application using a CPE. The surfactant−free sample solutions could be precisely analyzed for the presence of illicit drugs by any standard methods. Using PMI, a newly developed CPE, a rapid and practical method for the efficient detection, discrimination, and removal of SDS and SDBS at ppb levels from water and urine, under harsh conditions, and in natural chemical environments is demonstrated.

Chapter IV: Ultrasensitive detection of nitroexplosive−picric acid *via* a conjugated polyelectrolyte in aqueous media and solid support

Chapter IV described the application of water soluble cationic CP PMI in performing detection of a stronger nitroexplosive and a serious environment pollutant nitroexplosive picric acid (PA) in aqueous media and solid support. The fluorescence−amplified detection of picric acid is achieved at parts per trillion (ppt) levels for the first time using conjugated polyelectrolyte PMI. The polymer PMI displayed substantial fluorescence quenching exclusively for PA with a very high Stern−Volmer constant (K_{sv}) value of 0.1 × 10^{8} M^{-1} and a very low limit of detection value 0.56 × 10^{-9} M (128 ppt) in 100% aqueous media. Formation of ground state charge transfer complex, resonance energy transfer as well as favorable electrostatic interaction between PMI and PA were the key aspects for unprecedented selectivity and remarkable sensitivity of PMI towards PA.

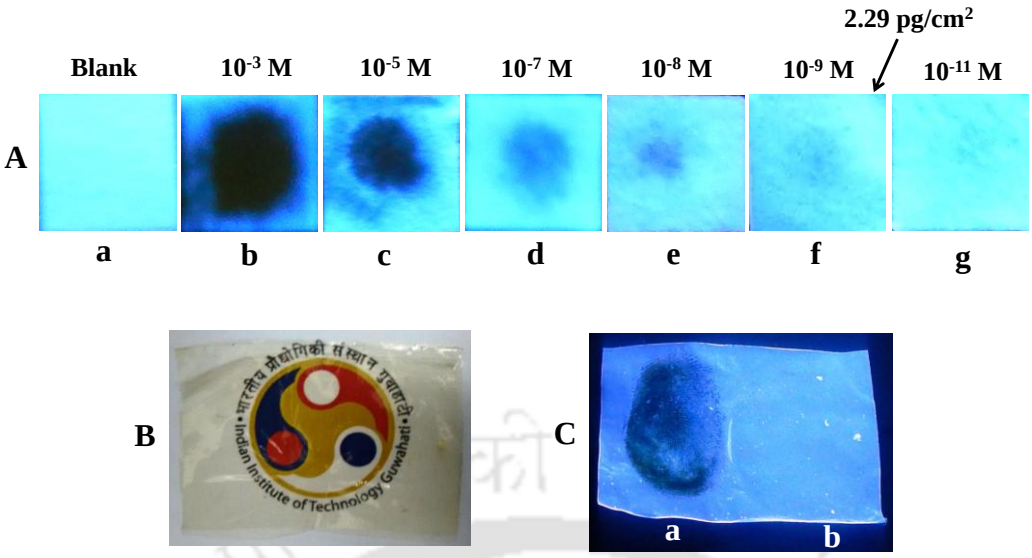

Figure 4. (A) Color of fluorescent test strips under UV light (a) before and after (b, c, d, e, f and g) adding 10 µL of various concentrations of PA solution. (B) PMI–doped transparent Chitosan (CS) film in day light. (C) Visualization of PMI-doped CS fluorescent film under UV light. (a) Dark spot of PA residual left thumb impression. (b) Right thumb impression as control (lamp excited at 365 nm).

Paper strips test using simple Whatman paper and contact mode detection using PMI-doped chitosan (Figure 4) film makes this method simple, portable and cost−effective in order to monitor environmental contamination and terrorist threats rapidly.

Chapter V: FRET−assisted selective detection of flavins *via* cationic conjugated polyelectrolyte under physiological conditions

Chapter V described the detection and discrimination of flavins using CP PMI under physiological conditions. Flavins *viz.* riboflavin (RF, Vitamin B_2), flavin mononucleotide (FMN) and flavin adenine dinucleotide (FAD) represent an important class of biomolecules ubiquitously found in living systems that are vital for numerous cellular activities inside the body. The fluorescence amplified detection of these flavins at ppb levels (RF−259 ppb, FMN−9.37 ppb and FAD−11.11 ppb) is achieved for the first time using water soluble cationic conjugated polymer PMI under physiological conditions. The substantial FRET, variable binding abilities of flavins with PMI *via* Columbic interaction and the subsequent displacement of FMN/FAD by simple chelating agent like Cu^{2+} affords a simple and consistent method to detect and discriminate them even in the

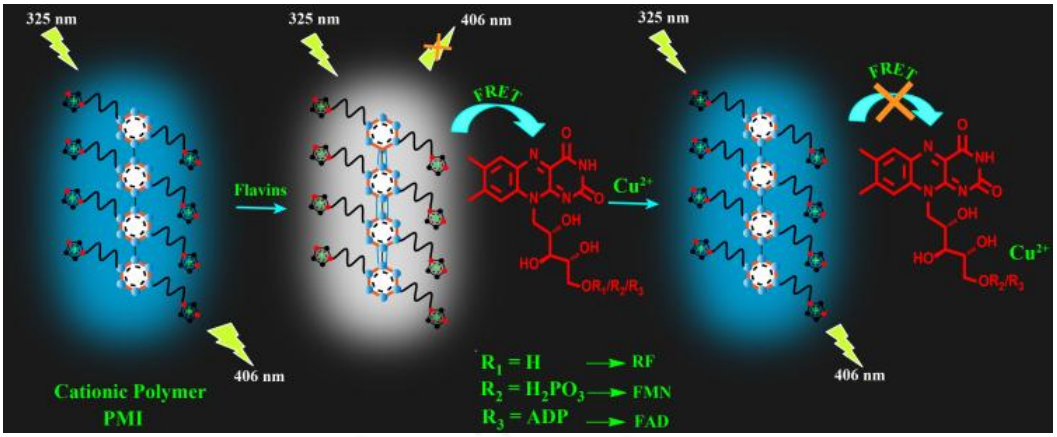

Figure 5. Schematic presentation for the detection and discrimination of flavins using conjugated polymer PMI and simple chelating metal ion Cu^{2+}.

presence of most common interfering analytes usually found in biosystems (Figure 5). This new strategy based on FRET provides more precise measurement using two different emission bands and hence, eliminates the environmental effects unlike in classical or direct fluorescence method. Furthermore, the determination of flavins in human blood serum using cationic conjugated polyelectrolyte PMI signifies the potential of this protocol in studying the metabolic processes and clinical assessment of diseases related to flavins.

Conclusion and thesis overview

In conclusion, the two new derivatives of poly(*p*−phenylene) i.e. PPT and PMI were synthesized using oxidative polymerization reaction followed by post functionalization technique. The polymer PPT was successfully utilized for the detection of I^- and Hg^{2+} in solution state as well as on solid support using simple and portable PPT doped polystyrene film. The water soluble cationic conjugated polyelectrolyte PMI was also employed for the detection of anionic surfactants (SDS/SDBS), nitroexplosive picric acid and ubiquitously found flavins (RF, FMN and FAD) in aqueous media. Furthermore, a new strategy was developed using CP PMI to catch drug abusers giving "false−negative test" in dope test due to adulteration of their urine specimens.

Contents

Chapter 1

Introduction

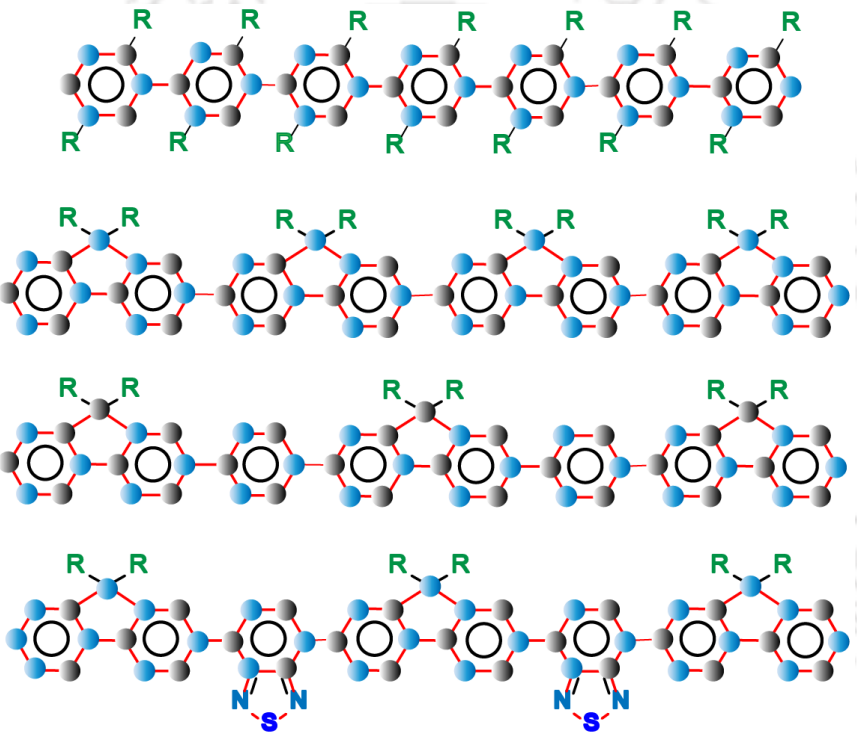

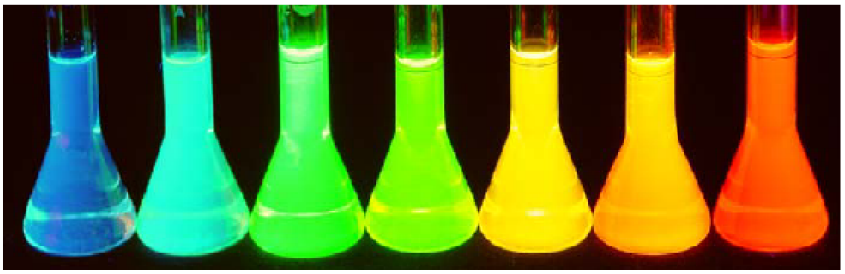

1.1 Introduction

Conjugated polymers (CPs) are organic macromolecules consisting of alternate single and double bonds along their backbone. The π−bonds are delocalized over the entire polymer chain and responsible for the unique photophysical and electrochemical properties of CPs. Conducting property of such organic materials were first discovered[1] in halogen doped polyacetylene by three eminent scientists Alan MacDiarmid, Hideki Shirakawa and Alan Heeger in 1977 that led them to win Nobel Prize of Chemistry in 2000. Owing to numerous features of CPs, they considered them as an unique class of materials for optoelectronic devices[2−13] and used worldwide today for light emitting diodes (LEDs), organic−field effect transistors (OFETs), photovoltaics, plastic lasers and sensors. CPs can be acquired with variable backbone chains, *viz.* poly(*p*−phenylene vinylene) (PPV), poly(*p*−phenylene) (PPP), poly(*p*−phenylene ethynylene) (PPE), polyfluorene (PF), polythiophene (PT), polypyrrole (PPy), etc. as shown in Figure 1.1.

1.2 Conjugated polymers as sensory material

For any sensor system, there are several parameters that need to be fulfilled in order to define it as an effective or "Ideal" sensor. These parameters include high selectivity, reasonable sensitivity, water solubility, low toxicity etc. as shown in Figure 1.2. The use of CPs as highly sensitive material represents a new and promising direction in multi−disciplinary areas of chemical sciences, biological sciences and material sciences. On the basis of signal response, CP based optical sensors can be classified into two categories *viz.* colorimetric and fluorometric. Colorometric detection is primarily based on the change in absorption spectra of CP or change in the color of the polymer solution

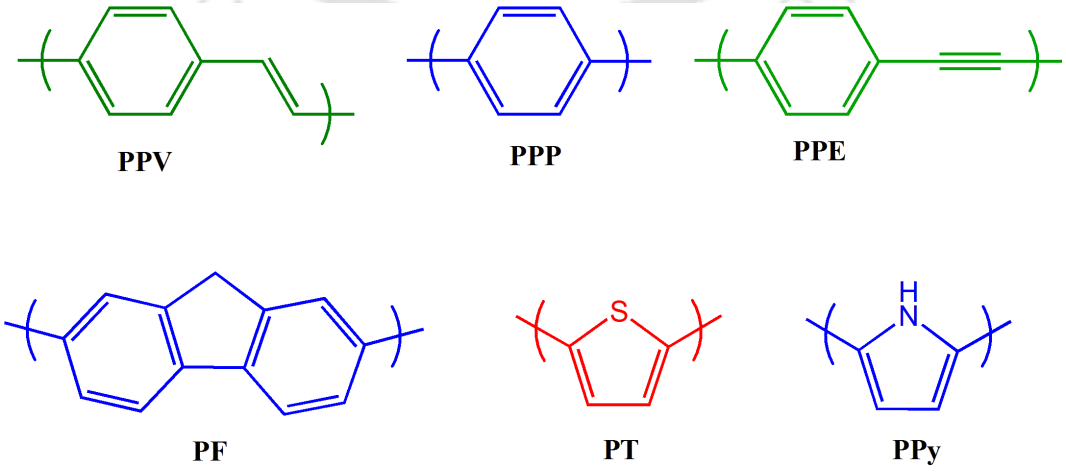

Figure 1.1 Structure of some well−known fluorescent conjugated polymers.

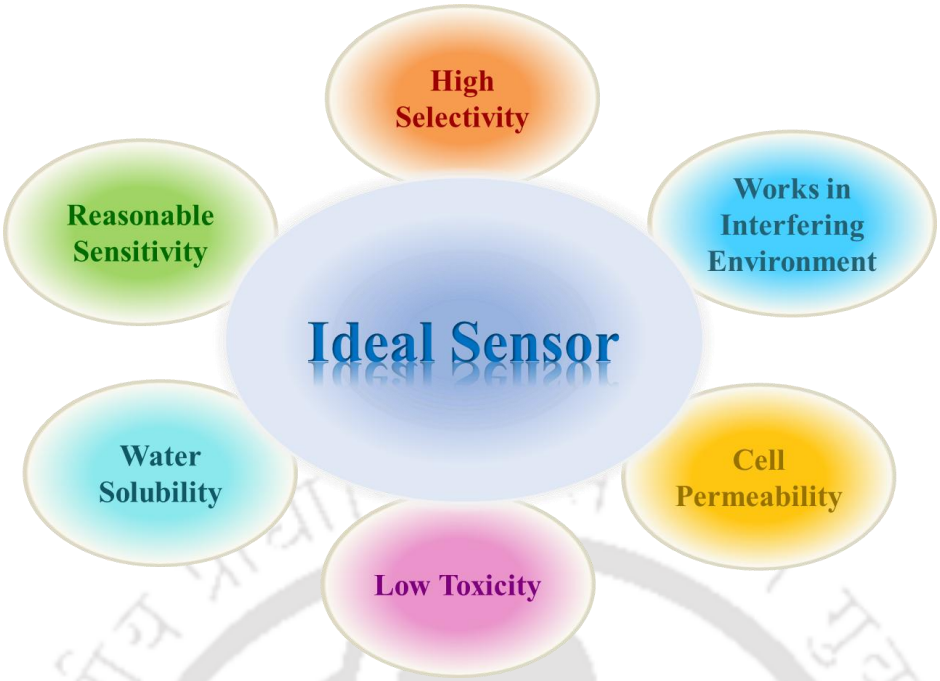

Figure 1.2 Graphical representation of an ideal sensor system.

under visible eye. In fluorometric detection, change in the emission intensity/wavelength, and/or fluorescence lifetime is usually observed. Such changes in the optical properties of CPs can be achieved *via* favorable signal transduction processes like intra and/or inter chain polymer aggregation, photoinduced electron transfer (PET), Förster resonance energy transfer (FRET) etc. These signal transduction processes are typically operative *via* favorable non−covalent interactions between the sensing analyte and probe that brings them in close proximity to bring the change in signal. Several research groups have demonstrated[8−13] that CP based sensing platforms are very efficient in detecting various chemical and biological species. The solubility of CPs in water is essential for performing sensing in biological environments. This can be accomplished by incorporating suitable ionic pendant groups like sulphate, sulphonate, carboxylate, quaternary ammonium, imidazolium etc. onto the side chains of polymer. Such water soluble conjugated polymers (WSCPs) are termed as conjugated polyelectrolytes (CPEs) that act as a link between the electronic and biological world. In addition to providing the solubility in aqueous media, charged character of CPEs further facilitates the electrostatic interactions between the desirable sensing analyte and probe that assists in efficient signal transduction process. Thus, the combined water solubility and light harvesting property of CPs offer exceptional opportunities for the development of chemical and biological sensors with enhanced sensitivity that is superior to small molecule based sensors.

1.3 Amplifying signal response in conjugated polymers

Conjugated polymers exhibit strong absorption and emission due to the migration of excitons along the backbone chain. These excitons can be transferred to low energy/electron acceptor sites over a particular distance that subsequently results in signal amplification of the acceptors or amplified quenching of the fluorescence. The photophysical properties of CPs depend on effective conjugation length, chemical nature, intramolecular arrangements and intermolecular packing that provide suitable mechanisms for sensing applications. Sensors based on CPs are considered more sensitive than small molecule due to their ability to amplify the signal from a recognition event. On binding of an analyte to a receptor attached to CP, the conducting properties of the entire backbone or several absorbing units are collectively affected as shown in Figure 1.3. Such recognition process eventually results in signal amplification or super quenching of the fluorescence compared to small molecule based sensors where change in fluorescence usually occurred due to single chromophore after the binding event (Figure 1.3). This signal amplification process in CPs was first discovered[14] by Swager in 1995 and termed as a "molecular−wire effect". Such remarkable feature of CPs endorses its widespread application as chemo− and biosensors, since extremely dilute concentrations of the probe is required.

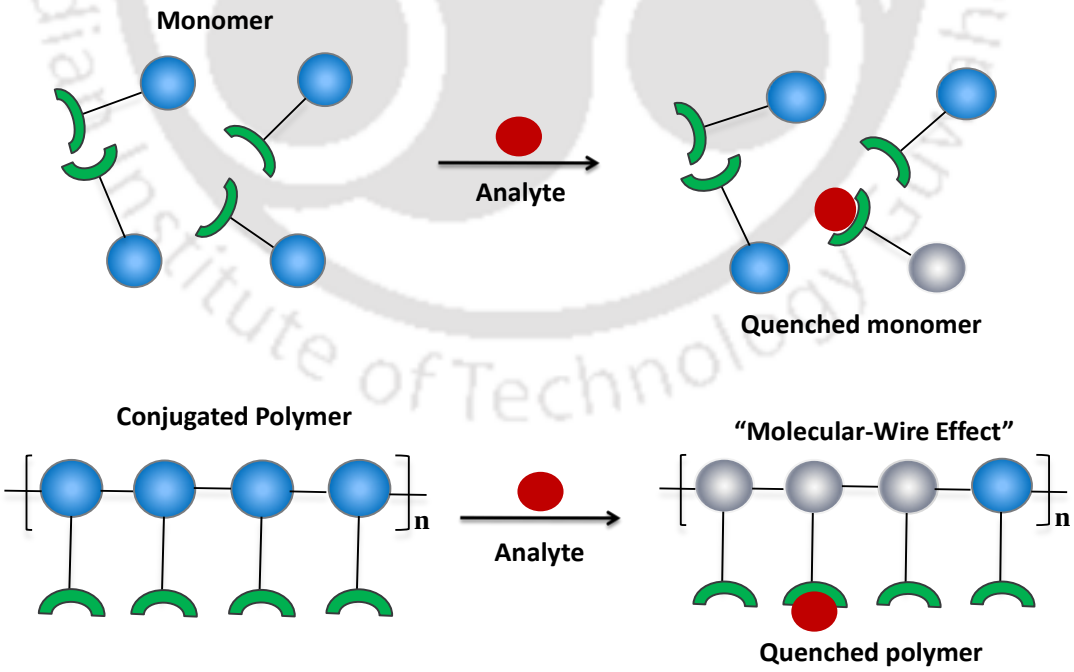

Figure 1.3 Pictorial representation of fluorescence quenching in monomer and conjugated polymer by a particular analyte.

1.4 Quenching and dequenching process

This is the change in the optical signal response in CPs after binding event has taken place either *via* fluorescence "turn−off" (quenching) or "turn−on" (dequenching) process. In a quenching process, the emission of a CP is effectively quenched *via* non−radiative relaxation pathways or the aggregation of the polymer chains.[10] The signal amplification in such process depends upon the exciton diffusion length and the form of material (Figure 1.4 ABC). While employing solution based quenching studies, the level of signal gain is limited because the diffusion of exciton is constrained to a 1−D random walk process. The exciton can revisit the same sites several times, since it is randomly diffused along an isolated polymer chain. However, the level of signal gain can dramatically increase on allowing the excitons to diffuse more freely in three dimensions. Therefore, continuous polymer films exhibit superior signal amplification properties compared to the same polymers in solution state. In a dequenching process, the analyte binding perturbs the electron density along the polymer backbone or alter the conformation of the polymer chain that subsequently results in appearance of emission. Note that dequenching process usually exhibits lower sensitivity than a quenching process (Figure 1.4 DEF). This is due to the fact that to attain highly quenched state, few quencher molecules will inevitably be positioned inside the exciton diffusion length and removal of such quenchers during the dequenching process will be difficult to recover all the potential fluorescence.

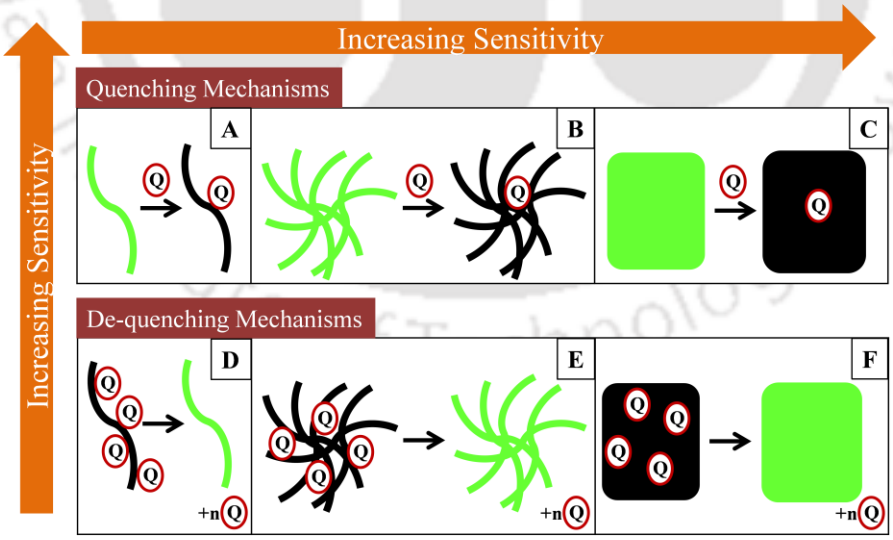

Figure 1.4 Effect of dimensionality on the sensitivity of conjugated polymers *via* quenching and de−quenching mechanism. Quenching mechanisms are generally more sensitive than dequenching mechanisms. Higher dimension materials exhibit greater sensitivity than 1−Dimensional or isolated polymer chains. Reprinted with permission from ref 12. Copyright 2013 American Chemical Society.

1.5 Conjugated polymers for chemo− and bio− sensing applications

During past years, CPs have been extensively used as a sensory material for the detection of various chemical and biological species[7−13] like metals ions, anions, pollutants, explosives, proteins, enzymes, etc. owing to remarkable sensitivity, excellent film forming ability, high photoluminescence quantum yield, portability, photo− and thermal stability of these CPs. Selected examples of such CP based sensing platforms are discussed below.

1.5.1 Detection of metal ions and anions

In 2005, Bunz[15] *et al.* reported a carboxylated water−soluble poly(*p*−phenylene ethynylene) **1** (Figure 1.5) that displayed remarkable fluorescence quenching exclusively towards Pb^{2+} ions with a K_{sv} value ~10^6 M^{-1} in aqueous solution. A variety of other divalent metal ions (Zn^{2+}, Hg^{2+}, Mg^{2+}, Ca^{2+}, Mn^{2+} and Cu^{2+}) were also examined and found ~10 times less sensitive towards Pb^{2+} ions. The sensitivity for the detection of Pb^{2+} ions was ~100 times lower in phosphate buffer than in PIPES (piperazine−1,4−bis−2−ethanesulfonic acid) buffer that may probably be due to the ability of phosphate anions to interfere with Pb^{2+} ions. However, the anionic polymer **1** was found to be ~1500 fold more sensitive towards Pb^{2+} ions than its model compound **2** (Figure 1.5) that consists of total two carboxylic acid groups along the side chains. Such a high sensitivity was attributed to the enhanced quenching of **1** due to "molecular−wire effect" compared to monomer **2.** It was presumed that lead ions could bind upto three carboxylate groups of **1** in solution, whereas model compound **2** could not bind strongly with Pb^{2+}, since the second carboxylate arm appeared to be too far away. Furthermore, based on the electrostatic complex between the **1** and papain (a cationic cysteine protease), same group[16] have also developed a fluorescence−based assay for Hg^{2+} ions.

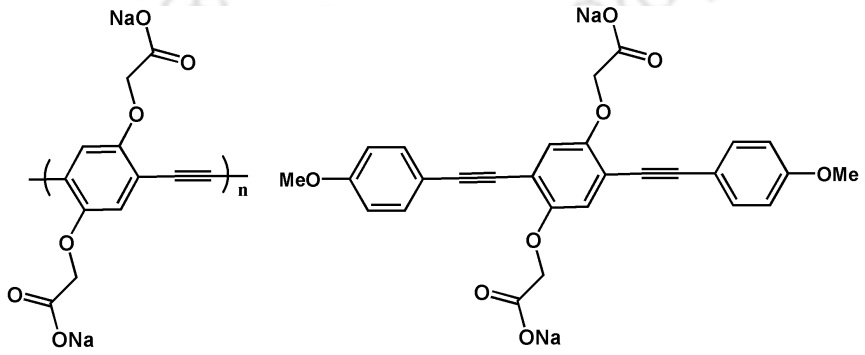

Figure 1.5 Structure of anionic polymer **1** and model compound **2** reported by Bunz *et al.* for the detection of Pb^{2+} ions.

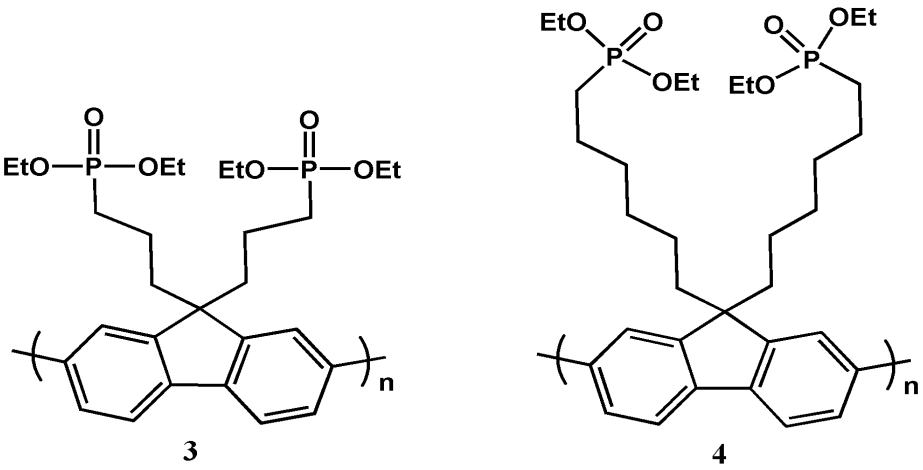

Figure 1.6 Structure of polyfluorene derivatives **3** and **4** reported by Wang *et al.* for the detection of Fe^{3+} ions.

In 2005, Wang and co−workers[17] reported two new derivatives of poly(fluorene) **3** and **4** (Figure 1.6) as synthesized *via* Yamamoto polycondensation method. Both polymers **3** and **4** were incorporated with phosphonate groups along the side chains that act as receptor sites with variable number of carbon. These polymers displayed an amplified fluorescence quenching by Fe^{3+} ions in dichloromethane solutions while other metal ions (Li^+, Na^+, K^+, Mg^{2+}, Ca^{2+}, Sr^{2+}, Cd^{2+}, Mn^{2+}, Fe^{2+}, Cu^{2+}, Co^{2+}, Ni^{2+}, Ag^+, Zn^{2+} and Pb^{2+}) did not significantly affect the absorption/emission spectra of these polymers. The quenching efficiency was found to be strongly dependent on the length of spacer alkyl chains. The quenching constant value (K_{sv}) was reduced by the factor of 2 on increasing the number of carbon in alkyl spacers from three (**3**) to six (**4**). Similarly, the quenching efficiency was reduced in ethanol solution by 1 order of magnitude due to competitive binding of phosphonate groups with solvent. When the sensing experiments of **3** and **4** were performed in THF solution, the quenched fluorescence was recovered after the addition of ammonia solution (14 M) which indicates that these polymers can act as reversible chemosensors for Fe^{3+} ions.

In 2011, Iyer[18] *et al.* reported a highly water soluble anionic poly(fluorene) **5** (Figure 1.7), synthesized by Suzuki copolymerization technique. The polymer **5** was incorporated with two sulphate groups on the side chains that provide solubility to the polymer in aqueous media (100 mg/mL) and also facilitate the selective and sensitive detection of Fe^{3+} ions under physiological conditions. The polymer **5** displayed remarkable fluorescence quenching ($K_{sv} = 1.98 \times 10^6\ M^{-1}$) of ~97% after interaction with Fe^{3+} ions at physiological pH, whereas several other interfering metal ions (Mn^{2+}, Mn^{3+}, Al^+, Mg^{2+}, Ca^{2+}, Fe^{2+}, Fe^+,

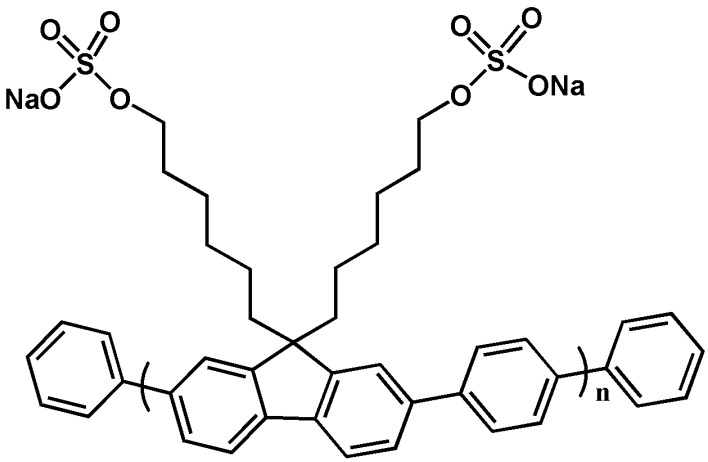

5

Figure 1.7 Structure of anionic poly(fluorene) **5** reported by Iyer *et al.* for the detection of Fe^{3+} and phosphate ions.

Co^{2+}, Ni^{2+}, Cu^{2+}, Zn^{2+} and Cd^{2+}) did not affect the emission of **5** significantly. Furthermore, **5**–Fe^{3+} complex was employed as "turn–on" fluorometric assay for inorganic phosphate (Pi), since emission of **5** was ~95% recovered after introducing Pi. Several other common anions *viz.* sulfide, acetate, sulfate, chloride, carbonate, thiosulfate, nitrate, cyanate, thiocyanate, and dicyanamide did not displayed significant fluorescence enhancement with **5**–Fe^{3+} complex. However, fluorescence recovery with other phosphates like PPi, ATP, ADP and AMP was found to be substantial but very slow (2–8 h incubation). Using **5**–Fe^{3+} assay, the concentration of Pi was also monitored in a competing biological medium like blood serum that validates potential of this rapid and label free system for clinical application.

In 2012, Iyer[19] *et al.* reported another conjugated polymer **6** (Figure 1.8), a derivative of poly(*p*–phenylene), synthesized by simple and economical method of oxidative polymerization followed by post functionalization with imidazole. Sensing studies were performed in 4:1 THF/water mixture, considering environmental conditions and insolubility of **6** in 100% aqueous media. This neutral polymer **6** displayed excellent fluorescence quenching of ~97% exclusively with Cu^{2+} ions with K_{sv} value as high as 3.03×10^5 M^{-1}. Interestingly, control studies with other common metal ions (Fe^{2+}, Zn^{2+}, Mn^{2+}, Fe^{3+}, Ca^{2+}, Hg^{2+}, Ni^{2+}, Pb^{2+} and alkali metals) indicate the selectivity of probe exclusively towards Cu^{2+} ions, since it is well–known that imidazole groups attached onto the side chains of polymer act as specific recognition site for Cu^{2+} ions. Based on the displacement technique, **6**–Cu^{2+} complex was also employed as "turn–on" fluorescent

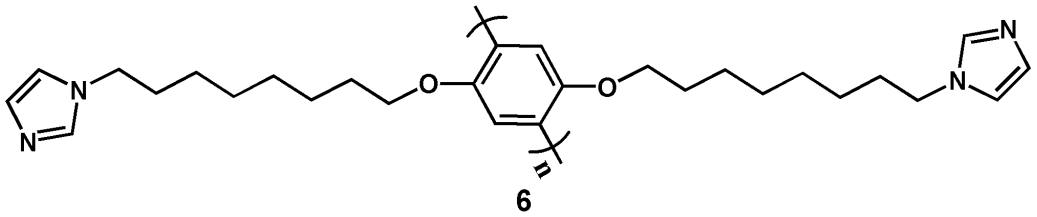

6

Figure 1.8 Structure of neutral poly(*p*–phenylene) **6** reported by Iyer *et al.* for the detection of Cu^{2+} and fluoride ions.

probe for the sensitive and selective detection of fluoride (F^-) ions in natural water systems. Finally, sensing studies were extended on solid state platform using simple TLC plate and membrane by blending 1% of probe with polystyrene that validates the potential of this system for real time and on–site detection of these analytes at ppb levels from natural water systems.

In 2003, Leclerc's group[20] has developed a new water soluble cationic polythiophene derivative **7** (Figure 1.9) *via* oxidative polymerization in chloroform using $FeCl_3$ as oxidizing agent. The aqueous solution of cationic polymer **7** displayed significant fluorescence quenching as well as change in the color from yellow to red–violet on the addition of iodide (I^-) ions. Interference with several other anions (CO_3^{2-}, HCO_3^-, $H_2PO_4^-$, PO_4^{2-}, F^-, Cl^-, Br^-, CH_3COO^-, $EDTA^{4-}$, SO_4^{2-} and $(C_6H_5)_4B^-$) was found negligible. Such a remarkable selectivity is attributed to the exclusive ability of iodide to promote aggregation and planarization of polymer chains *via* electrostatic attraction that was not observed by other anions.

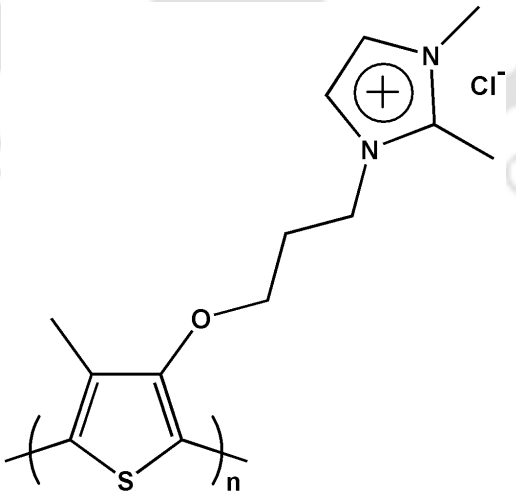

7

Figure 1.9 Structure of water soluble cationic polythiophene **7** reported by Leclerc *et al.* for the colorimetric and fluorometric detection of iodide ions.

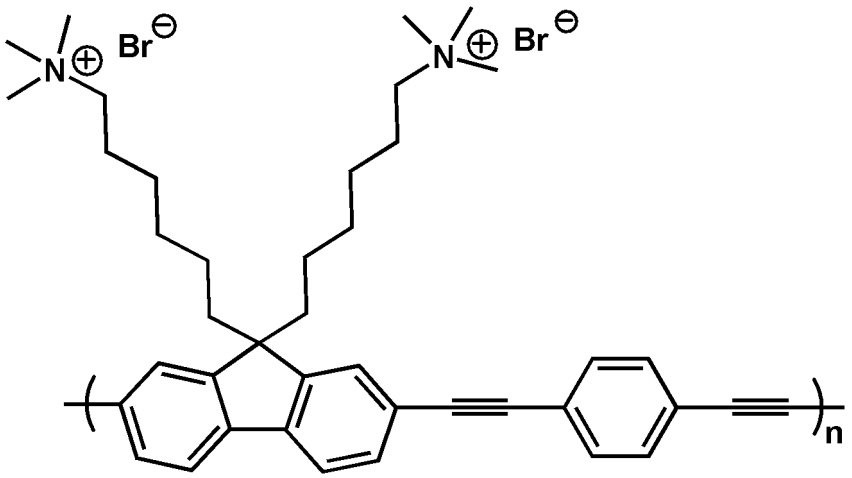

8

Figure 1.10 Structure of cationic polymer **8** reported by Li *et al.* for the detection of citrate and Al^{3+} ions.

In 2013, Li and co–workers[21] reported a cationic conjugated polymer **8** (Figure 1.10) that contains fluorene units in the PPE–like structure. The polymer **8** exhibited strong aggregation in the presence of sodium citrate and resulted in amplified fluorescence self–quenching ($K_{sv} = 2.66 \times 10^5\ M^{-1}$) *via* π– π stacking of the polymer chains. Among various other anions (sodium tartrate, sodium succinate, sodium benzoate, sodium lactate, sodium oxalate, sodium malate etc.), only citrate was found to be the most efficient quenching analyte. Since, Al^{3+} ions can selectively chelate sodium citrate, an assay was developed for the selective and sensitive detection of Al^{3+} using the citrate–induced aggregation properties of **8**. The formation of Al^{3+}–citrate complexes limited the quenching effect *via* disaggregation; subsequently resulting in the recovery of fluorescence. Other metal ions (Mn^{2+}, Mg^{2+}, Fe^{2+}, Fe^{3+}, Cu^{2+}, Co^{2+}, Hg^{2+}, Ag^{+} and Zn^{2+}) except Cr^{3+}, Ga^{3+} and Pb^{2+} were found to have insignificant effect on the fluorescence recovery of **8** owing to their weak interaction with citrate.

1.5.2 Detection of nitroexplosives

In 2013, Dichtel and co–workers[22] synthesized a cross–linked network (Figure 1.11) of CP **9** *via* acyclic dienemetathesis (ADMET) polymerization technique. Due to strong scattering of light, the powdered form of polymer **9** was unsuitable for detecting explosives *via* fluorescence quenching, hence, drop casted or spin coated films of **9** on fused SiO_2 substrates were employed for sensing purposes. The fluorescence of the fabricated film was quenched by the traces of RDX introduced from solution or vapor

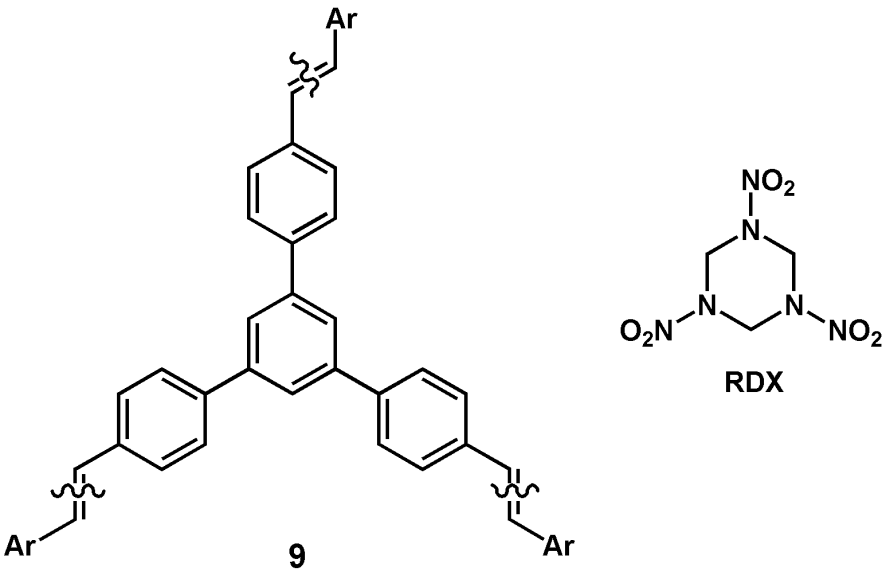

Figure 1.11 Structure of conjugated polymer network **9** reported by Dichtel *et al.* for the detection of RDX.

phase. The sensing response was strongly dependent on the film's growth time and displayed enhanced quenching as a function of time. However, the polymer network was not very selective and also showed some response towards TNT and PETN.

In 2001, Schanze[23] *et al.* reported a new derivative of polyacetylene **10 (**Figure 1.12) having a molecular weight as high as 293000. The polymer **10** gives emission maximum at 520 nm with a high quantum yield ($\phi = 0.25$) and a shorter lifetime (50 ps) in toluene. Upon casting the polymer into thin films, the emission maximum shifts slightly to 533 nm. This is attributed to the weak aggregation of **10** in the solid state due to rigidity in backbone and bulky phenyl side groups that restricts the inter–chain stacking and self–quenching of the fluorescence. This unique structure produces a high fractional free volume that imparts permeability to the analyte vapors to diffuse rapidly into the polymer. The fluorescence of the film was significantly quenched on exposing vapors of different nitroaromatics (1,4–dinitrotoluene, 2,6–dinitrotoluene, 1,3–dinitrobenzene and 4–nitrotoluene) ranging from ppm to ppb levels in air. The signal response time of the film increases with increasing vapor pressure of nitroaromatics and decreasing the thickness of the film. The quenching is attributed to the formation of charge–transfer complexes between the electron–rich polymer **10** and electron–deficient nitroaromatics. Interestingly, the films can be recycled, since the fluorescence intensity of the exposed films were recovered after allowing it to stand in air or on heating.

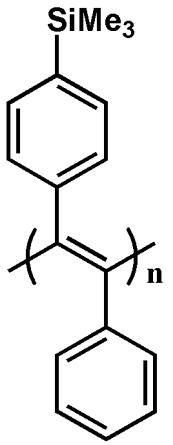

10

Figure 1.12 Structure of conjugated polymer network **9** reported by Schanze *et al.* for the detection of nitroexplosives.

In 2014, Wang and co–workers[24] reported a new conjugated polymer **11 (**Figure 1.13) comprising pentiptycene and aggregation induced emission (AIE) active tetraphenylethene (TPE) units in the backbone linked by acetylene. This neutral polymer **11** was employed for the direct detection of nitroexplosives both in solution as well in vapor mode. The polymer **11** displayed remarkable fluorescence quenching of ~98% towards picric acid (PA) at concentration of 4.7 μM in 9:1 water/THF mixture, where TPE units remain in highly emissive aggregated state. The sensing behavior is attributed to the Lewis acid–base interaction between electron–rich polymer **11** and electron–

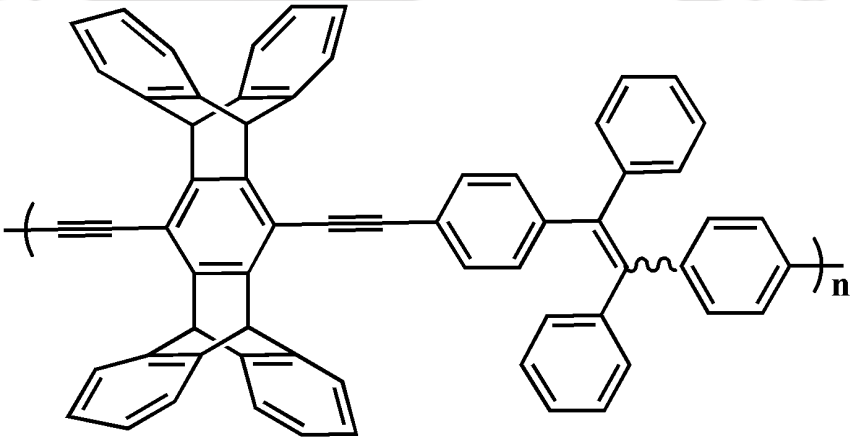

11

Figure 1.13 Structure of AIE active conjugated polymer **11** reported by Wang *et al.* for the detection of PA.

deficient nitroexplosive PA. There was also a possibility of photoinduced electron transfer (PET) from the lower unoccupied molecular orbital (LUMO) of **11** nanoaggregates to LUMO of PA as studied by cyclic voltammetry studies. For achieving vapor mode detection, fluorescent films of **11** with various thicknesses were fabricated and used. Thin film (4 nm) of **11** displayed reduction in the emission intensity by ~48% after exposure of DNT vapors for 10 s which was further reduced to 97% on exposure till 300 s. Thicker film (75 nm) of **11** displayed considerably less quenching response towards DNT vapors. These results indicate that polymer **11** is very efficient for direct detection of nitroexplosives in both solution as well as vapor phase at ppb levels without the need for any further film modifications.

In 2015, Cao[25] *et al.* reported the synthesis of two new porous luminescent covalent–organic polymers (COP) **12** and **13** (Figure 1.14) *via* nickel–catalyzed Yamamoto–type Ullmann cross–coupling reaction. The blue emitting polymers **12** and **13** displayed fluorescence quenching behavior towards various nitroaromatic explosives *viz.* TNT, PA, DNT, NB and *m*–DNB in the solution of methanol. The order of quenching was found to be PA > TNT > DNT > *m*–DNB > NB for both the polymers. The quenching constant (K_{sv}) value of **12** for PA (8.3×10^4 M^{-1}) was found to be ~200 times greater than other nitroaromatics, while polymer **13** exhibit K_{sv} of 2.6×10^5 M^{-1} which is ~100 times greater than other analytes, respectively. The disappearance of blue emission of **12** and **13** was also clearly visible under UV–light upon the addition of PA solution. The order of quenching is attributed to the ease of PET from LUMO of polymers to the LUMO of nitroaromatics. High sensitivity of **13** towards PA compared to **12** is attributed to the higher LUMO level in the former. High sensitivity of these polymers for nitoraromatic explosives (about 1 ppm) and remarkable selectivity towards PA indicates that COPs can be employed as promising luminescent probes for the detection of nitroexplosives.

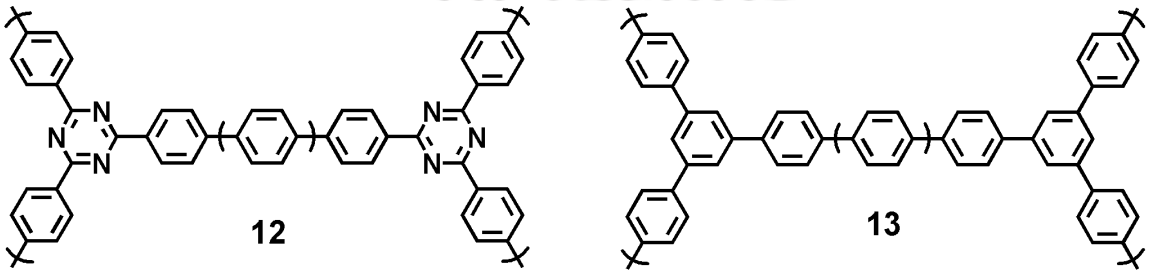

Figure 1.14 Structure of covalent–organic polymers (COPs) **12** and **13** reported by Cao *et al.* for the selective detection of PA.

1.5.3 Detection of biomolecules

In 2004, Bazan and co−workers[26] synthesized a multipurpose cationic conjugated polymer **14** (Figure 1.15) using Suzuki–coupling copolymerization technique by introducing 5% 2,1,3−benzothiadiazole (BT) units into cationic poly(fluorene−*co*−phenylene) to obtain two distinct emission colors from a single polymer chain. The cationic polymer **14** interacts with oppositely charged DNA molecule in aqueous solution, resulting in aggregation of polymer chains. Such inter–polymer interactions lead to increase in the local concentration of benzothiadiazole (BT) units (responsible for FRET) and inter−chain contacts that subsequently improve electronic coupling between the optical partners. This ultimately facilitates the energy transfer process from the fluorene−phenylene segments to BT units, thus enabling the change in emission color of solution from blue−to−green that aided in the determination of DNA concentration. Furthermore, the authors demonstrated that polymer **14** could also be employed as a three−color DNA assay using a PNA−C* strand. Depending upon the content of solution, three different emission colors could be obtained i.e. (i) blue (in the absence of DNA), (ii) green (in the presence of non−complementary ssDNA) and (iii) red (in the presence of complementary ssDNA). Taking advantage of the signal amplification effect of CPs, fine−tuning of electrostatic and optical events leads to multicolor biosensing assay.

In 2013, Iyer[27] *et al.* developed an assay consisting of Fe^{3+} bound anionic conjugated polymer **5** for the continuous and real time detection of acid phosphatase (ACP) enzyme (Figure 1.16) under acidic conditions at very low nanomolar levels. The widely used ACP substrate *p*−nitrophenyl phosphate (*p*−NPP) was ineffective towards the dequenching of

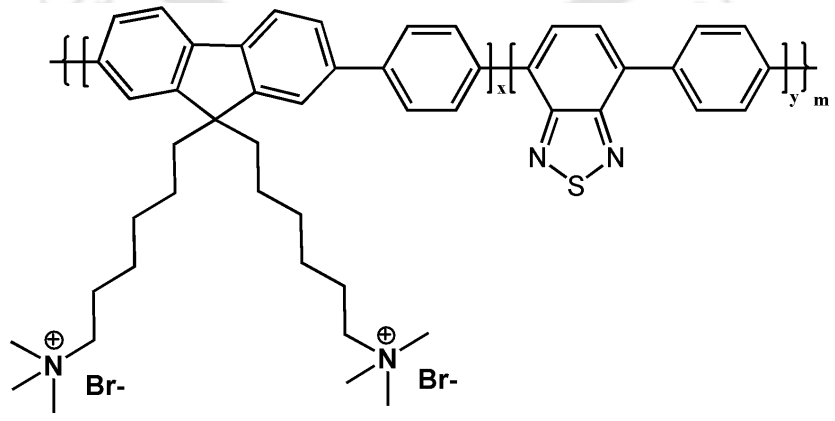

14

Figure 1.15 Structure of cationic conjugated polymer **14** reported by Bazan *et al.* for the detection of DNA.

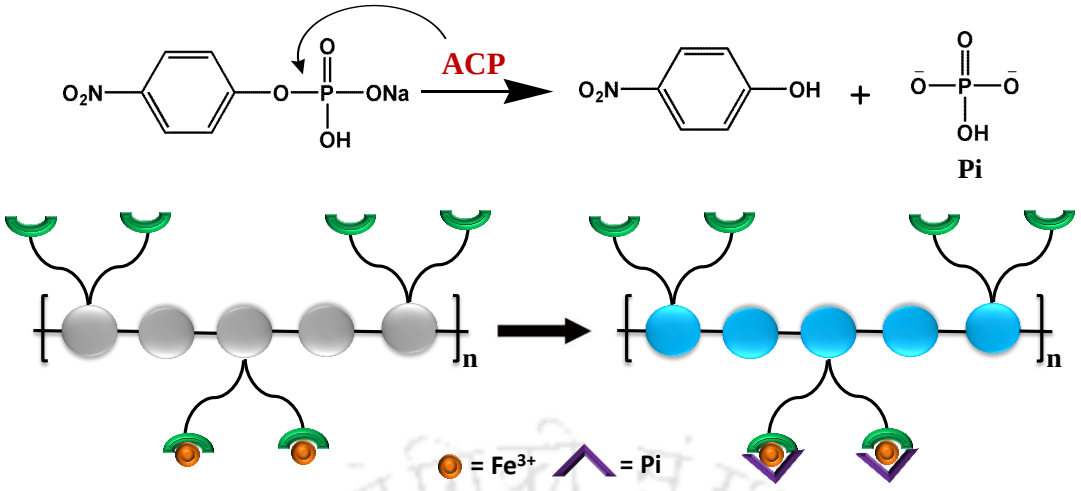

Figure 1.16 An assay for the continuous and real time detection of ACP using anionic conjugated polyfluorene **5** reported by Iyer *et al.*

5–Fe^{3+} fluorescence even after 8 h incubation at pH 6.0 in 15 mM Tris–HCl buffer. The system was then utilized for the hydrolysis of substrate *p*–NPP employing ACP enzyme which indicated that a very low quantity (in nanomolar regime) of ACP was adequate to generate significant fluorometric changes during the enzymatic hydrolysis. In a control experiment, the fluorescence intensity of **5**–Fe^{3+} system was also monitored after introducing ACP and the results demonstrated that enzyme itself did not affect the emission of **5**. Enzyme catalyzed hydrolysis of *p*–NPP as a function of time and with variable concentration of ACP confirmed the feasibility of **5**–Fe^{3+} system as continuous and real time assay for ACP activity.

In 2014, Lee[28] and his co–workers reported a color tunable conjugated polyelectrolyte **15** (Figure 1.17) for the highly sensitive and selective detection of serine protease thrombin. The water soluble polymer **15** exhibits unique color tunable property from blue (λ_{em} = 420 nm) to red emission (λ_{em} = 653 nm) *via* aggregation in solution state. Protein fibrinogen was first introduced into the solution of **15** in 20 mM HEPES buffer at pH 7.4 that did not instigate strong aggregation of polymer chains due to weak hydrophobic interaction between negatively charged polyelectrolyte and fibrinogen. On adding thrombin to the same solution, the blue–to–red color transformation occurred due to the formation of water insoluble fibrin clot from fibrinogen that aggregates the polyelectrolyte *via* hydrophobic as well as electrostatic interaction. The detection limit calculated for thrombin was found to be 1.75×10^{-10} M signifying the practicability of this system for real sample analysis. To demonstrate the selectivity of this system for thrombin, various

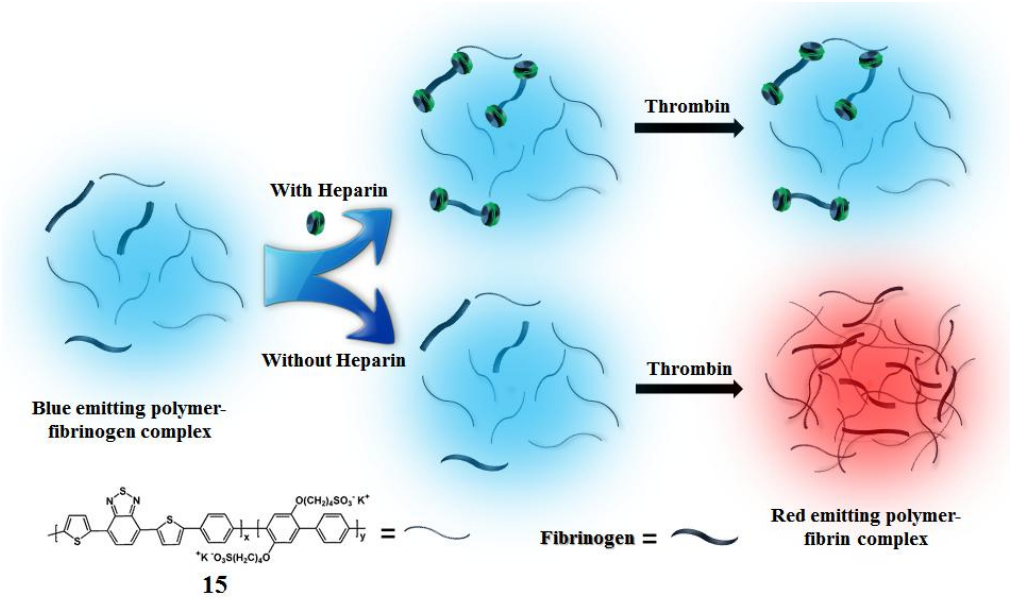

Figure 1.17 An assay for the detection of thrombin and implementation of logic gate in the presence and absence of heparin using anionic conjugated polymer **15** reported by Lee *et al.* Reproduced from Ref. 28 with permission from The Royal Society of Chemistry.

other enzymes *viz.* trypsin, pepsin and glucose oxidase (GO_x) were checked and found ineffective. Moreover, the influence of heparin (inhibitor) on the enzymatic activity of thrombin in this system was also investigated. It was observed that thrombin could not hydrolyze fibrinogen when heparin is present in the system, hence prevented the aggregation process and subsequently the change in the emission color from blue to red. Finally, a combined logic gate was implemented and realized taking fibrinogen, thrombin and heparin as inputs and red emission enhancement of **15** as optical readout signal.

In 2016, Iyet[29] *et al.* reported another water soluble polyfluorene **16** (Figure 1.18) for the detection of spermine which is considered as an excellent biomarker for early cancer diagnosis. The polymer **16** displayed significant changes in its photophysical properties after interacting with most widely used anionic surfactants *viz.* SDS and SDBS *via* electrostatic as well as hydrophobic interactions in aqueous media. The emission peak of polymer **16** at 415 nm was almost quenched on addition of SDS/SDBS with the enhancement of new peak at 545 nm due to an efficient FRET from the fluorine segments to benzothiadiazole units induced by surfactant induced aggregation of polymer chains. The change in color of the solution from blue to yellowish green assisted in naked−eye detection of SDS/SDBS in aqueous media. The detection limit calculated for SDS and

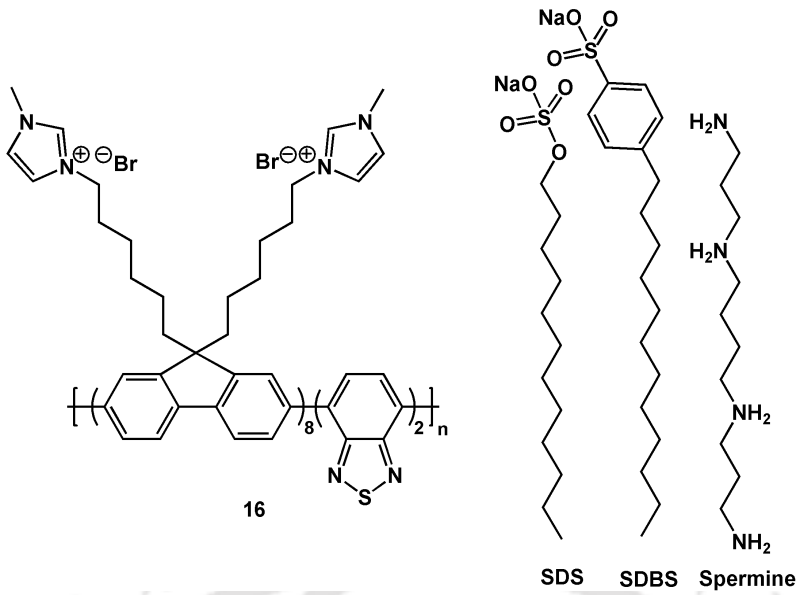

Figure 1.18 Structure of color tunable cationic conjugated polymer **16** reported by Iyer *et al.* for the detection of surfactants SDS/SDBS and biogenic amine spermine.

SDBS was found to be as low as 34 ppb and 45 ppb, respectively. Moreover, the polymer−surfactant complex assembly is utilized for the sensitive detection of spermine in urinary samples at very low ppb levels which indicates the potential of the system in early cancer diagnosis.

Similarly several other CPEs have also been reported for the detection of various important biomolecules *viz.* pyrophosphate[30], phospholipase C[31], protease[32], alkaline phosphatase[33], peptidase[34] etc.

1.6 Objective and conclusion of the thesis work

The main focus of the thesis work was to design and develop fluorescent sensors based on CPs for the highly selective and sensitive detection of environmental and biological important analytes with the aim to overcome the challenges and drawbacks arising in the existing sensing systems. Among various CPs, poly(*p*−phenylene) (PPP) was chosen for sensing studies due to its ease of synthesis, low−cost, good solubility, high quantum yield and excellent film forming ability. The main objective and conclusion for each work is described below−

- Mercury poisoning remains one of the foremost threat to human as well as marine lives due to which several agencies like WHO and US−EPA imposed certain regulations and permissibility limit (10 nM) for its contamination in water. Most of the existing sensors (including conjugated polymer based probes) for mercury

displayed fluorescence quenching behavior and low sensitivity. Chapter II described the synthesis of a neutral conjugated polymer PPT and its application in the colorimetric/fluorometric detection of iodide and mercury in aqueous environment, both in solution state as well as on solid platform with the detection limit for mercury as low as 2.1 nM.

- SDBS and SDS are most common anionic surfactants that are indispensable in detergent industry, emulsification, lubrication and catalysis. Owing to their versatile applications, it has become necessary to determine their presence in pharmaceutical/food formulations, waste−water treatment plants, environment and biological fluids, since they are regarded as "emerging pollutants". Another critical problem associated with these surfactants is their extensive misuse as an adulterant and masking agents along with abusive and performance enhancing drugs to evade detection such as doping tests. Chapter III discussed the synthesis of a new water soluble conjugated polymer PMI and its application in the detection and discrimination of widely used anionic surfactants SDS/SDBS in the natural water systems. Furthermore, this chapter also discussed about the practicability of polymer PMI in illicit drug analysis that has not previously been realized with any synthetic material.

- Picric acid (PA) is a stronger explosive and serious environmental pollutant generated from various industries. Owing to its high solubility in water, it can easily contaminate soil and groundwater and is liable for acute health effects. Development of highly specific and sensitive probe for PA detection remains a challenging task for the investigators due to the absence of any suitable receptor for PA and interference from other electron deficient nitroexplosives. Chapter IV highlighted the application of cationic polymer PMI in the detection of potent explosive and highly water soluble pollutant PA both in solution as well as solid phase with the detection limit reaching ppt levels for the first time using conjugated polymer. The developed method is simple, portable and cost–effective in order to prevent environmental contamination and terrorist threats rapidly under very realistic conditions.

- Flavins *viz.* riboflavin (RF, Vitamin B_2), flavin mononucleotide (FMN) and flavin adenine dinucleotide (FAD) represent an important class of biomolecules ubiquitously found in living systems that are vital for numerous cellular activities inside the body. B_2 hypervitaminosis in the body is a matter of concern, since RF has unique ability to react with light, resulting in adverse cellular effects including the generation of toxic peroxides as well as riboflavin–tryptophan photo adduct that is prone to impairment of cells and liver. Such tendency of RF is concerning patients, infants who are fed intravenously and athletes engaged in various sports activities that usually takes vitamin supplements. Chapter V discussed the practicability of polymer PMI in monitoring the elevated levels of flavins in biological fluids like serum which will be helpful in minimizing the hazards of flavin–induced radical formation in the humans. Furthermore, the PMI based system was employed to recognize and discriminate all the three flavins in biosystems with the advantage of exterminating environmental effects and possible applications in the clinical valuation of the diseases related to flavins and examining metabolic processes.

References

(1) Shirakawa, H.; Louis, E. J.; MacDiarmid, A. G.; Chiang, C. K.; Heeger, A. J. *J. Chem. Soc., Chem. Commun.* **1977**, 578.

(2) Kraft, A.; Grimsdale, A. C.; Holmes, A. B. *Angew. Chem. Int. Ed*. **1998**, *37*, 402.

(3) Friend, R. H.; Gymer, R. W.; Holmes, A. B.; Burroughes, J. H.; Marks, R. N.; Taliani, C.; Bradley, D. D. C.; Dos Sontos, D. A.; Bredas, J. L.; Logdlund, M.; Salaneck, W. R. *Nature* **1999**, *397*, 121.

(4) Bunz, U. H. F. *Chem. Rev*. **2000**, *100*, 1605.

(5) Gong, X.; Matthew, R. R.; Ostrowski, J. C.; Moses, D.; Bazan, G. C.; Heeger, A. J. *Adv. Mater*. **2002**, *14*, 581.

(6) Yu, G.; Gao, J.; Hummelen, J. C.; Wudl, F.; Heeger, A. J. *Science* **1995**, *270*, 1789.

(7) McQuade, D. T.; Pullen, A. E.; Swager, T. M. *Chem. Rev*. **2000**, *100*, 2537.

(8) Zhu, C.; Liu, L.; Yang, Q.; Lv, F.; Wang, S. *Chem. Rev.* **2012,** *112*, 4687.

(9) Liang, J.; Li, K.; Liu, B. *Chem. Sci.* **2013**, *4*, 1377.

(10) Rochat, S.; Swager, T. M. *ACS Appl. Mater. Interfaces* **2013**, *5*, 4488.

(11) Kim, H. N.; Guo, Z.; Zhu, W.; Yoon, J.; Tian, H. *Chem. Soc. Rev.* **2011**, *40*, 79.

(12) Thomas, S. W.; Joly, G. D.; Swager, T. M. *Chem. Rev.* **2007**, *107*, 1339.

(13) Lee, K.; Povlich, L. K.; Kim, J. *Analyst* **2010**, *135*, 2179.

(14) Zhou, Q.; Swager, T. M. *J. Am. Chem. Soc.* **1995**, *117*, 12593.

(15) Kim, I.–B.; Dunkhorst, A.; Gilbert, J.; Bunz, U. H. F. *Macromolecules* **2005**, *38*, 4560.

(16) Kim, I.–B.; Bunz, U. H. F. *J. Am. Chem. Soc.*, **2006**, 128, 2818.

(17) Zhou, G.; Qian, G.; Ma, L.; Cheng, Y.; Xie, Z.; Wang, L.; Jing, X.; Wang, F. *Macromolecules* **2005**, *38*, 5416.

(18) Dwivedi, A. K.; Saikia, G.; Iyer, P. K. *J. Mater. Chem.* **2011**, *21*, 2502.

(19) Saikia, G.; Dwivedi, A. K.; Iyer, P. K. *Anal. Methods*, **2012**, *4*, 3180.

(20) Ho, H. A.; Leclerc, M. *J. Am. Chem. Soc.* **2003**, *125*, 4412.

(21) Wang, H.; He, F.; Yan, R.; Wang, X.; Zhu, X.; Li, L. *ACS Appl. Mater. Interfaces* **2013**, *5*, 8254.

(22) Gopalakrishnan, D.; Dichtel, W. R. *J. Am. Chem. Soc.* **2013**, *135*, 8357.

(23) Liu, Y.; Mills, R. C.; Boncella, J. M.; Schanze, K. S. *Langmuir* **2001**, *17*, 7452.

(24) Ghosh, K. R.; Saha, S. K.; Wang, Z. Y. *Polym. Chem.* **2014**, *5*, 5638.

(25) Sang, N.; Zhanb, C.; Cao, D. *J. Mater. Chem. A*, **2015**, *3*, 92.

(26) Liu, B.; Bazan, G. C. *J. Am. Chem. Soc.* **2004**, *126*, 1942.

(27) Dwivedi, A. K.; Iyer, P. K. *Anal. Methods*, **2013**, *5*, 2374.

(28) Kim, D.; Lee, T. S. *Chem. Commun.* **2014**, *50*, 5833.

(29) Malik, A. H.; Hussain, S.; Iyer, P. K. *Anal. Chem.* **2016**, *88*, 7358.

(30) Yang, J.; Acharya, R.; Zhu, X.; Köse, M. E.; Schanze, K. S. *ACS Omega*, **2016**, *1*, 648.

(31) Liu, Y.; Ogawa, K.; Schanze, K. S. *Anal. Chem.*, **2008**, *80*, 150.

(32) Wang, Y.; Zhang, Y.; Liu, B. *Anal. Chem.*, **2010**, *82*, 8604.

(33) Liu, Y.; Schanze, K. S. *Anal. Chem.*, **2008**, *80*, 8605.

(34) An, L.; Tang, Y.; Feng, F.; Hea, F.; Wang, S. *J. Mater. Chem.*, **2007**, *17*, 4147.

Chapter 2

Thiazole-Containing Conjugated Polymer as a Visual and Fluorometric Sensor for Iodide and Mercury

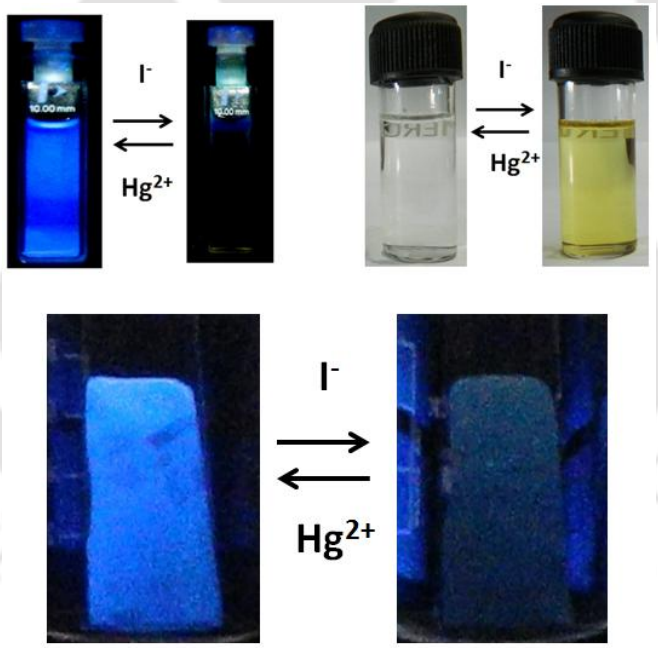

Hussain, S.; De, S.; Iyer, P. K., *ACS Appl. Mater. Interfaces* **2013**, *5*, 2234−2240.

Abstract

A new poly(*p*−phenylene) (PPP) derivative, poly(1,4−bis−(8−(4−phenylthiazole−2−thiol)−octyloxy)−benzene) (PPT) was prepared using a very simple and economical method of oxidative polymerization reaction. This neutral conjugated polymer (CP) PPT was characterized by means of Fourier transform infrared spectroscopy (FT−IR), ^{1}H nuclear magnetic resonance (^{1}H NMR), ultraviolet−visible (UV−Vis) and fluorescence spectroscopy. The CP PPT displayed fluorescence "turn−off/ turn−on" characteristics and colorimetric responses towards I^- and Hg^{2+} in aqueous based media. The UV−Vis and fluorescence spectra of the PPT showed significant shift in λ_{max} *via* the addition of iodide and mercury ions. A colorless PPT solution turned to deep yellow in the presence of iodide ions, which subsequently became colorless upon the addition of mercury ions that was easily detected visually by naked eye. The Stern−Volmer constant (K_{sv}) value obtained for the detection of iodide was found to be 0.13×10^5 M^{-1}, confirming very high sensitivity of polymer PPT for iodide ions. The detection limit calculated for Hg^{2+} was found to be 2.1 nM which is compatible with the WHO and US−EPA maximum permissible limit (10 nM) set for mercury in natural water systems. The detection of both iodide and mercury ions was also possible in solid state by using a membrane film prepared by mixing 1% PPT in polystyrene. This membrane changed its color in the presence of iodide as well as mercury ions. These results confirm that the PPT polymer can be applied for the colorimetric as well as fluorometric sensing of I^- and Hg^{2+} ions in a competent environment in solution, as well as in the solid state, using a membrane film rapidly.

2.1 Introduction

Iodine is an indispensable element in human life and plays a key role in several biological activities, such as neurological and thyroid functions.[1–3] However, its excessive application can cause serious environmental pollution and health disorders.[4] Because of its larger size and weaker basicity than other halides, the binding ability of I^- ions with receptors are the weakest, compared to other halogen ions, with the following binding order–[5–9]

$$F^- > Cl^- > Br^- > I^-$$

Therefore, it remains a challenge to design chemo sensors that can bind iodide selectively in the natural environment.

CPs with extended π−electron system and receptors on the side chain or main chain have been widely employed as organic light−emitting diodes (OLEDs),[10–12] organic thin−film transistors (OFETs), chemical sensors[13,14] and in various photonic and electronic devices.[15,16] High sensitivity of CPs toward a range of analytes is believed to be due to the phenomenon known as "molecular wire effect". Fluorescence is the most common and highly sensitive optical transduction method to observe analyte binding events that usually produces an enhancement, reduction, or wavelength shift in the emission and can be employed to generate a functional sensor.[17] CPs with suitable receptors present a simple and consistent approach to attain selectivity while performing sensing studies or observing changes in absorption and emission spectra.[18–23] CPs that comprise poly(*p*−phenylene)s, poly(*p*−phenylene vinylene)s, polyfluorenes etc. with receptor groups on the side chain or main chain have been successfully used for detecting various chemical and biological species. Many supramolecular systems capable of recognizing and sensing halides and several other negatively charged species have also been developed and studied extensively.[24] However, very few examples using CPs for sensing iodide ions have been reported.[25,26]

According to the survey from the World Health Organization (WHO), iodide deficiency still causes serious public health problems in many countries.[27,28] As a strong nucleophilic reagent, I^- ions are also commonly employed in many important organic reactions. Therefore, it is desirable to detect I^- ions rapidly with high sensitivity and selectivity in either aqueous or non−aqueous media. Among the range of biologically important anions, iodide is of particular interest, because of its essential role in the functioning of thyroid gland. In addition, elemental iodine is used in synthesizing several organic chemicals, in

manufacturing dyes, in medicine (its radioactive isotope), in analytical chemistry and in several other applications.

Among toxic metals, mercury poisoning remains one of the foremost threat to human health and it has caused serious environmental and health problems.[29−31] Severe damage to human central nervous system and endocrine system due to mercury ingestion have been reported.[32−35] Among different forms of mercury, Hg^{2+} is considered as the most common water pollutant owing to its highest solubility in water. In this context, several researchers have focused on the development of colorimetric and/or fluorometric[36−44] probes for Hg^{2+} but most of them suffer from the issue of selectivity, portability, slow signal response time, etc.[45] Few polymer−based chemo sensors for detection of Hg^{2+} have also been reported.[46−55] In all types of detection platforms, it is stressed to selectively detect Hg^{2+} in the presence of other competing metal ions usually found in the environment. Furthermore, most of the existing sensors for Hg^{2+} displayed "turn−off" fluorometric responses due to its quenching nature[56−60] and the development of "turn−on" probe for Hg^{2+} with high sensitivity/selectivity remains a challenging task.

Herein, we report the synthesis and characterization of a new conjugated poly(*p*−phenylene) derivative strapped with 4−phenylthiazole−2−thiol, which can optically and visually detect the presence of iodide and mercury ions over a wide range of other competent ions in an aqueous medium.

2.2 Experimental

2.2.1 Materials and measurements

All reagents and solvents were purchased from commercial sources and were of reagent grade. Ultraviolet−visible light (UV−Vis) and photoluminescence (PL) spectra were recorded on a Perkin−Elmer Model Lambda−25 spectrophotometer and a Varian Cary Eclipse spectrophotometer, respectively. Tetrahydrofuran (THF) was purified by distillation over sodium under a nitrogen atmosphere. ^{1}H NMR (400 MHz) and ^{13}C NMR (100 MHz) spectra were obtained with a Varian−AS400 NMR spectrometer. GPC was recorded with a Waters−2414 instrument (polystyrene calibration). Polystyrene (PS) used for film studies was obtained from Total Petrochemicals, USA and had the following specifications: grade 500b general−purpose PS, M_w = 215010; density = 1.04 g/cm^3; MFI = 14 g/10 min at 200 °C and 5 kg load.

2.2.2 Synthesis of monomer (M1)

Synthesis of 1,4−bis−(8−bromooctyloxy)−benzene was carried out using a previously established procedure from the literature.[61-63] In a 250 mL round−bottomed flask, K_2CO_3 and dry acetone were stirred under inert atmosphere for 30 min at room temperature. To this, hydroquinone (2 g, 18.17 mmol) and 1,8−dibromooctane (19.62 g, 72.6 mmol) was added and stirred continuously for additional 2 days at 60º C. The brown colored solution thus obtained was diluted with acetone and passed through a celite bed to remove excess base. Anhydrous Na_2SO_4 was then added to the solution to remove traces of water and evaporated to obtain a yellow−brown liquid. Excess 1,8−dibromooctane was distilled out under reduced pressure and the crude on further purification by column chromatography (ethyl acetate:hexane, 0.5:9.5) yielded the desired monomer as white solid flakes. Yield: 82%.

^{1}H NMR (400 MHz, $CDCl_3$): δ ppm, 6.89(s), 3.89(t), 3.41(t) 1.89(m), 1.76(m), 1.44(m), 1.35(m). ^{13}C NMR (100 MHz, $CDCl_3$): δ ppm, 153.3, 115.5, 68.7, 42.1, 34.1, 32.9, 29.5, 29.2, 28.8, 28.2, 26.1. GC−MS: m/z = 491.11 (M + 1) (calculated 490.108).

2.2.3 Synthesis of poly(1,4−bis−(8−bromo−octyloxy)−benzene) (PBr)

Polymer was prepared by methods reported earlier.[64,65] The synthesis of PPB was performed as follows. In a 100 mL three−necked round−bottom flask equipped with a nitrogen inlet, anhydrous ferric chloride (0.74 g, 4.57 mmol) was dissolved in 10 mL of nitrobenzene. M1 (1.0 g, 2.03 mmol) dissolved in 10 mL of nitrobenzene was added to the flask using a syringe. The reaction mixture was stirred at room temperature for 36 h, followed by precipitation from methanol. This was stirred for 1 h, centrifuged, and washed repeatedly with methanol. The resulting polymer was dried under reduced pressure to obtain product as a light brown powder. Yield: 70%.

^{1}H NMR (400 MHz, $CDCl_3$): δ ppm, 7.07(b), 3.91(b), 3.36(m) 1.80(b), 1.67(b), 1.37(b), 1.2(b). ^{13}C NMR (100 MHz, $CDCl_3$): δ ppm, 150.2, 115.1, 67.8, 40.1, 33.6, 33.1, 28.9, 28.0, 27.8, 27.2, 26.3. $M_w = 3.52 \times 10^4$; PDI = 1.9 (GPC in THF, polystyrene standard).

2.2.4 Synthesis of PPT

PPB (0.20 g. 0.41 mmol) and 4−phenylthiazole−2−thiol (0.32g, 1.6 mmol) were dissolved in dry THF (5 mL) in the presence of K_2CO_3 (4 eq.). The reaction mixture was kept for reflux under stirring for 12 h. The mixture was then filtered to remove the unreacted base and poured into 50 mL of cold methanol (MeOH), followed by stirring for 1 h to obtain a

yellow precipitate. The obtained solid was dissolved in THF and reprecipitated in methanol (100 mL). The precipitant was then collected, washed with acetone, and dried in a vacuum desiccator to obtain the product. Yield: 72%.

^{1}H NMR ($CDCl_3$, δ, ppm): 7.78(b), 7.41(b), 7.31(b), 7.06(b), 6.90(b), 3.81(b), 3.07(b), 1.76(b), 1.56(b), 1.30(b), 1.25(b). FT−IR (KBr, cm^{-1}): 2930.43, 2853.65, 1467.86, 1261.23, 1099.46, 1027.72, 802.32.

2.2.5 Optical measurements

The absorption measurements and fluorescence titrations of the polymer PPT with different anions and metal cations in aqueous based solution were run by directly adding small aliquots (typically 5 μL) to 3mL of the 4:1 THF/water solution containing 6.6×10^{-6} M PPT in a quartz cuvette (1 cm × 1 cm). After being mixed thoroughly the absorption or fluorescence spectra were recorded at room temperature.

2.2.6 Calculating fluorescence quantum yield changes

Fluorescence quantum yield changes of PPT with iodide was determined using quinine sulfate ($\Phi_r = 0.52$ in 0.1 M H_2SO_4) as standard and it was calculated by the equation;

$$\Phi_s = \Phi_r (A_r F_s / A_s F_r) (\eta_s^2 / \eta_r^2)$$

where, s and r denote the sample and reference, respectively, A is the absorbance, F is the relative integrated fluorescence intensity, and η is the refractive index of the solvent.

2.2.7 PPT film preparation

Ninety nine milligrams (99 mg) of blending polymer (polystyrene in this experiment) and 1 mg CP were taken in a glass vial and dissolved in 2 mL of THF by mixing for 2 h to make a homogeneous mixture. The clear solution was spread onto a smooth glass plate and allowed to dry at room temperature in open air. As the film dried, it was carefully peeled from the glass plate, cut into rectangular shapes, and used for sensor application experiments.

2.2.8 Sensor experiment method

The rectangular film was placed on a small glass plate and kept in a beaker filled with distilled water. Under UV light, the film showed bright blue fluorescence. Dilute I^- and Hg^{2+} solutions were prepared and added to the beaker (drop−wise) and the fluorescence of the film was observed under UV−lamp illumination.

2.3 Results and discussion

2.3.1 Synthesis of poly (1,4−Bis-(8−4−phenylthiazole−2−thiol−octyloxy) −benzene) (PPT) and evaluating the sensing properties

The synthesis of PPT presented in Scheme 2.1, involves mainly room temperature reaction steps without requiring costly metal catalysts/phase−transfer catalysts, while still employing very easy and mild reaction conditions. The 4−phenylthiazole−2−thiol moiety was introduced onto the side chain of PBr by substituting the terminal Br atoms to obtain the desired PPT polymer using a post-polymerization functionalization method in 72% yield. Both the synthesized polymers were characterized by ^{1}H-NMR spectroscopy (See Appendix). The molecular weight of the polymer before 4−phenylthiazole−2−thiol functionalization was reported to be M_w = 3.52 × 10^4, PDI = 1.9 (GPC in THF, polystyrene standard).[66] Thiazoles are one of the important classes of sulfur containing heterocyclic compounds among the many found in living organisms.[67] Due to their several vital biological properties, they are regarded as the main tools in pharmaceutical research.[68−69] Some nitrogen, oxygen and sulphur containing ligands *viz.* carbazole, oxazole, thiazole have also been reported[26,70-71] sensitive to iodide anion.

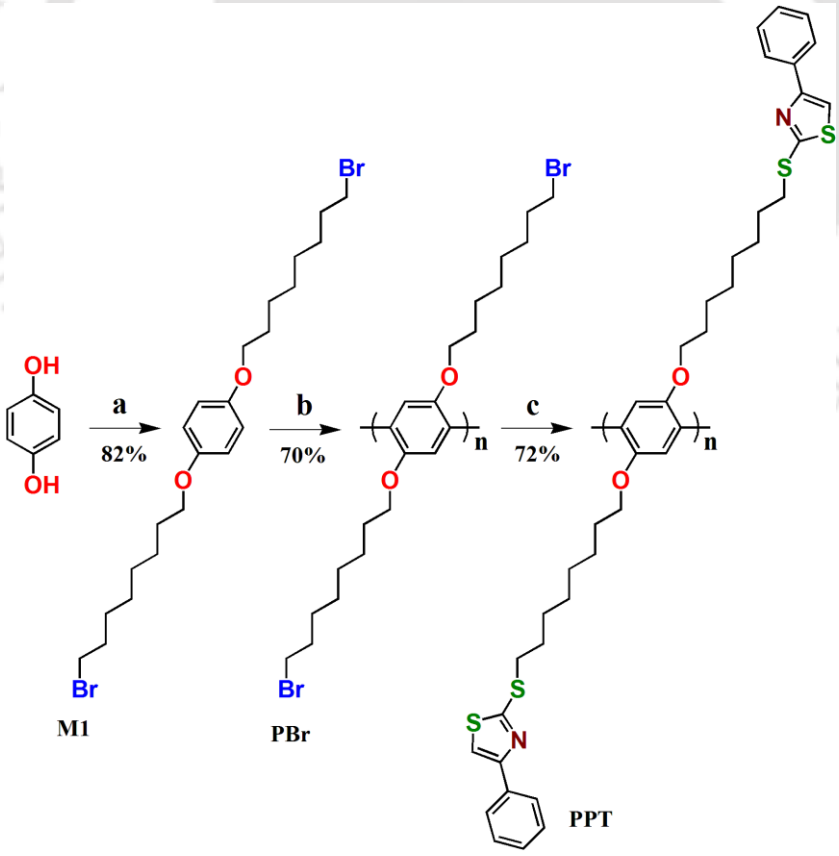

Scheme 2.1 Synthesis of poly(1,4−Bis(8−4−phenylthiazole−2−thiol−octyloxy)−benzene (a) K_2CO_3, dry acetone, 1,8−dibromooctane, 60 °C. (b) $FeCl_3$, nitrobenzene, RT. (c) K_2CO_3, 4−phenylthiazole−2−thiol, THF, reflux, 12 h.

CPs of the type PPT display strong blue luminescence under UV−light that can be visualized in diluted organic solvents. PPT shows absorption maximum at 335 nm and an emission maximum at 402 nm. The fluorescence quenching studies of polymer PPT by I^- ions were initially investigated using UV−lamp (lamp excitation−365 nm), where the disappearance of the blue luminescence in the presence of the I^- ions and, again, the reappearance of the blue color in the presence of Hg^{2+} ions was very clear (Figure 2.1a). The initial colorless solution of the polymer PPT also changes to a yellow color upon the addition of I^-, which subsequently become colorless again on the addition of dilute Hg^{2+} salt solution (Figure 2.1b). Upon the addition of I^-, with increasing time, the intensity of the yellow color increases, whereas, introducing Hg^{2+} in the same solution results in the disappearance of the yellow color. The polymer PPT showed no significant change in color upon the addition of anions (Figures 2.2a), halides (Figures 2.2b) other than I^- and cations (Figures 2.2c) other than Hg^{2+}. The sensing properties of PPT were studied in a THF/water (4:1) solution using aliquots of aqueous solution of tetrabutylammonium salts of anions and the perchlorate metal salts. Interestingly, the polymer PPT detects only I^- among common anions such as fluorides, chlorides, bromides, nitrate, nitrite, thiocyanate, hydrogen phosphate, dihydrogen phosphate, acetate, tetrafluoroborate, etc. The nature of counter cations such as tetrabutylammonium, potassium, etc. does not influence the color change while performing the detection experiments. The effect of pH on PPT solution was also studied. It was observed that pH does not significantly affect the detection ability of PPT and the fluorescence of PPT is retained from pH 5.5 to basic pH. The quenching mechanism can be explained by the formation of weak, transient charge transfer complex *via* "heavy−atom" interaction between the polymer PPT and the iodide ions that leads to an enhancement of the spin−orbit coupling.[72−75]

Figure 2.1 Color of the PPT solution in 4:1 THF/water under (a) UV light (b) naked-eye.

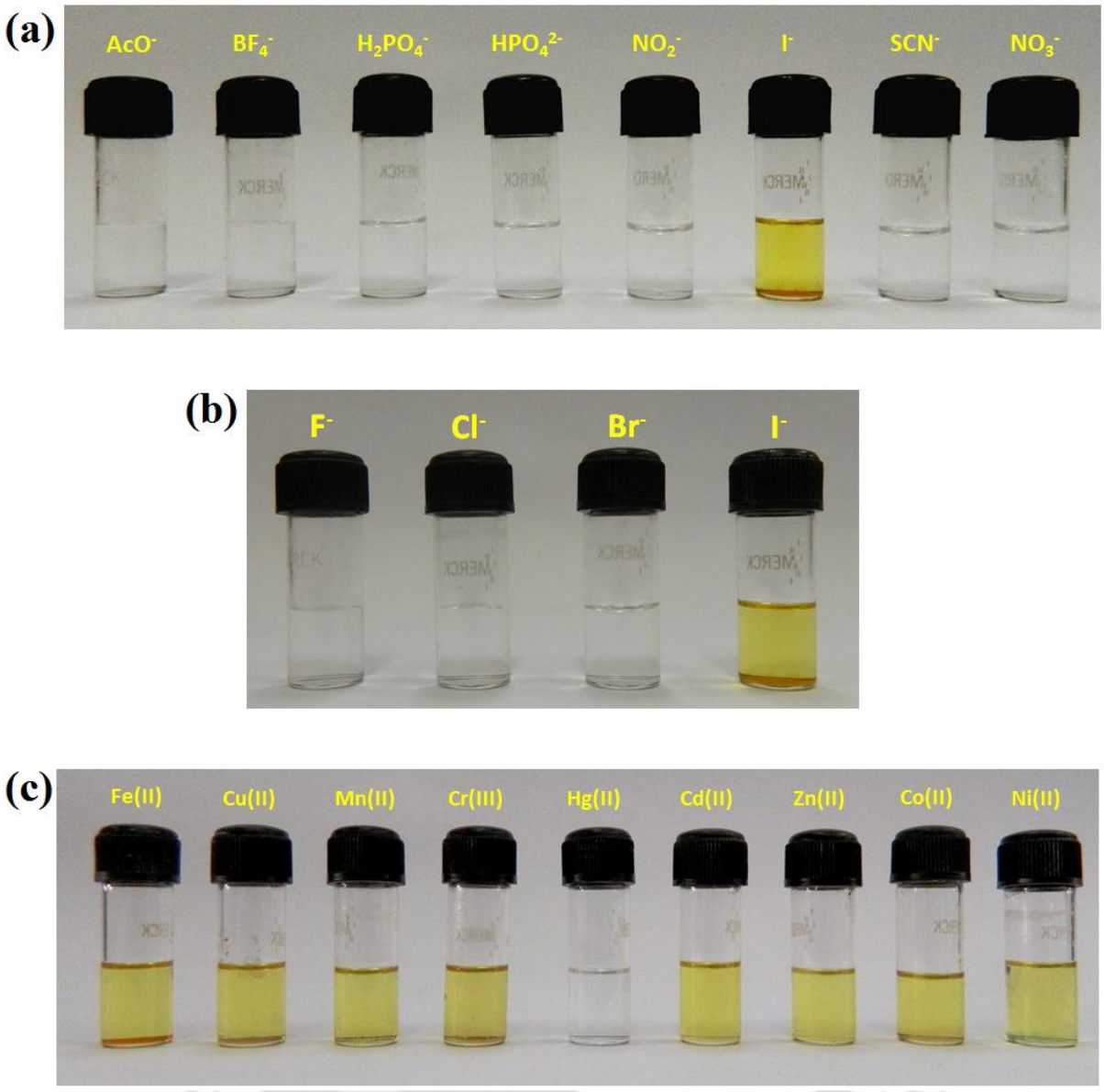

Figure 2.2 Color changes of PPT solution in 4:1 THF/water upon addition of (a) anions and (b) halides; in both panels a and b, the concentration of PPT and anions are 6.6×10^{-6} M and 3.3×10^{-4} M, respectively. (c) Color changes of PPT−I^- solution in 4:1 THF/water upon addition of metal salts in water; in panel c, the concentration of metal salts is 5×10^{-5} M.

The decrease in fluorescence intensity was investigated by adding successive aliquots of aqueous stock solutions of I^- ions (TBAI) to the solution of PPT (6.6×10^{-6} M) in a 4:1 THF/water solution (Figure 2.3). PL quenching of PPT was >96% at a concentration of 1.67×10^{-4} M of I^- ions. A similar experiment was also repeated with KI to verify the counter cation effect and is presented in Appendix as Figure A2.1 Both TBAI and KI displayed nearly same quenching behavior with PPT confirming that I^- is responsible for

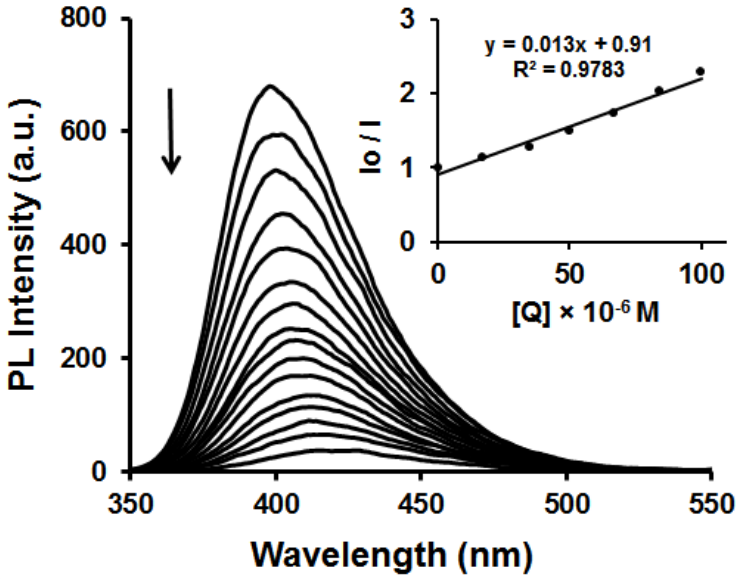

Figure 2.3 Photoluminescence spectra of PPT in a 4:1 THF/water solution with increasing concentration of I^-. Inset shows a Stern−Volmer plot of PPT upon the addition of I^-.

fluorescence quenching rather than the counter cation. The efficiency of quenching was studied by plotting a Stern−Volmer plot[76,77] (I_0/I *vs* [Q], where I_0 is the initial fluorescence intensity of PPT and I is the fluorescence intensity of PPT after the addition of a given concentration of quencher [Q], where [Q] = I^- ion concentration) to obtain a Stern−Volmer constant (K_{sv}). The K_{sv} value calculated from the plot was found to be 0.13 × 10^5 M^{-1} (Inset of Figure 2.3), confirming high sensitivity of PPT towards iodide ions.

The fluorescence quantum yield of polymer PPT was found to be 0.24, which decreases rapidly to 0.0095 with the addition of iodide. To check the selectivity of the system, sensing studies of PPT were than performed with several other anions. Except with I^-, the intensity of PPT was indistinctly affected upon the addition of anions such as F^-, Cl^-, Br^-, NO_2^-, CH_3COO^-, HPO_4^{2-}, $H_2PO_4^-$, BF_4^-, and SCN^- (Figure 2.4).

Titration of I^- ions with PPT was also monitored *via* UV−Vis spectroscopy. The absorption maxima of PPT showed a significant 26 nm red shift (Figure 2.5) upon titration with tetrabutylammonium iodide salts. A similar UV−Vis study of the PPT polymer was done with KI and the results were found comparable (Figure A2.2). The red shift in the absorption and emission maxima can be explained through charge transfer *via* the heavy atom effect between the polymer PPT and the I^- anions, as discussed earlier.[26,72−75] In addition, a new peak was observed developing at 295 nm upon the continuous addition of I^- anions, which may be due to the interaction of the thiazole

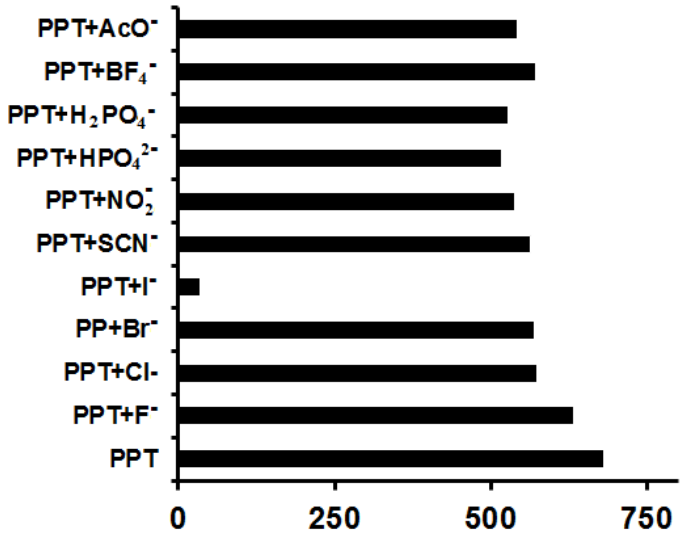

Figure 2.4 Bar diagram depicting effect of various anions on the fluorescence intensity of PPT. Photoluminescence titration of different anions (3.3×10^{-4} M) was performed with PPT (6.6×10^{-6} M) in 4:1, THF/water at room temperature.

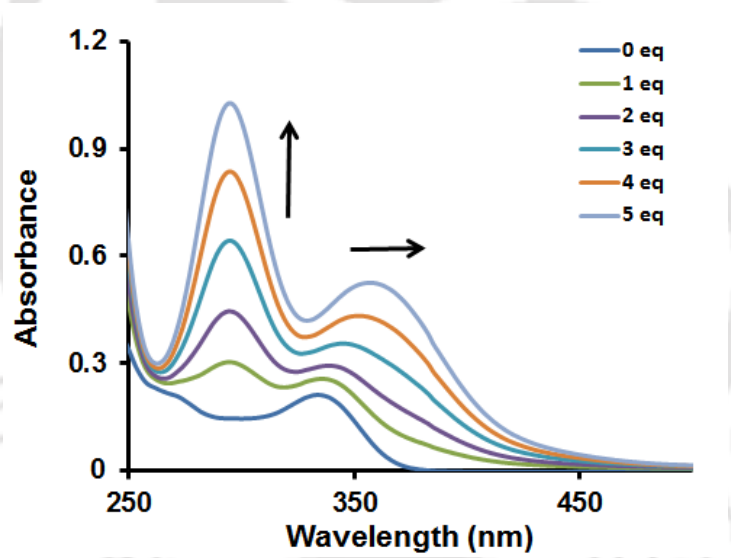

Figure 2.5 UV−Vis titration spectra of PPT in a 4:1 THF/water solution with increasing concentration of I^- (TBAI) solution in water.

moiety with iodide. From these results, it could be concluded that, in this sensory system, the thiazole groups in PPT serve as coordination sites for I^- and facilitates very high fluorescence quenching of >96%. To the best of our knowledge, fluorescence quenching of neutral PPT−type thiazole containing CPs in an aqueous−based environment, as well as a mixture of aqueous and organic-based environments by I^- remains unreported.

We further noticed that the quenched fluorescence of PPT−I^- complex was restored in the presence of an aqueous solution of Hg^{2+} salts (Figure 2.6). Significant color changes that could be both visualized with the naked eye, as well as fluorescent enhancement, occurred at a very low concentration of Hg^{2+} in the presence of other metals salts of cadmium, zinc, iron, etc. The quenched fluorescence intensity of PPT−I^- was ~60% recovered upon the addition of Hg^{2+} in concentrations as low as 8.3×10^{-6} M (Figure 2.7). Titration performed with various other metal ions (Figure 2.8) that are known to compete with Hg^{2+} showed no significant effect on the enhancement of the fluorescence intensity of PPT−I^-. This can be attributed to ultra−strong binding between Hg^{2+} and I^- with very high association constants (8.3×10^{23} for HgI_2 and 6.31×10^{29} for $[HgI_4]^{2-}$). The detection limit (LOD) calculated for Hg^{2+} using the equation 3σ/k, where σ is the

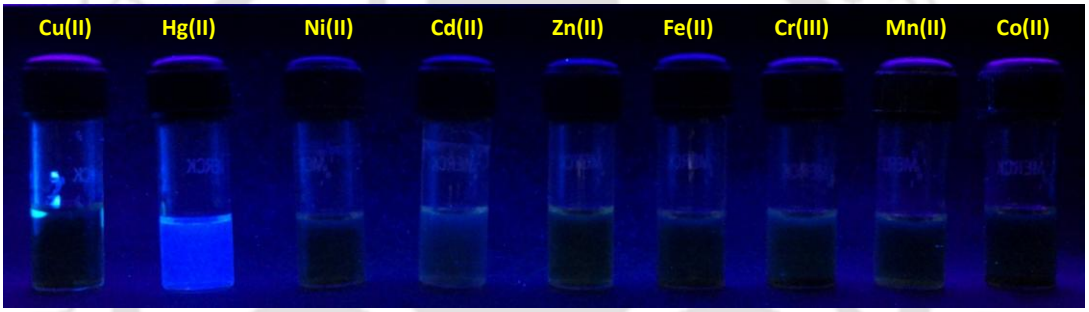

Figure 2.6 Color changes of PPT−I^- solution in a 4:1 THF/water solution upon the addition of metal salts under UV light. The concentration of each metal salt is 5×10^{-5} M.

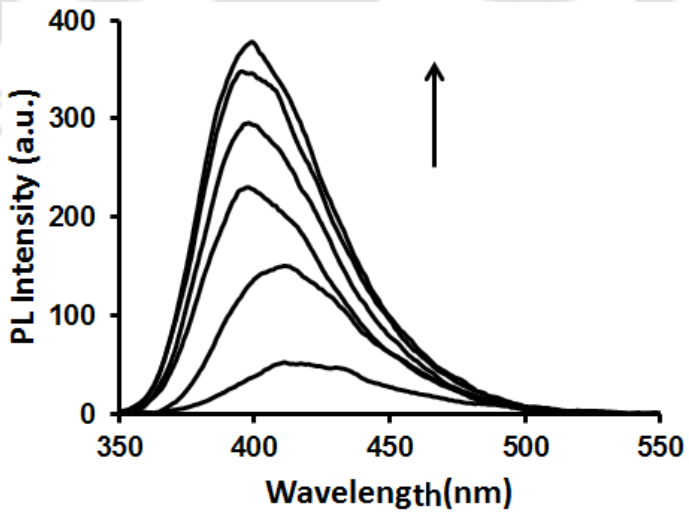

Figure 2.7 Photoluminescence spectra of PPT−I^- in a 4:1 THF/water solution with increasing concentration of Hg^{2+}. Dequenching was ~60% at a concentration of 8.3×10^{-6} M of Hg^{2+}.

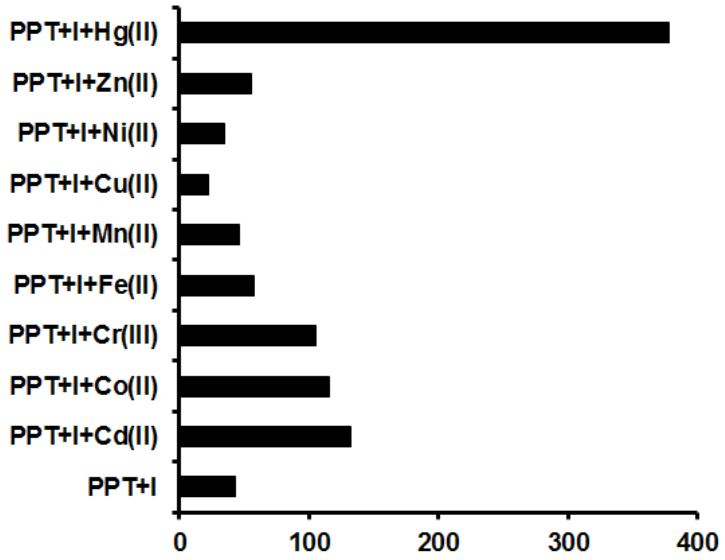

Figure 2.8 Bar diagram depicting the effects of various metal ions (5×10^{-5} M) on the fluorescence intensity of PPT−I^- in a 4:1 THF/water solution at room temperature.

standard deviation in the absence of Hg^{2+} and k represents slope of the plot was found to be 2.1 nM (Figure A2.3) which is compatible with maximum permissible limit (10 nM) set by WHO and US−EPA.

Interaction between the PPT−I^- and Hg^{2+} was also monitored *via* UV−Vis spectroscopy (Figure 2.9). Significant changes in peaks were observed after adding 3 eq. of Hg^{2+} ions. Upon addition of Hg^{2+} ions to the solution of PPT−I^-, the 365 nm absorption peak of PPT−I^- disappeared completely and a new peak was appeared at 260 nm with the clear formation of an isosbestic point at 276 nm. The absorption peak at 295 nm also showed a bathochromic shift of 15 nm. Detection of Hg^{2+} can be explained *via* two probable mechanisms (1) displacement of I^- by Hg^{2+} and (b) formation of new complex between PPT−I^- and Hg^{2+}. Since the initial absorption peak of PPT does not recover after the addition of Hg^{2+} to PPT−I^-, we can assume that a new complex between PPT−I^- with mercury has formed. The red shift in absorbance maximum and appearance of new peak further justified this assumption.

2.3.2 Analysis of real water samples

The real tap water samples were collected and filtered through a 0.2 μm membrane. The water samples were spiked with standard iodide and mercury solutions separately at certain concentrations and then used for sensing purposes. The amounts of iodide and mercury ions in tap water were estimated after preparing a standard calibration curve and

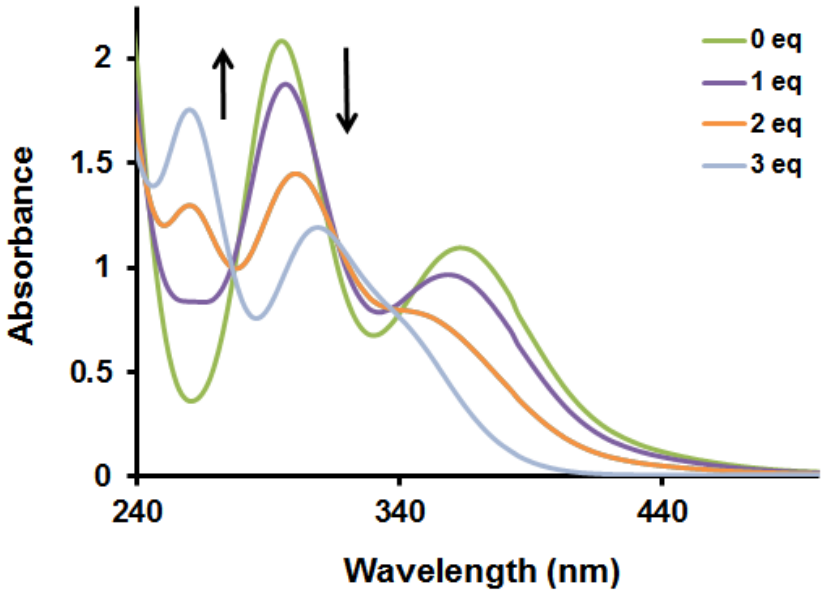

Figure 2.9 UV−Vis titration spectra of PPT−I^- in a 4:1 THF/water solution with increasing concentration of Hg^{2+} in water.

Table 1. Detection of I^- in tap water samples

Tap water samples	I^- added (µm)	I^- found[a] (µm)	Recovery (%)
Sample 1	2.0	1.96	98.0
Sample 2	2.67	2.60	97.4

[a]from calibration curve

Table 2. Detection of Hg^{2+} in tap water samples

Tap water samples	Hg^{2+} added (nM)	Hg^{2+} found[a] (nM)	Recovery (%)
Sample 1	16.7	15.6	93.4
Sample 2	33.0	34.2	103.6

[a]from calibration curve

comparing it with the changes caused in the fluorescence spectra of the polymer PPT upon the addition of these tap water samples (Tables 1 and 2).

2.3.3 Evaluating the sensing properties of PPT in the membrane form

Most of the I^- and Hg^{2+} detection systems are generally solution based which is difficult and sometimes not practical for carrying out analysis at distant places. Hence, to realize practical applications, the fluorescence response of the PPT had to be utilized on a solid

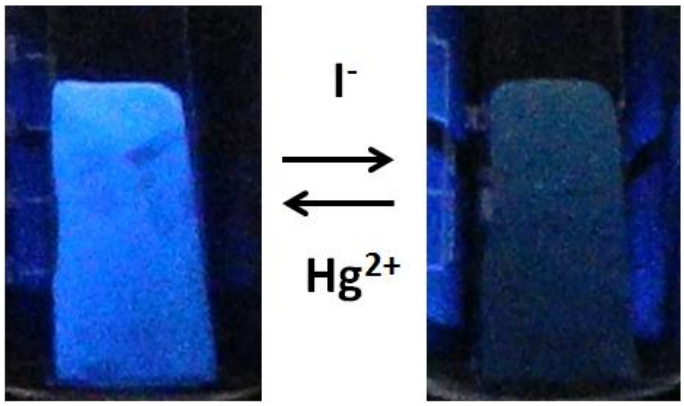

Figure 2.10 A bright blue PS + PPT membrane (left image) under UV light in water loses its fluorescence (right image) upon being dipped in a 3.3×10^{-5} M I^- solution in water. This film regains its fluorescence upon being dipped in a fresh 5×10^{-5} M solution of Hg^{2+}.

support based platform for better mobility. Since CPs can form films on desired substrates or membranes with any other polymer, we utilized these properties to make a handy membrane of PPT with commercial polystyrene and performed membrane based I^- and Hg^{2+} detection in aqueous medium. This technique is energy and cost−effective method if the concentration levels of the pollutants are very low (ca. ppm or sub−ppm). A membrane film was prepared by doping 1% PPT in a polystyrene (PS) solution dissolved in THF (w/w) and cast gently over a glass slide (Figure 2.10). The membrane was peeled off on drying and cut into desired shape and size. The bright fluorescence of the PPT film was completely quenched and clearly visualized in the presence of a 3.3×10^{-5} M I^- solution. The same film was dipped in a fresh 5×10^{-5} M solution of Hg^{2+} to visualize fluorescence recovery that could also be easily distinguished. The PPT based polymeric sensory system shows outstanding optical selectivity and sensitivity for I^- as well as Hg^{2+} ions in water even in the presence of other competing anions and cations. The lowest limit of detection calculated for Hg^{2+} by visible eye using membrane method was found to be 1.6 μM.

2.4 Conclusion

A neutral conjugated polymer (CP), poly(1,4−bis−(8−(4−phenylthiazole−2−thiol)−octyloxy)−benzene) (PPT), was synthesized using an oxidative polymerization reaction. The polymer PPT showed high optical activity in the presence of I^- and Hg^{2+} ions, which could be detected by

fluorescence spectroscopy as well by colorimetric responses at very low quantities by the naked eye. The colorless PPT solution changed to a deep yellow color upon the addition of iodide salts. The yellow color disappeared in the presence of dilute Hg^{2+} salts that could be visualized by the naked eye. The PPT−based detection platform was further extended to the solid state by preparing a membrane using 1% PPT in polystyrene, and this free−standing membrane also showed the capability to detect and respond to both iodide and mercury ions. The PPT−based detection system is very simple and economical to prepare, highly sensitive, and can rapidly detect iodide and mercury in competitive environments.

References

(1) Ravikumar, I.; Lakshminarayanan, P. S.; Suresh, E.; Ghosh, P. *Inorg. Chem*. **2008**, *47*, 7992.

(2) Rodriguez−Docampo, Z.; Pascu, S. I.; Kubik, S.; Otto, S. *J. Am. Chem. Soc.* **2006**, *128*, 11206.

(3) Martínez−Máñez, R.; Sancenón, F. *Chem. Rev*. **2003**, *103*, 4419.

(4) Dwight, S. J.; Gaylord, B. S.; Hong, J. W.; Bazan, G. C. *J. Am. Chem. Soc*. **2004**, *126*, 16850.

(5) Hossain, M. A.; Kang, S. O.; Powell, D.; Bowman-James, K. *Inorg. Chem*. **2003**, *42*, 1397.

(6) Gale, P. A.; Sessler, J. L.; Král, V.; Lynch, V. *J. Am. Chem. Soc*. **1996**, *118*, 5140.

(7) Choi, K.; Hamilton, A. D. *J. Am. Chem. Soc.* **2001**, *123*, 2456.

(8) Kang, J.; Kim, J. *Tetrahedron Lett*. **2005**, *46*, 1759.

(9) Davis, A. P.; Perry, J. P.; Williams, R. P. *J. Am. Chem. Soc.* **1997**, *119*, 1793.

(10) Kraft, A.; Grimsdale, A. C.; Holmes, A. B. *Angew. Chem. Int. Ed*. **1998**, *37*, 402.

(11) Friend, R. H.; Gymer, R. W.; Holmes, A. B.; Burroughes, J. H.; Marks, R. N.; Taliani, C.; Bradley, D. D. C.; Dos Santos, D. A.; Brédas, J. L.; Lögdlund, M.; Salaneck, W. R. *Nature* **1999**, *397*, 121.

(12) Bunz, U. H. F. *Chem. Rev*. **2000**, *100*, 1605.

(13) McQuade, D. T.; Pullen, A. E.; Swager, T. M. *Chem. Rev*. **2000**, *100*, 2537.

(14) Zhu, C.; Liu, L.; Yang, Q.; Lv, F.; Wang, S. *Chem. Rev.* **2012,** *112,* 4687.

(15) Gong, X.; Robinson, M. R.; Ostrowski, J. C.; Moses, D.; Bazan, G. C.; Heeger, A. J. *Adv. Mater.* **2002**, *14*, 581.

(16) Yu, G.; Gao, J.; Hummelen, J. C.; Wudl, F.; Heeger, A. J. *Science* **1995**, *270*, 1789.

(17) Bissell, R. A.; de Silva, A. P.; Gunaratne, H. Q. N.; Lynch, P. L. M.; Maguire, G. E. M.; McCoy, C. P.; Sandanayake, K. R. A. S. *Sensors. In Topics in Current Chemistry,* Springer−Verlag, Berlin Heidelberg, **1993**.

(18) Harrison, B. S.; Ramey, M. B.; Reynolds, J. R.; Schanze, K. S. *J. Am. Chem. Soc.* **2000**, *122*, 8561.

(19) Fan, C.; Plaxco, K. W.; Heeger, A. J. *J. Am. Chem. Soc*. **2002**, *124*, 5642.

(20) Gaylord, B. S.; Heeger, A. J.; Bazan, G. C. *J. Am. Chem. Soc*. **2003**, *125*, 896.

(21) Kim, J.; McQuade, D. T.; McHugh, S. K.; Swager, T. M. *Angew. Chem. Int. Ed*. **2000**, 3*9*, 3868.

(22) Chen, L.; McBranch, D. W.; Wang, H. L.; Helgeson, R.; Wudl, F.; Whitten, D. G. *Proc. Natl. Acad. Sci. U.S.A*. **1999**, *96*, 12287.

(23) Beer, P. D.; Gale, P. A. *Angew. Chem. Int. Ed.* **2001**, *40*, 486.

(24) Bianchi, A.; Bowman-James, K.; García-España, E. *Supramolecular Chemistry of Anions*, Wiley−VCH, New York **1997**.

(25) Hoang, A. H.; Leclerc, M. *J. Am. Chem. Soc*. **2003**, *125*, 4412.

(26) Vetrichelvan, M.; Nagarajan, R.; Valiyaveettil, S. *Macromolecules* **2006**, *39*, 8303.

(27) Hetzel, B. S. *Bull. W.H.O.* **2002***, 80,* 410.

(28) Andersson, M.; Takkouche, B.; Egli, I.; Allen, H. E.; de Benoist, B. *Bull.W.H.O.* **2005***, 83*, 518.

(29) Zhang, Z.; Wu, D.; Guo, X.; Qian, X.; Lu, Z.; Xu, Q.; Yang, Y.; Duan, L.; He, Y.; Feng, Z. *Chem. Res. Toxicol.* **2005**, *18*, 1814.

(30) Grandjean, P.; Weihe, P.; White, R. F.; Debes, F. *Environ. Res.* **1998**, *77*, 165.

(31) Harris, H. H.; Pickering, I. J.; George, G. N. *Science* **2003**, *301*, 1203.

(32) Boening, D. W. *Chemosphere* **2000**, *40*, 1335.

(33) Benoit, J. M.; Fitzgerald, W. F.; Damman, A. W. *Environ. Res.* **1998**, *78*, 118..

(34) Kuwabara, J. S.; Arai, Y.; Topping, B. R.; Pickering, I. J.; George. G. N. *Environ. Sci. Technol.* **2007**, *41*, 2745.

(35) Yoon, S.; Albers, A. E.; Wong, A. P.; Chang, C. J. *J. Am. Chem. Soc.* **2005**, *127*, 16030.

(36) Zhu, X.-J.; Fu, S.-T.; Wong, W.-K.; Guo, J.-P.; Wong, W.−Y. *Angew. Chem. Int. Ed*. **2006**, *45*, 3150.

(37) Caballero, A.; Martínez, R.; Lloveras, V.; Ratera, I.; Vidal−Gancedo, J.; Wurst, K.; Tárraga, A.; Molina, P.; Veciana, J. *J. Am. Chem. Soc.* **2005**, *127*, 15666.

(38) Hennrich, G.; Sonnenschein, H.; Resch.-G. U. *J. Am. Chem. Soc.* **1999**, *121*, 5073.

(39) Nolan, E. M.; Lippard, S. J. *J. Am. Chem. Soc.* **2003**, *125*, 14270.

(40) Ros-Lis, J. V.; Marcos, M. D.; Martínez-Máñez, R.; Rurack, K.; Soto, J. *Angew. Chem. Int. Ed*. **2005**, *44*, 4405.

(41) Kim, I. B.; Erdogan, B.; Wilson, J. N.; Bunz, U. H. F. *Chem. Eur. J.* **2004**, *10*, 6247.

(42) Ou, S.; Lin, Z.; Duan, C.; Zhang, H.; Bai, Z. *Chem. Commun.* **2006**, *42,* 4392.

(43) Wang, J.; Qian, X. *Org. Lett*. **2006**, *8*, 3721.

(44) Ono, A.; Togashi, H. *Angew. Chem. Int. Ed*. **2004**, *43,* 4300.

(45) Nolan, E. M.; Lippard, S. J. *Chem. Rev.* **2008**, *108*, 3443.

(46) Fan, L.−J.; Zhang, Y.; Jones, W. E. *Macromolecules* **2005**, *38*, 2844.

(47) Kim, I.−B.; Bunz, U. H. F. *J. Am. Chem. Soc.* **2006**, *128*, 2818.

(48) Tang, Y.; He, F.; Yu, M.; Feng, F.; An, L.; Sun, H.; Wang, S.; Li, Y.; Zhu, D. *Macromol. Rapid Commun.* **2006**, *27,* 389.

(49) Liu, X.; Tang, Y.; Wang, L.; Zhang, J.; Song, S.; Fan, C.; Wang, S. *Adv. Mater.* **2007**, *19*, 1471.

(50) Li, C.; Zhou, C.; Zheng, H.; Yin, X.; Zou, Z.; Liu, H.; Li, Y. *J. Polym. Sci. A Polym. Chem.* **2008**, *46*, 1998.

(51) Liu, X.; Zhu, J. *J. Phys. Chem. B* **2009**, *113*, 8214.

(52) Zou, Y.; Wan, M.; Sang, G.; Ye, M.; Li, Y. *Adv. Funct. Mater.* **2008**, *18*, 2724.

(53) Li, J.; Wu, Y.; Song, F.; Wei, G.; Cheng, Y.; Zhu, C. *J. Mater. Chem.* **2012**, *22*, 478.

(54) Huang, X.; Meng, J.; Dong, Y.; Cheng, Y.; Zhu, C. *Polymer* **2010**, *51*, 3064.

(55) Ma, B.; Zeng, F.; Zheng, F.; Wu, S. *Chem. Eur. J.* **2011**, *17*, 14844.

(56) Huang, X.; Xu, Y.; Miao, Q.; Zong, L.; Hu, H.; Cheng, Y. *Polymer* **2009**, *50*, 2793.

(57) Huang, X.; Meng, J.; Dong, Y.; Cheng, Y.; Zhu, C. *J. Polym. Sci. A Polym. Chem.* **2010**, *48*, 997.

(58) Ha−Thi, M.−H.; Penhoat, M.; Michelet, V.; Leray, I. *Org. Lett*. **2007**, *9*, 1133.

(59) Moon, S.−Y.; Youn, N. J.; Park, S. M.; Chang, S.−K. *J. Org. Chem*. **2005**, *70*, 2394.

(60) Kim, J. H.; Kim, H. J.; Kim, S. H.; Lee, J. H.; Do, J. H.; Kim, H.-J.; Lee, J. H.; Kim, J. S. *Tetrahedron Lett.* **2009**, *50*, 5958.

(61) Paul, G. S.; Sarmah, P. J.; Iyer, P. K.; Agarwal, P. *Macromol. Chem. Phys*. **2008**, *209*, 417.

(62) Zheng, J.; Zhan, C.; Wu, S.; Zhou, L.; Yang, X.; Zhan, R.; Qin, J. *Polymer* **2002**, *43*, 1761.

(63) van Breemen, A. J. J. M.; Herwig, P. T.; Chlon, C. H. T.; Sweelssen, J.; Schoo, H. F. M.; Benito, E. M.; de Leeuw, D. M.; Tanase, C.; Wildeman, J.; Blom, P. W. M. *Adv. Funct. Mater*. **2005**, *15*, 872.

(64) Saikia, G.; Singh, R.; Sarmah, P. J.; Akhtar, M. W.; Sinha, J.; Katiyar, M.; Iyer, P. K. *Macromol. Chem. Phys*. **2009**, *210*, 2153.

(65) de Halleux, V. M.; Geerts, Y. H. *React. Funct. Polym*. **2000***, 43*, 145.

(66) Saikia, G.; Dwivedi, A. K.; Iyer, P. K. *Anal. Methods* **2012**, *4*, 3180.

(67) Metzger, J. V. *Comprehensive Heterocyclic Chemistry*; Pergamon:New York, **1984**.

(68) Lu, Y.; Li, C.−M.; Wang, Z.; Ross, C. R.; Chen, J.; Dalton, J. T.; Li, W.; Miller, D. D. *J. Med. Chem*. **2009**, *52*, 1701.

(69) Miwatashi, S.; Arikawa, Y.; Kotani, E.; Miyamoto, M.; Naruo, K.−I.; Kimura, H.; Tanaka, T.; Asahi, S.; Ohkawa, S. *J. Med. Chem*. **2005**, *48*, 5966.

(70) Sarigiannis, Y.; Spiliopoulos, I. K. *J. Polym. Sci. A Polym. Chem.* doi:10.1002/pola.28362.

(71) Shia, W.; Mab, F.; Xie, Z. *Sens. Actuators, B.* **2015**, *220*, 600.

(72) Lakowicz, J. R. *Principles of Fluorescence Spectroscopy*, 2nd ed.; Plenum Press: New York **1999**.

(73) Watkins, A. R. *J. Phys. Chem*. **1974**, *78*, 1885.

(74) Kasha, M. J. *Chem. Phys*. **1952**, *20*, 71.

(75) McGlynn, S. P.; Azumi, T.; Khinoshita, M. *Molecular Spectroscopy of the Triplet State*; Prientice-Hall: Englewood Cliffs, NJ. **1969**.

(76) Wang, J.; Wang, D.; Miller, E. K.; Moses, D.; Bazan, G. C.; Heeger, A. J. *Macromolecules* **2000**, *33*, 5153.

(77) Sandanaraj, B. S.; Demont, R.; Aathimanikandan, S. V.; Savariar, E. N.; Thayumanavan, S. *J. Am. Chem. Soc.* **2006**, *128*, 10686.

Appendix

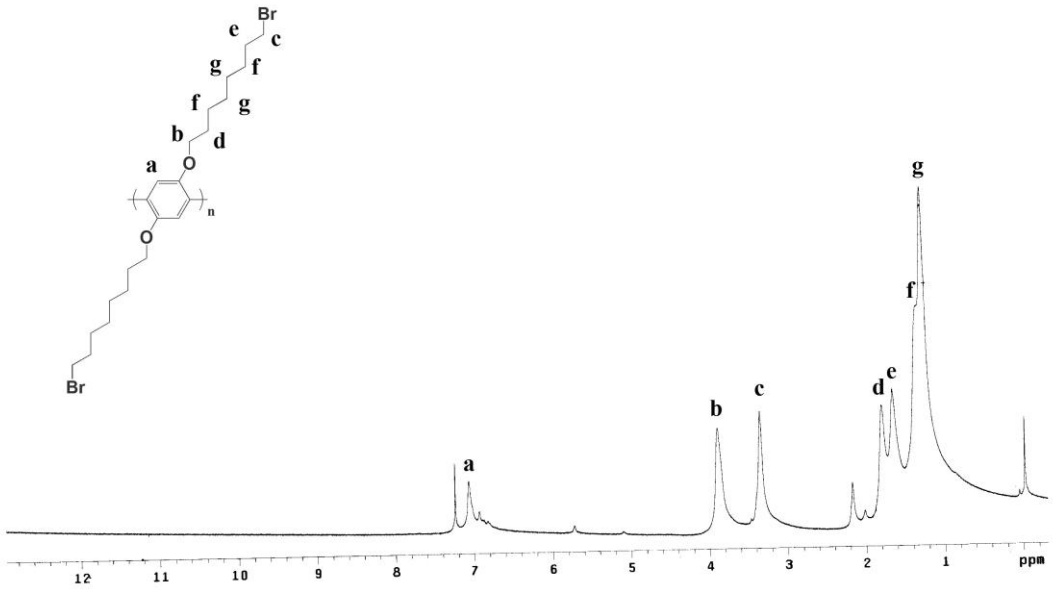

[1]H-NMR spectrum of PBr.

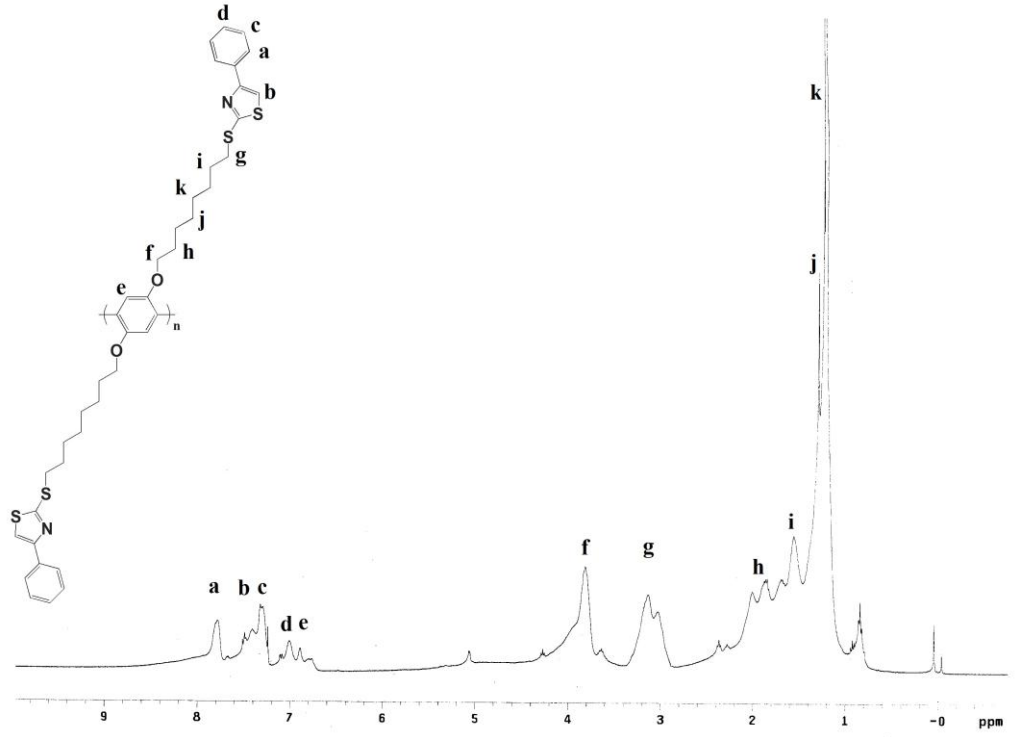

[1]H-NMR spectrum of PBT.

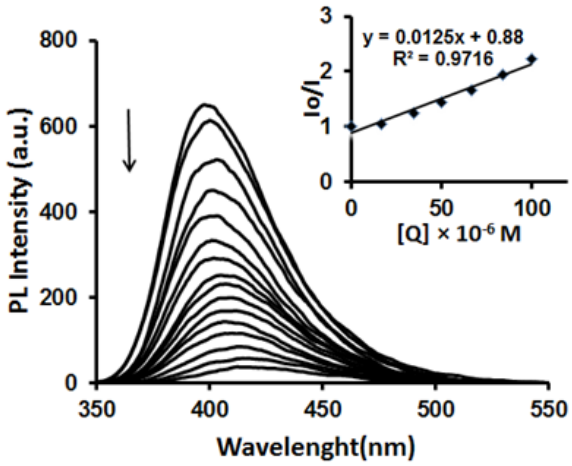

Figure A2.1 Photoluminescence spectra of PPT (6.6×10^{-6} M) with increasing concentration of I^- (KI) in 4:1 THF−water. Fluorescence quenching was >95% at a concentration of 2×10^{-4} M of I^-.

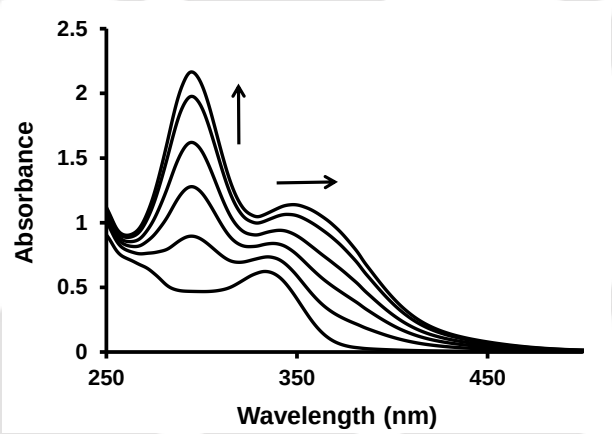

Figure A2.2 UV−Vis titration spectra of PPT with increasing concentration of I^- (KI) in 4:1 THF–water.

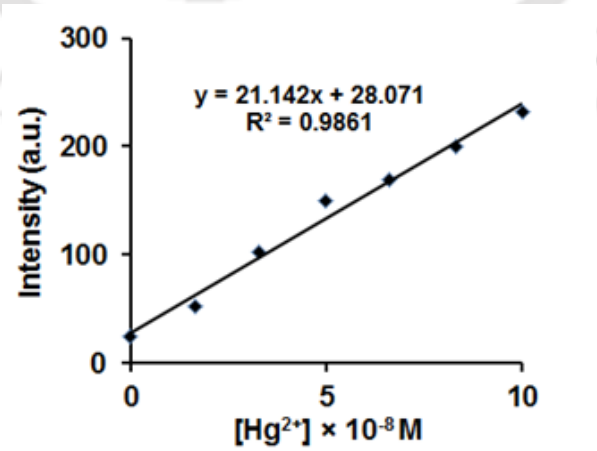

Figure A2.3 Fluorescence intensity of PPT–I as a function of Hg^{2+} concentration in 4:1 THF/water.

Chapter 3

Highly Precise Detection, Discrimination, and Removal of Anionic Surfactants over the Full pH Range via Cationic Conjugated Polymer: An Efficient Strategy to Facilitate Illicit-Drug Analysis

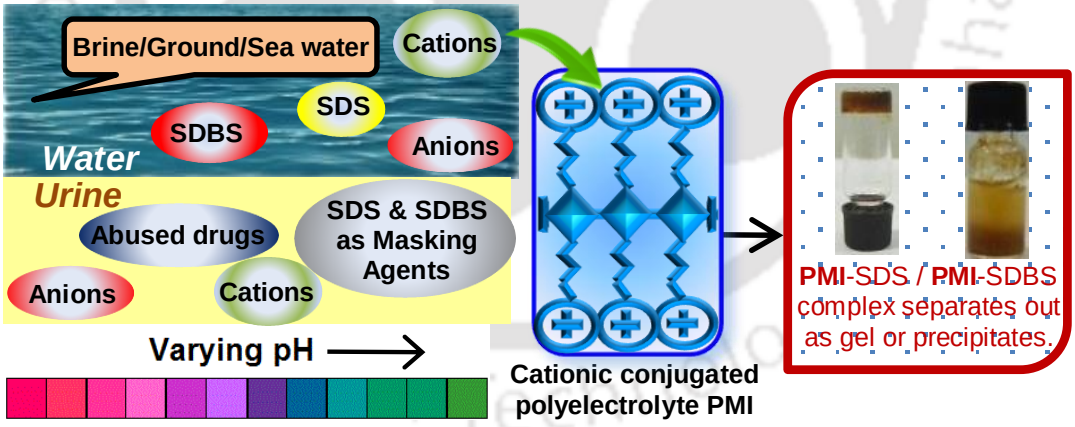

Hussain, S.; Malik, A. H.; Iyer, P. K., *ACS Appl. Mater. Interfaces* **2015**, *7*, 3189−3198.

Abstract

A water−soluble cationic conjugated polyelectrolyte (CPE), poly(1,4−bis(6−(1−methylimidazolium)−hexyloxy)−benzene bromide) (PMI) was synthesized that displayed extraordinary stability over the full pH range of 1−14 as well as in seawater, brine, urine and other harsh solutions yet retains the ability to carry out efficient detection, discrimination and removal of moderately dissimilar anionic surfactants (*viz.,* sodium dodecyl benzenesulfonate (SDBS) and sodium dodecyl sulfate (SDS)) at very low levels of 31.7 and 17.3 parts per billion (ppb), respectively. PMI formed stable hydrogels in the presence of SDS that remained unaffected by strong acids/bases, heating, ultrasonication, or exposure to light, whereas SDBS formed precipitates with PMI as a result of its different inter−polymer cofacial arrangement *via* Coulombic attraction. The complex−forming ability of PMI with SDS and SDBS facilitated their elimination from water or drug−doped urine samples without the use of any organic solvent, chromatographic technique, or solid support. This protocol, the first of its kind for the removal of anionic surfactants at very low concentrations from any type of solution and competitive environments, demonstrates an original application using a CPE. The surfactant−free sample solutions could be precisely analyzed for the presence of illicit drugs by any standard methods. Using PMI−a newly developed CPE, a rapid and practical method for the efficient detection, discrimination and removal of SDS and SDBS at ppb levels from water and urine, under harsh conditions and in natural chemical environments was demonstrated.

3.1 Introduction

Anionic surfactants that possess hydrophobic alkyl chains (nonpolar) and hydrophilic groups (polar) are indispensable in the detergent industry; for emulsification, lubrication, and catalysis; and for their well−known interaction with biomolecules such as proteins, DNA and peptides, even possessing the ability to penetrate cell membranes.[1−5] Because of their large application base and extensive industrial scale production, it has become extremely important to determine their presence in pharmaceutical and food formulations, as drug−abuse−masking agents, in waste water treatment plants, in the environment and in biological fluids as well as to analyze them in trace quantities because they are well−recognized contaminants.[6,7] Another critical problem associated with anionic surfactants (*viz.*, sodium dodecyl benzenesulfonate (SDBS) and sodium dodecyl sulfate (SDS)) is their extensive misuse as adulterants and masking agents, along with abused and performance−enhancing drugs, to evade detection by doping tests.[8,9] It is estimated that approximately 20 million individuals are screened each year in the United States alone for illicit drug abuse. Thus, adulterants are a severe challenge for testing of abused drugs. Detergents containing SDS and SDBS have also been found to be one of the most common specimens in adulterated forensic urine drug tests because they can interfere with the immunoassay/initial test via a combination of pH and ionic strength, remove the drug by forming an insoluble complex, or cause impediments with gas chromatography−mass spectrometry (GC−MS) confirmation procedures.[9−12] Most of the fluorometric sensors developed for anionic surfactants have been employed for either the analysis of industrial samples in quality control processes or environmental monitoring. To the best of our knowledge, no conjugated polymers/polyelectrolytes (CPE) platforms, recognized for their superior chemical stability, tunable photophysical properties, and high sensitivity, have been developed to detect and distinguish among anionic surfactants in water, urine and biological fluids or under extremely harsh conditions such as seawater and brine as well as over the full pH range of 1−14. This unique property of poly(1,4−bis(6−(1−methylimidazolium)−hexyloxy)−benzene bromide) (PMI) was utilized to efficiently remove anionic surfactants used as masking agents in drug testing by simple gelation or by precipitation, thereby enabling efficient and error−free analysis of the illicit drugs and demonstrating a novel application of CPEs that has not previously been realized with any synthetic material.

Several surfactant−analysis techniques, such as the methylene blue active substances (MBAS) method,[13] ion−selective electrodes, capillary electrophoresis,[14] high−performance liquid chromatography[15] (HPLC), gas chromatography and mass spectroscopy[16] (GC−MS) are widely used but have multiple limitations in their applicability, owing to tedious procedures, irreproducibility, and signal instability as well as requiring the use of large amounts of chlorinated solvents that are not readily biodegradable. Despite the enormity of the problem, the limitations in the existing surfactant−analysis systems and the necessity to have efficient alternate detection platforms, very few reports on the use of fluorescence and/or UV/Vis spectra have been developed to detect anionic surfactants.[17−19] In addition, these surfactants tend to form micelles or to accumulate at the air−water interface as a stable foam, with the hydrophobic tail in the air and hydrophilic head in the water, posing serious separation problems; as a result, no existing methods can remove these large organic contaminants, e.g., SDS and SDBS. Therefore, the development of superior probes and efficient methods to detect anionic surfactants at low concentrations in water, under acidic/basic conditions and in a competitive environment and to remove them from biological fluids has immense technological significance, yet remains an unsolved problem.

Charged polyelectrolytes have a strong tendency to form stable complexes with oppositely charged surfactant molecules and the resulting complexes may have different conformations than the free polymer.[20−24] Among the various receptors, imidazolium has been widely reported as a suitable coordination site for anions via both electrostatic and hydrogen-bonding interactions.[25,26] Recent studies have also shown their ability for the recognition of anionic surfactants.[17,18,27,28]

Herein, we report the synthesis and characterization of PMI, a new cationic CPE, that neither degrades nor shows loss of activity over the full pH range of 1−14 and that displays significant photophysical and conformational changes in the presence of anionic surfactants SDBS and SDS with precise and highest selectivity. This PMI system was found to be highly effective for detecting and distinguishing SDS and SDBS in aqueous media, most notably, over the full working pH range at which the solubilities of both surfactants are very high and which was not perceived with any synthetic sensors in prior instances. We also demonstrate that by combining the CPE (PMI) with dissimilar anionic surfactants, the geometric conformation of the CPE is altered, thereby bringing significant photophysical changes that in principle form the basis on which to distinguish anionic surfactants with minor structural variations. On the basis of this principle, the PMI system

was utilized to detect the presence of anionic surfactants in aqueous samples, random urine specimens and drug formulations and to remove them efficiently.

3.2 Experimental

3.2.1 Materials and measurements

Chemicals (*viz.*, SDBS, triton−X−100, tween−20, cetyltrimethylammonium bromide (CTAB), sodium laurate, sodium stearate, sodium *p*−toluenesulfinate, sodium *p*−toluenesulfonate, 1,6−dibromohexane, 1−methyl imidazole and metal salts (used as their perchlorates)) were purchased from Sigma-Aldrich chemicals. SDS was purchased from Merck. Scheme 3.1 shows the structures of SDS and SBDS. Four different classes of benzodiazepines that are available as commercial drugs were purchased and used. UV/vis and PL spectra were recorded on a PerkinElmer Lambda−25 spectrophotometer and a Horiba Fluoromax−4 spectrofluorometer using 10 mm path length quartz cuvettes with a slit width of 2 nm at 298 K. Atomic microscopy images were recorded on an Agilent 5500−STM instrument. FT−IR spectra were recorded on a Perkin Elmer spectrometer with samples that were prepared as KBr pellets. ^{1}H NMR (400 MHz) and ^{13}C NMR (100 MHz) spectra were recorded with a Varian−AS400 NMR spectrometer. GPC data was recorded with a Waters−2414 instrument (polystyrene calibration). Urine specimens were collected via a laboratory from different individuals voluntarily at different time intervals.

3.2.2 Synthesis of 1,4−Bis(6−bromohexyloxy)−benzene (M1)

Synthesis of monomer M1 was carried out using a previously reported method from the literature.[29-31] In a 250 mL round−bottomed flask, K_2CO_3 and dry acetone were stirred under inert atmosphere for 15 min at room temperature. To this, hydroquinone (2 g, 18.16

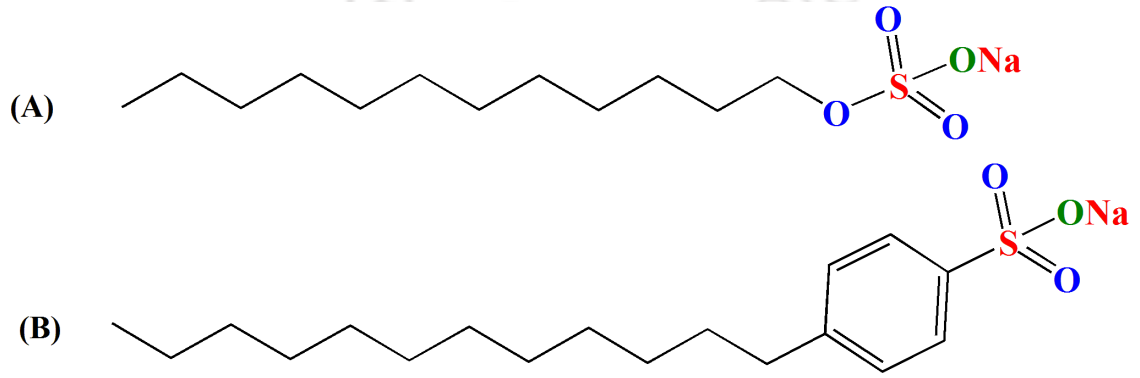

Scheme 3.1 Structures of anionic surfactants (A) Sodium dodecyl sulfate (SDS) and (B) Sodium dodecyl benzene sulfonate (SDBS).

mmol) and 1,6−dibromohexane (17.73 g, 72.6 mmol) was added and stirred continuously for additional 2 days at 60 ºC. The brown colored solution thus obtained was diluted with acetone and passed through celite bed to remove excess base. Anhydrous Na_2SO_4 was then added to the solution to remove traces of water and evaporated to obtain a yellow−brown liquid. Excess 1,6−dibromohexane was distilled out under reduced pressure and the crude on further purification by column chromatography (ethyl acetate : hexane, 0.5 : 9.5) yielded the desired monomer as white solid flakes. Yield: 82%.

3.2.3 Synthesis of poly(1,4−bis(6−bromo−hexyloxy)−benzene) (PBr)

Synthesis of polymer PBr were carried out by using a previously established procedure.[32,33] To prepare PBr, anhydrous ferric chloride (0.74 g, 4.57 mmol) was dissolved in 10 mL of nitrobenzene and transferred to a three−necked round−bottomed flask that was equipped with a nitrogen inlet. Using a syringe, M1 (1.0 g, 2.03 mmol, dissolved in 15 mL of nitrobenzene) was introduced into the flask. The reaction mixture was then stirred for 36 h at room temperature, followed by precipitation from methanol. The reaction mixture was centrifuged and washed repeatedly with methanol. The resulting polymer was finally dried under reduced pressure to obtain a brown−colored powder. Yield: 70%.

^{1}H NMR (400 MHz, $CDCl_3$, δ): 7.07 (s, 2H), 3.94 (m, 4H), 3.36 (m, 4H), 1.81 (m, 4H), 1.69 (m, 4H), 1.52 (m, 4H), 1.41 (m, 4H). GPC in THF, polystyrene standard: $M_w = 2.32 \times 10^4$, PDI = 1.7.

3.2.4 Synthesis of poly(1,4−bis(6−(1−methylimidazolium)−hexyloxy)−benzene bromide) (PMI)

To a 100 mL round−bottomed flask, PBr (0.12 mmol, 1 eq.) and an excess of 1−methyl imidazole were added and kept at reflux under stirring in an oil bath at 80 °C for 24 h. The reaction mixture was then poured into excess chloroform and stirred for 1 h to obtain a precipitate. The process was repeated twice to remove excess 1−methyl imidazole and PBr. The precipitate was filtered out and dried to get a brownish−colored sticky product. Yield: 85%.

^{1}H NMR (600 MHz, DMSO−d_6, δ): 9.38 (b, 2H), 7.75 (b, 2H), 7.69 (b, 2H), 7.02 (b, 2H), 4.18 (b, 2H), 3.87 (b, 10H), 1.90 (b, 4H), 1.76 (b, 4H), 1.29 (b, 4H), 1.24 (b, 4H).

^{13}C NMR (150 MHz, DMSO−d_6, δ): 149.47, 136.50, 128.64, 123.50, 122.25, 114.20, 68.73, 48.69, 35.78, 29.79, 28.70, 28.49, 25.53.

FT−IR (ν_{max}/cm^{-1}): 2928.08, 2855.31, 1634.02, 1571.27, 1463.99, 1381.17, 1206.33, 1168.33, 1021.93, 757.54.

3.2.5 Method of calculating fluorescence quantum yield

Fluorescence quantum yield of PMI in water and methanol was determined using quinine sulfate (Φ_r = 0.54 in 0.1 M H_2SO_4) as the standard and was calculated from the following equation.[34]

$$\Phi_s = \Phi_r (A_r F_s / A_s F_r) (\eta_s^2 / \eta_r^2)$$

Here, s and r denote the sample and reference, respectively; A is the absorbance, F is the relative integrated fluorescence intensity, and η is the refractive index of the solvent used.

3.2.6 Preparation of stock solutions and fluorescence and absorbance studies of PMI

Surfactants, anions and various metal stock solutions were prepared (10.0×10^{-3} M in Milli−Q water). The stock solutions were diluted to the desired concentrations with Milli−Q water when needed. A solution of PMI (2×10^{-5} M) in repeat units in HEPES buffer (pH 7.2, 10 mM) was placed in a 3 mL cuvette (10.0 mm width) and then the fluorescence spectrum was recorded. Different analyte solutions were introduced and the changes in the fluorescence intensity were recorded at room temperature each time (λ_{ex} = 325 nm). Similarly, the absorbance of PMI (2×10^{-5} M in HEPES buffer (pH 7.2, 10 mM)) was recorded at room temperature, and the stock solutions of SDS and SDBS were introduced separately to observe the changes in absorbance induced by each addition.

3.2.7 Methods for calibration curve and detection limit

Different solutions of PMI (2×10^{-5} M) each containing SDBS (0, 2, 4, 6, 8, 10, 12, 14, and 16 μM) and SDS (0, 2, 4, 6, 8, 10, 12, 14, 16, 18, and 20 μM) were prepared separately in HEPES buffer (pH 7.2, 10 mM). The fluorescence spectrum was then recorded for each sample by excitation at 325 nm at room temperature. The calibration curve for SDBS/SDS was obtained by plotting change in the fluorescence intensity versus the concentration of SDBS/SDS. The curve demonstrates a linear relationship and the correlation coefficient (R^2) value as determined via linear regression analysis was found to be 0.9900 (SDBS) and 0.9893 (SDS), respectively. The limit of detection (LOD) was calculated on the basis of the standard method reported in the literature[35] using the equation below−

$$LOD = 3 \times \sigma / k$$

where k is the slope of the curve equation and σ represents the standard deviation for the intensity of the PMI solution in the absence of these analytes.

3.2.8 Gel formation and precipitation

Stock solutions of PMI and surfactants SDS and SDBS (0.05 M) were prepared separately in Milli−Q water. Similarly, 0.05 M solutions of SDS and SDBS were prepared in untreated urine as well as in drug-doped specimens. Mixing was done by drop−wise addition of the homogeneous surfactant solutions to the aqueous polyelectrolyte solutions. The PMI−SDS complex formed a gel, whereas the PMI−SDBS separated out as a precipitate. Micro-centrifugation of the PMI−SDS complex at 14000 rpm produced a highly stable hydrogel. The hydrogel and the precipitate complexes of anionic surfactants with PMI were separated and the aqueous solution was analyzed by thin layer chromatography analysis to confirm the presence of the drug.

3.2.9 Detection of SDS and SDBS in various ground water (GW), sea water (SW) and brine samples (BW)

Two different ground water (GW) samples were collected from various places inside the IITG campus and filtered through a 0.2 μm membrane filter, respectively. Fluorometric titration was performed initially by adding aliquots of all these samples to the solution of PMI (2×10^{-5} M) in HEPES buffer (pH=7.2, 10 mM) to monitor their interference. No significant change in fluorescence of PMI was observed after adding a total 50 μL of each sample. Each GW sample was then spiked with SDBS (10^{-3} M) and SDS (10^{-3} M) separately to make the standard stock solutions. Different random volumes of SDBS−spiked GW samples (GW1: 6 μL, GW2: 15 μL) and SDS−spiked GW samples (GW1: 5 μL, GW2: 25 μL) were added to the solution of PMI (2×10^{-5} M) in HEPES buffer (pH=7.2, 10mM) and fluorescence changes were monitored by exciting at 325 nm. The results obtained were compared with the standard calibration curves of SDBS and SDS. Similar experiments were also performed with two sea water (SW) and brine (BW) samples that were filtered through a 0.2 μm membrane filter before use. Under similar conditions as above, each SW and BW samples were spiked with SDBS (10^{-3} M) and SDS (10^{-3} M) separately. Different random volumes of SDBS−spiked SW samples (SW1: 0.5 μL, SW2: 20 μL), SDS−spiked SW samples (SW1: 5 μL, SW2: 20 μL), SDBS−spiked BW samples (BW1: 10 μL, BW2: 30 μL) and SDS−spiked BW samples (BW1:12 μL, BW2: 27 μL) were added to the solution of PMI (2×10^{-5} M) in HEPES buffer (pH=7.2, 10 mM) and fluorescence changes were monitored by exciting at 325 nm.

The results obtained were compared with the standard calibration curves of SDBS and SDS.

3.2.10 Control experiment using drug−doped urine specimens

Tablets (*viz.*, Lonazep (0.25 mg of clonazepam), Nitrest (5 mg of zolpidem), Alzolam (0.25 mg of alprazolam) and Clampose (5 mg of diazepam)) were crushed and independently mixed with 3 mL of a urine specimen and then subjected to Whatman filtration to remove any insoluble components. A total of 50 μL of each sample was added to an aqueous solution of PMI, and changes in fluorescence were recorded. Each sample was then independently doped with SDBS (10^{-2} M) or SDS (10^{-2} M) to prepare standard stock solutions, set aside for 2 d, and used for sensing purposes.

3.3 Result and discussion

3.3.1 Synthesis and characterization of PMI

The synthesis of PMI is shown in Scheme 3.2. N−Methyl imidazole was introduced onto the terminal bromide atoms of the neutral conjugated polymer (PBr), using post polymerization functionalization, resulting in the formation of cationic polymer PMI. All of the products at each step were well characterized by NMR, FT−IR and GPC (Figures A3.1−A3.4). The molecular weight (M_w) of the polymer PBr was found to be 2.32×10^4, PDI = 1.7 (GPC in THF, PS standard). Fluorescence quantum yield (Φ_s) of PMI was calculated in water and methanol and found to be 0.32 and 0.36, respectively.

3.3.2 Effect of pH on the emission of PMI

Water−soluble cationic polymer PMI shows an absorption maximum at 325 nm and an emission maximum at 406 nm (λ_{ex} = 325 nm) in aqueous media. The pH studies using NaOH/HCl and a buffer demonstrated that the fluorescence of PMI is retained over the full pH range of 1−14, with negligible fluorescence quenching of 2−12% observed at higher pH (Figure 3.1). Furthermore, no changes in the emission maxima and shape of the spectra were observed over the full pH range studied here. Because the pH stability of PMI is extraordinarily high, the application of PMI could be extended over the full pH range; a range not accessible previously with any other synthetic probes. This also confirms that irrespective of the environment or sample source the loss of PMI activity would be insignificant.

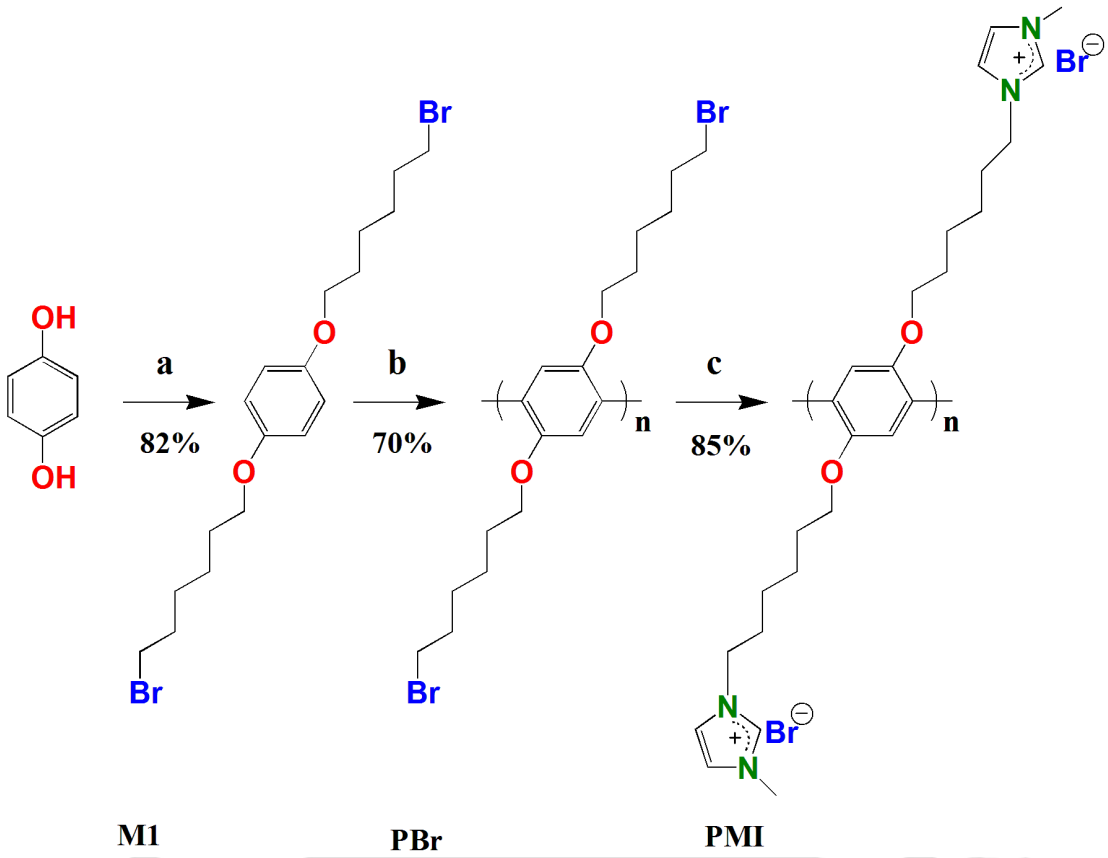

Scheme 3.2 Synthesis of poly(1,4−bis(6−(1−methylimidazolium)−hexyloxy)−benzene bromide) (PMI). (a) K_2CO_3, dry acetone, 1,6−dibromohexane, 70°C. (b) $FeCl_3$, nitrobenzene, RT, 36 h. (c) 1−methyl imidazole, reflux, 24 h.

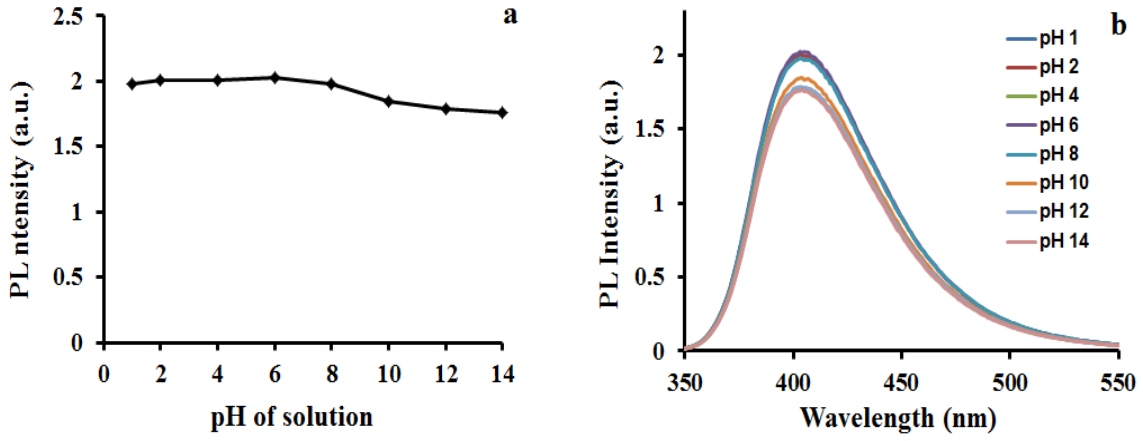

Figure 3.1 (a) Maximum fluorescence intensity of PMI (2×10^{-5} M) as a function of pH values in water. (b) Change in emission spectra of PMI (2×10^{-5} M) at different pH values.

3.3.3 Optical sensing of SDBS and SDS

At the outset, the photophysical changes of PMI were studied in the presence of the surfactants to demonstrate its detection ability. The fluorescence intensity of PMI decreased after the addition of successive aliquots of surfactants to the PMI solution (2×10^{-5} M in HEPES buffer (pH 7.2, 10 mM)). The addition of only 1 eq. of SDBS or SDS (2×10^{-5} M) to the solution of PMI caused a decrease (~90%) in the fluorescence intensity (λ_{ex} = 325 nm), with a red shift of ~12 and ~21 nm with SDBS and SDS, respectively (Figure 3.2ab). In addition to the red shift, the emission spectrum of the PMI−SDS complex (Figure 3.2b) shows a well−defined vibrational structure as a result of interchain charge−transfer reactions and excimer formation.[36,37] However, no such change was observed in the spectrum of the PMI−SDBS complex (Figure 3.2a). The Stern-Volmer constant (K_{sv}) values obtained (Figures A3.41) for SDBS (1.2×10^5 M^{-1}) and SDS (2.3×10^5 M^{-1}) were found to be sensibly high. The LOD (Figure 3.3) calculated for SDBS and SDS were found to be 110 nM (31.7 ppb) and 61 nM (17.3 ppb), respectively that confirms the ability of PMI to detect surfactants in aqueous media at very low levels that were previously inaccessible.[17,18,27,28]

3.3.4 Selectivity Studies

Other widely used surfactants (*viz.* triton−X−100, tween−20, cetyltrimethylammonium bromide (CTAB)) and several anions, including those found in urine such as halides (Cl^-), phosphates (PO_4^{3-}), and sulfates (SO_4^{2-}), did not cause any significant changes in the fluorescence emission of PMI (Figure 3.2c) when compared with the spectra of PMI with added SDS and SDBS. To identify the effect of the hydrophobic chains of SDS and SDBS on the photophysical properties of PMI, the sodium salts of SO_4^-, SO_4^{2-}, *p*−toluenesulfinate (SO_2^-) and *p*−toluenesulfonate (SO_3^-) were titrated with PMI. However, no noticeable changes were observed in the fluorescence emission peaks of PMI after the addition of these anionic salts (Figures 3.2c). Fluorometric titration of PMI with anionic surfactants (*viz.* sodium laurate and sodium stearate) were also carried out to ascertain the effect of polar head groups with characteristics (i.e., charge distribution and hydrophobic chain length) similar to those of SDS, however no remarkable changes in the fluorescence emission of PMI were observed, suggesting a lesser preference for carboxylate salts (Figures 3.2c). Common metal ions, such as Cu^{2+}, Co^{2+}, Ni^{2+}, Pb^{2+}, Cr^{3+},

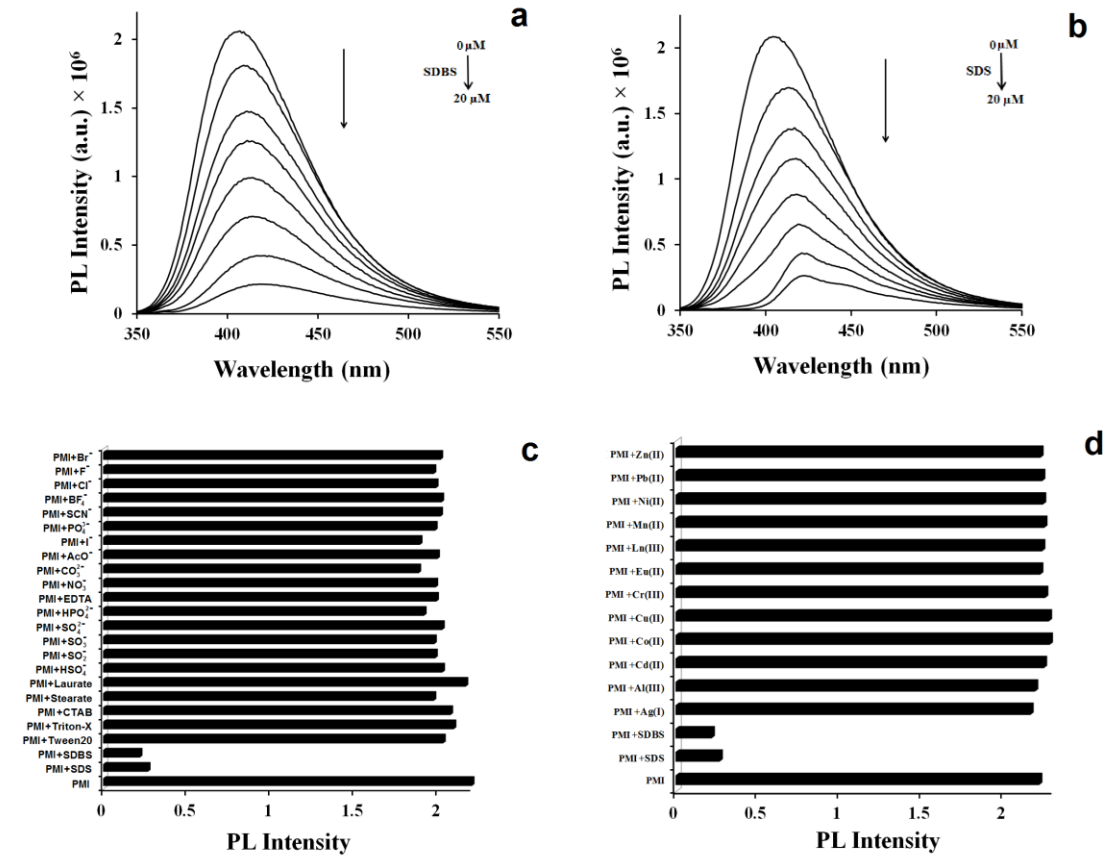

Figure 3.2 PL spectra of PMI with increasing concentration of (a) SDBS (λ_{ex}=325 nm) and (b) SDS (λ_{ex}=325 nm) in HEPES buffer (pH 7.2, 10 mM). Concentration of PMI inside the cuvette was 2×10^{-5} M. Final concentration of SDBS and SDS was 2×10^{-5} M. Bar diagrams depicting the effect of various (c) anions and surfactants and (d) metal ions on the fluorescence intensity of PMI in water. Concentration of PMI and other analytes are 2×10^{-5} and 2×10^{-4} M, respectively.

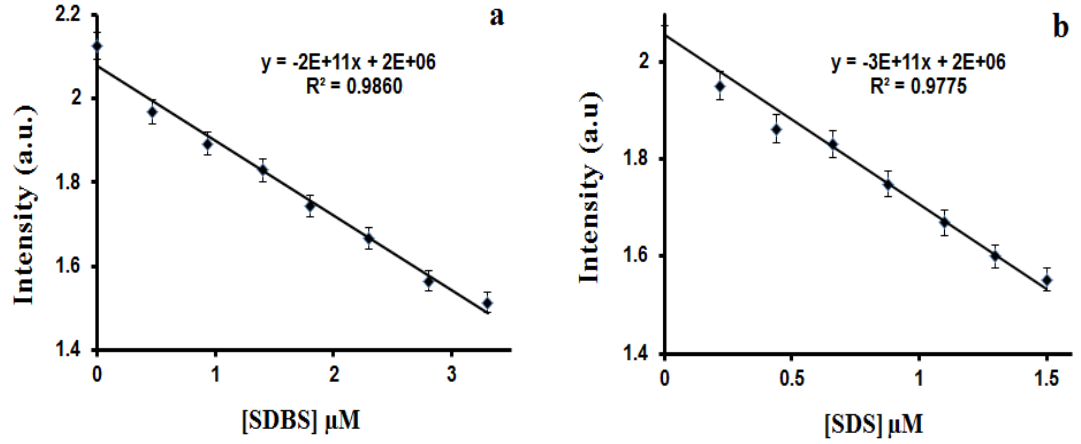

Figure 3.3 Detection limit plots for (a) SDBS and (b) SDS in HEPES buffer (pH 7.2, 10 mM).

Mn^{2+}, Cd^{2+}, Ln^{3+}, Zn^{2+}, Eu^{3+}, Ag^{+} and Al^{3+} were also ineffectual toward the fluorescence quenching of PMI (Figures 3.2d). These results confirm that the combination of the hydrophobic chains and the polar head groups of surfactants plays a key role in the assembly of PMI toward an interchain cofacial arrangement[19,23,36] and is vital for both sensitive and selective detection and conformational changes.

3.3.5 Monitoring complexation *via* UV/vis spectroscopy

The interaction of anionic SDBS and SDS with cationic PMI was also studied by UV/vis spectroscopy to gain further insight into the polymer−surfactant interactions. Significant shifts in the absorption peaks occurred after the addition of these surfactants to the aqueous solution of PMI (2×10^{-5} M). The absorption maximum peak of PMI was red−shifted by 15 nm (Figure 3.4a) after the addition of a total of 1 eq. of SDBS, with the formation of isosbestic point at 330 nm. However, the presence of SDS had a more remarkable effect on the structure of PMI, as observed by the significant 55 nm redshift of the 325 nm peak to 380 nm, with the clear formation of an isosbestic point at 345 nm after continuous addition of up to 1 eq. of SDS (Figure 3.4b). These red shifts are attributed to the J−type aggregation of PMI upon binding with SDBS or SDS as a result of an interpolymer cofacial arrangement; J−type aggregates generally display bathochromic shifted bands because of increased chain or aggregate length.[38] The appearance of isosbestic points in the absorption spectra with increasing SDBS/SDS concentration also provides strong evidence for an equilibrium between the polymer PMI and each surfactant.

3.3.6 Discrimination between SDBS and SDS

Interestingly, when PMI (2×10^{-5} M in HEPES buffer (pH 7.2, 10 mM)) was excited at 380 nm, the emission spectra showed remarkable fluorescence enhancement at 424 nm after the addition of SDS, with a well−defined vibrational structure (Figure 3.4c). Enhancement of PMI fluorescence was found to be ∼90% at 2×10^{-5} M SDS concentration. These spectral changes suggest that after the addition of SDS to the aqueous solution of PMI, the polymer shifts to a different conformation that has an emission peak at 424 nm. PMI starts out as the first species, but when the concentration of SDS reaches 2×10^{-5} M, the polymer shifts to a different conformation, i.e., a polymer−SDS complex that induces the formation of an excimer. However, no such fluorescent enhancement was observed in the emission spectra of PMI after the addition of SDBS (Figure 3.4d), indicating that excimer was formed with PMI−SDS but not with

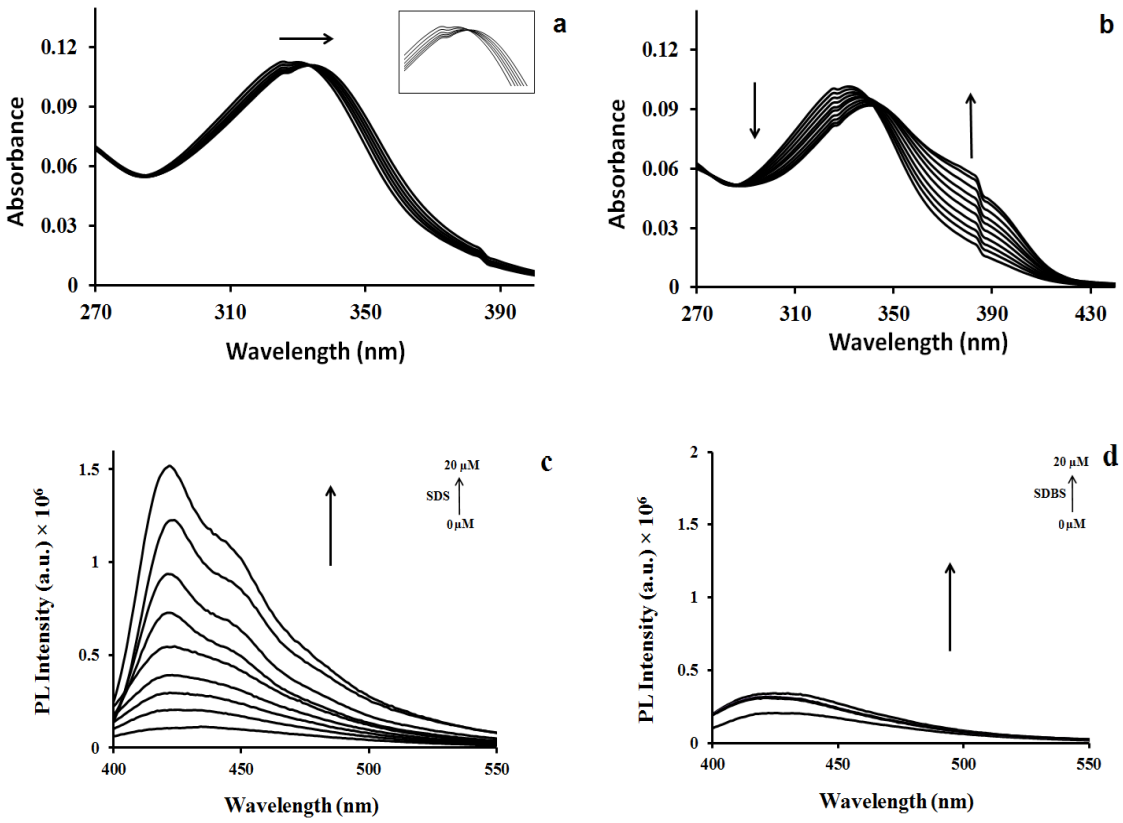

Figure 3.4 UV/vis titration spectra of PMI (2×10^{-5} M) with increasing concentrations of (a) SDBS (2×10^{-5} M) and (b) SDS (2×10^{-5} M). Photoluminescence spectra of PMI (2×10^{-5} M) with increasing concentrations of (c) SDS (λ_{ex} = 380 nm) and (d) SDBS (λ_{ex} = 380 nm) in HEPES buffer (pH 7.2, 10 mM). Fluorescent enhancement was found to be ~90% after the addition of 1 eq. of SDS. SDBS did not cause any significant change in fluorescence.

PMI−SDBS. On the basis of these observations, moderately dissimilar anionic surfactants (*viz.*, SDBS and SDS) can be easily discriminated in aqueous media by tuning the excitation wavelength of PMI.

Since the emission spectra were observed to change with the excitation wavelength, a thorough study was carried out by monitoring the change in emission spectra of both the PMI−SDBS and PMI−SDS complexes at different excitation wavelengths (300−400 nm). It was found that the PMI−SDBS complex does not show significant enhancement of fluorescence at any excitation (300−400 nm, Figure 3.5a). However, substantial fluorescence enhancement at 424 nm was observed in case of the PMI−SDS complex when changing the excitation wavelength (300−400nm, Figure 3.5b). The intensity of the emission maxima at 424 nm was highest when recorded at 380 nm, indicating that the

PMI−SDS complex induces excimer formation at this emission wavelength. Similarly, excitation spectra were also monitored at different emission wavelengths (400−500 nm) to examine the species present in the system. The excitation spectra of the PMI−SDBS complex (Figure 3.5c) has a peak at ~340 nm (at any emission between 400−500 nm), confirming the formation of a new species. However, the PMI−SDS excitation spectra (Figure 3.5d) showed a peak at ~380 nm (at any emission between 400−500 nm), indicating the formation of a complex between PMI and SDS. These results are in good agreement with the UV/vis studies and confirm the formation of a new species between PMI and SDBS/SDS detectable at 340 and 380 nm, respectively.

We have also demonstrated that the polymer PMI can efficiently distinguish between SDBS and SDS in a mixed and competitive environment. To confirm this unique ability of PMI to differentiate between moderately dissimilar anionic surfactants, the following experiment was carried out. A solution of SDS and SDBS in Milli−Q water (pH=7) was prepared by adding equimolar concentrations (10 mM each) of these surfactants and the solution was incubated for 2 d at room temperature. When this mixture (2×10^{-5} M) was

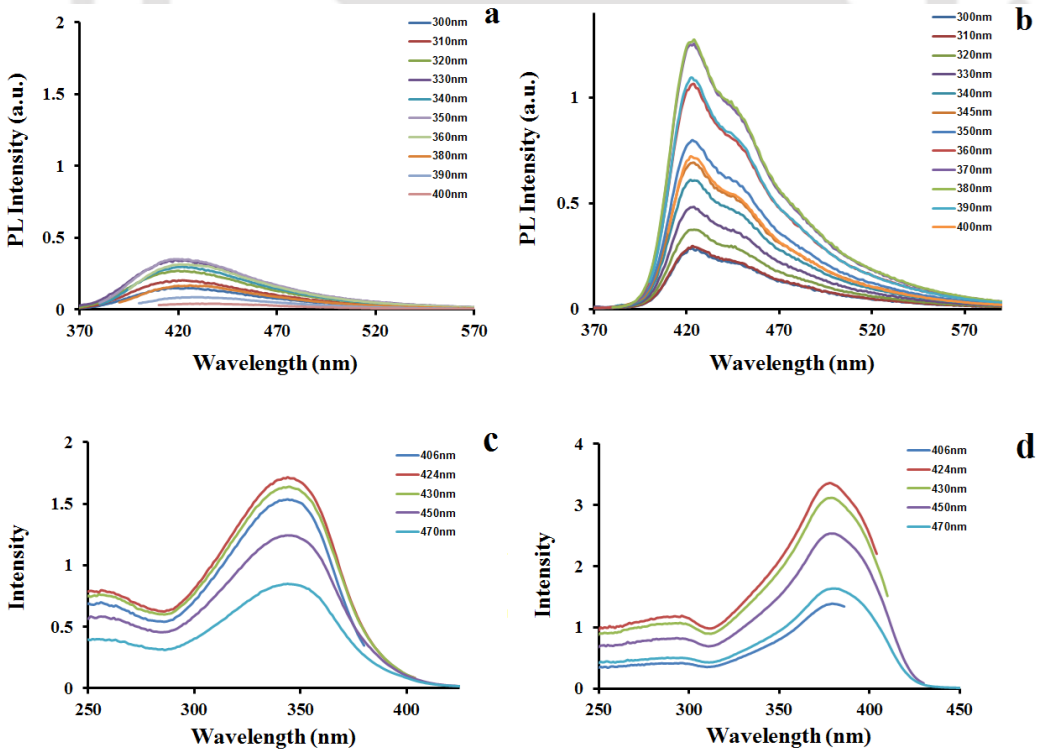

Figure 3.5 Emission spectra of (a) PMI−SDBS complex and (b) PMI−SDS complex at various excitation wavelengths. Excitation spectra of (c) PMI−SDBS complex and (d) PMI−SDS complex observed at various emission wavelengths. Concentrations of PMI and SDBS/SDS in each case were 2×10^{-5} M, respectively.

added to a solution of PMI (2×10^{-5} M, 325 nm excitation), ~90% fluorescent quenching was observed. However, when PMI was excited at 380 nm, the fluorescent enhancement was found to be ~55%. This result postulates that SDS and SDBS interact almost equally with PMI and that they can be distinguished by PMI even in a mixed environment.

3.3.7 Mechanistic studies of complexation

Generally, CPEs are present as weak aggregates in aqueous solution, with ionic side chains facing the water−polymer interface and π−π stacking occurring between the backbones within.[39] The complexation between PMI and surfactants SDBS and SDS *via* interpolymer cofacial arrangement and the interaction of hydrophobic chains with these anionic surfactants is driven by Coulombic interactions. Consequently, the interfacial water molecules are released during complexation, which may further assist the extension of the polymer chains by reducing conformation disorders.[19] After the addition of SDS to the aqueous solution of PMI, the extended chains promote interchain packing via the PMI−SDS complex and overlap to form excimers[36] that emit fluorescence at a longer wavelength (Figure 3.6A). The large red shift in the absorption spectra and the emission at a longer wavelength can be attributed to this observation. However, the SDBS/PMI mixture failed to show any excimer emission, indicating that the aromatic rings present in SDBS restrict the interchain packing of the PMI−SDBS complex (Figure 3.6B).

3.3.8 Gel formation and precipitation

To gain a better understanding of the complexation process, the polymer and the surfactants were mixed at higher concentrations of 0.05 M (1:1 mole ratio of

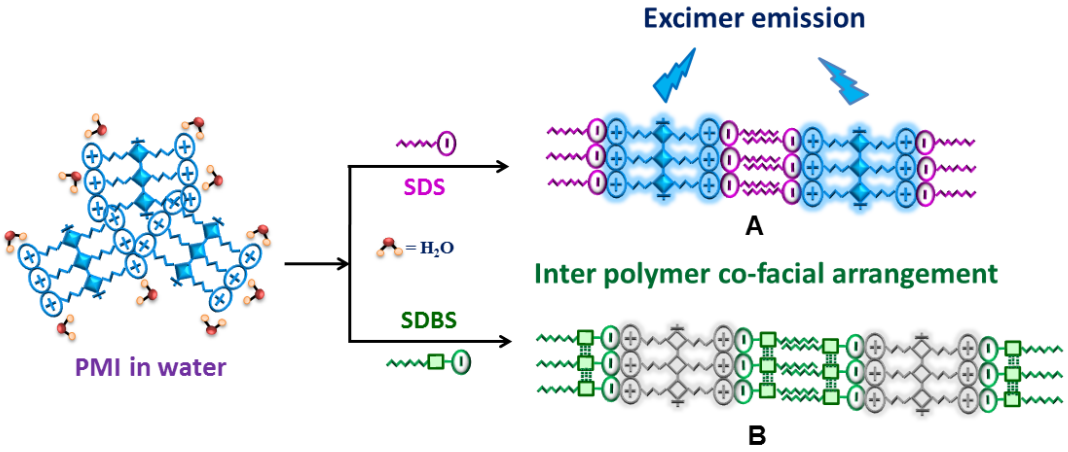

Figure 3.6 Schematic representation of the aggregation behavior of the (A) PMI−SDS and (B) PMI−SDBS complexes.

PMI/surfactant) by drop−wise addition of the surfactants to the PMI solution. When SDS (10^{-5} M) was added to the clear solution of PMI, the mixture became more viscous, resulting from intermolecular association and crosslinking *via* Coulombic attraction. As the SDS concentration is increased, a self−assembled 3D network with high viscosity and a semi−solid gel nature was formed[40] (Figure A3.5) because of the intermolecular association between PMI and SDS *via* hydrophobic chain interactions and efficient interchain interdigitations. The hydrogel thus obtained displayed extraordinary chemical, thermal and optical stability for a prolonged period of over six months. A similar observation was reported[23] for a P3KHT−CTAB complex, formed by the interaction of anionic polythiophene and cationic surfactant. Because of this high stability, the gel showed irreversible behavior when subjected to thermal, chemical, optical and mechanical stresses (Figure 3.7). Interestingly, this irreversible PMI−SDS hydrogel does not collapse even under extremely acidic or basic conditions (pH 1−14), at high temperature, in the presence of light, or under prolonged shaking/sonication. However, PMI did not form a gel in the presence of SDBS (10^{-5} M); instead, the complex precipitated out of the solution, a behavior of PMI with SDBS that clearly distinguishes it from the gel−forming PMI−SDS complex. The amount of PMI−SDBS precipitate that was formed further increased at higher SDBS concentration (10^{-5}−10^{-2} M) and could be

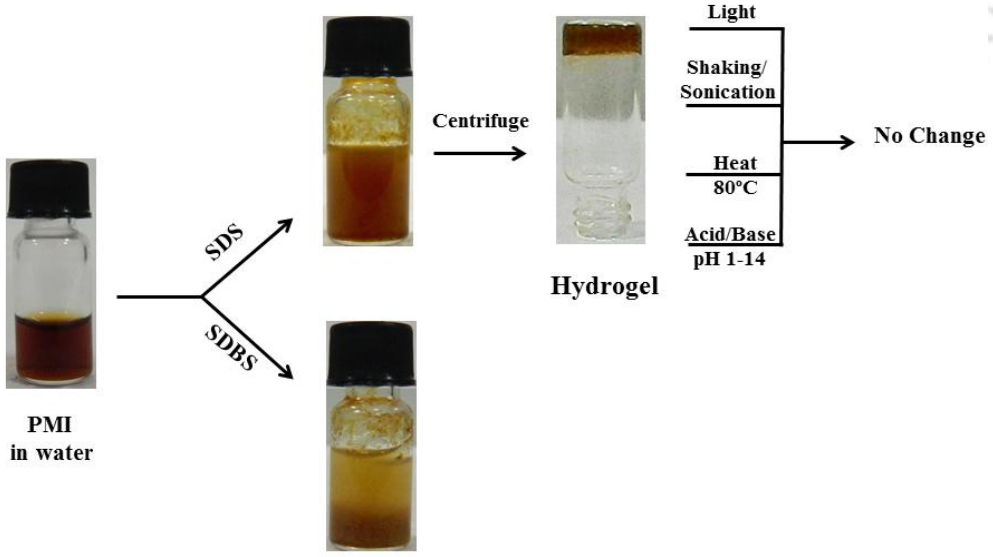

Figure 3.7 Solutions of PMI and SDS/SDBS in water were mixed and kept standing for a few minutes. PMI−SDS forms a stable hydrogel when this is followed by centrifugation, whereas PMI−SDBS separated out as a precipitate. The hydrogel showed very high stability when subjected to thermal, chemical, photo, and mechanical stresses and displayed irreversible behavior.

easily separated from the clear liquid after standing. It may be presumed that after the addition of SDBS to PMI the complex is favored to remain in a planar conformation rather than forming a 3D network.[23]

It has been reported earlier that anionic surfactants present at levels of 10^{-4} M or greater interfered with and gave false negative results in immunoassay and GC−MS procedures during drug−analysis tests[41] with several urine specimens. Hence, alternate strategies that can overcome the limitations in the existing methods with regard to eliminating anionic surfactants SDS or SDBS from the drugs are indispensable for the accurate analysis of illicit doping. Experiments utilizing PMI confirmed that it is possible to easily remove both SDS and SDBS from water and urine containing illicit drugs at concentrations much lower than those allowed by existing methods because both the PMI−SDS gel and the PMI−SDBS precipitate rapidly at room temperature without the use of any chromatographic technique or solid support, demonstrating a practical application of PMI that was previously unfeasible with any other material.

3.3.9 Detection of SDBS/SDS at varying pH

Furthermore, PMI showed extraordinarily high detection ability over the full pH range of 1−14, a range over which synthetic sensors are rarely recognized to operate. This unique feature of PMI was further verified by carrying out detection under harsh and unfavorable conditions, i.e., highly acidic and basic environments as well as seawater and brine samples. The quenching efficiency of PMI remained unperturbed over the full pH range, with a very negligible quenching of 2−12% at pH 8−14 in the presence of SDBS and SDS (Figure 3.8). Such high stability demonstrated by the PMI system was not perceived previously with synthetic sensors and is a unique feature of PMI.

3.3.10 Detection of SDBS and SDS in brine, groundwater, seawater, and urine specimens

To further confirm the feasibility of PMI as a sensor in practical applications, the detection studies of SDBS and SDS under competitive−environment conditions and natural samples were carried out since these surfactants are categorized as the most common pollutants to be found in technogenic water and natural water and as adulterants in urine specimens.[28] In a typical experiment, various groundwater, seawater, brine and random urine samples were independently spiked with known concentrations of SDBS and SDS and utilized for sensing. Experiments carried out using various ground water,

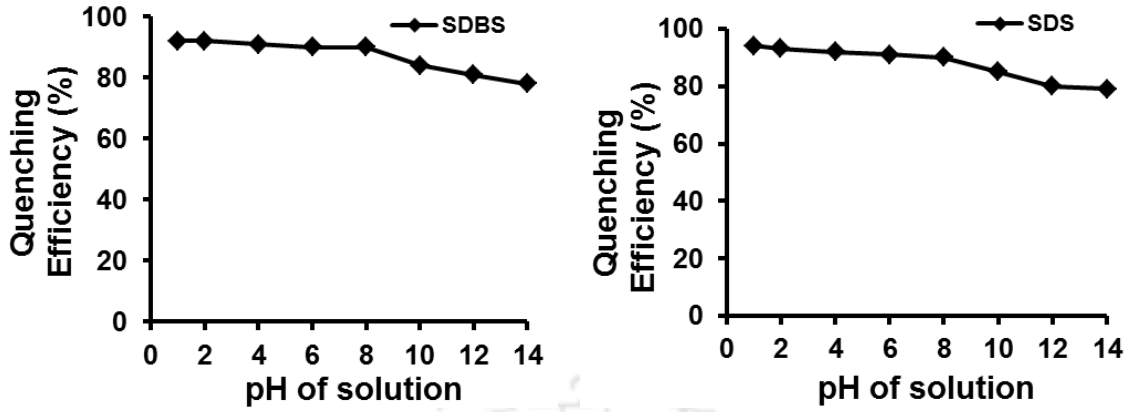

Figure 3.8 Quenching efficiency of PMI/surfactants at different pH values. Concentration of PMI and surfactants were 2×10^{-5} M, respectively.

Table 1. Determination of anionic surfactants in ground water samples.

Ground water samples	SDBS added (10^{-7}M)	SDBS found (10^{-7}M)[a]	SDS added (10^{-7}M)	SDS found (10^{-7}M)[a]
GW1	20	18.6 ± 0.5	17	15.7 ± 0.7
GW2	50	49.5 ± 1.5	83	82.1 ± 1.7

[a]An average of three replicate measurements with standard deviation

Table 2. Determination of anionic surfactants in sea water samples.

Sea water samples	SDBS added (10^{-7} M)	SDBS found (10^{-7}M)[a]	SDS added (10^{-7}M)	SDS found (10^{-7}M)[a]
SW1	1.7	1.6 ± 0.2	17	15.5 ± 1.7
SW2	67	64.6 ± 1.5	67	64.9 ± 2.0

[a]An average of three replicate measurements with standard deviation

Table 3. Determination of anionic surfactants in brine samples.

Brine samples	SDBS added (10^{-7} M)	SDBS found (10^{-7}M)[a]	SDS added (10^{-7}M)	SDS found (10^{-7}M)[a]
BW 1	33	27.8 ± 1.3	40	37.3 ± 1.1
BW 2	100	95.9 ± 1.4	90	88 ± 2.4

[a]An average of three replicate measurements with standard deviation

seawater, and brine samples confirm the practicability of PMI to detect both these surfactants efficiently under competitive−environment conditions at very low ppb levels (Tables 1−3). This protocol demonstrated enhanced features for the detection of anionic

surfactants (*viz.*, SDBS/SDS) in aqueous media without the use of hazardous chlorinated organic solvents.[13,41] Likewise, seawater is known to have high salinity and an excess of dissolved ions, yet PMI showed no loss of activity under such harsh environmental conditions and was able to detect both SDS and SDBS efficiently.

Similarly, six urine specimens (pH 6−7) were collected from different consenting individuals at varying time intervals and used without further treatment. Fluorometric titration was carried out by adding aliquots of urine to a solution of PMI (2×10^{-5} M in HEPES buffer (pH 7.2, 10 mM)). It was found that the interference of urine on the fluorescence emission of PMI was negligible. To acquire enhanced and accurate results, three samples that caused minimum change in the fluorescence emission of PMI were then separately spiked with known concentration of SDBS and SDS (10^{-3} and 10^{-3} M, respectively). After adding known volumes of these spiked samples to a solution of PMI (2×10^{-5} M), the fluorescence spectra were then recorded and the peaks were compared with the standard calibration curves (Table 4, Figure A3.6) after taking three replicate measurements. It could be established from these experiments that even in urine samples, PMI could detect and estimate the presence of SDBS and SDS at very low levels (10^{-7} M) that were inaccessible in the past with any sensors.[17,28] This study formed the basis for carrying out further analysis of surfactants with high stability that are used as adulterants and masking agents in biological fluids.

3.3.10 Detection of SDBS and SDS in drug−doped urine specimens

To determine the ability of PMI to detect SDS and SDBS being used as adulterants and masking agents with recreational, abused and performance−enhancing drugs, detection experiments were carried out by spiking these surfactants with several prescription drugs commonly used as abused agents. The most popular recreational drugs used worldwide include amphetamines, cocaine, cannabinoids, and heroin. Subjects abusing these drugs

Table 4. Determination of anionic surfactants in urine specimens.

Urine samples	SDBS added (10^{-7} M)	SDBS found (10^{-7} M)[a]	SDS added (10^{-7}M)	SDS found (10^{-7}M)[a]
U1	40.00	33.40 ± 2.00	50.00	51.51± 1.73
U2	90.00	86.05± 2.64	33.33	30.70± 1.00
U3	123.33	122.67± 3.60	90.00	85.40± 3.00

[a]An average of three replicate measurements with standard deviation

may adulterate the urine specimens with anionic surfactants to mask them and to evade illicit drug detection during testing[12] because these surfactants are stable in a biological environment for extended periods. Benzodiazepines are also considered to be one of the most commonly abused[42,43] drugs because of their high misuse as a medical prescription and their categorization as Schedule IV controlled drugs[44] by the International Narcotics Control Board. They enhance the effect of the neurotransmitter γ−aminobutyric acid, resulting in sedative, anxiolytic (antianxiety) and muscle−relaxant properties. They generally have long detection periods in urine (up to 7 d with therapeutic use and 4 to 6 weeks with chronic use). Urinalysis is the most common type of test employed for drug testing because drug metabolites can be detected for a longer time in urine than in other biological specimens such as blood, saliva, and sweat.[45] Hence, control studies were carried out by doping urine specimens separately with a few medically prescribed and commercially available benzodiazepines (*viz.*, clonazepam (D1), zolpidem (D2), alprazolam (D3), and diazepam (D4); Figures 3.9). It was found that when these drugs

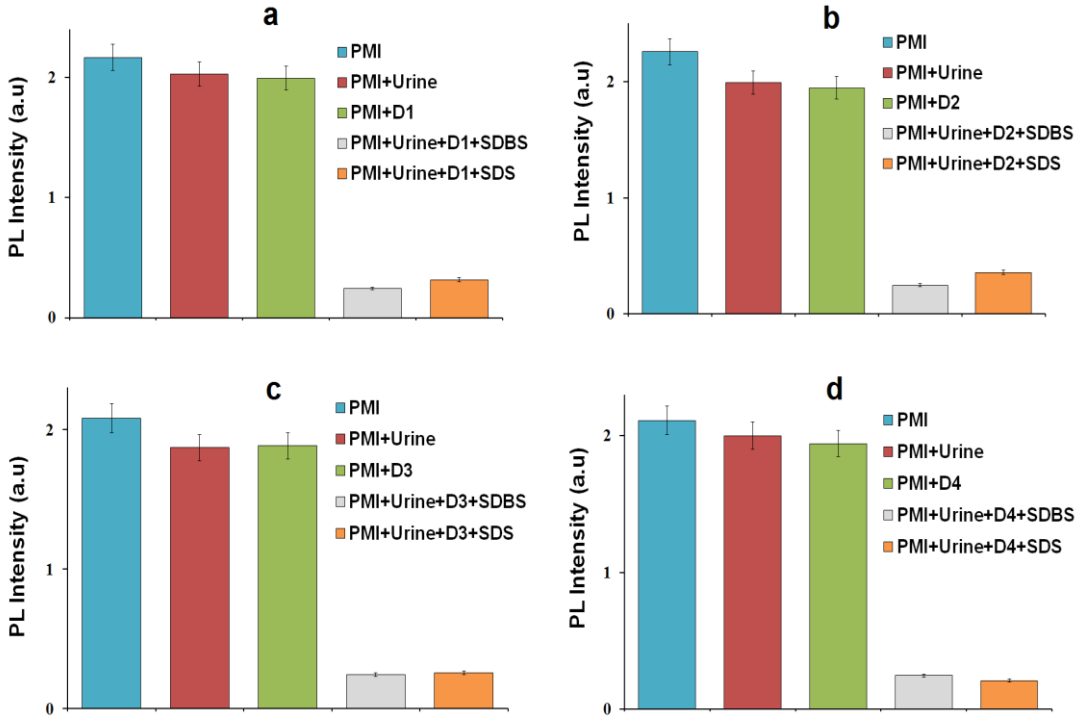

Figure 3.9 (a), (b), (c), and (d) Fluorescence changes observed after the addition of urine samples, various drugs (clonazepam (D1), zolpidem (D2), alprazolam (D3), and diazepam (D4)), and drug−doped urine samples that contained SDBS and SDS to a solution of PMI in HEPES buffer (pH 7.2, 10 mM). Concentration of PMI inside the cuvette was 2×10^{-5} M. Final concentration of SDBS and SDS after the addition of drug−doped urine samples was 2×10^{-5} M. Error bars=±5%.

were mixed with urine specimens they have an insignificant effect on the fluorescence emission of PMI. However, surfactants doped with these recreational drugs in urine showed significant fluorescence quenching, even after a prolonged time of 2−7 d. These results confirm that the PMI−based system can efficiently detect anionic surfactants, i.e., SDBS and SDS that are exploited as adulterants in urine with recreational drugs at concentrations as low as 10^{-7} M in a highly competitive environment, containing drug formulations and components of urine, under varying pH conditions. SDS molecules form ion pairs with the cationic side chains of PMI *via* Coulombic attraction, leading to an increase in the conjugation length. The extended chains can then overlap and form excimers that emit fluorescence at a longer wavelength. PMI forms complexes with SDS and SDBS and separates them efficiently in the form of hydrogels or precipitates from water or urine samples, thereby facilitating analysis of illicit drugs that remain in the analysis fluid and are utilized for confirmation tests.

3.4 Conclusion

An efficient strategy for the detection, discrimination and removal of anionic surfactants having very small structural variation (*viz.*, sodium dodecyl benzenesulfonate (SDBS) and sodium dodecyl sulfate (SDS)) is developed on the basis of different aggregation behavior *via* interpolymer cofacial arrangement. The polymer PMI was found to be highly effective over viable range of pH range from 1−14 for the detection and removal of these moderately dissimilar surfactants, even at parts per billion levels (SDS = 17.3 ppb and SDBS = 31.7 ppb) in urine specimens, under acidic and basic conditions, in seawater, brine, and aqueous media. The removal of these surfactants irrespective of the fluid in which they exist has remained an unresolved problem; hence, they are frequently exploited by doping suspects as the most common masking agents and adulterants in urine specimens to elude detection in drug testing. PMI demonstrated high optical activity in the presence of these surfactants and facilitated the rapid elimination of both SDS and SDBS in the form of gel or precipitate from water and biological medium, thereby enabling accurate analysis of illicit drugs. This simple approach provides for the first time a highly stable and practical method that rapidly detects and discriminates SDS and SDBS, eliminates them from urine samples without the use of hazardous organic solvents, as well as facilitates the precise investigation of illicit drugs by doping suspects at very low concentrations.

References

(1) Patel, R.; Patel, K. S. *Analyst* **1998**, *123*, 1691.

(2) Chan, W. H.; Lee, A. W. M.; Lu, J. *Anal. Chim. Acta.* **1998**, *361*, 55.

(3) Sakai, T.; Harada, H.; Liu, X.; Ura, N.; Takeyoshi, K.; Sugimoto, K. *Talanta* **1998**, *45*, 543.

(4) Cserháti, T.; Forgács, E.; Oros, G. *Environ. Int.* **2002**, *28*, 337.

(5) Nielsen, A. D.; Borch, K.; Westh, P. *Biochim. Biophys. Acta−Protein Struct. Mol. Enzymol.* **2000**, *1479*, 321.

(6) Oshima, M.; Motomizu, S.; Doi, H. *Analyst* **1992**, *117*, 1643.

(7) Taguchi, S.; Takahashi, K.; Hata, N.; Kasahara, I. *Analyst* **2001**, *126*, 2078.

(8) Dasgupta, A. *Am. J. Clin. Pathol.* **2007**, *128*, 491.

(9) Mikkelsen, S. L.; Ash, K. O. *Clin. Chem.* **1988**, *34*, 2333.

(10) Cody, J. T. *Adulteration of Urine specimens: Handbook of Workplace Drug Testing*, AACC Press: Washington, D.C.,1995, pp−181.

(11) Duc, V. T. *Clin. Chem.* **1985**, *31*, 658.

(12) Warner, A. *Clin. Chem.* **1989**, *35*, 648.

(13) Clesceri, L. S.; Greenberg, A. E.; Eaton, A. D. *Standard Methods for the Examination of Water and Wastewater*, 20th ed; American Public Health Association: Washington, D.C., 1999.

(14) Heinig, K.; Vogt, C. *Electrophoresis* **1999**, *20*, 3311.

(15) Villar, M.; Callejón, M.; Jiménez, J. C.; Alonso, E.; Guiráum, A. *Anal. Chim. Acta* **2007**, *599*, 92.

(16) Moldovan, Z.; Avram, V.; Marincas, O.; Petrov, P.; Ternes, T. *J. Chromatogr. A* **2011**, *1218*, 343.

(17) Chen, X.; Kang, S.; Kim, M. J.; Kim, J.; Kim, Y. S.; Kim, H.; Chi, B.; Kim, S.−J.; Lee, J. Y.; Yoon, J. *Angew. Chem. Int. Ed. Engl.* **2010**, *49*, 1422.

(18) Kumar, S.; Arora, S.; Singh, P.; Kumar, S. *RSC Adv.* **2012**, *2*, 9969.

(19) Evans, R. C.; Knaapila, M.; Willis−fox, N.; Kraft, M.; Terry, A.; Burrows, H. D.; Scherf, U. *Langmuir* **2012**, *28*, 12348.

(20) Kabanov, A. V; Bronich, T. K.; Kabanov, V. A.; Yu, K.; Eisenberg, A. *J. Am. Chem. Soc.* **1998**, *7863*, 9941.

(21) Dutta, K.; Mahale, R. Y.; Arulkashmir, A.; Krishnamoorthy, K. *Langmuir* **2012**, *28*, 10097.

(22) Lavigne, J. J.; Broughton, D. L.; Wilson, J. N.; Erdogan, B.; Bunz, U. H. F. *Macromolecules* **2003**, *36*, 9.

(23) Danesh, C. D.; Starkweather, N. S.; Zhang, S. *J. Phys. Chem. B* **2012**, *116*, 12887.

(24) Heeley, M. E. H.; Gallaher, J. K.; Nguyen, T. L.; Woo, H. Y.; Hodgkiss, J. M. *Chem. Commun.* **2013**, *49*, 4235.

(25) Yoon, J.; Kim, S. K.; Singh, N. J.; Kim, K. S. *Chem. Soc. Rev.* **2006**, *35*, 355.

(26) Xu, Z.; Kim, S. K.; Yoon, J. *Chem. Soc. Rev.* **2010**, *39*, 1457.

(27) Coll, C.; Martínez−Máñez, R.; Marcos, M. D.; Sancenón, F.; Soto, J. *Angew. Chem., Int. Ed.* **2007**, *46*, 1675.

(28) Climent, E.; Giménez, C.; Marcos, M. D.; Martínez-Máñez, R.; Sancenón, F.; Soto, J. *Chem. Commun.* **2011**, *47*, 6873.

(29) Paul, G. S.; Sarmah, P. J.; Iyer, P. K.; Agarwal, P. *Macromol. Chem. Phys.* **2008**, *209*, 417.

(30) van Breemen, A. J. J. M.; Herwig, P. T.; Chlon, C. H. T.; Sweelssen, J.; Schoo, H. F. M.; Benito, E. M.; de Leeuw, D. M.; Tanase, C.; Wildeman, J.; Blom, P. W. M. *Adv. Funct. Mater.* **2005**, *15*, 872.

(31) Saikia, G.; Singh, R.; Sarmah, P. J.; Akhtar, M. W.; Sinha, J.; Katiyar, M.; Iyer, P. K. *Macromol. Chem. Phys.* **2009**, *210*, 2153.

(32) Hussain, S.; De, S.; Iyer, P. K. *ACS Appl. Mater. Interfaces* **2013**, *5*, 2234.

(33) Muthuraj, B.; Hussain, S.; Iyer, P. K. *Polym. Chem.* **2013**, *4*, 5096.

(34) Melhuish, W. H. *J. Phys. Chem.* **1961**, *65*, 229.

(35) McNaught, A. D.; Wilkinson, A. *IUPAC Compendium of Chemical Terminology*, Wiley Blackwell: New York, 1997.

(36) Treger, J. S.; Ma, V. Y.; Gao, Y.; Wang, C.−C.; Wang, H.−L.; Johal, M. S. *J. Phys. Chem. B* **2008**, *112*, 760.

(37) Chen, L.; Xu, S.; Mcbranch, D. *J. Am. Chem. Soc.* **2000**, *298*, 9302.

(38) Maiti, N. C.; Mazumdar, S.; Periasamy, N. *J. Phys. Chem. B* **1998**, *5647*, 1528.

(39) Wang, H.; He, F.; Yan, R.; Wang, X.; Zhu, X.; Li, L. *ACS Appl. Mater. Interfaces* **2013**, *5*, 8254.

(40) Tam, K. C.; Wyn−jones, E. *Chem. Soc. Rev.* **2006**, *35*, 693.

(41) Jones, J. T.; Esposito, F. M. *J Anal Toxicol* **2000**, *24*, 323.

(42) White, J. M.; Irvine, R. J. *Addiction* **1999**, *94*, 961.

(43) Hindmarch, J.; Beaumont, G.; Brandon, S.; Leonard, B. E. *Benzodiazepines: Current Concepts−Biological, Clinical and Social Perspectives*, John Wiley & Sons, 1990.

(44) *Drugs Included in Schedule IV of the 1971 Convention*: International Narcotics Control Board (INCB), 50th ed; 2011.

(45) Dasgupta, A. *Drugs of Abuse Analysis. Encyclopedia of Analytical Chemistry*, John Wiley & Sons Ltd., vol 2, 2013.

Appendix

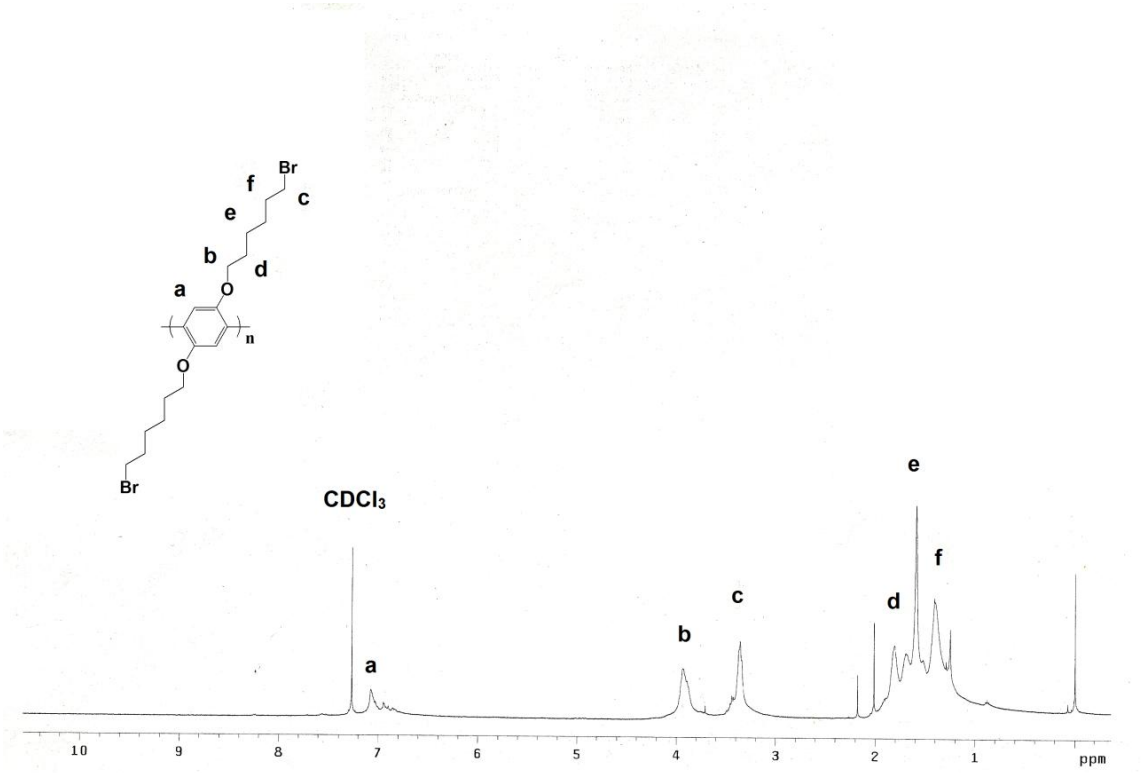

Figure A3.1 ^{1}H NMR (400 MHz, $CDCl_3$) spectrum of PBr.

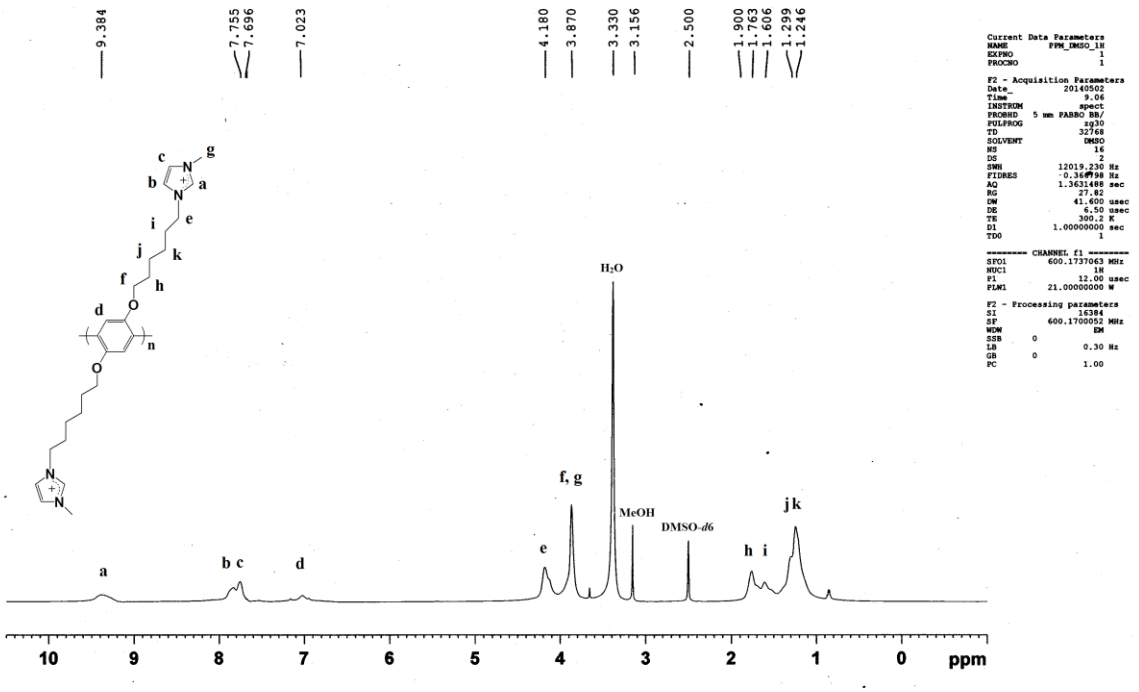

Figure A3.2 ^{1}H NMR (600 MHz, DMSO−d_6) spectrum of PMI**.**

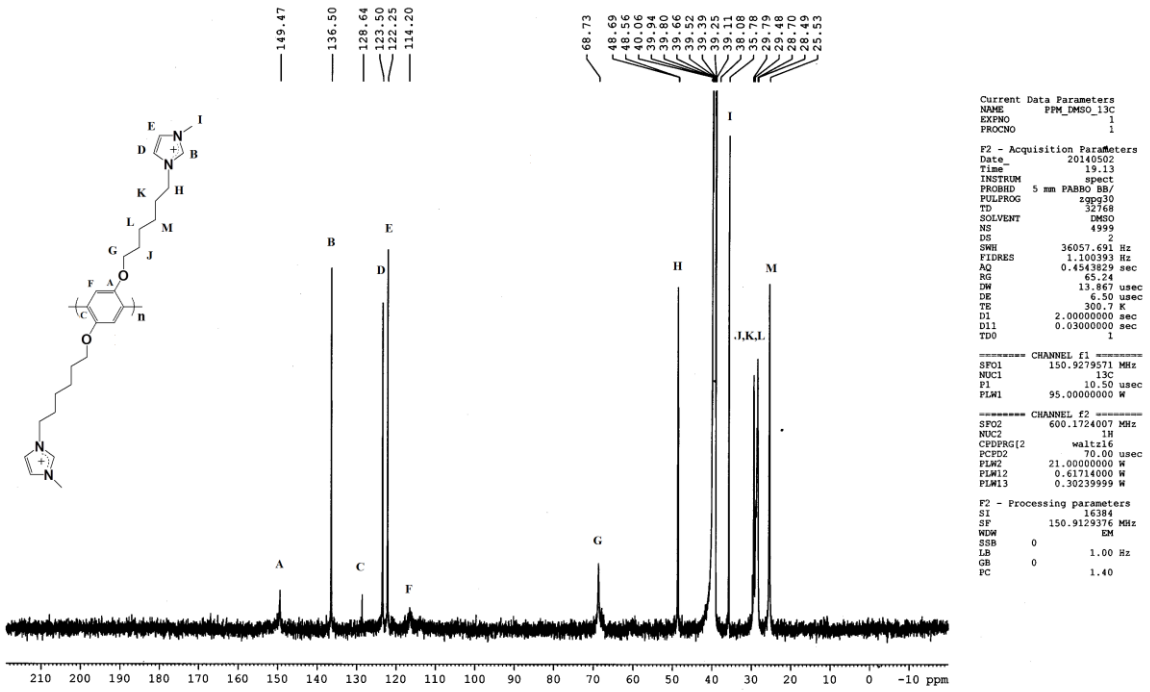

Figure A3.3 ^{13}C NMR (150 MHz, DMSO–*d6*) spectrum of PMI**.**

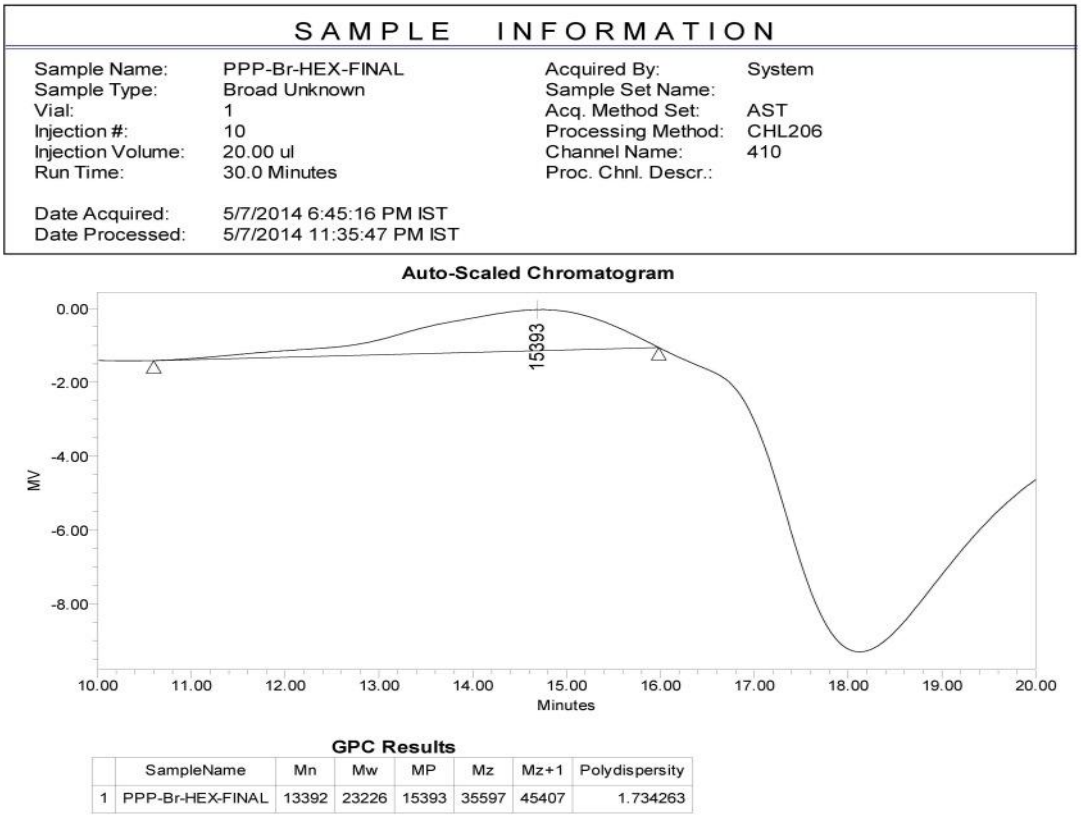

GPC Results

	SampleName	Mn	Mw	MP	Mz	Mz+1	Polydispersity
1	PPP-Br-HEX-FINAL	13392	23226	15393	35597	45407	1.734263

Figure A3.4. GPC Chromatogram of PBr.

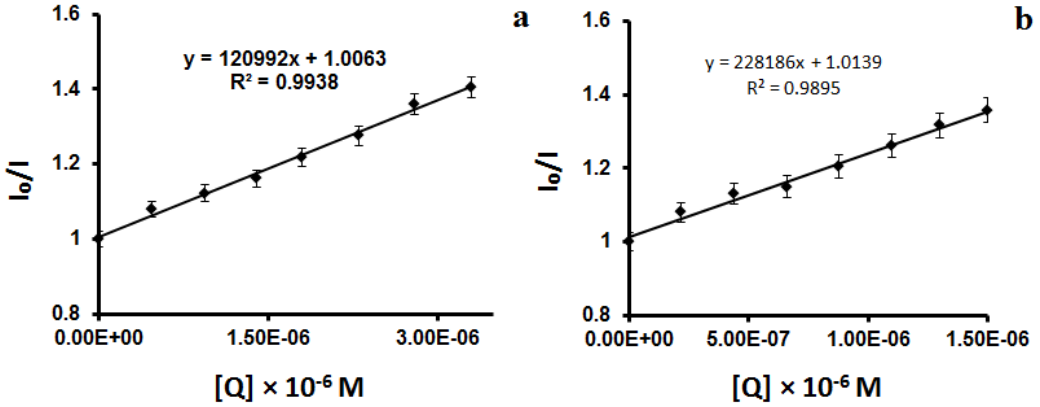

Figure A3.41 Stern-Volmer plots for SDBS and SDS.

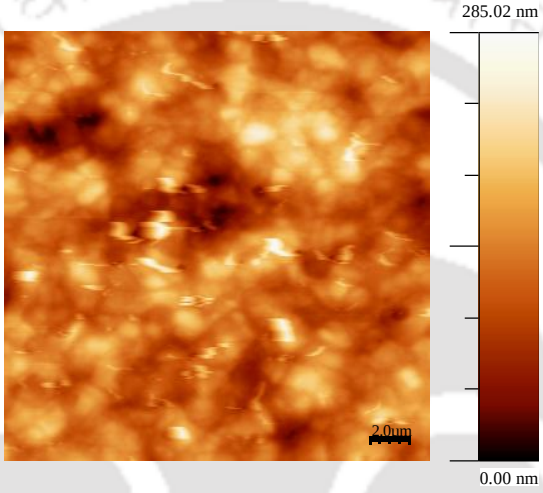

Figure A3.5 AFM image of PMI−SDS hydrogel on glass substrate were examined *via* the tapping model.

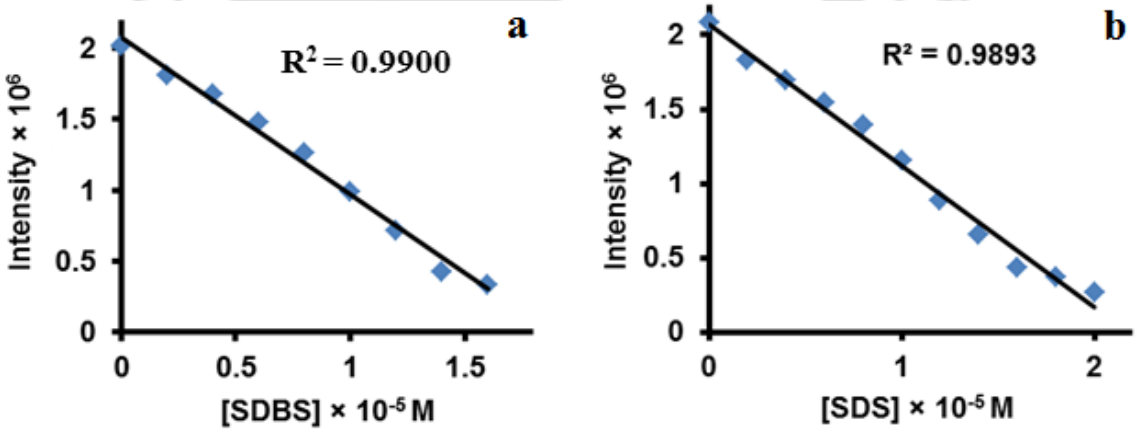

Figure A3.6 Calibration curve of PMI (2×10^{-5} M) as a function of (a) SDBS and (b) SDS concentration.

Chapter 4

Ultrasensitive Detection of Nitroexplosive – Picric Acid via Conjugated Polyelectrolyte in Aqueous Media and Solid Support

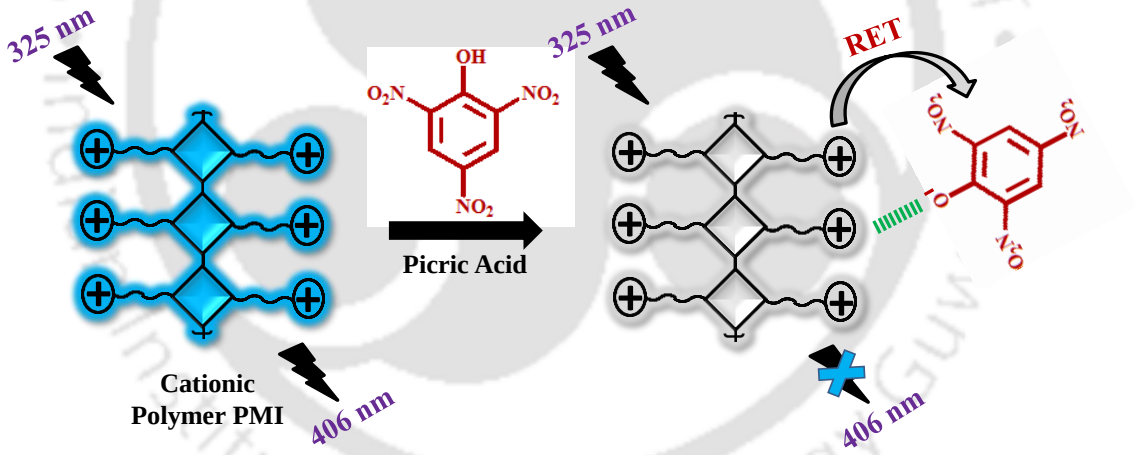

Hussain, S.; Malik, A. H.; Afroz, M. A.; Iyer, P. K. *Chem. Commun.* **2015**, *51*, 7207−7210.

Abstract

The fluorescence−amplified detection of trinitrophenol/picric acid (TNP/PA), a stronger nitroexplosive and a serious environmental pollutant is achieved at parts per trillion (ppt) levels for the first time using conjugated polyelectrolyte PMI. The polymer PMI displayed substantial fluorescence quenching exclusively for PA with very high Stern−Volmer constant (K_{sv}) value of 0.1×10^{8} M^{-1} and a very low limit of detection value 0.56×10^{-9} M (128 ppt) in 100% aqueous media. Formation of ground state charge transfer complex, resonance energy transfer as well as favorable electrostatic interaction between PMI and PA were the key aspects for unprecedented selectivity and remarkable sensitivity of PMI towards PA. Paper strips test using simple Whatman paper and contact mode detection using PMI−doped chitosan film makes this method simple, portable and cost−effective in order to monitor environmental contamination and terrorist threats rapidly.

4.1 Introduction

The rapid and selective detection of nitroexplosives is an imperative challenge with respect to national security and environmental protection.[1] Among various nitroaromatics, 2,4,6−trinitrotoluene (TNT), 2,4−dinitrotoluene (2,4−DNT), 2,6−dinitrotoluene (2,6−DNT) and 2,4,6−trinitrophenol/picric acid (TNP/PA) are the primary constituents of industrial explosives, found in several unexploded land mines worldwide.[2] Picric acid (PA) was an extensively used explosive up to World War−I due to its superior explosive power compared to its well−known counterpart TNT even at picomolar concentrations. Additionally, it remains a serious environmental pollutant generated from leather, pharmaceutical, chemical and dye industries.[3] Owing to the high solubility of PA in water, it easily contaminates soil and groundwater and is liable for acute health effects like strong irritation to the skin/eye and potential damage to respiratory organs.[4,5] During metabolic processes, PA transforms into picramic acid (2−amino−4,6−dinitrophenol), which has ten times more mutagenic activity than PA.[6] Hence, the development of reliable, selective and sensitive methods to detect PA to prevent terrorist threats and environmental contamination is highly significant in the present context.

Although detection of explosives has been performed with sophisticated instruments,[2] they suffer primarily from low selectivity, portability and on−field use issues making them unviable and expensive. Fluorescence−based detection of nitroexplosives is gaining attention due to their simplicity, high sensitivity, short response time and viability both in solution and solid phase.[7−12] In this regard, numerous sensors for explosives based on polymers,[13−16] metal–organic frameworks,[17−20] self−assemblies,[21,22] nanoaggregates,[23−26] etc. have been designed. However, due to similar electron affinities of nitroaromatics, the development of a reliable and effective chemosensor for PA with high selectivity and sensitivity remains a challenging task. Conjugated polymers (CPs) have proven to be excellent candidates for the detection of nitroexplosives due to their excellent molar absorptivity, good film forming ability, high quantum efficiency and amplified signal responses.[1,14,27−31] In recent years, few approaches to design CP based sensors for detection of PA have been reported.[16,32−34] However, most of them work in organic media with lesser detection limit, low selectivity and moderate quenching efficiencies. Interference by other nitroexplosives is another key problem associated with the existing systems due to the absence of specific receptors for PA.[14,16] This was the motivation to

develop a sensitive platform based on CPs with an specific receptor for the amplified and selective detection of PA both in the aqueous phase as well as solid support.

Herein, a highly selective detection of PA at parts per trillion (ppt) levels using a conjugated polyelectrolyte (PMI) in aqueous media as well as by contact mode/instant spot testing *via* paper strips and efficient fluorescent films is reported for the first time.

The cationic CP PMI was developed using post−functionalization polymerization method.[35] Imidazolium groups strapped along the side chain of PMI provided good solubility in polar solvents like DMSO, methanol and water and also acts as a specific recognition site for PA due to favorable electrostatic attraction. The fluorescence signal amplification properties of CPs encouraged us to utilize PMI for specific recognition of PA at very low concentrations.[36]

4.2 Experimental

Caution!

The nitroaromatics used in the study, especially picric acid, are highly explosive in nature and should be handled cautiously in small quantities with safety measures to avoid any explosion.

4.2.1 Materials and measurements

The structure of various analytes used in the experiments are shown in Scheme 4.1 Nitroexplosives *viz*. 2,6−DNT, 2,4−DNT, 4−NT, 1,3−DNB and chitosan were purchased from Aldrich Chemicals. Picric acid was purchased from Loba Chemie. All other chemicals and reagents were purchased from Alfa−Aesar and/or Merck and were used without further purification. Milli−Q water was used in all the experiments. UV/visible spectra were recorded on a Perkin Elmer Lambda−25 spectrophotometer. Photoluminescence spectra were recorded on a Horiba Fluoromax−4 spectrofluorometer using 10 mm path length quartz cuvettes with a slit width of 2 nm at 298 K. Electrochemical measurements were performed using a CH instruments Model 700D series electrochemical workstation. Paper strip tests were performed using Whatman® qualitative filter paper, Grade 1. Time resolved fluorescence studies were performed in an Edinburgh Instruments Life Spec II instrument.

4.2.2 Synthesis of M1 and PBr

Synthesis of monomer M1 and polymer PBr was carried out using a previously established procedure shown in chapter 2.[37−39]

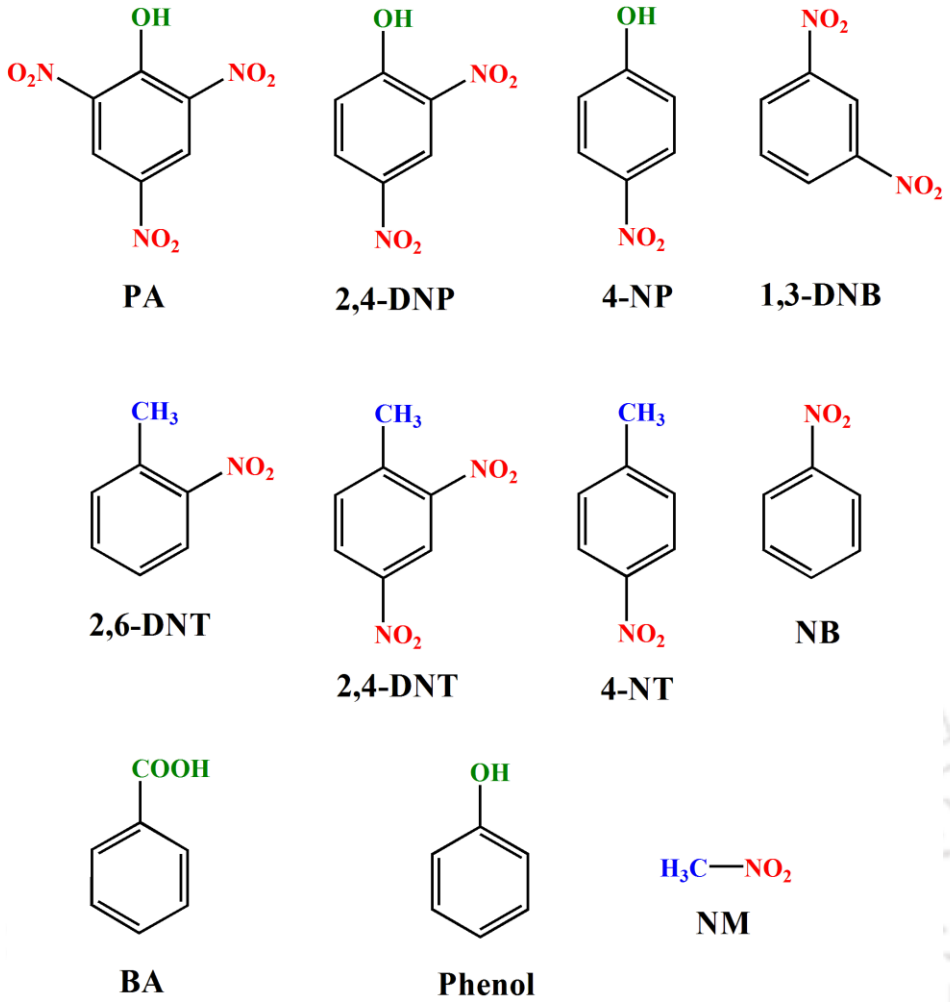

Scheme 4.1: Structures of various nitroexplosives and electron deficient compounds used in the sensing experiment.

4.2.3 Synthesis of PMI

The polymer PMI was prepared according to the previously reported procedure[35] shown in chapter 3 (Scheme 4.2). In a 100 mL round−bottom flask, PBr (0.12 mmol, 1eq.) and excess 1−methyl imidazole were taken and heated under stirring condition in an oil bath at 80 ºC for 24 h. The reaction mixture was then poured into excess chloroform and stirred for 1 h to observe precipitates. The process was repeated twice to remove excess 1−methyl imidazole and PBr. The precipitates were then filtered out and dried to obtain brownish colored product. Yield: 85%

^{1}H NMR (600 MHz, DMSO−d_6, δ): 9.38 (b, 2H), 7.75 (b, 2H), 7.69 (b, 2H), 7.02 (b, 2H), 4.18 (b, 2H), 3.87 (b, 10H), 1.90 (b, 4H), 1.76 (b, 4H), 1.29 (b, 4H), 1.24 (b, 4H).

^{13}C NMR (150 MHz, DMSO−d_6, δ): 149.47, 136.50, 128.64, 123.50, 122.25, 114.20, 68.73, 48.69, 35.78, 29.79, 28.70, 28.49, 25.53.

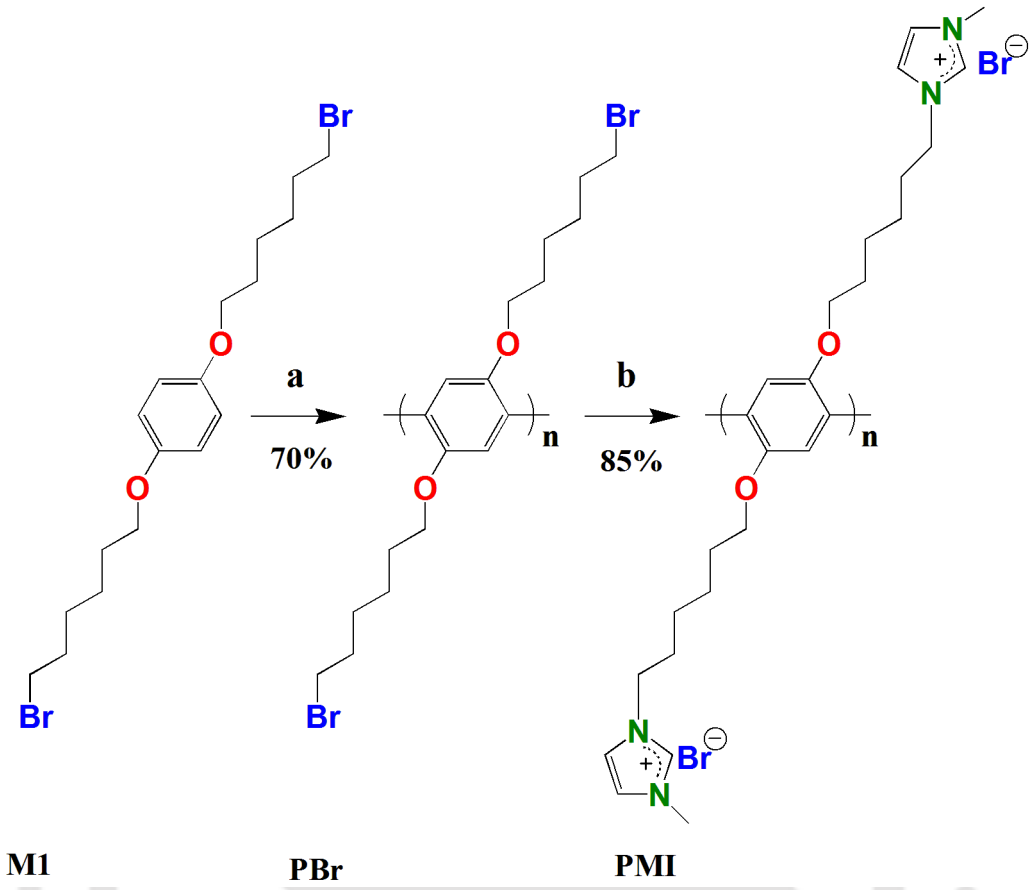

Scheme 4.2 Synthesis of cationic polymer PMI. (a) $FeCl_3$, nitrobenzene, RT, 36 h (b) 1−methyl imidazole, 80ºC, 24 hr.

4.2.4 Sensing studies in aqueous solution

Stock solution of the polymer PMI and other analytes *viz.* nitrobenzene, nitromethane, benzoic acid, phenol, 4–nitrophenol, 2,4–dinitrophenol were prepared in Milli–Q water at concentrations of 1×10^{-3} M and 1×10^{-4} M, respectively. Stock solution of other nitroaromatics *viz.* 2,6–dinitrotoluene, 2,4–dinitrotoluene, 4–nitrotoluene, 1,3–dinitrobenzene were prepared at concentrations of 1×10^{-4} M in HPLC grade THF. The absorption measurements and fluorescence titrations of the polymer PMI with different analytes were carried out by sequentially adding 1 µL to 3 mL aqueous solution containing 2×10^{-5} M PMI in a quartz cuvette (1 cm × 1 cm). The absorption and fluorescence spectra of the resultant mixtures were then recorded after mixing thoroughly at room temperature.

4.2.5 Calculation of overlap integral values and Förster radius

To identify the extent of energy transfer, overlap integral values for all analytes were calculated using the equation[40] shown below;

$$J(\lambda) = \int_0^\infty F_D(\lambda)\, \varepsilon_A(\lambda)\lambda^4 d\lambda$$

where, F_D (λ) denotes the corrected fluorescence intensity of donor in the range of λ to λ + Δλ with the total intensity normalized to unity, ε_A is molar absorptivity of the acceptor at λ in M^{-1} cm^{-1}. The Förster distance R_0 was also calculated for PMI–PA interaction using the expression shown below;

$$R_0 = 0.211[(J)Q(\eta^{-4})(k^2)]^{1/6}$$

where, J is the degree of spectral overlap between donor fluorescence spectrum and the acceptor absorption spectrum, Q is fluorescence quantum yield of the donor (without acceptor), η is the refractive index of the medium and k^2 is the dipole orientation factor usually taken as 0.667.

4.2.6 Preparation of fluorescence test strips

Test strips were prepared by dip−coating Whatman filter paper (70 mm diameter) in the methanolic solution of PMI (10^{-4} M) followed by removal of solvent in an air stream. PMI coated filter papers were then cut into desired number of pieces (1 cm × 1 cm) and used as solid support for the surface sensing purpose.

4.2.7 Preparation of fluorescence film and its sensing towards PA

In a 50 mL beaker containing PMI (5 mg) and purified chitosan (95 mg), 10 mL Milli−Q water and 100 µL of acetic acid were added followed by continuous stirring for about 15 min to ensure complete dissolution of chitosan. This led to the formation of highly viscous liquid which was spread on pre-cleaned glass plate/petri dish and dried for 2 h at 50 ºC in a vacuum oven. A homogeneous transparent film was obtained that could be easily lifted using forceps for sensing purposes.

For contact mode sensing, 2 mg of PA was rubbed with the left hand thumb and brushed properly to remove all visible PA particles. Left thumb was then pressed onto the film for 10 sec, kept aside and the impression observed under UV light. Right hand thumb was used as control without using PA. Similar procedure was applied for studying selectivity of the film. 5 mg of each solid analyte was rubbed with fingertip and brushed properly to remove all visible particles before pressing it onto the film. For liquid samples, 2 drops of each analyte was casted on fingertip followed by air drying and pressed onto the film.

4.2.8 Calculation of detection limit

For calculating the detection limit, different samples of PMI (2×10^{-5} M) each containing PA (0 nM, 5 nM, 10 nM, 15 nM, 20 nM, 25 nM, 30 nM, 35 nM and 40 nM) were prepared separately and fluorescence spectrum was then recorded for each sample by exciting at 325 nm. The detection limit plot for PA was obtained by plotting the change in the fluorescence intensity *vs* concentration of PA. The curve demonstrates a linear relationship and the correlation coefficient (R^2) value *via* linear regression analysis was calculated to be 0.9980. The limit of detection (LOD) was then determined using the equation 3σ / K, where σ denotes the standard deviation for the intensity of PMI in the absence of picric acid and K represents slope of the equation.

4.2.9 Cyclic voltammetry

The electrochemical study for PMI was performed using three−electrode cell at room temperature in inert atmosphere using argon. A glassy carbon electrode was used as working electrode. Pt wire and the saturated Ag/Ag^+ electrode were used as counter and reference electrodes, respectively. The Fc^+/Fc couple was used as an internal reference with 0.1M tetrabutylammonium hexafluorophosphate ($TBAPF_6$) as supporting electrolyte in CH_3CN. Noticeable reduction potential was observed for PMI (E_{red} = −0.736 V) and LUMO (−4.364 eV) energy level was determined through onset calculation according to the method[41] reported for conjugated polymers.

4.2.10 Computational studies

The monomer of PMI (without two Br^- anions) was used as a model to obtain energy optimized structures by density functional theory (DFT) using B3LYP functional and 6−31G basis set in Gaussian 03[42] program. Picric acid, its corresponding picrate ion and various other nitroexplosives have also been optimized for the analysis of charge transfer phenomenon.

4.3 Result and discussion

4.3.1 Sensing Studies

Cationic polymer PMI shows absorption and emission maximum at 325 nm and 406 nm (325 nm excitation) in aqueous media. Sensing studies were performed in aqueous solution and HEPES buffer (pH = 7, 10 mM), and the results were comparable. To investigate the interaction of nitroexplosives with PMI, fluorescence quenching titration

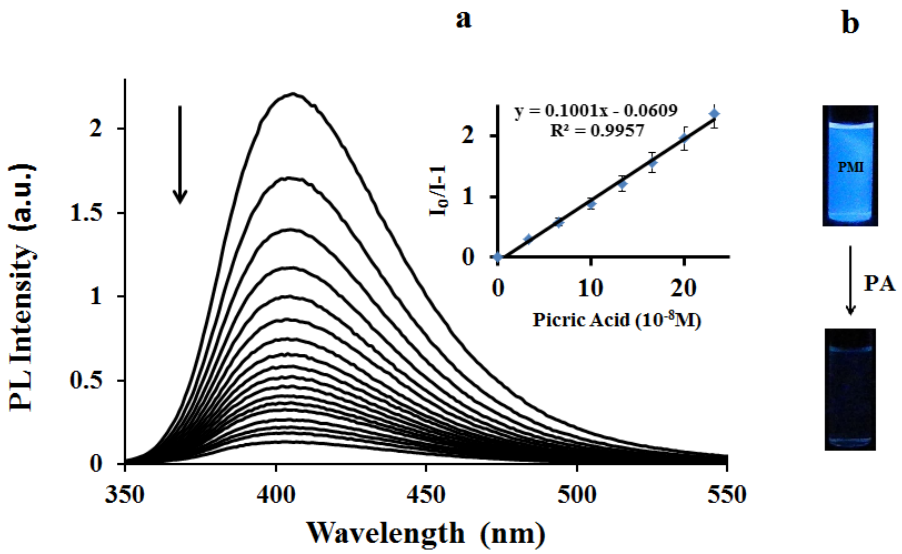

Figure 4.1 (a) Photoluminescence spectra of PMI (2×10^{-5} M) with increasing concentration of PA in aqueous media. ~95% quenching was observed at 6.67×10^{-7} M of PA. Inset: the Stern–Volmer plot of PMI upon addition of PA. (b) Color of PMI solution in water before and after adding PA (irradiation under a UV lamp at 365 nm).

was performed by adding aliquots of various analytes to the aqueous solution of PMI. Immediate fluorescence quenching of ~25% was observed upon adding just 3.3×10^{-8} M solution of PA, which is further quenched ~95% upon adding 6.67×10^{-7} M PA solution (Figure 4.1a). The disappearance of the blue luminescence of PMI in the presence of PA was clearly visible under UV light (Figure 4.1b). The efficiency of quenching studied by linear fitting of the Stern–Volmer plot (K_{SV}) was found to be 0.1×10^{8} M^{-1} (inset of Figure 4.1a), confirming the very high sensitivity of PMI towards PA. The limit of detection (LOD) calculated (Figure 4.2) for PA was 56.11×10^{-11} M (128 ppt), which is the best value reported in the literature (Table A4.1).

4.3.2 Competitive Studies

Other interfering analytes, *viz.* 2,6–DNT, 2,4–DNT, 4−nitrotoluene (4–NT), 1,3–dinitrobenzene (1,3–DNB), nitrobenzene (NB), nitromethane (NM), benzoic acid (BA) and phenol did not influence the fluorescence emission of PMI even in large quantities (Figure 4.3). It is evident (Figure 4.4a) that at lower PA concentrations, the S–V plot is close to linear, whereas at higher concentrations it deviates from linearity and increases nearly exponentially demonstrating an amplified quenching process. The non–linear nature of the S–V plot also suggests self−absorption or an additional effective energy

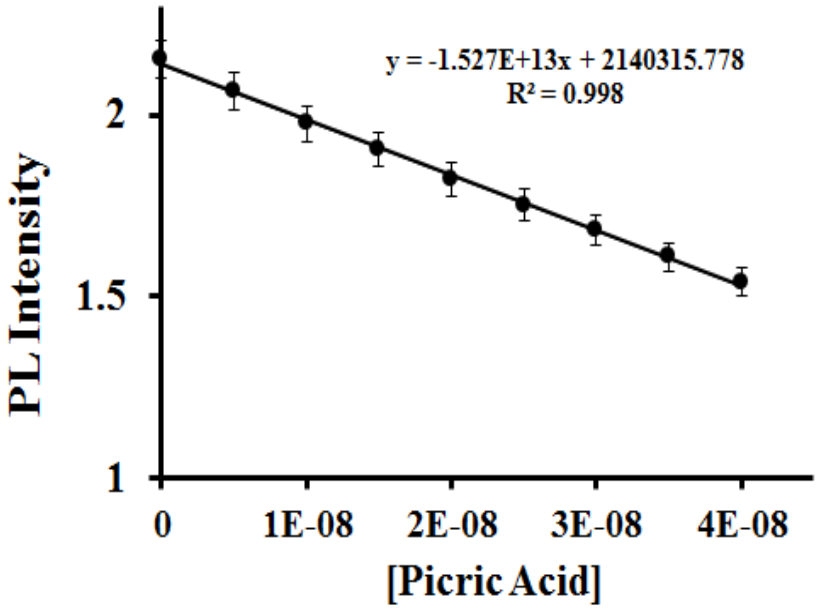

Figure 4.2 Fluorescence intensity of PMI (2×10^{-5} M) in aqueous solution as a function of PA concentration.

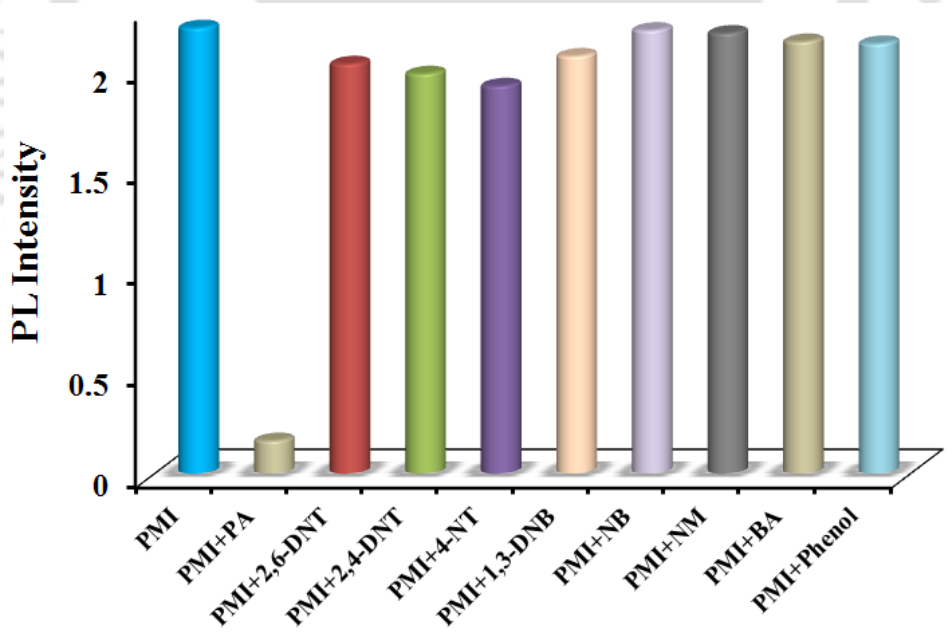

Figure 4.3 Bar diagram depicting the effect of various analytes (6.67×10^{-6} M) on fluorescence emission of PMI (2×10^{-5} M) in aqueous media.

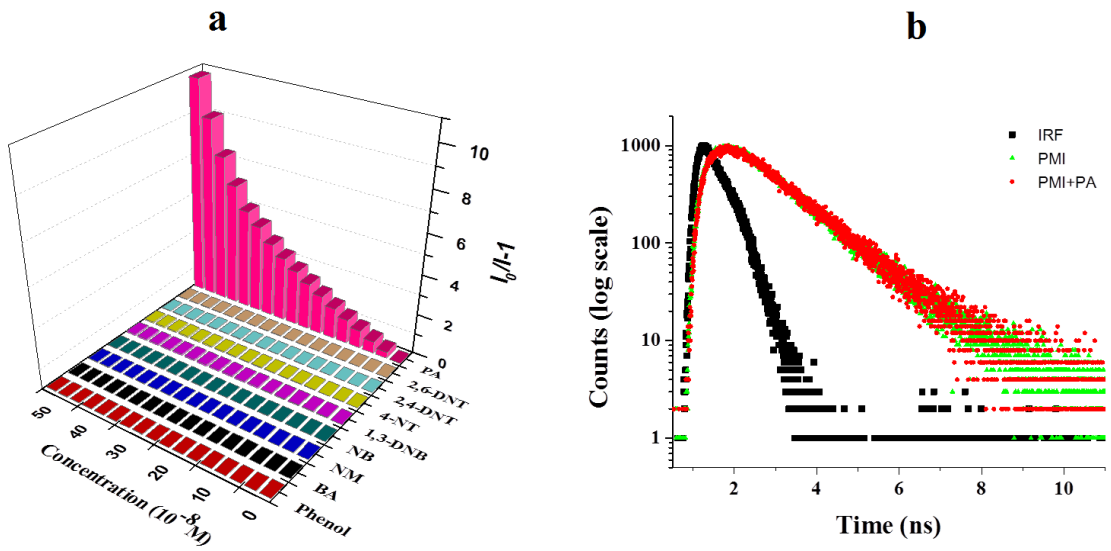

Figure 4.4 (a) Stern–Volmer plots for different analytes in water. (b) Lifetime decay profile for PMI with PA (λ_{ex} = 308 nm, monitored at 406 nm).

transfer mechanism.[1,43] However, all other analytes showed only a linear increase in S–V plots (Figure 4.4a). The significantly higher K_{SV} value obtained for PA compared to other analytes confirms predominant selectivity and exceptional quenching ability of PA towards PMI. Time resolved fluorescence studies validated the mechanism of quenching as static and further confirms the ground state complex formation since the fluorescence lifetime of PMI remains unchanged in the presence of PA[10,12] (Figure 4.4b). For practical applications, the selective recognition of PA in an aquatic system is in great demand. In this regard, we have performed titration experiments in the presence of various nitroaromatics and electron–deficient analytes to monitor the selectivity of PMI for PA (Figure 4.5 & Figure A4.1–A4.8). These plots demonstrate that PMI can detect PA even in the presence of other interfering analytes. Since most of the PA chemosensors suffer largely from the interference of other electron–deficient compounds, the higher selectivity of PMI provides a very rare and unique platform for the highly selective detection of PA in aqueous media.

4.3.3 Sensing mechanism

Encouraged by these results, the origin of remarkable selectivity was also investigated. The high quenching efficiency of PA compared to other nitrocompounds is explained *via* deprotonation of the strongly acidic phenolic –OH group in aqueous media, resulting in anion exchange with the polymer PMI.[11] The complex thus formed may facilitate the

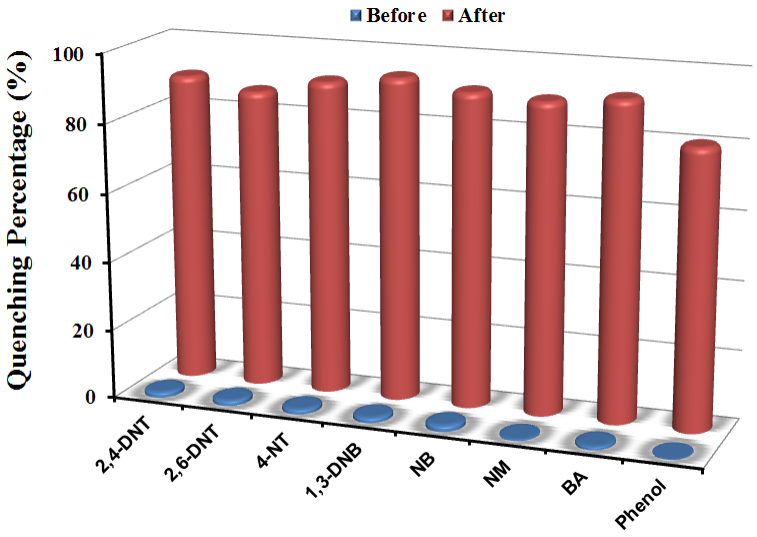

Figure 4.5 Percentage fluorescence quenching of PMI (2×10^{-5} M) with several analytes (6.67×10^{-7} M) in aqueous media before and after the addition of PA (6.67×10^{-7} M)

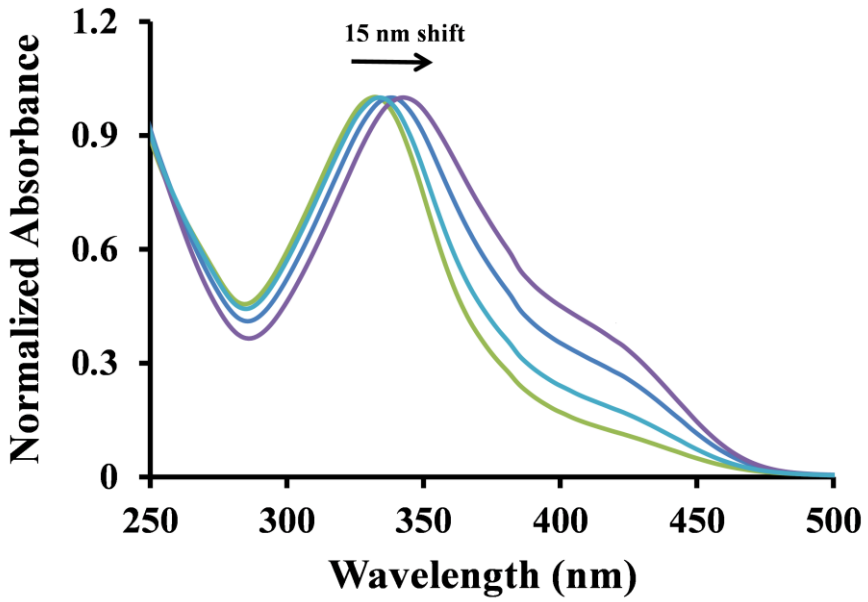

Figure 4.6 UV–Vis spectra of PMI upon addition of PA in water. The red shift in the spectra indicates the complex formation in ground state.

ground state electron transfer between PMI and picrate. The UV–Vis spectrum of PMI displayed a significant red shift of ~15 nm upon gradual addition of PA (Figure 4.6) in aqueous media, suggesting the formation of a ground state non-fluorescent complex[10,11] between PMI and PA, which is also in agreement with the lifetime studies. To comprehend the mode of interaction between PMI and PA, cyclic voltammetry studies were carried out that displayed noticeable reduction potential for PMI (Figure A4.9).

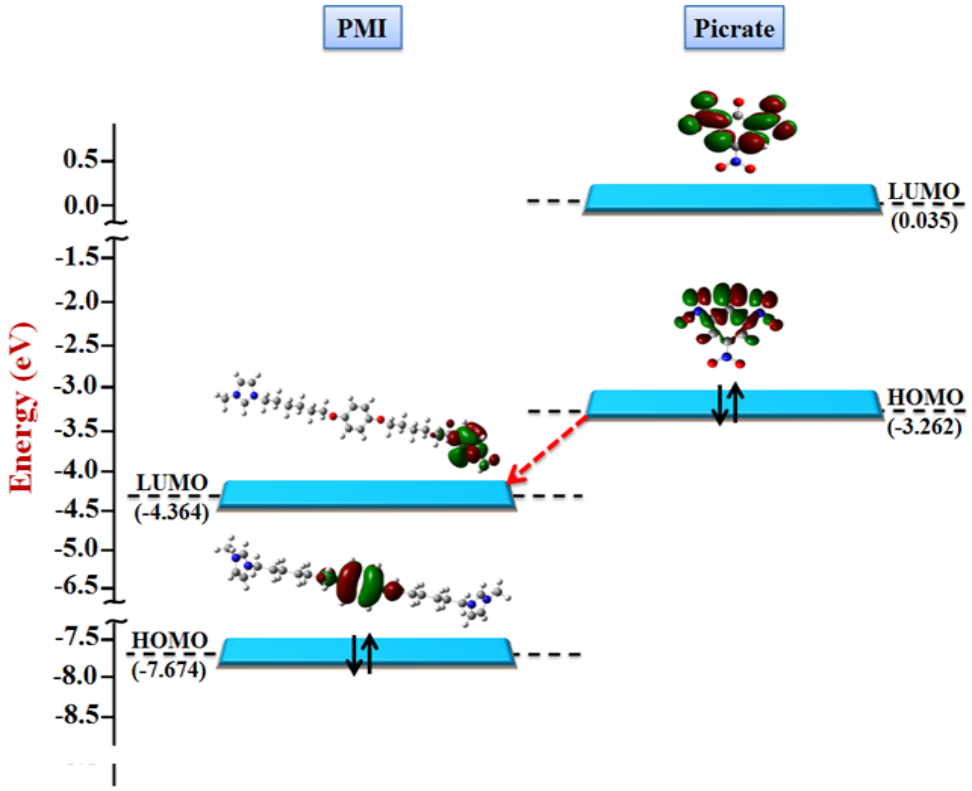

Figure 4.7 Schematic representation showing possibility of ground state electron transfer from HOMO of the picrate to the LUMO of PMI.

The lowest unoccupied molecular orbital (LUMO) value calculated for PMI (–4.364 eV) was found to be lower than the HOMO of picrate (–3.262 eV).[10-11] Hence, there is a strong possibility of ground state electron transfer from the HOMO of the picrate to the LUMO of positively charged PMI (Figure 4.7), resulting in high quenching efficiency. However, HOMOs of other nitroexplosives were found to have low energy levels than the LUMO of the sensor molecule (PMI), thereby discarding the possibility of ground state electron transfer, resulting in low quenching efficiencies (Figure A4.10).

The high sensitivity of PMI towards PA and the non–linear nature of the S–V plot for PA suggests that an energy transfer process may also be involved in the quenching process.[10] There is a possibility of RET from the fluorophore (donor) to non–emissive analytes (acceptor) if the emission band of the donor overlaps efficiently with the absorption band of the acceptor. Since RET has moderately higher efficiency compared to the electron transfer process,[23] it can significantly enhance the quenching efficiency *viz–a–viz*

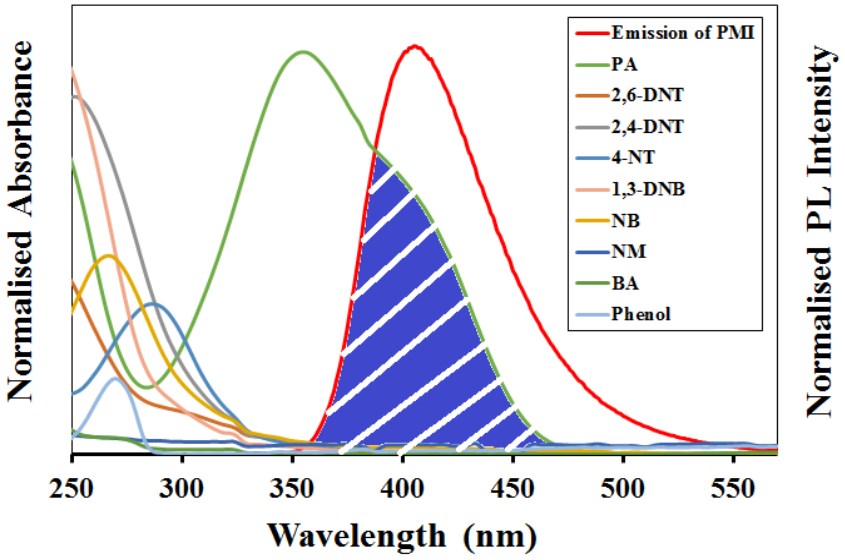

Figure 4.8 Spectral overlap between the normalized emission spectrum of PMI and normalized absorption spectra of various electron–deficient compounds.

sensitivity. Figure 4.8 confirms a large overlap between the absorption spectrum of PA and the emission spectrum of PMI, resulting in dramatic florescence quenching unlike other analytes that have almost no overlap. To identify the extent of energy transfer, overlap integral values for all analytes were calculated. The integral value J (λ) observed for PA was highest (2.63×10^{14} M^{-1} cm^{-1} nm^4) compared to other analytes by ~100 times (Table 1). The Förster distance R_0 value obtained for PMI–PA interaction was 35.30 Å, which falls well in the range of 10–100 Å applicable for RET. Thus, unprecedented sensitivity and remarkable selectivity of PMI towards PA in 100% aqueous media is a unique feature accountable to the well–known ‘‘molecular–wire effect’’, formation of a ground state charge transfer complex as well excited state energy transfer process. However, both theoretical and experimental studies suggest that charge transfer is a predominant process.

Finally, a control experiment was performed to elucidate the unprecedented selectivity of PMI towards PA using nitro–compounds comprising only one hydroxyl group, *viz.* PA, 4–nitrophenol (NP) and 2,4–dinitrophenol (2,4–DNP). The fluorescence quenching efficiencies of these analytes follow the order PA > DNP > NP (Figure 4.9), which are in good agreement with the acidity of these nitrocompounds (PA > DNP > NP). Since PA is a strong acid with a pKa value of ~0.38, it can easily dissociate in aqueous medium, which can accelerate the electrostatic interactions between cationic PMI and PA. TFA, a stronger acid than PA, had no effect on the emission of PMI, thereby negating the

Table 1. Overlap integral J(λ) values obtained for various analytes.

Compounds	J (λ) values (M^{-1} cm^{-1} nm^4)
PA	2.63×10^{14}
2,6–DNT	3.90×10^{12}
2,4–DNT	1.54×10^{12}
4–NT	1.98×10^{12}
1,3–DNB	5.16×10^{12}
NB	4.86×10^{12}
NM	8.32×10^{12}
BA	1.30×10^{12}
Phenol	6.24×10^{12}

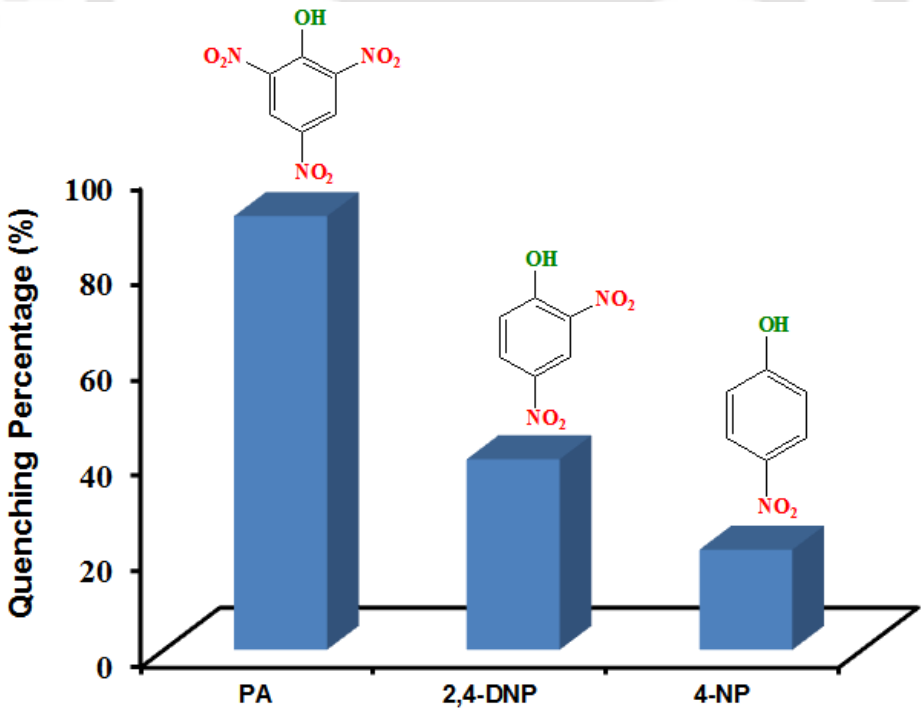

Figure 4.9 Comparison of percentage fluorescence quenching obtained on addition of PA, 2,4–DNP and 4–NP to the solution of PMI in water. Concentration of PMI and each analyte were 2×10^{-5} M and 6.67×10^{-7} M, respectively.

possibility of quenching by the acidity effect (Figure A4.11). Consequently, it can be concluded that homogeneity of both PMI and PA in aqueous media is another key factor involved, which brings PMI and PA in close proximity *via* electrostatic attraction and facilitates efficient charge transfer and/or energy transfer mechanisms, thereby providing excellent and unprecedented fluorescence quenching towards PA.

4.3.4 On–site detection

To realize practical applications with PMI, the sensing of explosives at the actual site is of immense significance. In this context, the instant surface sensing of explosives by preparing PMI coated fluorescent test strips using Whatman filter paper was performed. To check the sensitivity of PMI, the PA solutions with varying concentrations (10^{-3}–10^{-11} M) were spotted onto the different test strips. A solvent blank was also spotted as control. For better reliability, each deposition was performed taking a 10 µL volume, thereby producing a spot of 0.5 cm in diameter. After drying, the filter paper was visualized under UV light (lamp excited at 365 nm). Dark spots of different strengths were observed, which vary with the concentration of PA (Figure 4.10A). The minimum amount of PA detectable by the naked eye was 10 mL (1×10^{-9} M) providing a very low detection limit of ~2.29 pg, which is among the best reported values.[12,21,44–46] Other interfering analytes

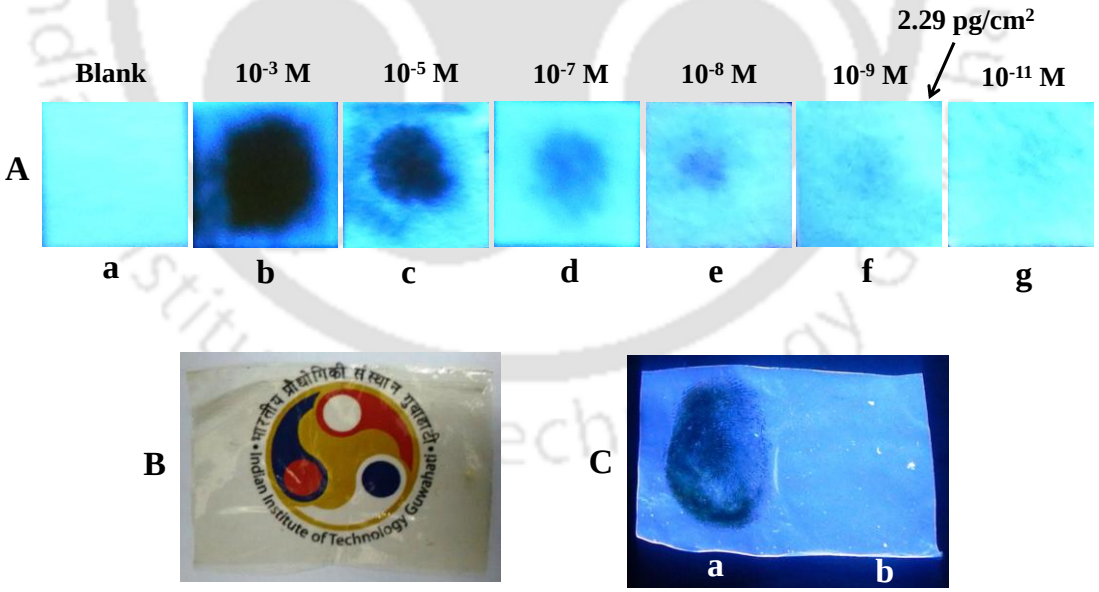

Figure 4.10 (A) Color of fluorescent test strips under UV light (a) before and after (b, c, d, e, f and g) adding 10 µL of various concentrations of PA solution. (B) PMI–doped transparent CS film in day light. (C) Visualization of PMI–doped CS fluorescent film under UV light. (a) Dark spot of PA residual left thumb impression. (b) Right thumb impression as control (lamp excited at 365 nm).

were found to be ineffective towards paper strip test confirming the high selectivity of PMI towards PA (Figure A4.12). These results validate the unprecedented efficacy of the test strips for on–site instant and accurate detection of PA. PA can contaminate the human body, apparel and other materials in the environment during manufacturing of rocket fuel, preparation and packaging of fireworks. Hence, contact mode detection of PA has huge demand in the field of analytical and forensic sciences, yet no efficient methods exist. To achieve this objective, we prepared a transparent fluorescent film by doping 5% PMI with commercial chitosan (CS) (Figure 4.10B) and described its fluorescence response towards PA *via* contact mode. CS is an ideal substrate due to its excellent film–forming ability, ease of modification, economy, ready availability and environmental biocompatibility.[47,48] Since PA is a strong acid while CS film is rich in amino groups, the affinity of PA towards CS film is enhanced due to electrostatic interaction, thereby increasing its detection ability. The image (Figure 4.10C) under ultraviolet light confirms that PMI–doped CS film can detect even trace residues of PA very clearly, providing an exceptional, cheap and reliable platform for PA detection on a solid support. Other common interfering analytes did not cause any significant change in the fluorescence of film even in higher quantities (Figure A4.13).

4.4 Conclusion

In conclusion, the fluorescence–amplified detection of PA at parts per trillion levels in 100% aqueous media as well as on solid based platforms is achieved using a cationic conjugated polyelectrolyte PMI for the first time. PMI exhibits remarkable selectivity even in the presence of most commonly interfering nitroaromatics. The formation of a ground state non-fluorescent complex, RET as well as favorable electrostatic interaction between PMI and PA are the key aspects for unprecedented selectivity and remarkable sensitivity of PMI towards PA. A paper strip test and a contact mode sensing platform using PMI–doped chitosan film confirm this method as simple, portable and cost–effective in order to prevent environmental contamination and terrorist threats rapidly under very realistic conditions.

References

(1) Salinas, Y.; Martínez–Máñez, R.; Marcos, M. D.; Sancenón, F.; Costero, A. M.; Parra, M.; Gil, S. *Chem. Soc. Rev.*, **2012**, *41*, 1261.

(2) Germain, M. E.; Knapp, M. J. *Chem. Soc. Rev.*, **2009**, *38*, 2543.

(3) Akhavan, J. *Chemistry of Explosives*, Royal Society of Chemistry, 2nd ed., 2004.

(4) Ashbrook, P. C.; Houts, T. A. *Chem. Health Safety*, **2003**, *10*, 27.

(5) *Innovative Treatment Technologies: Annual Status Report*, U.S. Environmental Protection Agency: Washington, D.C., 8th ed., 1996.

(6) Wollin, K.–M.; Dieter, H. H.; *Arch. Environ. Contam. Toxicol.*, **2005**, *49*, 18.

(7) Peng, Y.; Zhang, A.–J.; Dong, M.; Wang, Y.–W. *Chem. Commun.*, **2011**, *47*, 4505.

(8) Dey, N.; Samanta, S. K.; Bhattacharya, S. *ACS Appl. Mater. Interfaces*, **2013**, *5*, 8394.

(9) Dinda, D.; Gupta, A.; Shaw, B. K.; Sadhu, S.; Saha, S. K. *ACS Appl. Mater. Interfaces*, **2014**, *6*, 10722.

(10) Mukherjee, P. S.; Acharyya, K. *Chem. Commun.*, **2014**, *50*, 15788.

(11) Roy, B.; Bar, A. K.; Gole, B.; Mukherjee, P. S. *J. Org. Chem.*, **2013**, *78*, 1306.

(12) Bhalla, V.; Gupta, A.; Kumar, M.; Rao, D. S. S.; Prasad, S. K. *ACS Appl. Mater. Interfaces*, **2013**, *5*, 672.

(13) Dong, W.; Fei, T.; Palma–Cando, A.; Scherf, U. *Polym. Chem.*, **2014**, *5*, 4048.

(14) Sohn, H.; Sailor, M. J.; Magde, D.; Trogler, W. C. *J. Am. Chem. Soc.*, **2003**, 3821.

(15) Kartha, K. K.; Babu, S. S.; Srinivasan, S.; Ajayaghosh, A. *J. Am. Chem. Soc.*, **2012**, *134*, 4834.

(16) Xu, B.; Wu, X.; Li, H.; Tong, H.; Wang, L. *Macromolecules*, **2011**, *44*, 5089.

(17) Nagarkar, S. S.; Joarder, B.; Chaudhari, A. K.; Mukherjee, S.; Ghosh, S. K. *Angew. Chem. Int. Ed. Engl.*, **2013**, *52*, 2881.

(18) Lan, A.; Li, K.; Wu, H.; Olson, D. H.; Emge, T. J.; Ki, W.; Hong, M.; Li, J. *Angew. Chem. Int. Ed. Engl.*, **2009**, *48*, 2334.

(19) Bhalla, V.; Pramanik, S.; Kumar, M. *Chem. Commun.*, **2013**, *49*, 895.

(20) Gong, Y.–N.; Jiang, L.; Lu, T.–B.; *Chem. Commun.*, **2013**, *49*, 11113.

(21) Bhalla, V.; Kaur, S.; Vij, V.; Kumar, M. *Inorg. Chem.*, **2013**, *52*, 4860.

(22) Ma, J.; Lin, T.; Pan, X.; Wang, W. *Chem. Mater.*, **2014**, *26*, 4221.

(23) Vij, V.; Bhalla, V.; Kumar, M. *ACS Appl. Mater. Interfaces*, **2013**, *5*, 5373.

(24) Sk, M. P.; Chattopadhyay, A. *RSC Adv.*, **2014**, *4*, 31994.

(25) Hou, X.–G.; Wu, Y.; Cao, H.–T.; Sun, H.–Z.; Li, H.–B.; Shan, G.–G.; Su, Z.–M. *Chem. Commun.*, **2014**, *50*, 6031.

(26) Feng, H.–T.; Zheng, Y.–S.; *Chem. Eur. J.* **2014**, *20*, 195.

(27) Toal, S. J.; Trogler, W. C.; *J. Mater. Chem.*, **2006**, *16*, 2871.

(28) Wang, Y.; La, A.; Brückner, C.; Lei, Y. *Chem. Commun.*, **2012**, *48*, 9903.

(29) Ghosh, K. R.; Saha, S. K.; Wang, Z. Y. *Polym. Chem.*, **2014**, *5*, 5638.

(30) Gopalakrishnan, D.; Dichtel, W. R. *J. Am. Chem. Soc.*, **2013**, *135*, 8357.

(31) Sohn, H.; Calhoun, R. M.; Sailor, M. J.; Trogler, W. C. *Angew. Chem. Int. Ed. Engl.*, **2001**, *40*, 2104.

(32) Shaligram, S.; Wadgaonkar, P. P.; Kharul, U. K.; *J. Mater. Chem. A*, **2014**, *2*, 13983.

(33) Sang, N.; Zhan, C.; Cao, D.; *J. Mater. Chem. A*, **2015**, *3*, 92.

(34) Wei, W.; Lu, R.; Tang, S.; Liu, X. *J. Mater. Chem. A*, **2015**, *3*, 4604.

(35) Hussain, S.; Malik, A. H.; Iyer, P. K. *ACS Appl. Mater. Interfaces*, **2015**, *7*, 3189.

(36) McQuade, D. T.; Pullen, A. E.; Swager, T. M. *Chem. Rev. 2000*, *100*, 2537.

(37) Paul, G. S.; Sarmah, P. J.; Iyer, P. K.; Agarwal, P. *Macromol. Chem. Phys.*, **2008**, *209*, 417.

(38) van Breemen, A. J. J. M.; Herwig, P. T.; Chlon, C. H. T.; Sweelssen, J.; Schoo, H. F. M.; Benito, E. M.; de Leeuw, D. M.; Tanase, C.; Wildeman, J.; Blom, P. W. M.; *Adv. Funct. Mater.*, **2005**, *15*, 872.

(39) Saikia, G.; Singh, R.; Sarmah, P. J.; Akhtar, M. W.; Sinha, J.; Katiyar, M.; Iyer, P. K. *Macromol. Chem. Phys.*, **2009**, *210*, 2153.

(40) Lakowicz, J. R. *Principles of Florescence spectroscopy*, 3rd ed; Springer: Singapore, **2010**; pp 443–472.

(41) Cardona, M.; Li, W.; Kaifer, A. E.; Stockdale, D.; Bazan, G. C. *Adv. Mater.*, **2011**, *23*, 2367.

(42) Gaussian 03, Revision E.01, Frisch, M. J.; Trucks, G. W.; Schlegel, H. B.; Scuseria, G. E.; Robb, M. A.; Cheeseman, J. R.; Montgomery, J. A.; Jr., Vreven, T.; Kudin, K. N.; Burant, J. C.; Millam, J. M.; Iyengar, S. S.; Tomasi, J.; Barone, V.; Mennucci, B.; Cossi, M.; Scalmani, G.; Rega, N.; Petersson, G. A.; Nakatsuji, H.; Hada, M.; Ehara, M.; Toyota, K.; Fukuda, R.; Hasegawa, J.; Ishida, M.; Nakajima, T.; Honda, Y.; Kitao, O.; Nakai, H.; Klene, M.; Li, X.; Knox, J. E.; Hratchian, H. P.; Cross, J. B.; Bakken, V.; Adamo, C.; Jaramillo, J.; Gomperts, R.; Stratmann, R. E.; Yazyev, O.; Austin, A. J.; Cammi, R.; Pomelli, C.; Ochterski, J. W.; Ayala, P. Y.; Morokuma, K.; Voth, G. A.; Salvador, P.; Dannenberg, J. J.; Zakrzewski, V. G.; Dapprich, S.; Daniels, A. D.; Strain,

M. C.; Farkas, O.; Malick, D. K.; Rabuck, A. D.; Raghavachari, K.; Foresman, J. B.; Ortiz, J. V.; Cui, Q.; Baboul, A. G.; Clifford, S.; Cioslowski, J.; Stefanov, B. B.; Liu, G.; Liashenko, A.; Piskorz, P.; Komaromi, I.; Martin, R. L.; Fox, D. J.; Keith, T.; Al-Laham, M. A.; Peng, C. Y.; Nanayakkara, A.; Challacombe, M.; Gill, P. M. W.; Johnson, B.; Chen, W.; Wong, M. W.; Gonzalez, C.; Pople, J. A. *Gaussian, Inc.*, Wallingford CT, **2004**.

(43) Zhao, D.; Swager, T. M. *Macromolecules*, **2005**, *38*, 9377.

(44) Xiong, J.–F.; Li, J.–X.; Mo, G.–Z.; Huo, J.–P.; Liu, J.–Y.; Chen, X.–Y.; Wang, Z.–Y. *J. Org. Chem.* **2014**, *79*, 11619.

(45) Rong, M.; Lin, L.; Song, X.; Zhao, T.; Zhong, Y.; Yan, J.; Wang, Y.; Chen, X. *Anal. Chem.* **2015**, *87*, 1288.

(46) Ding, A.; Yang, L.; Zhang, Y.; Zhang, G.; Kong, L.; Zhang, X.; Tian, Y.; Tao, X.; Yang, J. *Chem. Eur. J.* **2014**, *20*, 12215.

(47) Notin, L.; Viton, C.; David, L.; Alcouffe, P.; Rochas, C.; Domard, A. *Acta Biomater.*, **2006**, *2*, 387.

(48) He, G.; Peng, H.; Liu, T.; Yang, M.; Zhang, Y.; Fang, Y.; *J. Mater. Chem.* **2009**, *19*, 7347.

Appendix

Detection limit calculation for PA

LOD = 3 × S.D./k, where S.D = 2856.067 and k = 1.527×10^{13} (from Figure 4.2)

LOD = $3 \times 2856.067/1.527 \times 10^{13}$

= 56.11×10^{-11} M (128ppt)

Table A4.1. A comparative study of present work with other the reported literature.

Literature	Material used	K_{sv} (M^{-1})	LOD	Medium used
Present Work	***Conjugated polyelectrolyte***	***1.0×10^7***	***5.6×10^{-10} M (128 ppt)***	***H_2O***
Angew. Chem. Int. Ed., **2013**, *52*, 2881	Metal–organic framework	3.5×10^4	-	CH_3CN
Chem. Eur. J., **2014**, *20*, 12215	α–cyanostilbene derivative	3.3×10^5	2.8×10^{-7} M	H_2O/THF (v/v=7:3)
Chem. Eur. J. **2014**, 20, 195	Tetraphenylethelene Nanosphere	3.0×10^4	5×10^{-9} M	H_2O/THF (v/v=9:1)
Chem. Mater., **2014**, *26*, 4221	Graphene derivative	8.9×10^5	300 ppb	H_2O/THF (v/v=9:1)
Chem. Commun., **2014**, *50*, 15788	Organic cage	2.2×10^5	6.4 ppb	DCM
ACS Appl. Mater. Interfaces, **2014**, *6*, 10722	Graphene oxide	1.3×10^5	125 ppb	Buffer
ACS Appl. Mater. Interfaces. **2013**, *5*, 5373	Hexa−peri−hexabenzocoronene derivative	3.2×10^6 & 2.0×10^6	4×10^{-9} M & 9×10^{-9} M	H_2O/THF (v/v=4:6)
Inorg. Chem. **2013**, *52*, 4860	Hexaphenylbenzene derivative	1.9×10^5	6.8 ppb	H_2O/THF (v/v=4:6)
ACS Appl. Mater. Interfaces, **2013**, *5*, 672	Pentacenequinone derivative	1.5×10^4	3.5×10^{-7} M	Toluene/DCM (v/v=8:2)
Chem. Commun., **2014**, *50*, 6031	Iridium (III) complex	5.2×10^4	-	H_2O/Acetone (v/v=9:1)
J. Org. Chem. **2013**, *78*, 1306	Tris imidazolium salt	3.8×10^4 & 3.3×10^4	-	DMSO

Chem. Commun., **2012**, *48*, 5007	Fluoranthene derivative	9.9×10^4	20 ppb	Ethanol
ACS Appl. Mater. Interfaces, **2013**, *5*, 8394	*p*−phenylenevinylene derivative	5.5×10^4	1.1×10^{-8}	Bri−58 Micelles

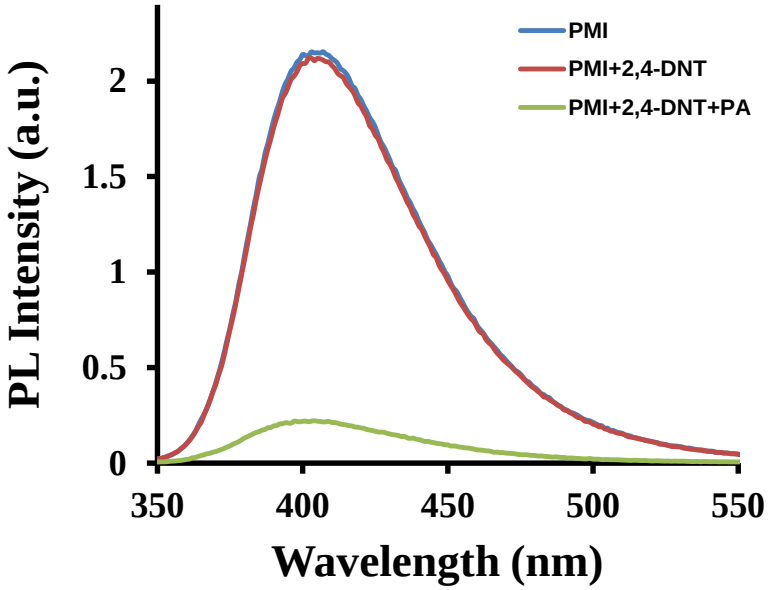

Figure A4.1 Change in emission spectra of PMI (2×10^{-5} M) with 2,4−DNT (6.67×10^{-7} M) followed by addition of PA (6.67×10^{-7} M).

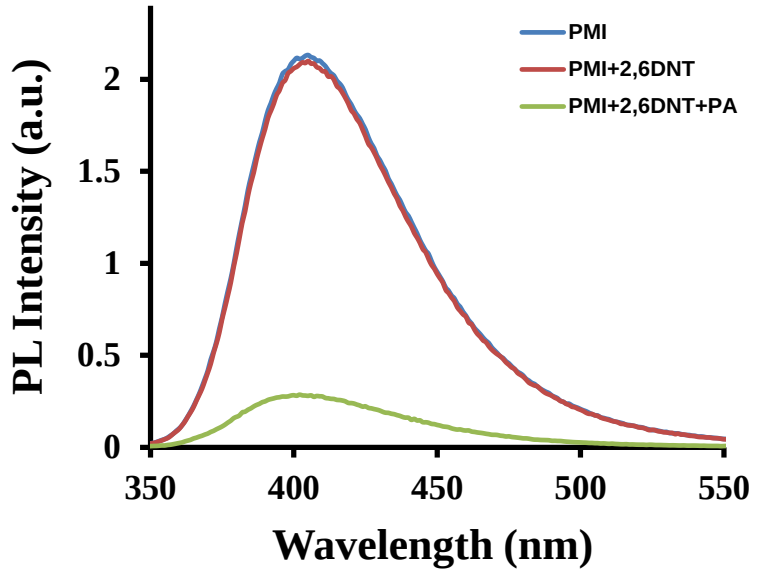

Figure A4.2 Change in emission spectra of PMI (2×10^{-5} M) with 2,6−DNT (6.67×10^{-7} M) followed by addition of PA (6.67×10^{-7} M).

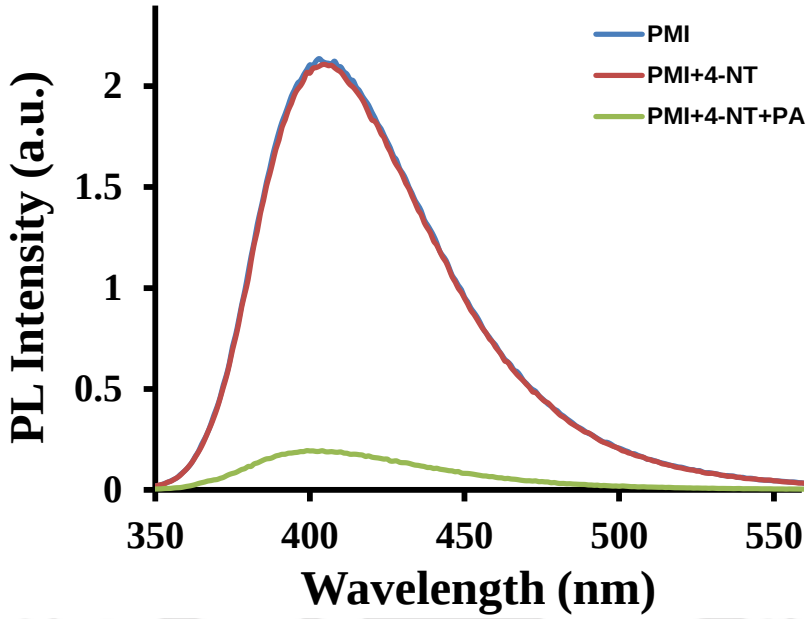

Figure A4.3 Change in emission spectra of PMI (2×10^{-5} M) with 4−NT (6.67×10^{-7} M) followed by addition of PA (6.67×10^{-7} M).

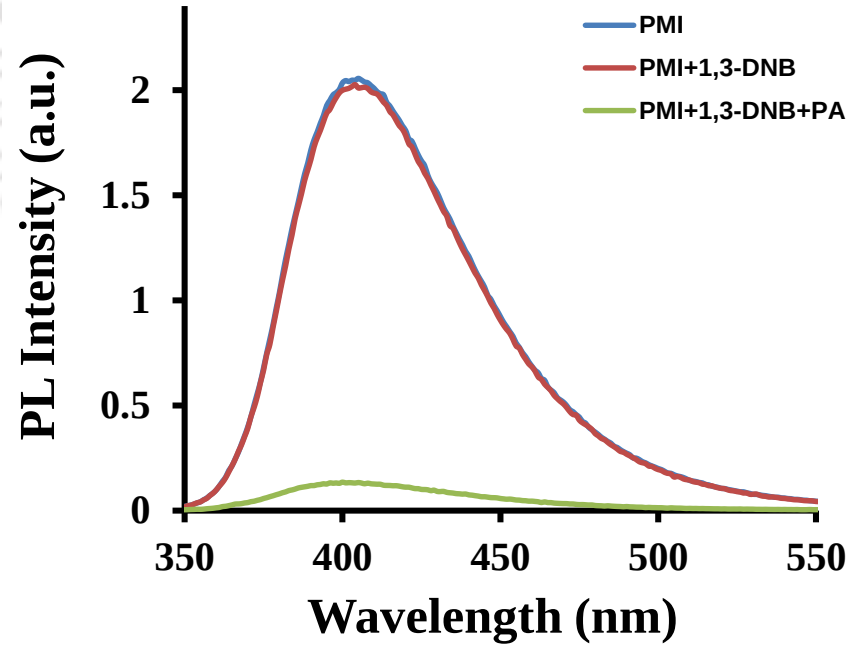

Figure A4.4 Change in emission spectra of PMI (2×10^{-5} M) with 1,3−DNB (6.67×10^{-7} M) followed by addition of PA (6.67×10^{-7} M).

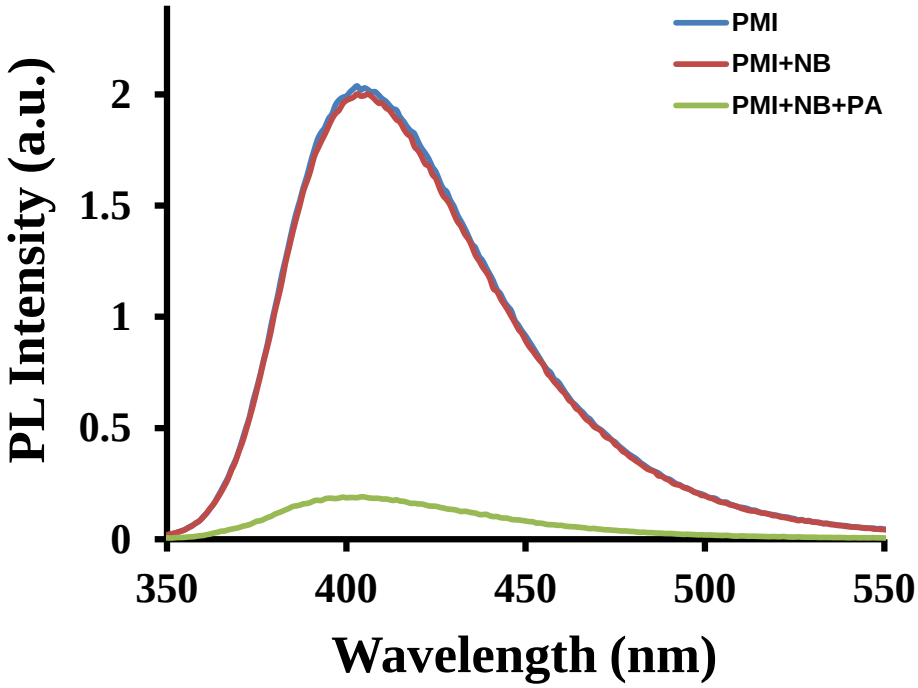

Figure A4.5 Change in emission spectra of PMI (2×10^{-5} M) with NB (6.67×10^{-7} M) followed by addition of PA (6.67×10^{-7} M).

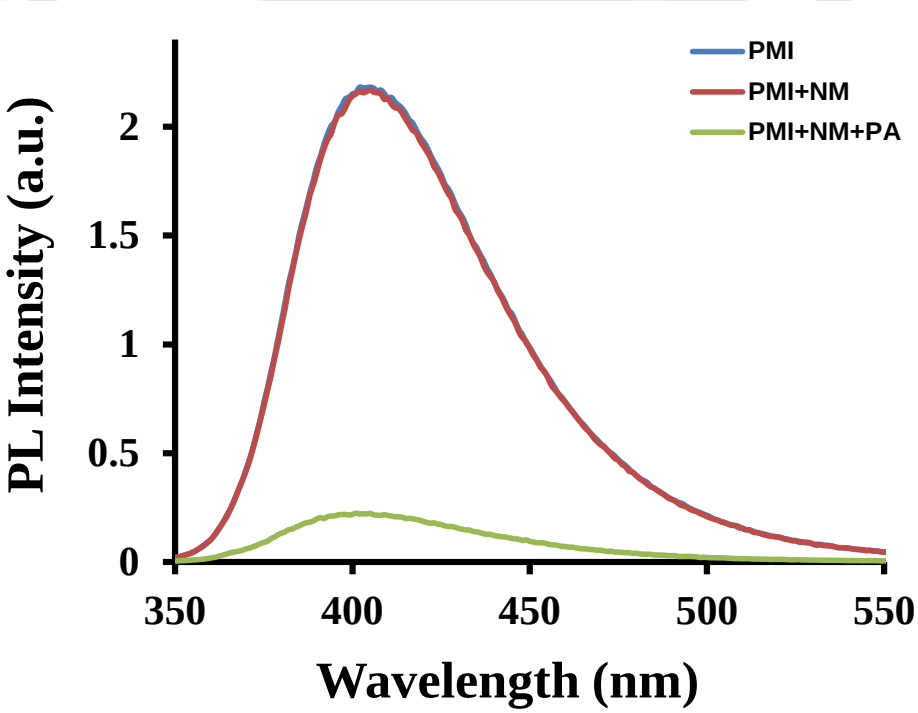

Figure A4.6 Change in emission spectra of PMI (2×10^{-5} M) with NM (6.67×10^{-7} M) followed by addition of PA (6.67×10^{-7} M).

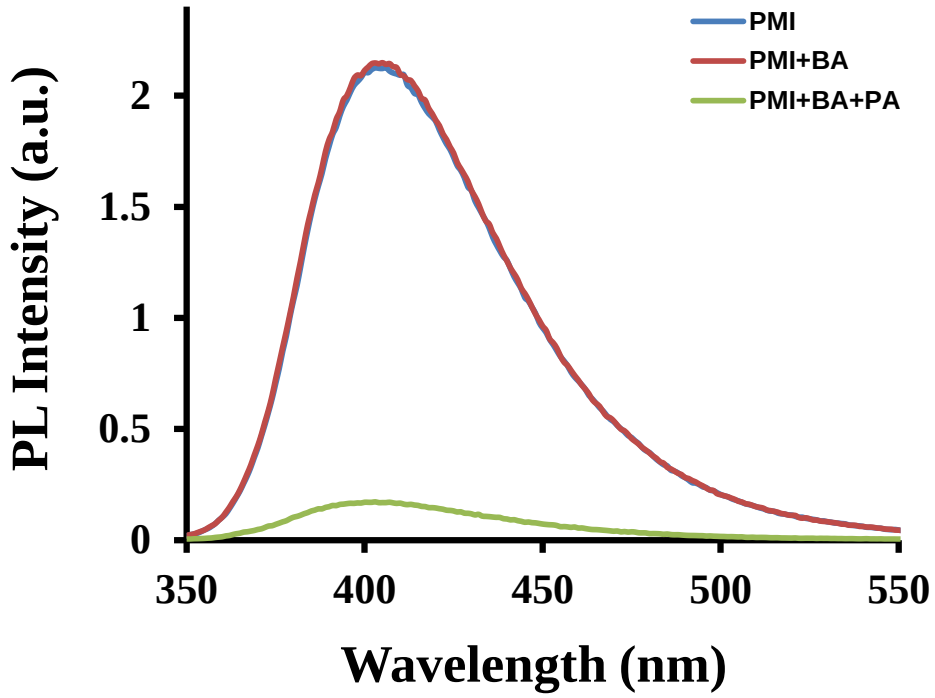

Figure A4.7 Change in emission spectra of PMI (2×10^{-5} M) with BA (6.67×10^{-7} M) followed by addition of PA (6.67×10^{-7} M).

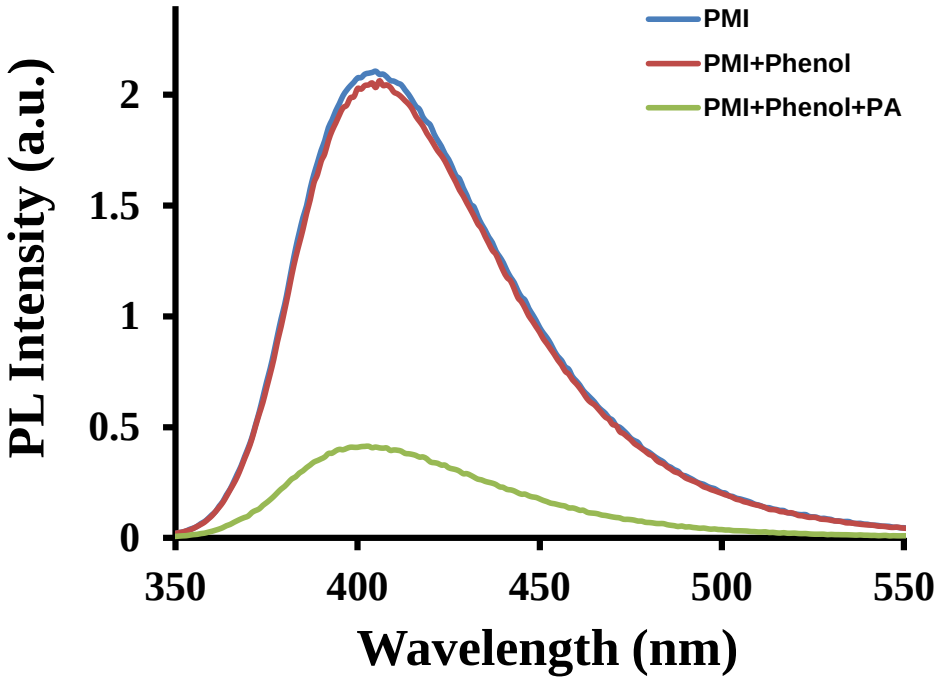

Figure A4.8 Change in emission spectra of PMI (2×10^{-5} M) with Phenol (6.67×10^{-7} M) followed by addition of PA (6.67×10^{-7} M).

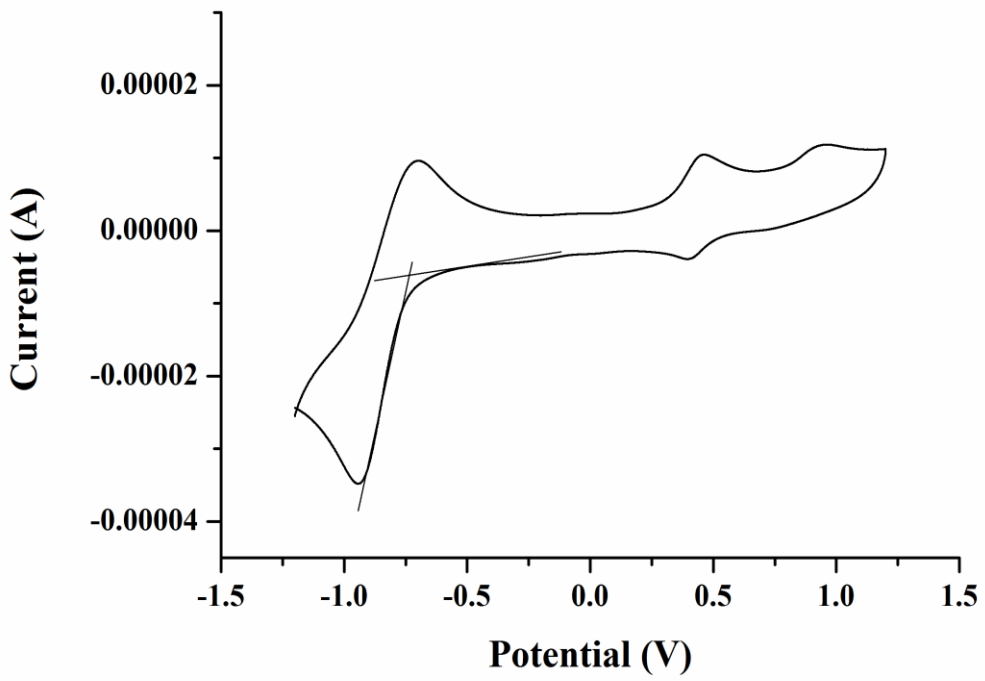

Figure A4.9 Cyclic voltammogram of PMI film on glassy carbon electrode in (0.1 M) $TBAF_6$, CH_3CN solution with a scan rate of 50 mV/s.

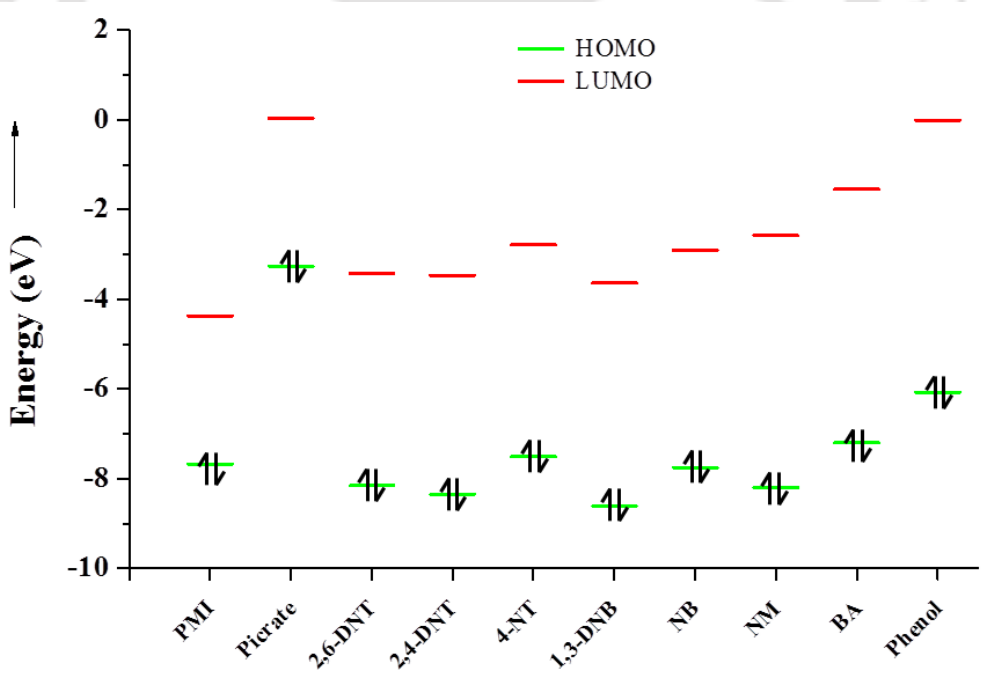

Figure A4.10 HOMO−LUMO energy levels for PMI and different sensing analytes.

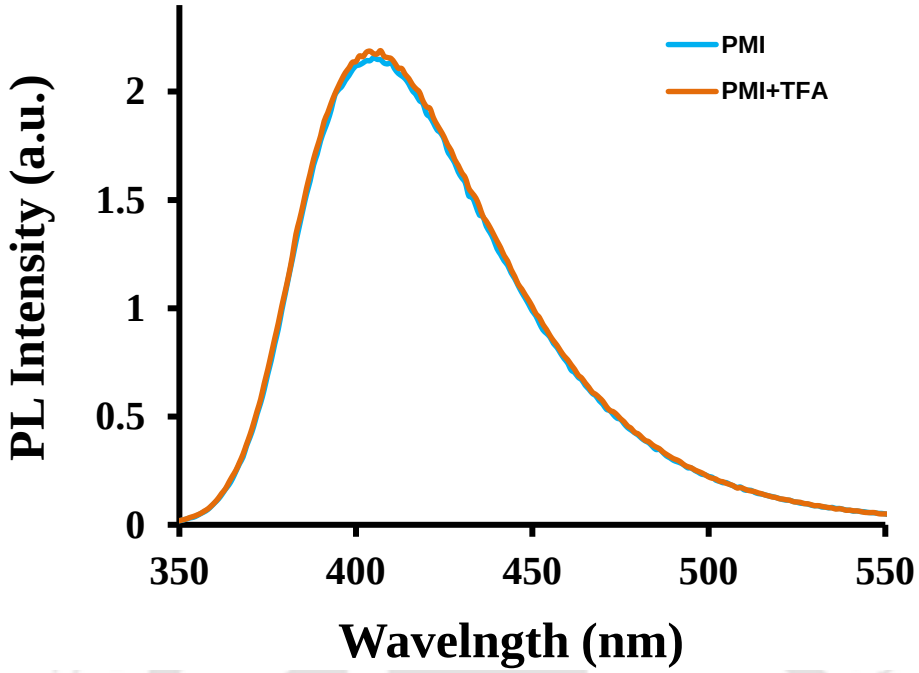

Figure A4.11 Change in emission spectra of PMI (2×10^{-5} M) after adding TFA (1×10^{-6} M) in aqueous media.

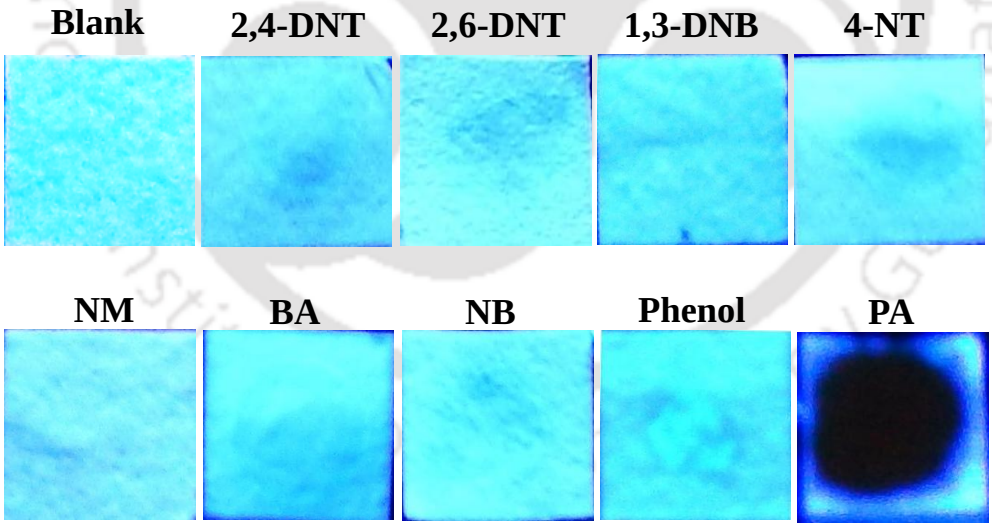

Figure A4.12 Color of fluorescent test strips under UV light before and after addition (10 µL) of 10^{-2} M solution of various analytes.

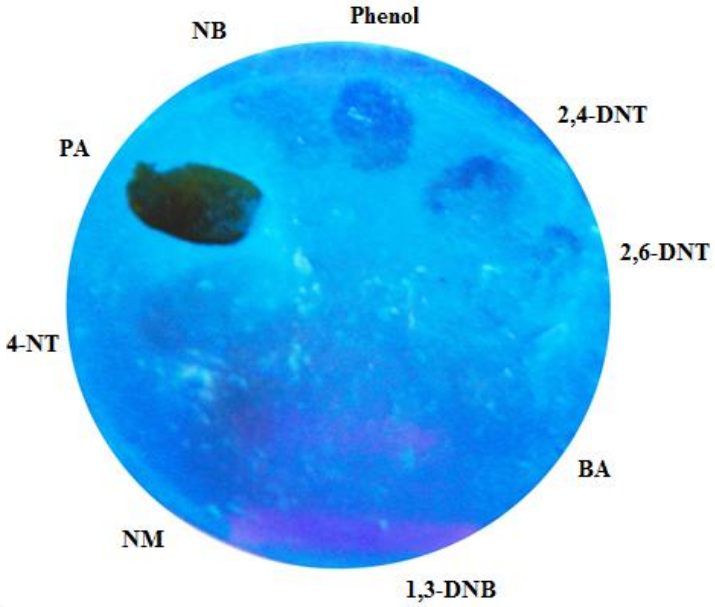

Figure A4.13 Visualization of PMI−doped CS fluorescent film under UV−light with fingertip impression of different analytes.

Optimized coordinates of PMI

Center Number	Atomic Number	Atomic Type	Coordinates (Angstroms) X	Y	Z
1	6	0	-1.289473	-0.031433	-0.528791
2	6	0	-0.649594	-1.259685	-0.326775
3	6	0	0.646319	-1.287314	0.196771
4	6	0	1.289820	-0.086571	0.517461
5	6	0	0.650053	1.141641	0.315278
6	6	0	-0.646013	1.169258	-0.208062
7	1	0	-1.162853	-2.176949	-0.593015
8	1	0	1.156779	-2.227768	0.371893
9	1	0	1.163117	2.059051	0.581427
10	1	0	-1.156319	2.109844	-0.382998
11	8	0	2.575134	-0.117100	1.094774
12	8	0	-2.574986	-0.001981	-1.105691
13	6	0	3.709551	-0.077885	0.165700
14	1	0	3.656849	-0.937794	-0.517062
15	1	0	3.661334	0.840384	-0.436600

16	6	0	4.972662	-0.120049	1.018234
17	1	0	4.953971	0.734017	1.707220
18	1	0	4.941443	-1.025792	1.637240
19	6	0	6.262801	-0.096295	0.178105
20	1	0	6.270403	-0.952153	-0.512941
21	1	0	6.282736	0.809451	-0.445828
22	6	0	7.529700	-0.139064	1.054433
23	1	0	7.521027	0.717854	1.743610
24	1	0	7.505527	-1.043299	1.679868
25	6	0	8.830094	-0.120987	0.225898
26	1	0	8.841158	-0.976807	-0.462509
27	1	0	8.868104	0.786718	-0.391033
28	6	0	10.068687	-0.174166	1.134577
29	1	0	10.096922	0.684954	1.810830
30	1	0	10.068536	-1.078957	1.749533
31	6	0	-3.708966	-0.040398	-0.176032
32	1	0	-3.657634	0.821553	0.504195
33	1	0	-3.658682	-0.956844	0.428941
34	6	0	-4.972603	-0.004084	-1.028060
35	1	0	-4.951568	0.906508	-1.640346
36	1	0	-4.944508	-0.852777	-1.723337
37	6	0	-6.262174	-0.049504	-0.187960
38	1	0	-6.281083	0.801207	0.509131
39	1	0	-6.269822	-0.959876	0.429556
40	6	0	-7.529807	-0.018497	-1.063730
41	1	0	-7.523728	0.895081	-1.675904
42	1	0	-7.504273	-0.864931	-1.765310
43	6	0	-8.829315	-0.076252	-0.235614
44	1	0	-8.867293	0.771745	0.461097
45	1	0	-8.838803	-0.990931	0.372496
46	6	0	-10.069021	-0.047910	-1.143891
47	1	0	-10.062772	-0.886472	-1.846441
48	1	0	-10.105225	0.874477	-1.730500
49	7	0	-11.345648	-0.129524	-0.381622

50	6	0	-12.163793	0.904489	-0.098851
51	6	0	-11.873665	-1.285660	0.192639
52	1	0	-12.020582	1.924574	-0.411050
53	6	0	-13.032396	-0.928822	0.827322
54	1	0	-11.393230	-2.243896	0.097859
55	1	0	-13.740797	-1.519536	1.382107
56	7	0	11.346784	-0.168605	0.370443
57	6	0	12.154809	0.896104	0.191631
58	6	0	11.886925	-1.257851	-0.313001
59	1	0	12.001218	1.879245	0.602016
60	6	0	13.042360	-0.829059	-0.908005
61	1	0	11.416069	-2.225491	-0.313218
62	1	0	13.757073	-1.355586	-1.516709
63	7	0	-13.197799	0.442709	0.635365
64	7	0	13.193925	0.518663	-0.582420
65	6	0	-14.329241	1.246985	1.140165
66	1	0	-15.259248	0.896833	0.688340
67	1	0	-14.385745	1.156156	2.226281
68	1	0	-14.171011	2.292385	0.875195
69	6	0	14.318006	1.379548	-1.003260
70	1	0	15.250561	0.997357	-0.583788
71	1	0	14.378305	1.394310	-2.092852
72	1	0	14.147684	2.392856	-0.639517

Optimized coordinates of picrate

Center Number	Atomic Number	Atomic Type	Coordinates (Angstroms) X	Y	Z
1	6	0	-0.571700	-1.231579	-0.000042
2	6	0	0.807625	-1.216591	0.000012
3	6	0	1.501818	-0.000098	0.000046
4	6	0	0.807783	1.216486	0.000045
5	6	0	-0.571539	1.231653	0.000004
6	6	0	-1.400198	0.000091	-0.000122
7	1	0	1.350805	-2.150897	0.000043
8	7	0	2.933134	-0.000191	0.000112

9	7	0	-1.184602	2.548924	0.000066
10	7	0	-1.184936	-2.548769	-0.000032
11	8	0	-2.654124	0.000172	-0.000147
12	8	0	-2.442360	2.669008	0.000304
13	8	0	3.547080	-1.119924	-0.000045
14	8	0	-0.408401	-3.570622	-0.000037
15	8	0	3.547225	1.119462	-0.000010
16	8	0	-2.442710	-2.668687	0.000118
17	8	0	-0.407933	3.570674	-0.000286
18	1	0	1.351086	2.150721	0.000096

Optimized coordinates of picric acid

Center Number	Atomic Number	Atomic Type	Coordinates (Angstroms) X	Y	Z
1	6	0	0.572349	-1.184898	-0.009717
2	6	0	-0.819827	-1.256628	0.018951
3	6	0	-1.546951	-0.076117	0.021583
4	6	0	-0.917302	1.170854	0.001065
5	6	0	0.466951	1.231065	-0.001214
6	6	0	1.267381	0.060771	-0.021674
7	1	0	-1.317540	-2.217189	0.032379
8	7	0	-3.009254	-0.138479	0.042913
9	7	0	1.071361	2.570342	0.013872
10	7	0	1.307567	-2.437524	-0.033071
11	8	0	2.601735	0.167551	-0.087213
12	1	0	3.016189	-0.742717	-0.111737
13	8	0	2.174640	2.726423	0.593387
14	8	0	-3.546470	-1.280711	0.052253
15	8	0	0.675038	-3.518581	0.000904
16	8	0	-3.640226	0.954373	0.051183
17	8	0	2.590885	-2.387249	-0.089001
18	8	0	0.403996	3.493953	-0.537085
19	1	0	-1.498755	2.083176	-0.016042

Chapter 5

FRET-Assisted Selective Detection of Flavins via Cationic Conjugated Polyelectrolyte Under Physiological Conditions

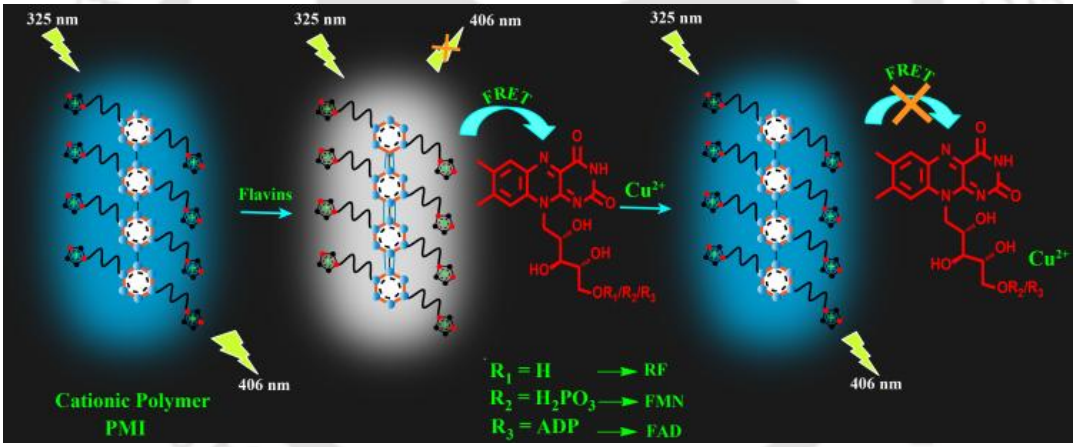

Hussain, S.; Malik, A. H.; Iyer, P. K. *J. Mater. Chem. B* **2016**, *4*, 4439−4446.

Abstract

Flavins *viz.* riboflavin (RF, Vitamin B_2), flavin mononucleotide (FMN) and flavin adenine dinucleotide (FAD) represent an important class of biomolecules ubiquitously found in living systems that are vital for numerous cellular activities inside the body. The fluorescence amplified detection of these flavins at ppb levels (RF−259 ppb, FMN−9.37 ppb and FAD−11.11 ppb) is achieved for the first time using water soluble cationic conjugated polymer PMI under physiological conditions. The substantial FRET, variable binding abilities of flavins with PMI *via* Columbic interaction and the subsequent displacement of FMN/FAD by simple chelating agent like Cu^{2+} affords a simple and consistent method to detect and discriminate them even in the presence of most common interfering analytes usually found in biosystems. This new strategy based on FRET provides more precise measurement using two different emission bands and hence, eliminates the environmental effects unlike in classical or direct fluorescence method. Furthermore, the determination of flavins in human blood serum using cationic conjugated polyelectrolyte PMI signifies the potential of this protocol in studying the metabolic processes and clinical assessment of diseases related to flavins.

5.1 Introduction

The three prime derivatives of flavin *viz.* riboflavin (RF, Vit B_2), flavin mononucleotide (FMN) and flavin adenine dinucleotide (FAD) are considered as key biomolecules due to their imperative roles in numerous redox reactions inside the living systems.[1−4] The heterocyclic isoalloxazine ring attached to RF, FMN and FAD chain are the main catalytic redox active component of the flavins (Scheme 1). RF is an abundant water soluble vitamin, ubiquitously found in biological system that aids in various cellular activities like cell apoptosis, nucleic acid repair process and electron transfer processes.[5,6] Inadequate dietary intake of RF leads to several health disorders[7,8] including slow growth, visual impairment, fatigue, digestive problems, hair loss, skin diseases, mental illness, anemia, angular stomatitis, glossitis and keratitis. RF is also a central component of essential co−enzymes FMN and FAD that catalyze a variety of biochemical reactions[9] including metabolism of carbohydrates, fats and proteins. These coenzymes are indispensable for the electron−transfer chains[1] inside the mitochondria of eukaryotes and plastids of plants. Among all the redox coenzymes only flavins have an exclusive capability of transferring one or two electrons at a time.[10] FAD is also known to generate hydrogen peroxide/superoxide inside the granules of human white blood cells eosinophils *via* redox reactions that can damage the parasitic organisms.[11,12] Since, flavins are not *de novo* produced inside the vertebrates, they have well−built salvage pathways involving the uptake of RF and quick conversion to FMN/FAD on the membrane of the mitochondria.[13,14] Thus, it is essential to develop an ultrasensitive and highly selective method for the determination of flavins to investigate the metabolic processes and clinical assessment of the associated diseases.

Owing to their high significance in biological transformations, the detection of flavins, especially RF has been performed typically *via* sophisticated methods.[15−20] However, most of these techniques are tedious, complicated, require large amount of costly/toxic solvents and suffer largely from the issue of selectivity and delayed response time. Fluorescence based detection platforms are versatile due to their simplicity, remarkable sensitivity, non−invasiveness, rapid signal response time and wider applicability.[21−23] In this context, few efforts have been made to detect flavins.[24−28] Yet, there are several limitations *viz.* (1) ineffective in physiological conditions, (2) low signal response, (3) low selectivity, (4) used classical/direct fluorescence method that generates insignificant and erroneous results due to the presence of other interfering species in the medium that

needs to be overcome. Förster resonance energy transfer (FRET) has emerged[29−36] as an outstanding and highly favorable method, since it has advantages of exterminating environmental effects thereby providing more precise measurement using two different emission bands.

Conjugate polyelectrolytes (CPEs) are extraordinary fluorescent materials used extensively in the field of sensing due to their amplified signal response *via* the "molecular−wire effect", excellent photophysical properties, high quantum efficiencies and viability in biological systems.[37−44] Sensors based on CPEs have been reported recently for the detection of toxic species, explosives, biomolecules, etc.[45−48] It is worth mentioning that despite their exceptional abilities no CPE based probe for the selective and sensitive detection and discrimination of flavins have been established yet, thereby providing immense opportunities to be explored.

Herein, a new protocol for the amplified detection of flavins under physiological conditions using CPE was developed for the first time. The cationic CPE, poly(1,4−bis−(6−(1−methylimidazolium)−hexyloxy)−benzene bromide) (PMI) (Scheme 5.1) displayed an amplified fluorescence quenching after interaction with flavins (RF, FMN and FAD) in aqueous solution with variable photo physical changes *via* the process of FRET. Interestingly, the emission of PMI was recovered on introducing chelating metal Cu^{2+} to the solution of PMI/FMN and PMI/FAD, respectively. However, PMI/RF solution did not reveal any fluorescence recovery, due to the absence of any phosphate group in RF unlike FMN/FAD. The significant FRET and the differential binding abilities of flavins with PMI *via* Columbic interaction and displacement of FMN/FAD using Cu^{2+} provided a novel and reliable method to recognize and discriminate them in aqueous/biological medium efficiently.

5.2 Experimental

5.2.1 Materials and measurements

Riboflavin (RF), flavin mononucleotide (FMN), flavin adenine dinucleotide, bovine serum albumin (BSA), lysozyme, vitamin B_1, vitamin B_{12} and organic phosphates were obtained from Sigma Aldrich. Vitamin B_7 was purchased from Fisher Scientific. All other chemicals and reagents were procured from Himedia, Alfa−Aesar and Merck. Sensing experiments were performed in Milli−Q water. Perkin Elmer Lambda−45 spectrophotometer was used to perform UV/visible studies. Photoluminescence spectra

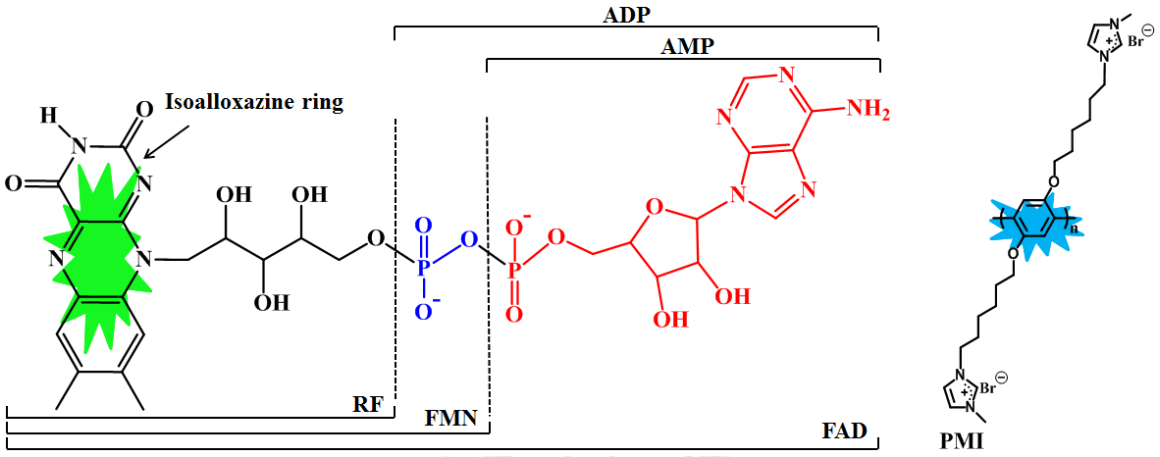

Scheme 5.1. Structure of flavins (RF, FMN and FAD) and cationic conjugated polymer PMI.

were recorded on a Horiba Fluoromax−4 spectrofluorometer using quartz cuvettes (10 mm path length) with a slit width of 2 nm at room temperature. Edinburgh Instruments Life Spec II instrument was used to perform fluorescence lifetime studies. The fresh human blood serum samples were obtained from IIT Guwahati hospital and analyzed on the same day.

5.2.2 Preparation of stock solution for sensing studies

Stock solutions of cationic polymer PMI (1mM), RF (0.1 mM), FMN (1 mM) and FAD (1 mM) were prepared in Milli−Q water. Similarly, the stock solutions of various amino acids, phosphates, vitamins and metal salts (as their perchlorate) were prepared according to their solubility in water. The solutions were then diluted to desired concentrations whenever needed. The sensing studies were carried out in 10 mM HEPES buffer (pH = 7.4) at room temperature.

5.2.3 Calculation for limit of detection (LOD)

For calculating detection limit, different PMI samples (10 μM) each containing variable concentrations of RF were prepared and subjected to fluorescent measurements by exciting at 325 nm. A curve was then obtained by plotting change in emission intensity *vs* concentration to calculate LOD using the equation shown below;

$$LOD = 3\sigma / k$$

where, σ represents standard deviation for emission intensity of PMI in the absence of RF and k denotes slope of the curve. Same method was used to calculate LOD for FMN and FAD, respectively.

5.2.4 Detection of favins in blood serum

The stock solution of FMN (1×10^{-3} M) and FAD (1×10^{-3} M) were prepared directly in fresh blood serum samples without any dilution. The stock solution of RF (1×10^{-4} M) was prepared in diluted serum sample considering its limited water solubility. The samples were analyzed immediately after doping. Three known concentrations of each flavin was then introduced into the cuvette containing PMI (10 μM) to monitor the changes in emission spectra. Each measurement was repeated thrice and compared with the calibration curves to obtain the results.

5.2.5 Determination of FRET parameters

To study the magnitude of energy transfer between flavins and cationic polymer PMI, overlap integral values were calculated using the equation[49] shown below−

$$J(\lambda) = \int_0^\infty F_D(\lambda)\, \varepsilon_A(\lambda)\lambda^4 d\lambda$$

where, J (λ) denotes overlap integral value, FD (λ) is the corrected fluorescence intensity of PMI from λ to λ + Δλ with the total intensity normalized to unity, ε_A represents molar extinction coefficient of the acceptor. The critical distance/Förster radius (R0) between flavins and polymer PMI was determined using the expression below−

$$R_0 = 0.211[(J)Q(\eta^{-4})(k^2)]^{1/6}$$

where, J is the overlap integral value, Q is photoluminescence quantum yield of polymer PMI (without acceptor), η is the refractive index of the medium and k^2 is the dipole orientation factor usually considered as 0.667 for randomly oriented dipole.

The FRET efficiency (E) for each flavin was determined using the equation below−

$$E = 1 - \frac{\tau_{DA}}{\tau_D}$$

where, τ_{DA} is the fluorescence lifetime of donor (D) in the presence of acceptor (A) and τ_D is the lifetime of donor in the absence of acceptor.

The appropriate donor−acceptor (D−A) distance (R) i.e. the distance between PMI and flavins was then calculated using the equation below-

$$R = R0\sqrt[6]{\frac{1-E}{E}}$$

5.3 Result and discussion

5.3.1 Sensing studies in physiological conditions

The cationic CPE PMI was synthesized using previously established method shown in chapter 3 and 4. PMI displayed absorption and emission maximum at 325 nm and 406 nm (λ_{ex} = 325 nm) in aqueous solution.[50] All the sensing studies were performed at room temperature in HEPES buffer (10 mM, pH=7.4) adhering physiological conditions. On continuously adding RF (0–25 μM) to the solution of PMI, the emission peak at 406 nm displayed considerable quenching with the appearance and enhancement of new peak at 526 nm *via* an isoemissive point at 485 nm (Figure 5.1a) indicating the occurrence of FRET. Nearly 80% quenching was observed at total 25 μM concentration of RF along with the hypsochromic shift of ~6 nm from 406 to 400 nm in the emission wavelength of PMI. FMN also showed similar response with ~90% fluorescence quenching at a concentration of 10.33 μM, i.e. ~2.5 times less than RF (Figure 5.1b). However, the enhancement of a new peak appearing at 526 nm was less prominent compared to RF. FAD causes ~90% fluorescence quenching at 10 times lower concentration (1.33 μM) of FMN without the appearance of any new emission peak (Figure 5.1c). Thus, three unique calibration curves were obtained using the change in intensity ratio (I_{526}/I_{406}) for RF and FMN and intensity at I_{406} for FAD that assisted in the determination and discrimination of these flavins in physiological conditions (Figure 5.2a–5.2c). The anomalous behavior in the sensing response can be attributed to the different binding affinities of flavins to PMI *via* Coulombic attraction as well as variable photo physical properties of the flavins in aqueous solution. Note that RF and FMN exhibit relatively high photoluminescence quantum yields[5,51] (ϕ_f = 0.26), while FAD displayed very weak fluorescence (ϕ_f = 0.03) in aqueous solutions owing to photo induced electron transfer[51] (PET) from the adenine unit to the isoalloxazine ring favored by stacked conformation in the latter. Hence, unlike RF and FMN, the FAD did not display any new emission peak on interacting with PMI. To study the efficiency of quenching, Stern−Volmer plots (K_{sv}) were obtained *via* linear regression analysis with correlation coefficient (R_2) values >0.99. The K_{sv} values were found to be 0.63×10^5 (RF), 0.18×10^7 (FMN) and 0.29×10^7 M^{-1} (FAD), (Insets of Figure

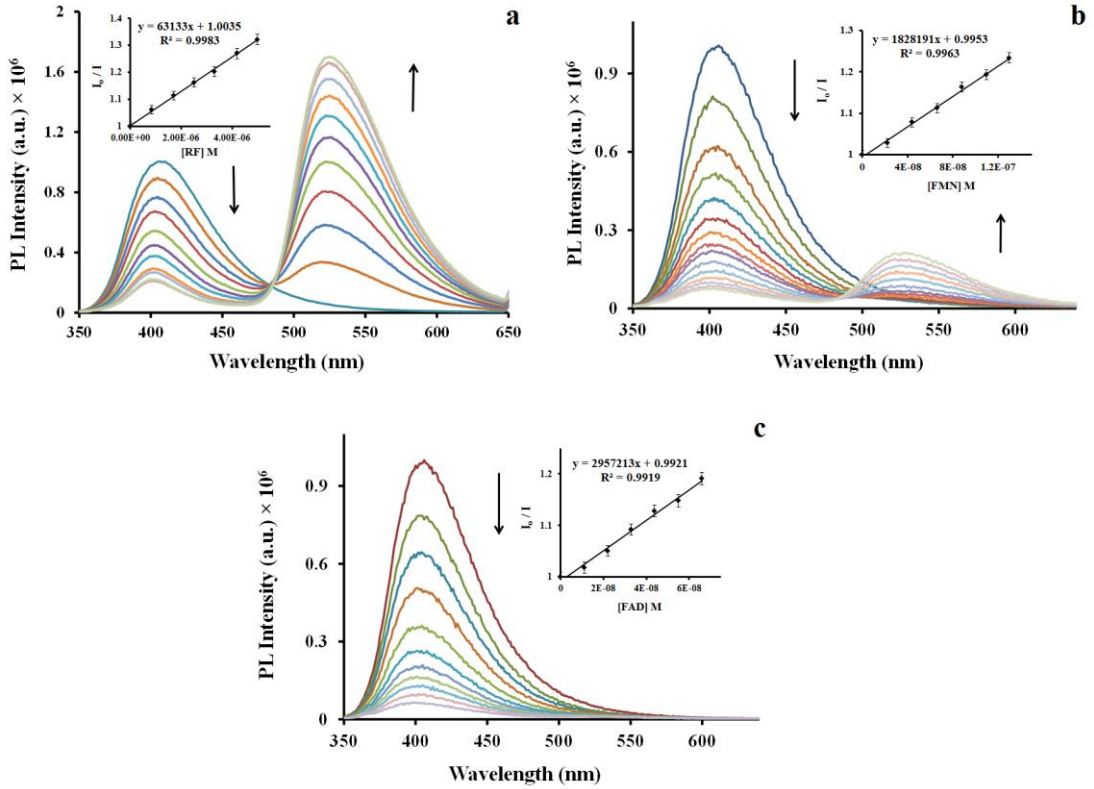

Figure 5.1 (a) Photolumenescence spectra of PMI (10 µM, λ_{ex} = 325 nm) with increasing concentration of (a) RF (b) FMN and (c) FAD in HEPES buffer (10mM, pH = 7.4). Final concentrations of RF, FMN and FAD were 25 µM, 10.33 µM and 1.33 µM, respectively. Inset: K_{sv} plots.

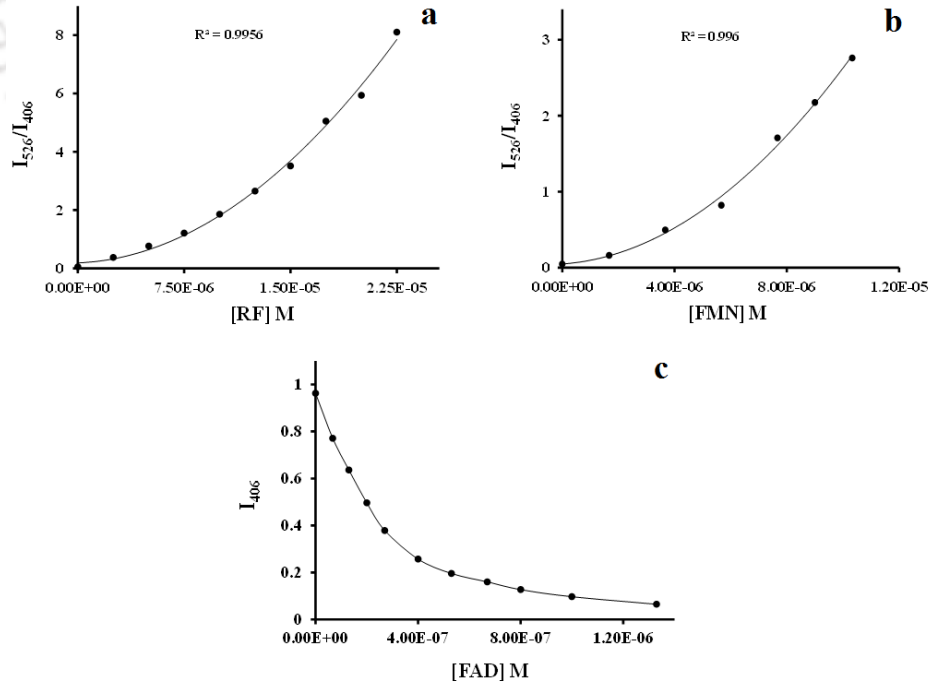

Figure 5.2 Calibration plot for (a) RF (b) FMN and (c) FAD in 10 mM HEPES buffer (pH=7.4) at room temperature.

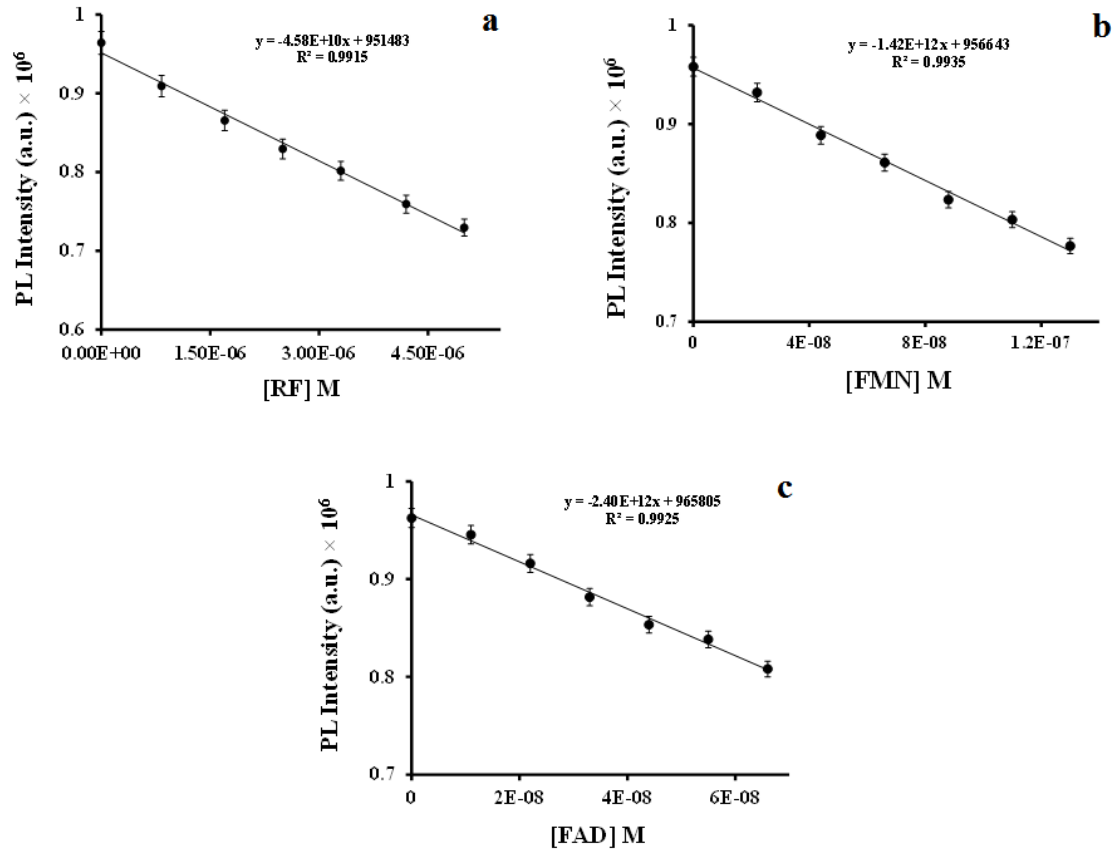

Figure 5.3 Detection limit plot for (a) RF (b) FMN and (c) FAD in 10 mM HEPES buffer (pH=7.4) at room temperature.

5.1) which are much superior among reported methods and described for the first time using CPE. The lower limit of detection (LOD) values as calculated was found to be 6.90 × 10^{-7} M (259 ppb), 1.96 × 10^{-8} M (9.37 ppb) and 1.34 × 10^{-8} M (11.11 ppb) for RF, FMN and FAD respectively (Figure 5.3a–5.3c) suggesting remarkable sensitivity of PMI towards the flavins. The sensing efficiency of these flavins followed the order FAD>FMN>RF which are in well agreement with the extent of Columbic interaction with PMI. Note that in addition to three –OH groups usually found in flavins, FAD molecule consists of two additional phosphates and –OH groups unlike FMN molecule which consist of only one phosphate, thus, more dipole interactions are expected in the former. RF, on the other hand lacks any phosphate groups, resulting in lesser interaction with PMI and requires larger amounts to quench the fluorescence of PMI.

5.3.2 Demonstrating FRET between PMI and flavins

FRET is a non–radiative process[23,51] in which the excited state energy of fluorophore (donor) is transferred to the acceptor at ground state without emitting a photon;

subsequently resulting in the reduction of fluorescence intensity of donor and increment in the fluorescence intensity of acceptor. However, there are several factors that must be satisfied for the occurrence of FRET in any system *viz.* (a) significant overlap between the emission band of donor and absorption band of acceptor, (b) appropriate spatial distance between the donor and acceptor (typical 1–10 nm), (c) the donor and acceptor must be oriented nearly parallel to each other, and (d) fluorescence quantum yield of donor should be adequate. These significant features of FRET endorse its widespread applications.[29,30,33,35,36] To demonstrate the possibility of FRET in PMI, a plot was obtained between the emission spectrum of PMI and absorption spectra of flavins. It was observed (Figure 5.4a) that the emission spectrum of PMI overlaps almost completely with the absorption bands of flavins, confirming the occurrence of energy transfer. Overlap integral values (J_λ) for the flavins were then obtained to ascertain the degree of energy transfer. The considerably high J_λ values *viz.* 3.68×10^{14} (RF), 2.62×10^{14} (FMN) and 2.15×10^{14} M^{-1} cm^{-1} nm^4 (FAD) supported the possibility of efficient FRET. The Förster distance (R0) values were also determined as 3.6 (RF), 3.4 (FMN) and 3.2 nm (FAD) which are well in the range (1–10 nm) desired for FRET.

To further confirm the quenching mechanism and occurrence of FRET from PMI to flavins, time−correlated single-photon counting (TCSPC) study was performed, since; decay time measurements are considered more sensitive than the steady state fluorescence quenching studies. The decay times of PMI were monitored using pulsed excitation of 336 nm (λ_{em} = 406 nm) before and after addition of RF, FMN and FAD, respectively (Figure 5.4b–d). The instrument response function (IRF) was measured using blank solvent (water). The fitting parameters are shown in Appendix as Figure A5.1. The decay curve of PMI was fitted mono−exponentially, whereas that of PMI/RF, PMI/FMN and PMI/FAD has been fitted bi−exponentially. The bi–exponential nature of curves indicates the presence of two populations[52] (a) donor (PMI) molecules bound with acceptor (flavins) and (b) unbounded donor molecules. The fast decay component is due to the acceptor bound donor molecules whose excited state lifetime is shortened due to FRET. The slow decay component is generally attributed to unbound donor molecules whose lifetime is not shortened by energy transfer. The average lifetime of polymer PMI (1.19 ns) was found to decrease sharply with the addition of RF (0.63 ns), FMN (0.79 ns) and FAD (0.85 ns), respectively that confirms the energy transfer from PMI to flavins. The FRET efficiency (E) determined for flavins were found to be 47% (RF), 34% (FMN) and

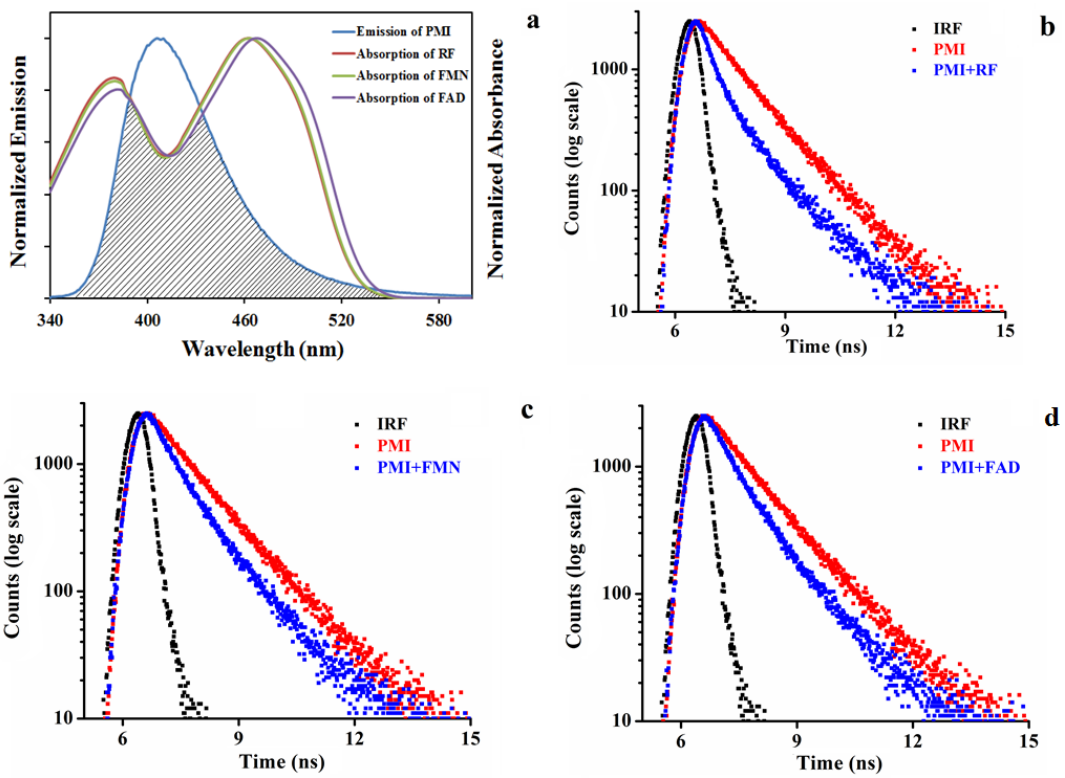

Figure 5.4 (a) Extent of spectral overlap between the absorption spectra of flavins and emission spectrum of PMI. Change in lifetime decay of PMI (10 µM) after adding (b) RF (25 µM), (c) FMN (10.33 µM) and (d) FAD (1.33 µM) (λ_{ex} = 336 nm, monitored at 406 nm).

29% (FAD), respectively. Using the values of E and R0, the appropriate distance between PMI and each flavin was also calculated and observed to be 3.67 nm (PMI/RF), 3.80 nm (PMI/FMN) and 3.71 nm (PMI/FAD), respectively. Since, FRET efficiency for all the flavins were found comparatively less than the steady−state fluorescence quenching efficiencies, hence, we presume that quenching process occurred *via* combination of both static and dynamic mechanism. FRET is an indication of dynamic quenching mechanism while static quenching usually occurred via formation of some ground state non−fluorescent complex.

The process of FRET was further demonstrated by monitoring the sensitized emission which is perhaps the simplest technique to validate the process of energy transfer. We monitored the emission spectrum of individual donor (PMI), acceptor (RF, FMN) and the mixture of donor and acceptor by exciting at the emission wavelength of donor (λ_{ex} = 325 nm). It was observed (Figure 5.5ab) that the acceptor fluorescence intensity was more in presence of donor indicating a sensitized emission and the occurrence of energy transfer

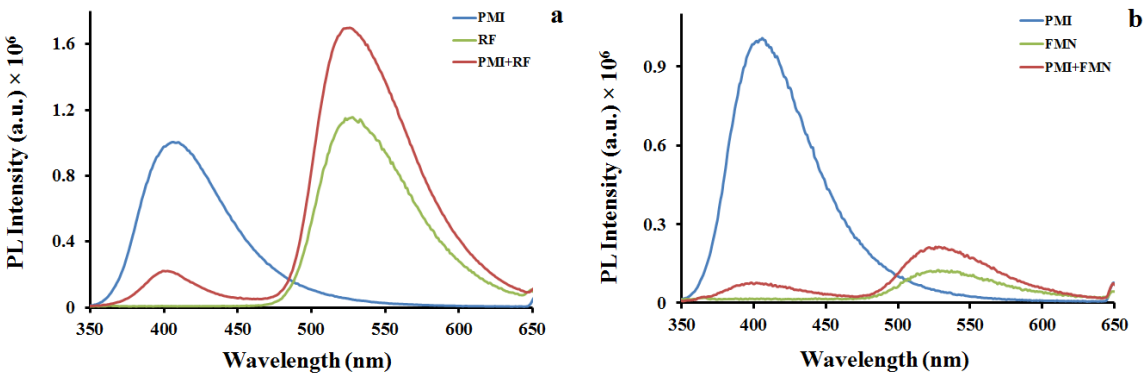

Figure 5.5 (a) Emission spectra of PMI (10 µM), RF (25 µM) and the PMI/RF (10 µM /25 µM) mixture at λ_{ex}=325 nm. (b) Emission spectra of PMI (10 µM), FMN (10.33 µM) and the PMI/FMN (10 µM/10.33 µM) mixture at λ_{ex}=325 nm.

from PMI to flavins. These results further confirm the occurrence of FRET and also demonstrated the light–harvesting property[53,54] of the conjugated polymer PMI.

5.3.3 Selectivity studies

For practical applications, the selective sensing of flavins in biological systems is highly desirable. To demonstrate the selectivity of this system, various other water soluble vitamins (Vit B_1, Vit B_3, Vit B_7, Vit C, and Vit B_{12}), serum protein (BSA), enzyme (Lyz) and amino acids (Met, Lys, Val, Thr, Leu, Ile, Phe, Gly, Trp, Ser, Ala, Gln, Glu, Arg, Cys and HomoCys) that are usually found in body fluids like blood serum or plasma were checked and found ineffectual towards the emission of PMI (Figure 5.6ab, Figure A5.2–5.3) compared to flavins. Since, the phosphate groups already present in FMN (as AMP) and FAD (as ADP) played a vital role in the sensing *via* FRET process, it was vital to check the effect of various inorganic (Pi, PPi, HPO_4^{2-} and $H_2PO_4^-$) and organic phosphates (G6–P, TMP, AMP, ADP, ATP, CTP, UTP and GTP) individually that are typically found in biological systems. None of these phosphates (including AMP & ADP) altered (Figure 5.6c, Figure A5.4) the emission of PMI. Insignificant spectral overlap between the absorption spectra of vitamins, protein, enzymes, phosphates and emission spectrum of PMI nullify the possibility of FRET (Figure 5.6d, Figure A5.5). Hence, it can be concluded that isoalloxazine ring present in flavins contributes to the sensing process *via* FRET and the attached phosphate groups (FMN & FAD) facilitate the electrostatic attraction between the sensor molecule and analyte to increase the efficiency of energy transfer.

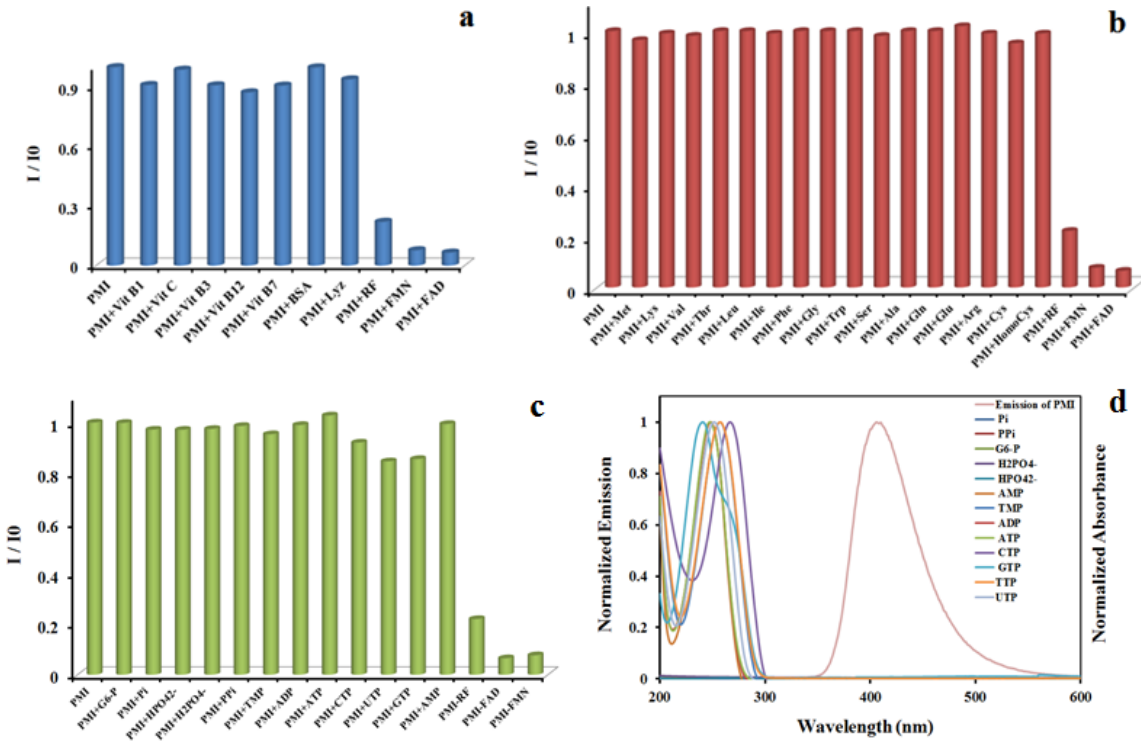

Figure 5.6 Bar chart showing the effect of (a) water soluble vitamins, serum protein, enzyme, (b) amino acids (c) phosphates on the emission of PMI in HEPES buffer (10mM, pH=7.4). Concentration of PMI and each analyte were 10 µM and 30 µM, respectively. (d) Spectral overlap between the emission spectrum of PMI and the absorption spectra of various phosphates.

5.3.4 Effect of ionic strength on FRET efficiency

The role of electrostatic interactions in the FRET was examined by varying the ionic strength of the solution using an electrolyte (NaCl). On introducing electrolyte (50–600 mM) to the solution of PMI/RF (10 µM/25 µM), PMI/FMN (10 µM/10.33 µM) and PMI/FAD (10 µM/1.33 µM), the intensity of the new peak at 526 nm decreased whereas the intensity of PMI peak at 406 nm increased (Figure A5.6–A5.8). This subsequent reduction in the quenching efficiency (Figure 5.7) with increasing ionic strength can be attributed to the weak Coulombic interaction between the oppositely charged PMI and flavin molecules and is in well agreement with Debye−Hückel theory.[34] Notably, the quenching efficiency was still ~50% at relatively high salt concentration indicating the bright prospects of the PMI system for bioanalytical applications.

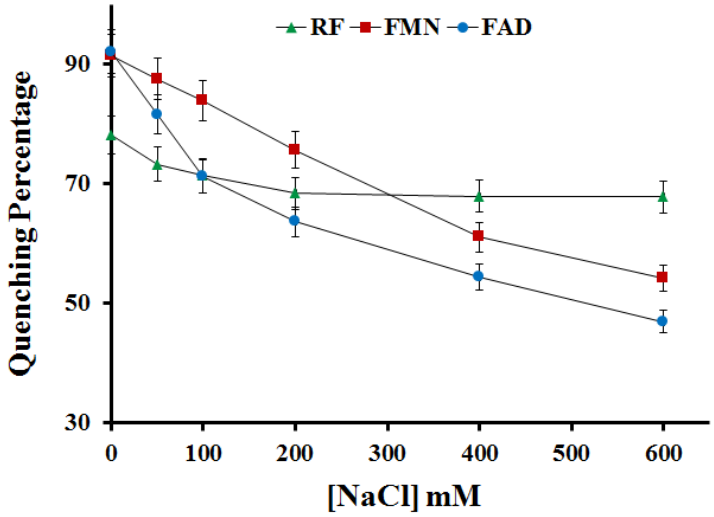

Figure 5.7 Effect of ionic strength on FRET efficiency.

5.3.5 Discrimination approach using simple chelating agent

Although the fluorescence responses by each flavin (RF, FMN & FAD) with PMI were dissimilar, yet it was not easy to discriminate FMN from RF due to the appearance of similar emission peak at 526 nm with only difference in their intensities. To overcome this problem and achieve an effective and clear discriminative assay, we developed an approach to recover the emission of polymer PMI *via* displacement technique using simple chelating agents like Cu^{2+}/Zn^{2+}, since it is well established that phosphates have high affinity for these transition metals.[55–57] In a typical experiment, Cu^{2+} metal ions were introduced into the solution of PMI/RF, PMI/FMN and PMI/FAD, separately. Interestingly, the emission of PMI was recovered by ~70% (PMI/FMN) and ~67% (PMI/FAD) (Figure 5.8ab). Similar results were obtained on adding Zn^{2+} ions, however, the peak intensities were quite less compared to Cu^{2+} ions. Hence, Cu^{2+} metal ions were found to be more efficient compared to Zn^{2+} ions and thus utilized. The LOD calculated for Cu^{2+} (Figure 5.9) was found to be 0.86 µM (PMI/FAD) and 0.56 µM (PMI/FMN), respectively. Note that PMI/RF solution did not reveal any significant change in their spectra after adding Cu^{2+} ions (Figure 5.8c). Since, FMN and FAD molecules comprise of phosphate groups unlike RF, an effective metal induced displacement is anticipated in the former. The overall sensing mechanism for the detection and discrimination of flavins is shown in Figure 5.10.

For realizing practicability of PMI based system, discrimination studies were also performed using different mixtures of flavins *viz.* RF/FMN, RF/FAD, FMN/FAD and

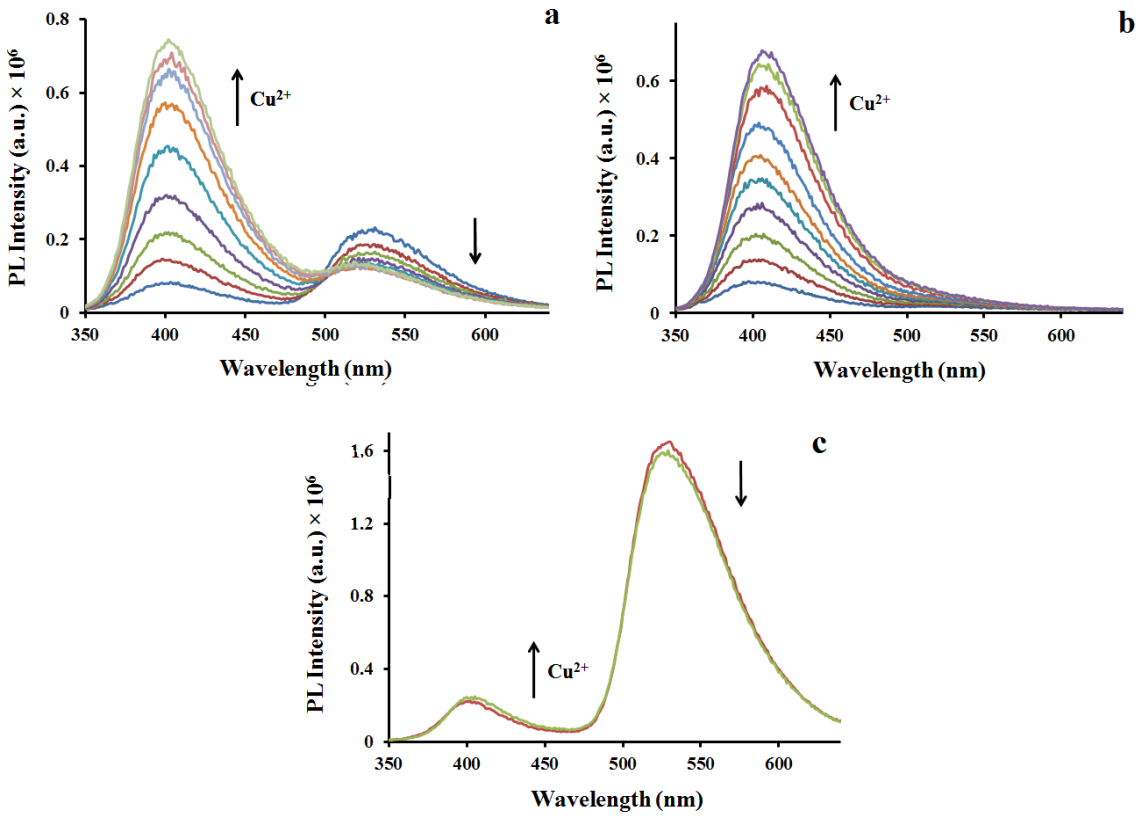

Figure 5.8 Photoluminescence spectra of (a) PMI/FMN (10 µM/10.33 µM), (b) PMI/FAD (10 µM/1.33 µM) and (c) PMI/RF (10 µM/25 µM) with increasing concentration of Cu^{2+} (6.6 ×10^{-4} M) in HEPES buffer (10 mM, pH = 7.4).

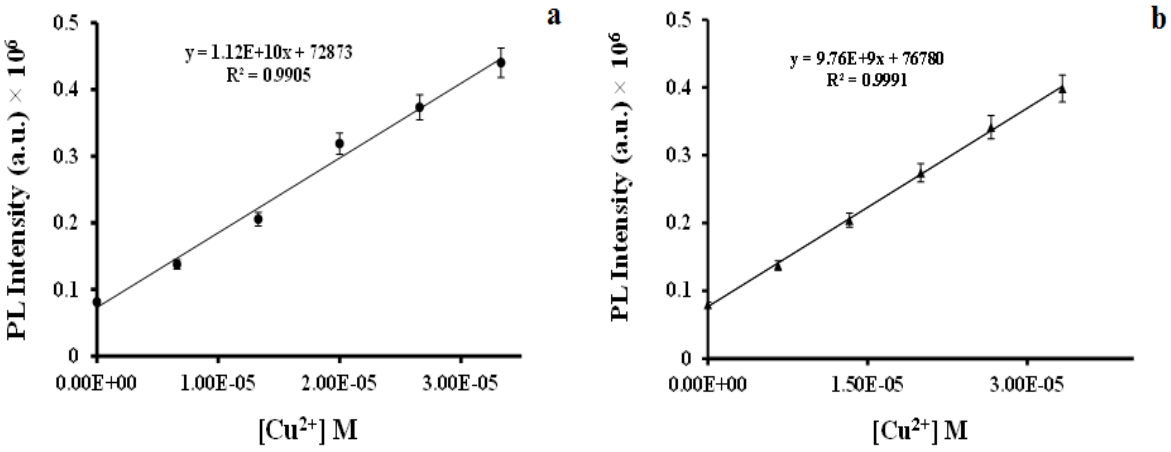

Figure 5.9 Detection limit plot for Cu^{2+} using (a) PMI/FMN complex and (b) PMI/FAD complex.

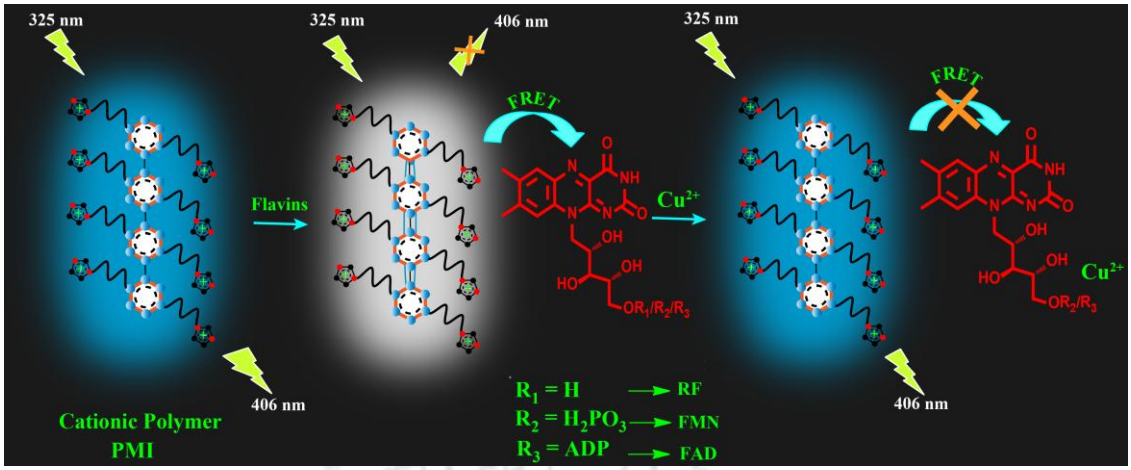

Figure 5.10 Schematic presentation for the detection and discrimination of flavins using conjugated polymer PMI and simple chelating metal (Cu^{2+}).

RF/FMN/FAD in buffer. On adding Cu^{2+} (6.6×10^{-5} M) to the solution of PMI (10 µM) containing RF/FMN (25 µM/10.33 µM) mixture, an enhancement in the fluorescence of PMI peak at 406 nm and decrement in the fluorescence of intense peak at 526 nm was observed (Figure A5.9a). Similar changes were also observed for PMI solution containing RF/FMN/FAD (25 µM/10.33 µM/1.33 µM) mixture with slightly greater intensity of emission peak at 406 nm (Figure A5.9d). However, on introducing Cu^{2+} to the solution of PMI containing RF/FAD (25 µM/1.33 µM) mixture, the emission peak at 406 nm displayed enhancement with no significant change in the intense peak at 526 nm (Figure A5.9b). On the other hand, PMI solution containing FMN/FAD (10.33 µM/1.33 µM) mixture displayed enhancement of emission peak at 406 nm with the decrement of less intense emission peak at 526 nm (Figure A5.9c). The enhancements in the peak at 406 nm in all the cases are attributed to the displacement of PMI bound FMN or FAD molecules from the mixture. From these results, it is evident that RF/FMN and RF/FAD molecules can be easily distinguished even in their mixture due to variable changes observed in the presence of Cu^{2+}. Moreover, FMN/FAD molecules were difficult to be distinguished from the mixture due to the similar changes observed with Cu^{2+}. Though, it was easy to determine the presence of RF in the mixture of all three flavins i.e. RF/FMN/FAD due to the appearance of more intense peak at 526 nm, yet distinguishing FMN/FAD in the same mixture was quite challenging. Thus, it can be said that metal induced displacement technique comprising of cationic polymer PMI was found to be most proficient in discriminating flavins, especially the fluorescence active flavins *viz.* RF and FMN that was impossible using classical or direct fluorescence methods (Table A5.1).[23–25,58–61]

5.3.6 Determination of flavins in blood serum

Dietary RF that is not being utilized into FMN and FAD exists as free RF in the body. On consuming excess RF (B_2 hypervitaminosis), there is a dramatic increment[62–66] of free RF in blood, tissues, and urine where the level reaches even upto micromolar concentrations. This remains a matter of concern because RF has the unique ability to react with light, resulting in adverse cellular effects[67–69] including the generation of toxic peroxides as well as riboflavin–tryptophan photo adduct that is prone to impairment of cells and liver. High doses of RF have also been reported to induce damage to retina cells in the eyes of research animals and cause cataract.[70] Such tendency of RF to generate both destructive free radicals as well as toxic photo adducts is a matter of great concern[63–65] especially for the patients, infants who are fed intravenously and athletes engaged in various sports activities that usually takes vitamin supplements. The PMI based system can be employed to monitor the elevated levels of flavins in all such cases which will be helpful in minimizing the hazards of flavin–induced radical formation in the humans.

Hence, to evaluate the feasibility of the proposed method for bioanalytical applications, sensing studies were performed in fresh human blood serum samples, which are vital media to investigate disorders/diseases related to flavins.[15–20] Note that untreated serum samples collected from healthy individuals did not affect the emission of PMI (Figure A5.10) significantly, since, the concentration of flavins remain extremely low under normal conditions.[15,71] Each flavin was then doped into serum samples and detected using standard addition method. The recoveries for each flavin were found to be well in the range 94.7-98.5% (Table 1–3, Figure A5.11–5.13). These results confirm that PMI is a highly efficient tool for real time monitoring abnormal / excess levels of flavins in the body fluids like serum.

Table 1. Detection of RF in serum samples.

Sample	Added (10^{-6} M)	Found (10^{-6} M)[a]	Recovery (%)
S1	2.50	2.39±0.13	95.6
S2	6.67	6.52±0.15	97.7
S3	10.00	9.71±0.20	97.1

Table 2. Detection of FMN in serum samples.

Sample	Added (10^{-7} M)	Found (10^{-7} M)[a]	Recovery (%)
S1	1.33	1.28±0.10	96.2
S2	2.67	2.63±0.19	98.5
S3	4.00	3.93±0.26	98.2

Table 3. Detection of FAD in serum samples.

Sample	Added (10^{-8} M)	Found (10^{-8} M)[a]	Recovery (%)
S1	3.30	3.20±0.30	96.9
S2	6.70	6.50±0.50	97.0
S3	13.30	12.60±0.70	94.7

5.4 Conclusion

In summary, the conjugated polyelectrolyte PMI displayed variable changes in its photo physical properties on interaction with flavins due to significant FRET and dissimilarity in charge density of flavins that forms the basis for their detection in the biological fluids like blood serum even in the presence of various interfering analytes. The discrimination of flavins (especially the fluorescent active RF and FMN) using simple chelating metal such as Cu^{2+} further makes this method unique and most reliable for distinguishing them that was impossible using classical fluorescence technique. Thus, the present protocol comprising of conjugated polyelectrolyte PMI provides the most efficient mode to recognize and discriminate flavins in biosystems with the advantage of exterminating environmental effects and possible applications in the clinical valuation of the diseases related to flavins and examining metabolic processes.

References

(1) Bruice, T. C. *Acc. Chem. Res.*, **1980**, *13*, 256.

(2) Silverman, R. B. *Acc. Chem. Res.*, **1995**, *28*, 335.

(3) Walsh, C. *Acc. Chem. Res.*, **1980**, *13*, 148.

(4) Bruice, T. C. *Flavins and Flavoproteins*, Walter De Gruyter and Co., New York, **1984**.

(5) Massey, V. *Biochem. Soc. Trans.*, **2000**, *28*, 283.

(6) Foraker, A. B.; Khantwal, C. M.; Swaan, P. W. *Adv. Drug Deliv. Rev.*, **2003**, *55*, 1467.

(7) Capo–chichi, C. D.; Feillet, F.; Gueant, J.–L.; Amouzou, K.; Zonon, N.; Sanni, A.; Lefebvre, E.; Assimadi, K.; Vidailhet, M. *Am J Clin Nutr*, **2000**, *71*, 978.

(8) Said, H. M.; Ortiz, A.; Moyer, M. P.; Yanagawa, N. *Am J Physiol Cell Physiol*, **2000**, *278*, 270.

(9) Leenheer, A. P. D.; Lambert, W. *Modern Chromatographic Analysis of Vitamins*, CRC Press, 3rd edn, **2000**.

(10) Roychowdhury–Saha, M.; Lato, S. M.; Shank, E. D.; Burke, D. H. *Biochemistry*, **2002**, *41*, 2492.

(11) Weil, G. J.; Chused, T. M. *Blood*, **1981**, *57*, 1099.

(12) Mayeno, A. N.; Hamann, K. J.; Gleich, G. J.; *J. Leukoc. Biol.*, **1992**, *51*, 172.

(13) Aw, T. Y.; Jones, D. P.; McCormick, D. B. *J. Nutr.*, **1983**, *113*, 1249.

(14) Gastaldi, G.; Ferrari, G.; Verri, A.; Casirola, D.; Orsenigo, M. N.; Laforenza, U.; *J. Nutr.*, **2000**, *130*, 2556.

(15) Hustad, S.; Ueland, P. M.; Schneede, J. *Clin. Chem.*, **1999**, *45*, 862.

(16) Qin, J.; Fung, Y.; Zhu, D.; Lin, B. *J. Chromatogr. A*, **2004**, *1027*, 223.

(17) Britz–McKibbin, P.; Otsuka, K.; Terabe, S. *Anal. Chem.*, **2002**, *74*, 3736.

(18) Britz–McKibbin, P.; Markuszewski, M. J.; Iyanagi, T.; Matsuda, K.; Nishioka, T.; Terabe, S.; *Anal. Biochem.*, **2003**, *313*, 89.

(19) Light, D. R.; Walsh, C.; Marletta, M. A. *Anal. Biochem.*, **1980**, *109*, 87.

(20) Wang, P.; Yin, Y.; Eremin, S. A.; Rybakov, V. B.; Zhang, T.; Xu, Z.; Ren, L.; He, X.; Meng, M.; Xi, R. *J. Agric. Food Chem.*, **2013**, *61*, 7048.

(21) Hargrove, A. E.; Nieto, S.; Zhang, T.; Sessler, J. L.; Anslyn, E. V. *Chem. Rev.*, **2011**, *111*, 6603.

(22) Zhou, Y.; Xu, Z.; Yoon, J. *Chem. Soc. Rev.*, **2011**, *40*, 2222.

(23) Choudhury, S. D.; Mohanty, J.; Bhasikuttan, A. C.; Pal, H. *J. Phys. Chem. B*, **2010**, *114*, 10717.

(24) Rhee, H.–W.; Choi, H.–Y.; Han, K.; Hong, J.–I. *J. Am. Chem. Soc.*, **2007**, *129*, 4524.

(25) Kundu, A.; Nandi, S.; Layek, R. K.; Nandi, A. K. *ACS Appl. Mater. Interfaces*, **2013**, *5*, 7392.

(26) Rhee, H.–W.; Choi, S. J.; Yoo, S. H.; Jang, Y. O.; Park, H. H.; Pinto, R. M.; Cameselle, J. C.; Sandoval, F. J.; Roje, S.; Han, K.; Chung, D. S.; Suh, J.; Hong, J.–I. *J. Am. Chem. Soc.*, **2009**, *131*, 10107.

(27) Kundu, A.; Nandi, S.; Das, P.; Nandi, A. K. *J. Colloid Interface Sci.*, **2016**, *468*, 276.

(28) Anderson, P. C.; Mecozzi, S. *Nucleic Acids Res.*, **2005**, *33*, 6992.

(29) Wu, J.; Liu, W.; Ge, J.; Zhang, H.; Wang, P. *Chem. Soc. Rev.*, **2011**, *40*, 3483.

(30) Carlson, H. J.; Campbell, R. E. *Curr. Opin. Biotechnol.*, **2009**, *20*, 19.

(31) Varghese, S. S.; Zhu, Y.; Davis, T. J.; Trowell, S. C. *Lab Chip*, **2010**, *10*, 1355.

(32) He, F.; Feng, F.; Wang, S.; Li, Y.; Zhu, D. *J. Mater. Chem.*, **2007**, *17*, 3702.

(33) Jares–Erijman, E. A.; Jovin, T. M. *Nat. Biotechnol.*, **2003**, *21*, 1387.

(34) He, F.; Tang, Y.; Yu, M.; Wang, S.; Li, Y.; Zhu, D. *Adv. Funct. Mater.*, **2006**, *16*, 91.

(35) Gaylord, B. S.; Heeger, A. J.; Bazan, G. C.; *Proc. Natl. Acad. Sci. U. S. A.*, **2002**, *99*, 10954.

(36) Wang, Y.; Li, S.; Feng, L.; Nie, C.; Liu, L.; Lv, F.; Wang, S. *ACS Appl. Mater. Interfaces*, **2015**, *7*, 24110.

(37) Zhu, C.; Liu, L.; Yang, Q.; Lv, F.; Wang, S. *Chem. Rev.*, **2012**, *112*, 4687.

(38) Liang, J.; Li, K.; Liu, B. *Chem. Sci.*, **2013**, *4*, 1377.

(39) Li, K.; Liu, B. *Chem. Soc. Rev.*, **2014**, *43*, 6570.

(40) Rochat, S.; Swager, T. M. *ACS Appl. Mater. Interfaces*, **2013**, *5*, 4488.

(41) Zhou, Q.; Swager, T. M. *J. Am. Chem. Soc.*, **1995**, *117*, 12593.

(42) McQuade, D. T.; Pullen, A. E.; Swager, T. M. *Chem. Rev.*, **2000**, *100*, 2537.

(43) Kim, H. N.; Guo, Z.; Zhu, W.; Yoon, J.; Tian, H. *Chem. Soc. Rev.*, **2011**, *40*, 79.

(44) Thomas, S. W.; Joly, G. D.; Swager, T. M. *Chem. Rev.*, **2007**, *107*, 1339.

(45) Sun, X.; Wang, Y.; Lei, Y.; *Chem. Soc. Rev.*, **2015**, *44*, 8019.

(46) Guan, W.; Zhou, W.; Lu, J.; Lu, C. *Chem. Soc. Rev.*, **2015**, *44*, 6981.

(47) Hussain, S.; Malik, A. H.; Afroz, M. A.; Iyer, P. K. *Chem. Commun.*, **2015**, *51*, 7207.

(48) Hussain, S.; De, S.; Iyer, P. K. *ACS Appl. Mater. Interfaces*, **2013**, *5*, 2234.

(49) Lakowicz, J. R. *Principles of Florescence spectroscopy*, 3rd edn, Springer, **2010**.

(50) Hussain, S.; Malik, A. H.; Iyer, P. K. *ACS Appl. Mater. Interfaces*, **2015**, *7*, 3189.

(51) Raszka, M.; Kaplan, N. O. *Proc. Natl. Acad. Sci. U. S. A.*, **1974**, *71*, 4546.

(52) Biskup, C.; Zimmer, T.; Kelbauskas, L.; Hoffmann, B.; Klöcker, N.; Becker, W.; Bergmann, A.; Benndorf, K. *Microsc. Res. Tech.*, **2007**, *70*, 442.

(53) Liu, B.; Gaylord, B. S.; Wang, S.; Bazan, G. C. *J. Am. Chem. Soc.*, **2003**, *125*, 6705–6714.

(54) McQuade, D. T.; Hegedus, A. H.; Swager, T. M. J. *Am. Chem. Soc.*, **2000**, *122*, 12389.

(55) Liu, Y.; Schanze, K. S. *Anal. Chem.*, **2008**, *80*, 8605.

(56) Malik, A. H.; Hussain, S.; Tanwar, A. S.; Layek, S.; Trivedi, V.; Iyer, P. K. *Analyst*, **2015**, *140*, 4388.

(57) Martinez, H. P.; Grant, C. D.; Reynolds, J. G.; Trogler, W. C. *J. Mater. Chem.*, **2012**, *22*, 2908.

(58) Burch, H. B.; Bessey, O. A.; Lowry, O. H.; *J Biol Chem.*, **1948**, *175*, 457.

(59) Hodson, A. Z.; Norris, L. C.; *J. Biol. Chem.*, **1939**, *131*, 621.

(60) Morell, D. B.; Slater, E. C. *Biochem J.*, **1946**, *40*, 652.

(61) Sankaran, N. B.; Nishizawa, S.; Seino, T.; Yoshimoto, K.; Teramae, N. *Angew. Chem. Int. Ed.*, **2006**, *45*, 1563.

(62) Ross, A. C. *Modern Nutrition in Health and Disease*, 11th edn, Lippincott Williams & Wilkins, **2012**.

(63) Chessex, P.; Lavoie, J.-C.; Rouleau, T.; Brochu, P.; St-Louis, P.; Lévy, E.; Alvarez, F. *Pediatr Res*, **2002**, *52*, 958.

(64) M. M. Manore. *Am J Clin Nutr*, **2000**, *72*, 598S–606S.

(65) Becker, K.; Wilkinson, K. A. R. *Biol Neonate*, **1993**, *63*, 80.

(66) Rassin, K. *Pediatr Res*, **1993**, *33*, 487.

(67) Kale, H.; Harikumar, P.; Kulkarni, S. B.; Nair, P. M.; Netrawali, M. S. *Mutat Res*, **1992**, *298*, 17.

(68) Jernigan Jr, H. M. *Exp Eye Res*, **1985**, *41*, 121.

(69) Speck, W. T; Chen, C. C.; Rosenkranz, H. S. *Pediatr Res*, **1975**, *9*, 150.

(70) Eckhert, C. D.; Hsu, M. H.; Pang, N. *Experientia*, **1993**, *49*, 1084.

(71) Hustad, S.; McKinley, M. C.; McNulty, H.; Schneede, J.; Strain, J. J.; Scott, J. M.; Ueland, P. M. *Clin Chem.*, **2002**, *48*, 1571.

Appendix

File: PMIex336em406cnt2500ns50.FL

v Discrete Components Analysis (Reconvolution)

Fitting range : [550; 1500] channels
c^2 : 1.055

Exp Num	B	err_B	f	err_f	t (ns)	err_t
1	0.081	0.017	100.0	15.96	1.190	0.003

Background : 2.613 Background error : 0.117
Shift : -1.474 ns Shift error : 20.53
IRF Background : 0.115 fixed

File: PMI+RFex336em406cnt2500ns50.FL

v Discrete Components Analysis (Reconvolution)

Fitting range : [550; 1600] channels
c^2 : 0.985

Exp Num	B	err_B	f	err_f	t (ns)	err_t
1	0.060	0.017	70.07	18.08	0.405	0.061
2	0.007	6.7e-4	29.93	2.971	1.186	0.009

Background : 1.978 Background error : 0.086
Shift : -0.415 ns Shift error : 10.04
IRF Background : 0.115 fixed

File: PMI+FMN336em406cnt2500ns50.FL

v Discrete Components Analysis (Reconvolution)

Fitting range : [550; 1450] channels
c^2 : 1.044

Exp Num	B	err_B	f	err_f	t (ns)	err_t
1	0.039	0.006	65.14	15.38	0.589	0.054
2	0.009	8.1e-4	34.86	3.579	1.182	0.017

Background : 1.983 Background error : 0.146
Shift : -0.354 ns Shift error : 8.275
IRF Background : 0.115 fixed

File: PMI+FADex336em406cnt2500ns50.FL

v Discrete Components Analysis (Reconvolution)

Fitting range : [550; 1500] channels
c^2 : 1.015

Exp Num	B	err_B	f	err_f	t (ns)	err_t
1	0.030	0.003	63.68	11.53	0.593	0.043
2	0.008	5.6e-4	36.32	3.025	1.206	0.010

Background : 1.891 Background error : 0.123
Shift : -0.219 ns Shift error : 5.530
IRF Background : 0.115 fixed

Figure A5.1 Fitting parameters correspond to lifetime measurements.

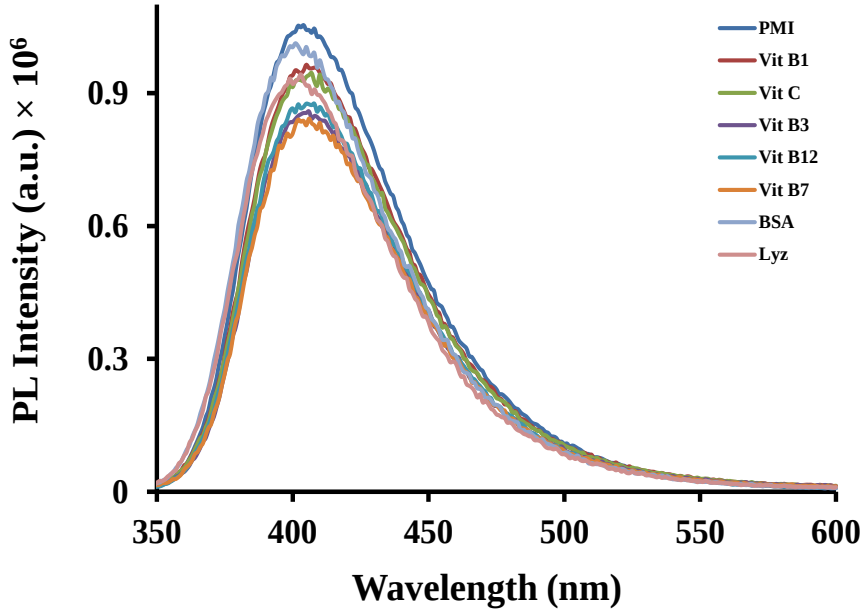

Figure A5.2 Effect of various other vitamins, protein (BSA) and enzyme (lysozyme) on the emission of PMI in 10 mM HEPES buffer (pH = 7.4) at room temperature. Concentration of PMI and each analyte were 10 µM and 25 µM, respectively.

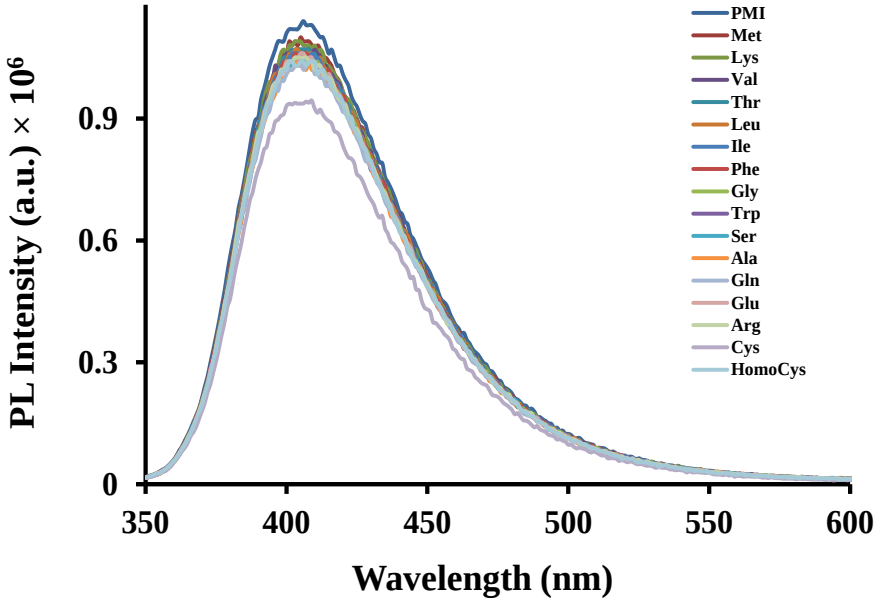

Figure A5.3 Effect of various amino acids (25 µM) on the emission of PMI (10 µM) in 10 mM HEPES buffer (pH = 7.4) at room temperature.

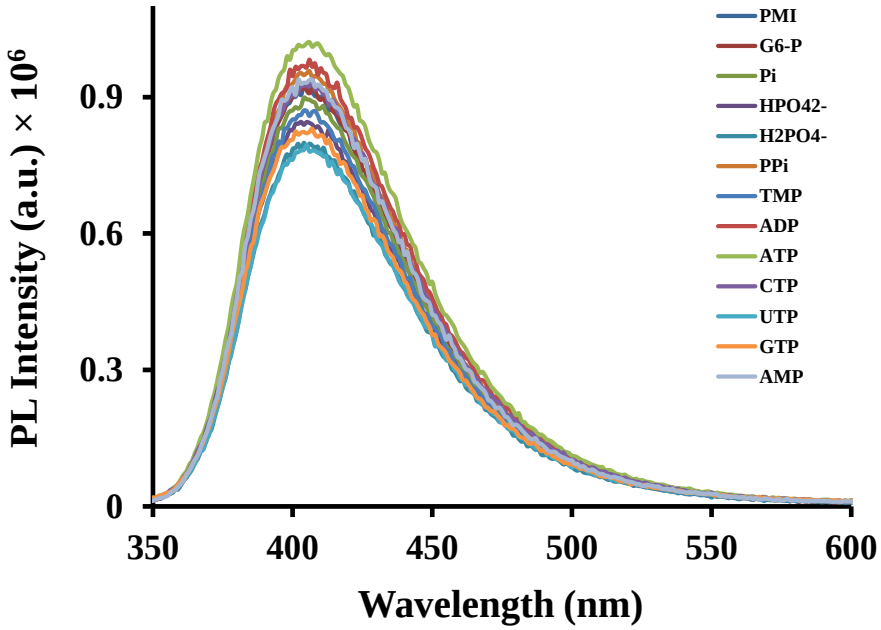

Figure A5.4 Effect of various inorganic and organinc phosphates on the emission of PMI in 10 mM HEPES buffer (pH = 7.4) at room temperature. Concentration of PMI and each analyte were 10 µM and 25 µM, respectively.

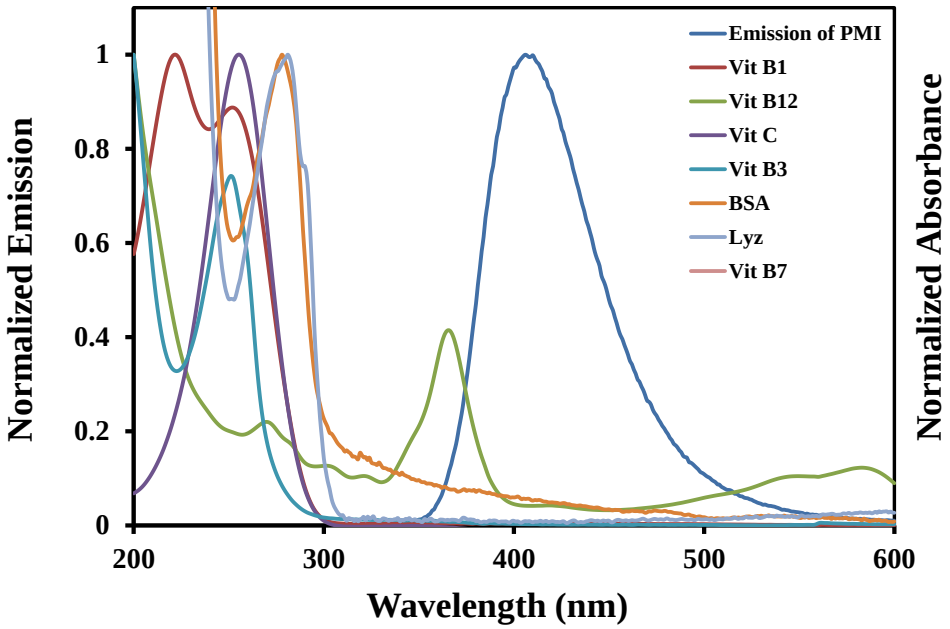

Figure A5.5 Spectral overlap between emission spectrum of PMI and absorbtion spectra of various other vitamins, protein (BSA) and enzyme (lysozyme).

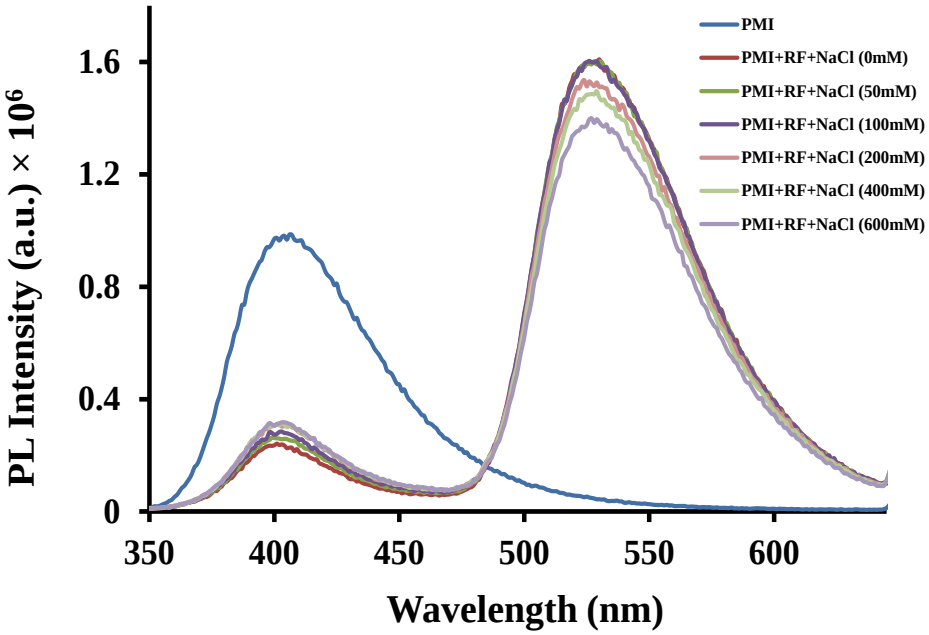

Figure A5.6 Effect of ionic strength on FRET efficency for RF detection. Concentration of PMI and RF were 10 μM and 25 μM, respectively.

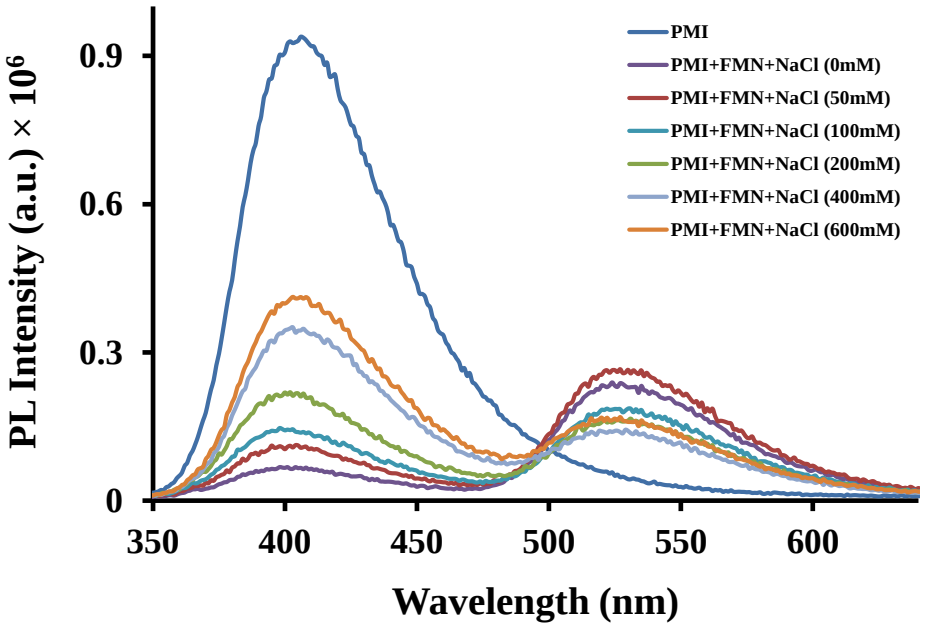

Figure A5.7 Effect of ionic strength on FRET efficency for FMN detection. Concentration of PMI and FMN were 10 μM and 10.33 μM, respectively.

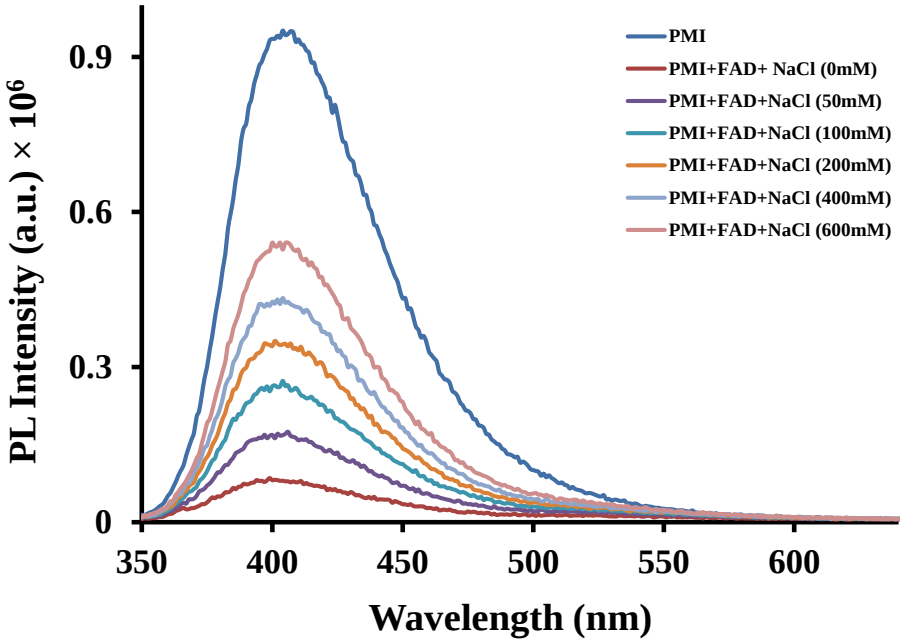

Figure A5.8 Effect of ionic strength on FRET efficency for FAD detection. Concentration of PMI and FAD were 10 µM and 1.33 µM, respectively.

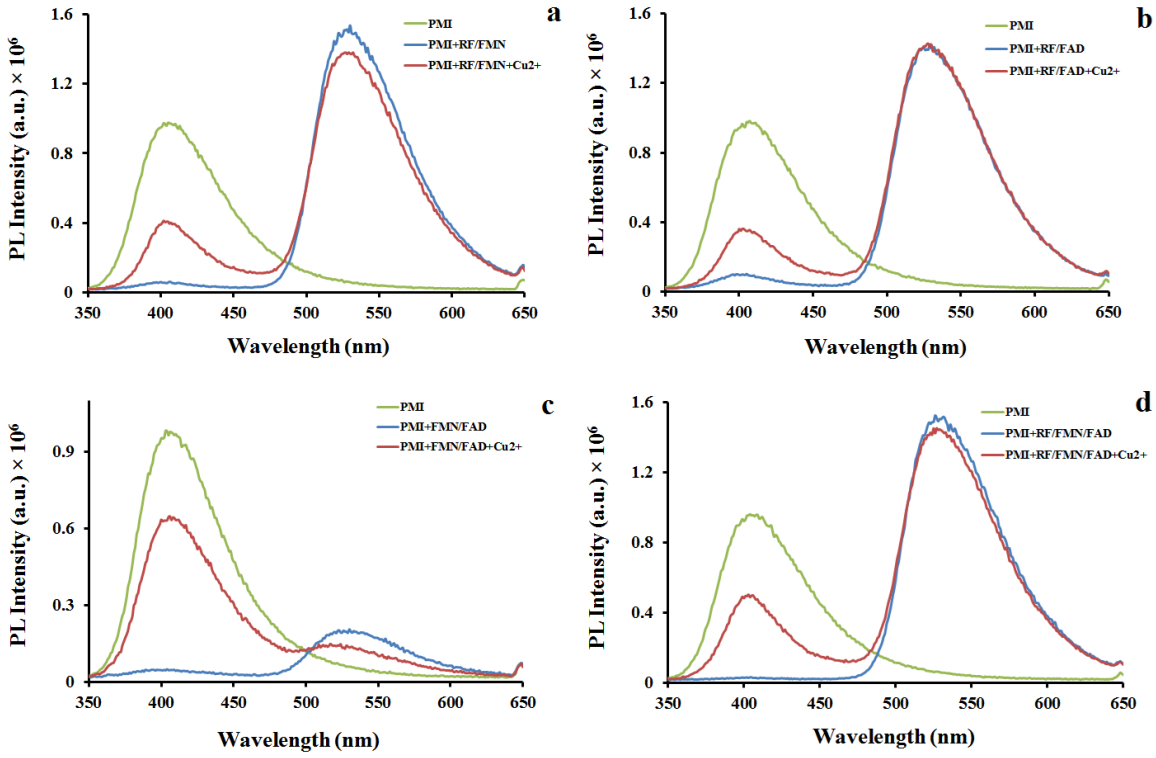

Figure A5.9 Change in emission spectra on adding Cu^{2+} (6.6×10^{-5} M) to the solution of PMI (10 µM) containing mixture of (a) RF/FMN (25 µM/10.33 µM), (b) RF/FAD (25 µM/1.33 µM), (c) FMN/FAD (10.33 µM/1.33 µM) and (d) RF/FMN/FAD (25 µM/10.33 µM/1.33 µM) in 10 mM HEPES buffer (pH = 7.4).

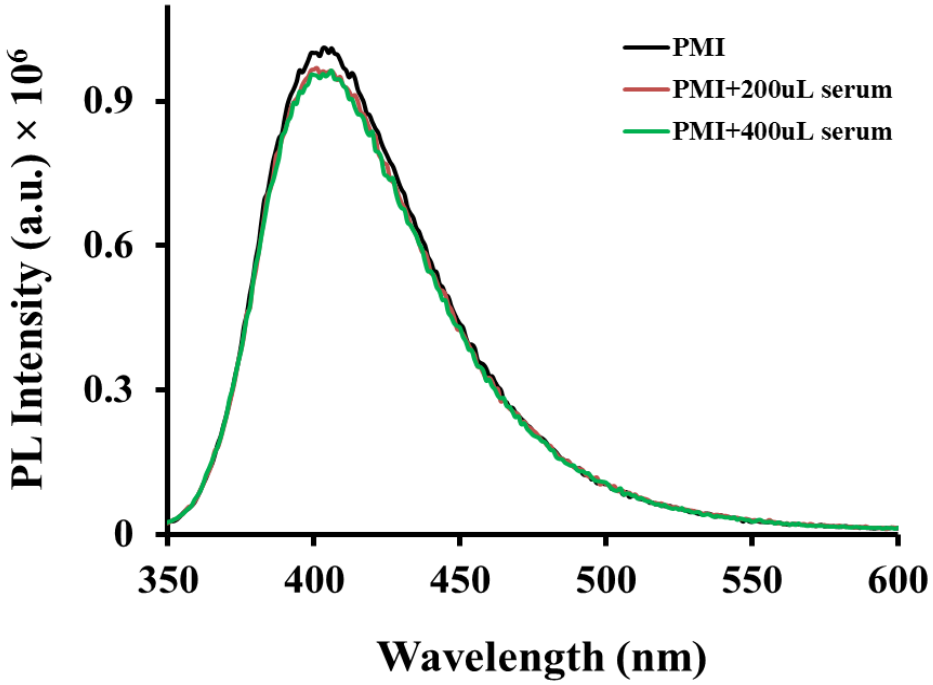

Figure A5.10 Change in emission of PMI after adding undoped serum samples.

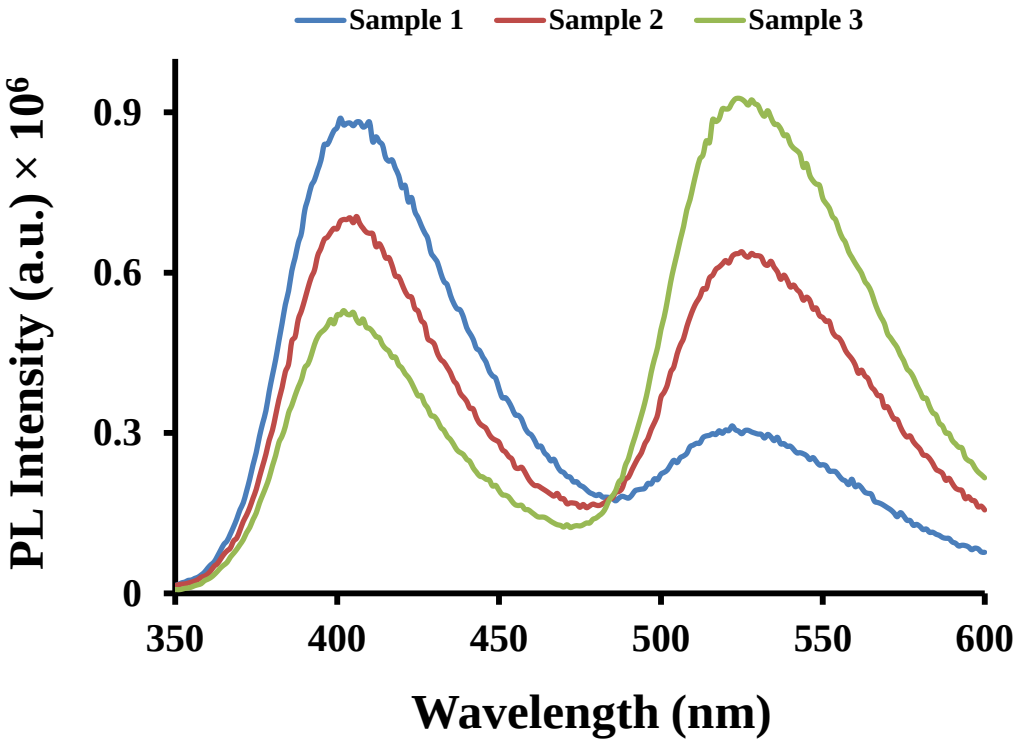

Figure A5.11 Change in emission of PMI after adding RF–doped serum samples.

Table A5.1 A comparative study of the some fluorometric based probes for the detection of flavins.

Publication	**Material used**	**Sensing analytes**	**Detection Method**	**Discrimination**	**LOD**
Current Work	***Conjugated Polyelectrolyte***	***RF, FMN, FAD and Cu^{2+}***	***FRET***	***RF/FMN and RF/FAD***	***RF–0.69 µM, FMN–19.68 nM, FAD–13.40 nM and Cu^{2+}–0.56 µM***
J. Am. Chem. Soc. **2007**, 129, 4524–4525	Bis(Zn^{2+}-dipicolylamine complex	FAD	Direct fluorescence method	Not shown	Not determined (Detection in µM range)
ACS Appl. Mater. Interfaces **2013**, 5, 7392–7399	Sulfonated Graphene	RF and FMN	FRET	Not shown	RF–1.6 µM
Angew. Chem. Int. Ed. **2006**, 45, 1563–1568	DNA-duplex Aptamer	RF	Direct fluorescence method	Not shown	Not determined
Organic Letters, **2013,** 15, 1210–1213	Pyrene bound Zn^{2+}–dipicolylamine	FMN and FAD	Ratiometric method	Only FMN and FAD	Not determined (Detection in µM range)
Org. Biomol. Chem. **2016**, 14, 447–450	RNA Aptamer	FAD	Direct fluorescence method	Not shown	Not determined
J. Phys. Chem. B **2010**, 114, 10717–10727	Cucurbit[7]uril	RF and FAD	Direct fluorescence method	Only RF and FAD	Not determined
J. Am. Chem. Soc. **1995**, 117, 1246–1257	RNA Aptamer	RF	Direct fluorescence method	Not shown	Not determined

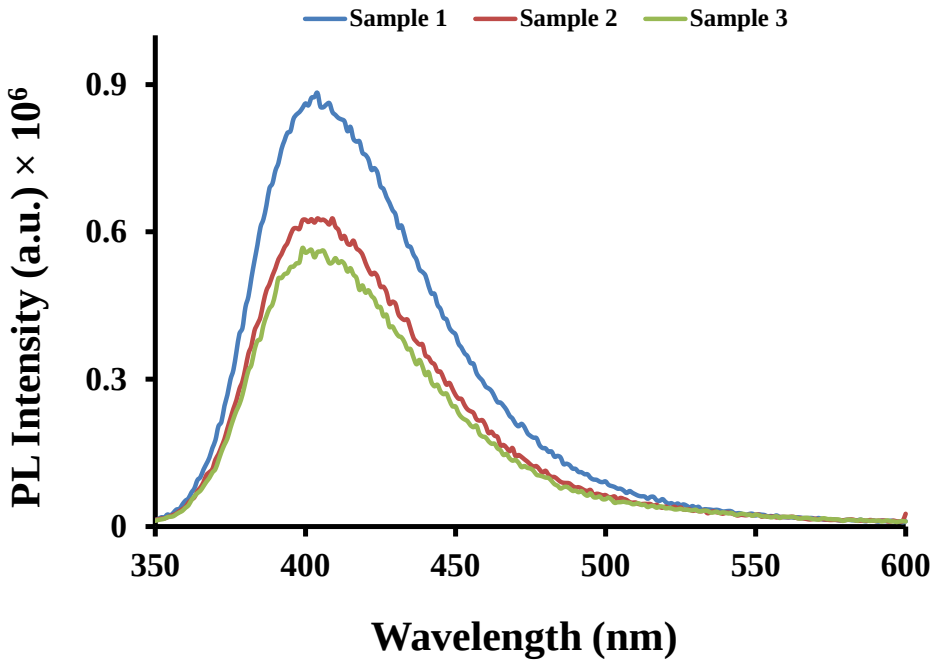

Figure A5.12 Change in emission of PMI after adding FMN–doped serum samples.

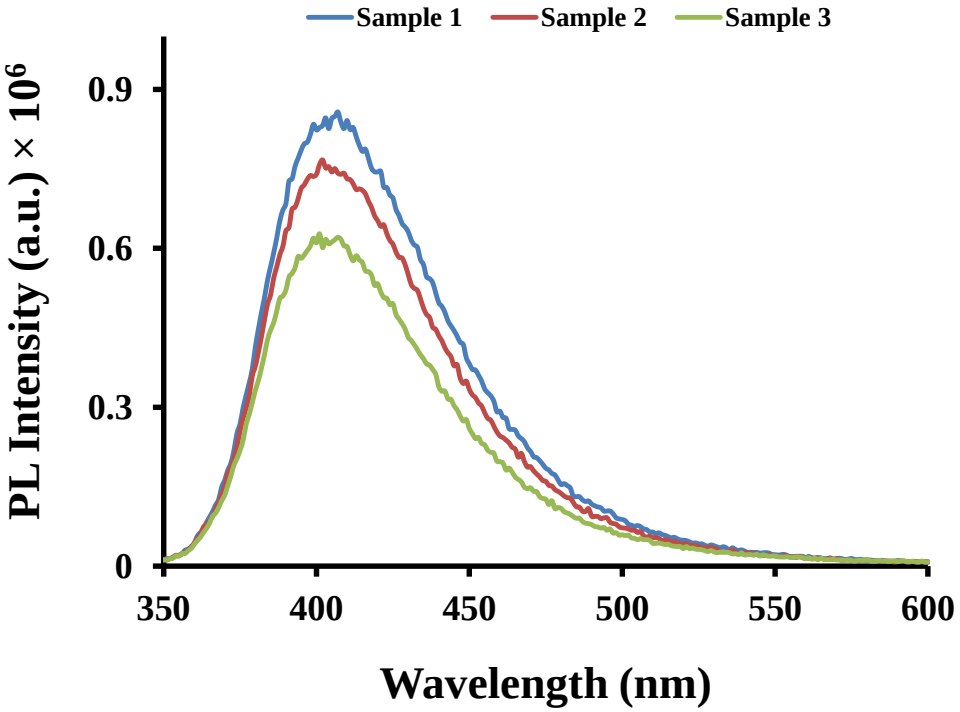

Figure A5.13 Change in emission of PMI after adding FAD–doped serum samples.

Publications

1. **Hussain, S.**; De, S.; Iyer, P. K. Thiazole–containing conjugated polymer as a visual and fluorometric sensor for iodide and mercury, *ACS Appl. Mater. Interfaces* **2013,** *5*, 2234–2240.

2. Muthuraj, B.; **Hussain, S.**; Iyer, P. K. A rapid and sensitive detection of ferritin at a nanomolar level and disruption of amyloid beta fibrils using fluorescent conjugated polymer, *Polymer Chem.* **2013**, *4*, 5096–5107. **(Work Highlighted by RSC as Paper and Author of the Week)**

3. **Hussain, S.**; Malik, A. H.; Iyer, P. K. Highly precise detection, discrimination, and removal of anionic surfactants over the full pH range *via* cationic conjugated polymer: An efficient strategy to facilitate illicit–drug analysis, *ACS Appl. Mater. Interfaces* **2015,** *7*, 3189–3198.

4. **Hussain, S.**; Malik, A. H.; Afroz, M. A.; Iyer, P. K. Ultrasensitive detection of nitro explosive–picric acid *via* conjugated polyelectrolyte in aqueous media and solid support, *Chem. Commun.* **2015**, *51*, 7207–7210.

5. Malik, A. H.; **Hussain, S.**; Tanwar, A. S.; Layek, S.; Trivedi, V.; Iyer, P. K. An anionic conjugated polymer as a multi–action sensor for the sensitive detection of Cu^{2+} and PPi, *Analyst* **2015**, *140*, 4388–4392.

6. Dar, A. A.; **Hussain, S.**; Dutta, D.; Iyer, P. K.; Khan. A. T. One–pot synthesis of functionalized 4–hydroxy–3–thiomethylcoumarins: Detection and discrimination of Co^{2+} and Ni^{2+} ions, *RSC Advances* **2015**, *5*, 57749–57756.

7. Valapa, R.; **Hussain, S.**; Iyer, P. K.; Pugazhenthi, G.; Katiyar, V. Non–isothermal crystallization kinetics of sucrose palmitate reinforced poly(lactic acid) bionanocomposites, *Polym. Bull.* **2015**, *23*, 21–38.

8. Valapa, R.; **Hussain, S.**; Iyer, P. K.; Pugazhenthi, G.; Katiyar, V. Influence of graphene on thermal degradation and crystallization kinetics behaviour of poly(lactic acid), *J. Polym. Res.* **2015**, *22*, 175.

9. Kalita, A.; **Hussain, S.**; Malik, A. H.; Subbarao, N. V. V.; Iyer, P. K. Vapor phase sensing of ammonia at the sub–ppm level using a perylene diimide thin film device, *J. Mater. Chem. C.* **2015**, *3*, 10767–10774.

Publications

10. Malik, A. H.; **Hussain, S.**; Kalita, A.; Iyer, P. K. Conjugated polymer nanoparticles for the amplified detection of nitro–explosive picric acid on multiple platforms, *ACS Appl. Mater. Interfaces* **2015**, *7*, 26968–26976.

11. **Hussain, S.**; Malik, A. H.; Iyer, P. K. FRET–assisted selective detection of flavins *via* cationic conjugated polyelectrolyte under physiological conditions, *J. Mater. Chem. B* **2016**, *4*, 4439–4446.

12. Malik, A. H.; **Hussain, S.**, Iyer, P. K. Aggregation–induced FRET *via* polymer–surfactant complexation: A new strategy for the detection of spermine, *Anal. Chem.* **2016**, *88*, 7358–7364.

13. Tanwar, A. S.; **Hussain, S.**; Malik, A. H.; Afroz, M. A.; Iyer, P. K. Inner–filter effect based selective detection of nitroexplosive–picric acid in aqueous solution and solid support using conjugated polymer, *ACS. Sens.* **2016**, *1*, 1070–1077.

14. Kalita, A.; **Hussain, S.**; Malik, A. H.; Barman, U.; Goswami, N.; Iyer, P. K. Anion–exchange induced strong π–π interactions in single crystalline naphthalene diimide for nitroexplosive sensing: An electronic prototype for visual on–site detection, *ACS Appl. Mater. Interfaces*, **2016**, *8*, 25326–25336.

Conferences & Seminars

1. Participated in "2nd National Workshop on NEMS/MEMS and Theranostics Devices" (NWNTD–2016) organized by Centre for Nanotechnology, IIT Guwahati during 21–22 March 2016.
2. Presented a ***POSTER*** in "Research Conclave '16" organized by Students' Academic Board (SAB), IIT Guwahati during 17–20 March 2016.
3. Attended "National Workshop on Advanced Probing Techniques in TEM" organized jointly by IIT Guwahati and Electron Microscopy Society of India during 15–16 February 2016.
4. Presented a ***POSTER*** in Materials and Research Society of India (MRSI) symposium on "Advanced Materials for Sustainable Applications" held at NEIST, Jorhat during 18–21 February 2016.
5. Presented a ***POSTER*** in "4th International Conference on Advanced Nanomaterials and Nanotechnology" (ICANN–2015) organized by Centre for Nanotechnology, IIT Guwahati during 08–11 December 2015.
6. Delivered an ***ORAL*** talk in the "11th International Conference on Advanced Polymers *via* Macromolecular Engineering" (APME 2015) held at Pacifico Yokohama in Yokohama, Japan, from 18–22 October 2015.
7. Delivered an ***ORAL*** talk on the occasion of Bharat Ratna Prof. C. N. R Rao's visit to IIT Guwahati in July 2015.
8. Attended "2–Day Familiarization Workshop on Nanofabrication Technologies" held at Tezpur University during 25–26 April 2015 funded by the Dept of Electronics and Information Technology (DeitY), the Ministry of Communication and Information Technology (MCIT), Govt. of India.
9. Delivered an ***ORAL*** talk in "ChemConvene 2015" organized by Department of Chemistry, IIT Guwahati on 8th April 2015.
10. Presented a ***POSTER*** in "TEQIP Short Term Course cum Workshop on "Emerging Micropollutants in the Environment: Occurrence, Transportation, Monitoring and Treatment" organized jointly by Centre for Education Technology and Department of Chemical Engineering, IIT Guwahati on 5th March 2015.

Conferences & Seminars

11. Presented a ***POSTER*** in "International Symposium on Polymer Science and Technology" (MACRO 2015) organized jointly by the Kolkata and Kharagpur chapters of the SPSI at the Indian Association for the Cultivation of Science (IACS), Kolkata during 23–26 January, 2015.
12. Attended "National Conference on Recent Advances in Cancer Biology and Therapeutics" (RACBT) organized by Department of Biotechnology, IIT Guwahati on 5th December, 2014.
13. Attended workshop on "Sensors and its Applications" conducted by Institute of Advanced Study in Science & Technology (IASST) Guwahati in 2013.

Awards & Achievements

1. Selected for the ***131st International Summer Course of BASF*** hosted by World's Leading Chemical Producing Company BASF at their headquarters in Ludwigshafen, Germany. From all over the world, 40 selected PhD students visited Germany as the guests of BASF to gain insight into an international company from various prospects.
2. Received ***Institute Best Poster Award (First)*** for the paper entitled "Ultrasensitive Detection of Nitro Explosive–Picric Acid *via* a Conjugated Polyelectrolyte in Aqueous Media and Solid Support" in Research Conclave '16 organized by Students' Academic Board (SAB), IIT Guwahati during 17–20 March 2016.
3. Received ***Departmental Best Poster Award (First)*** for paper entitled "Ultrasensitive Detection of Nitro Explosive–Picric Acid *via* Conjugated Polyelectrolyte in Aqueous Media and Solid Support" in Research Conclave '16 organized by Students' Academic Board (SAB), IIT Guwahati during 17–20 March 2016.
4. Awarded ***Travel Fellowship*** from Department of Science and Technology (DST), Govt. of India and Centre for International Co–operation in Science (CICS) for presenting a paper in 11th International Conference on Advanced Polymers *via* Macromolecular Engineering (APME 2015) held at Pacifico Yokohama in Yokohama, Japan, from 18–22 October 2015.
5. Received ***Best Poster Award (First)*** for paper entitled "Highly Precise Detection, Discrimination, and Removal of Anionic Surfactants over the Full pH Range *via* Cationic Conjugated Polymer: An Efficient Strategy to Facilitate Illicit–Drug Analysis" in Annual Chemical Engineering Festival "Reflux 2015" organized by Department of Chemical Engineering, IIT Guwahati during 27–29 March 2015.
6. Received ***Best Poster Award (First)*** for paper entitled "Highly Precise Detection, Discrimination, and Removal of Anionic Surfactants over the Full pH Range *via* Cationic Conjugated Polymer: An Efficient Strategy to Facilitate Illicit–Drug Analysis" in TEQIP National Course organized by Centre for Education Technology and Department of Chemical Engineering, IIT Guwahati on 5 March 2015.